

Supplementary Information for:

Hyoliths with pedicles constrain the origin of the  
brachiopod body plan

*Haijing Sun, Martin R. Smith, Han Zeng, Fangchen Zhao, Guoxiang Li and Maoyan Zhu*

2018-05-28

# Contents

<b>Supplementary Text</b>	<b>3</b>
<b>1 Phylogenetic dataset</b>	<b>4</b>
<b>2 Parsimony analysis</b>	<b>6</b>
2.1 Search parameters . . . . .	6
2.2 Analysis . . . . .	6
2.3 Results . . . . .	7
<b>3 Character reconstructions</b>	<b>14</b>
3.1 Sclerites . . . . .	15
3.2 Sclerites: Bivalved [2] . . . . .	16
3.3 Sclerites: Dorsal valve . . . . .	40
3.4 Sclerites: Ventral valve . . . . .	55
3.5 Sclerites: Ornament . . . . .	81
3.6 Sclerites: Composition . . . . .	86
3.7 Gametes . . . . .	100
3.8 Gametes: Spermatozoa . . . . .	102
3.9 Brephic shell . . . . .	108
3.10 Brephic shell: Setal sacs [79] . . . . .	115
3.11 Setae . . . . .	118
3.12 Pedicle [83] . . . . .	120
3.13 Mantle canals . . . . .	131
3.14 Lophophore . . . . .	139
3.15 Prominent pharynx [103] . . . . .	146
3.16 Anus [104] . . . . .	147
<b>4 Fitch parsimony</b>	<b>152</b>
4.1 Results . . . . .	152
<b>5 Bayesian analysis</b>	<b>156</b>
5.1 Parameter estimates . . . . .	157
5.2 Results . . . . .	157
<b>6 Taxonomic implications</b>	<b>159</b>
<b>Supplementary Figures</b>	<b>161</b>
<b>Supplementary Table</b>	<b>165</b>
<b>Bibliography</b>	<b>166</b>

# Supplementary Text

This document contains supplementary material to Sun et al. (2018). It is best viewed in HTML format at [ms609.github.io/hyoliths](https://ms609.github.io/hyoliths).

It opens with a detailed discussion of analyses of the morphological dataset constructed to accompany Sun et al. (2018), and their results.

The results presented in the main paper employ the algorithm described by Brazeau et al. (2018) for correct handling of inapplicable data in a parsimony setting. This document depicts how each character is most parsimoniously reconstructed on an optimal tree.

For completeness, we also document the results of standard Fitch parsimony analysis, and the results of Bayesian analysis, neither of which treat inapplicable data in a logically consistent fashion.

Supplementary figures and tables appear after the text.

# Chapter 1

## Phylogenetic dataset

Analysis was performed on a new matrix of 37 early brachiozoan taxa, including hyoliths, tommotiids and mickwitziids, which were coded for 107 morphological characters (62 neomorphic, 45 transformational).

*Namacalathus* was incorporated as a 38<sup>th</sup> taxon, but preliminary results did not uphold the homology of its potentially brachiozoan-like features. As such, we excluded it from our analysis due to its morphological distance from ingroup taxa, a likely source of long branch error. *Dalyatia* was instead selected as an outgroup as camenellans have been interpreted as the earliest diverging members of the Brachiozoa (Skovsted et al., 2015; Zhao et al., 2017).

Characters are coded following the recommendations of Brazeau et al. (2018):

- We have employed reductive coding, using a distinct state to mark character inapplicability. Character specifications follow the structural syntax of Sereno (2007) in order to highlight ontological dependence between characters and emphasize the structure of the dataset.
- We have distinguished between neomorphic and transformational characters (*sensu* Sereno, 2007) by reserving the token 0 to refer to the absence of a neomorphic (i.e. presence/absence) character. The states of transformational characters (i.e. characters that describe a property of a feature) are represented by the tokens 1, 2, 3, ...
- We code the absence of neomorphic ontologically dependent characters (*sensu* Vogt, 2017) as absence, rather than inapplicability.

The complete dataset comprises 3959 character codings, of which 451 are inapplicable and 2319 were neither ambiguous nor inapplicable. The amount and quality of data that *is* coded is more instructive than a measure of how many cells are ambiguous (Wiens, 1998, 2003). Of the 107 characters, the number that were coded with an applicable token for each taxon is:

<u>Acanthotretella spinosa</u>	59 &nbsp;	<u>Haplophrentis carinatus</u>	65 &nbsp;	<u>Orthis</u>
<u>Alisina</u>	75 &nbsp;	<u>Helio medusa orienta</u>	57 &nbsp;	<u>Paterimitra</u>
<u>Askepasma toddense</u>	65 &nbsp;	<u>Kutorgina chengjiangensis</u>	76 &nbsp;	<u>Pedunculotheca diania</u>
<u>Antigonambonites planus</u>	73 &nbsp;	<u>Lingula</u>	93 &nbsp;	<u>Pelagodiscus atlanticus</u>
<u>Botsfordia</u>	64 &nbsp;	<u>Lingulosacculus</u>	49 &nbsp;	<u>Phoronis</u>
<u>Clupeafumosus socialis</u>	66 &nbsp;	<u>Lingulellotreta malongensis</u>	70 &nbsp;	<u>Salanygolina</u>
<u>Coolinia pecten</u>	69 &nbsp;	<u>Longtancunella chengjiangensis</u>	49 &nbsp;	<u>Siphonobolus priscus</u>
<u>Craniops</u>	57 &nbsp;	<u>Micrina</u>	59 &nbsp;	<u>Terebratulina</u>
<u>Dailyatia</u>	32 &nbsp;	<u>Micromitra</u>	69 &nbsp;	<u>Ussunia</u>
<u>Eccentrotheca</u>	31 &nbsp;	<u>Mickwitzia muralensis</u>	63 &nbsp;	<u>Tomteluva perturbata</u>
<u>Eoobolus</u>	70 &nbsp;	<u>Mummpikia nuda</u>	45 &nbsp;	<u>Yuganotheca elegans</u>
<u>Glyptoria</u>	65 &nbsp;	<u>Nisusia sulcata</u>	73 &nbsp;	
<u>Gasconsia</u>	61 &nbsp;	<u>Novocrania</u>	86 &nbsp;	

The matrix can be viewed interactively and downloaded at Morphobank (project 2800). [This link will become live on publication of the paper. Referees should follow the pre-publication link to the dataset that has been provided in the main manuscript.]

A static version of the NEXUS file used to generate this supplementary information can be downloaded directly from [https://raw.githubusercontent.com/ms609/hyoliths/master/mbank\\_X24932\\_4-18-2018\\_656.nex](https://raw.githubusercontent.com/ms609/hyoliths/master/mbank_X24932_4-18-2018_656.nex).

# Chapter 2

## Parsimony analysis

The phylogenetic dataset contains a considerable proportion of inapplicable codings ( $451/3959 = 11.4\%$  of tokens), which are known to introduce error and bias to phylogenetic reconstruction when the Fitch algorithm is employed (Maddison, 1993; Brazeau et al., 2018). As such, we employed a new tree-scoring algorithm that correctly handles inapplicable data (Brazeau et al., 2018), implemented in the *MorphyLib* C library (Brazeau et al., 2017). We employed the R package *TreeSearch* v0.1.2 (Smith, 2018) to conduct phylogenetic tree search with this algorithm.

As this is a new method, we also employed the traditional, Fitch algorithm, even though this approach is known to generate erroneous trees. The results of this analysis can be viewed in a later section.

### 2.1 Search parameters

Heuristic searches were conducted using the parsimony ratchet (Nixon, 1999) under equal and implied weights (Goloboff, 1997). The consensus tree presented in the main manuscript represents a strict consensus of all trees that are most parsimonious under one or more of the concavity constants ( $k$ ) 2, 3, 4.5, 7, 10.5, 16 and 24, an approach that has been shown to produce higher accuracy (i.e. more nodes and quartets resolved correctly) than equal weights at any given level of precision (Smith, 2017).

### 2.2 Analysis

The R commands used to conduct the analysis are reproduced below. The results can most readily be replicated using the R markdown files (.Rmd) used to generate these pages.

#### 2.2.1 Initialize and load data

```
# Load data from locally downloaded copy of MorphoBank matrix
my_data <- ReadAsPhyDat(filename)
my_data$Namacalathus <- NULL # Exclude Namacalathus
iw_data <- PrepareDataIW(my_data)
```

#### 2.2.2 Generate starting tree

Start by quickly rearranging a neighbour-joining tree, rooted on the outgroup.

```

nj.tree <- NJTree(my_data)
rooted.tree <- EnforceOutgroup(nj.tree, outgroup)
start.tree <- TreeSearch(tree=rooted.tree, dataset=my_data, maxIter=3000,
                           EdgeSwapper=RootedNNISwap, verbosity=0)

```

### 2.2.3 Implied weights analysis

The position of the root does not affect tree score, so we keep it fixed (using RootedXXXSwap functions) to avoid unnecessary swaps.

```

for (k in kValues) {
  iw.tree <- IW Ratchet(start.tree, iw_data, concavity=k,
                         ratchHits = 60, searchHits=55,
                         swappers=list(RootedTBRSwap, RootedSPRSwap, RootedNNISwap),
                         verbosity=0L)
  score <- IWScore(iw.tree, iw_data, concavity=k)
  # Write a single best tree
  write.nexus(iw.tree,
              file=paste0("TreeSearch/hy_iw_k", k, "_",
                          signif(score, 5), ".nex", collapse=''))
  
  iw.consensus <- IW RatchetConsensus(iw.tree, iw_data, concavity=k,
                                         swappers=list(RootedTBRSwap, RootedNNISwap),
                                         searchHits=55,
                                         nSearch=150, verbosity=0L)
  write.nexus(iw.consensus,
              file=paste0("TreeSearch/hy_iw_k", k, "_",
                          signif(IWScore(iw.tree, iw_data, concavity=k), 5),
                          ".all.nex", collapse=''))
}

```

### 2.2.4 Equal weights analysis

```

ew.tree <- Ratchet(start.tree, my_data, verbosity=0L,
                     ratchHits = 25, searchHits=55, # ratchHits = 10 not enough
                     swappers=list(RootedTBRSwap, RootedSPRSwap, RootedNNISwap))
ew.consensus <- RatchetConsensus(ew.tree, my_data, nSearch=150, searchHits = 55,
                                   swappers=list(RootedTBRSwap, RootedNNISwap),
                                   verbosity=0L)
write.nexus(ew.consensus, file=paste0(collapse='', "TreeSearch/hy_ew_",
                                       Fitch(ew.tree, my_data), ".nex"))

```

## 2.3 Results

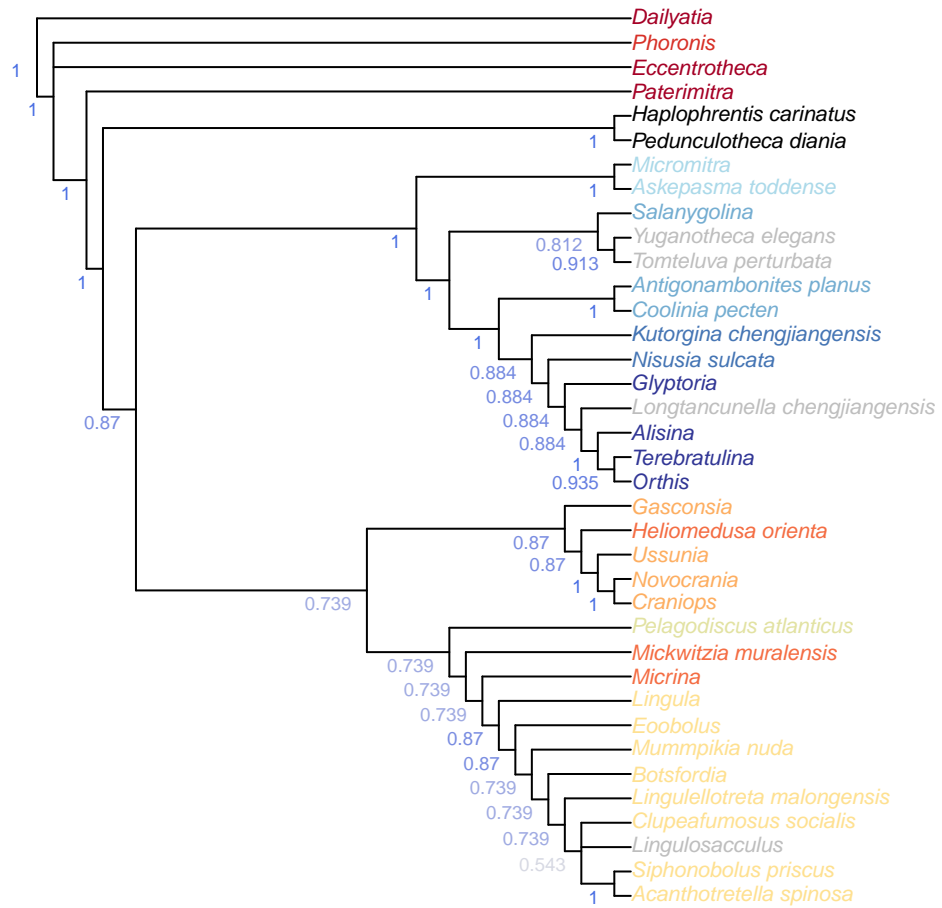


Figure 2.1: Consensus of all parsimony results. Node labels denote the proportion of trees obtained under all analytical conditions that support the clade.

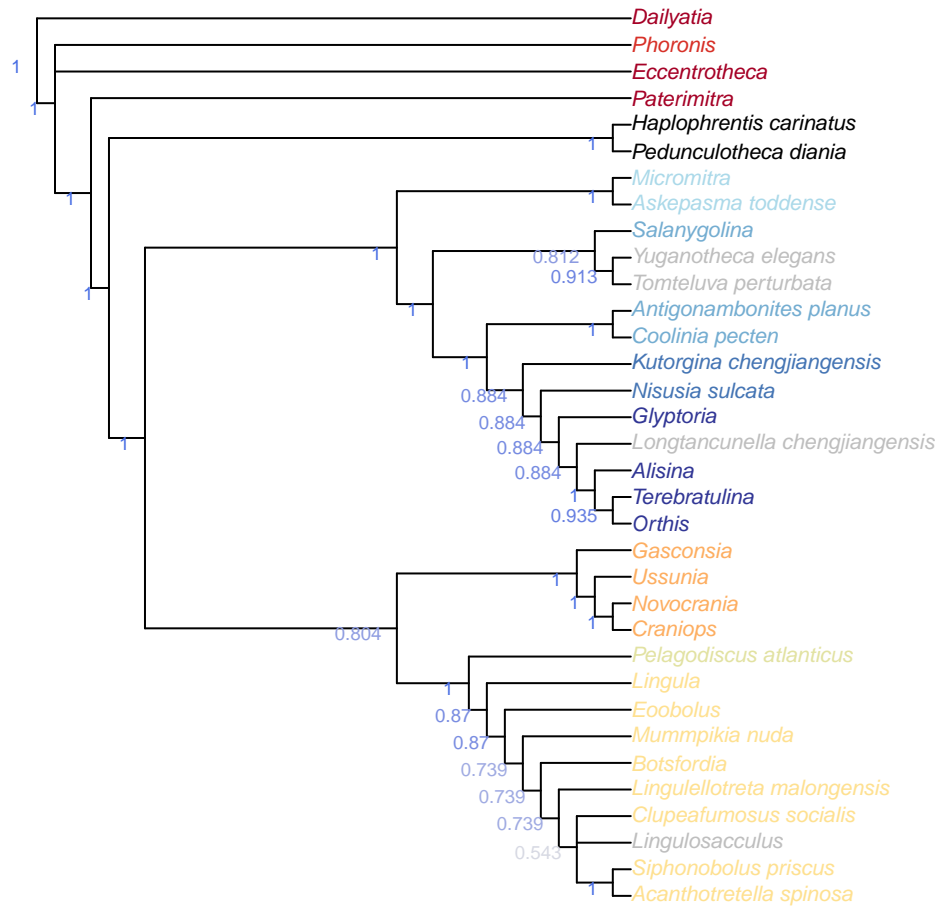


Figure 2.2: Consensus of all parsimony results. Node labels denote the proportion of trees obtained under all analytical conditions that support the clade.



Figure 2.3: Consensus of implied weights analyses at all values of  $k$ . Wildcard taxa have been excluded from the consensus tree shown above to improve resolution.

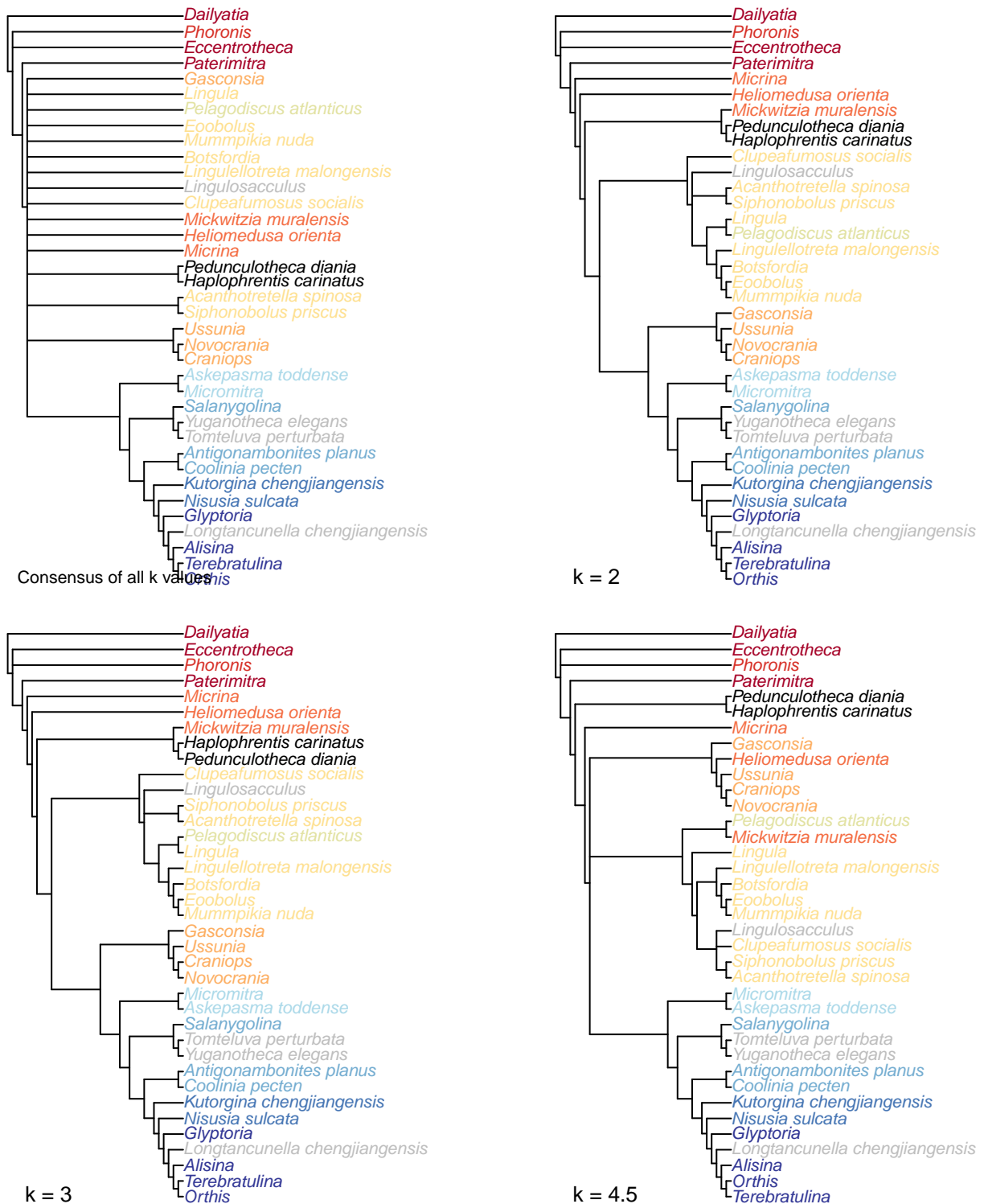


Figure 2.4: Consensus trees of implied weights analyses at all values of  $k$ , and at the individual values  $k = 2, 3$  and  $4.5$ .



Figure 2.5: Consensus trees of implied weights analyses at  $k = 7, 10.5, 16$  and  $24$ .



Figure 2.6: Strict consensus of most parsimonious trees under equally weighted parsimony

# Chapter 3

## Character reconstructions

This page provides definitions for each of the characters in our matrix, and justifies codings in particular taxa where relevant. Further citations for codings that are not discussed in the text can be viewed by browsing the morphological dataset on MorphoBank (project 2800). This link will become live on publication of the paper. Referees should follow the pre-publication link to the dataset that has been provided in the main manuscript.

Alongside its definition, each character has been mapped onto a tree. Here, we have arbitrarily selected one most parsimonious tree obtained under implied weighting,  $k = 4.5$ . Other trees can be viewed in the HTML version of this document at [ms609.github.io/hyoliths](https://ms609.github.io/hyoliths). Each tip is labelled according to its coding in the matrix. These states have been used to reconstruct the condition of each internal node, using the parsimony method of Brazeau et al. (2018) as implemented in the *Inapp R* package.

We emphasize that different trees will give different reconstructions. The character mappings are not intended to definitively establish how each character evolved, but to help the reader quickly establish how each character has been coded, and to visualize at a glance how well the character fits onto the given tree. Consistency indices (Archie, 1989) are also provided for each character.

### 3.1 Sclerites

#### [1] Present in adult



#### Character 1: Sclerites: Present in adult

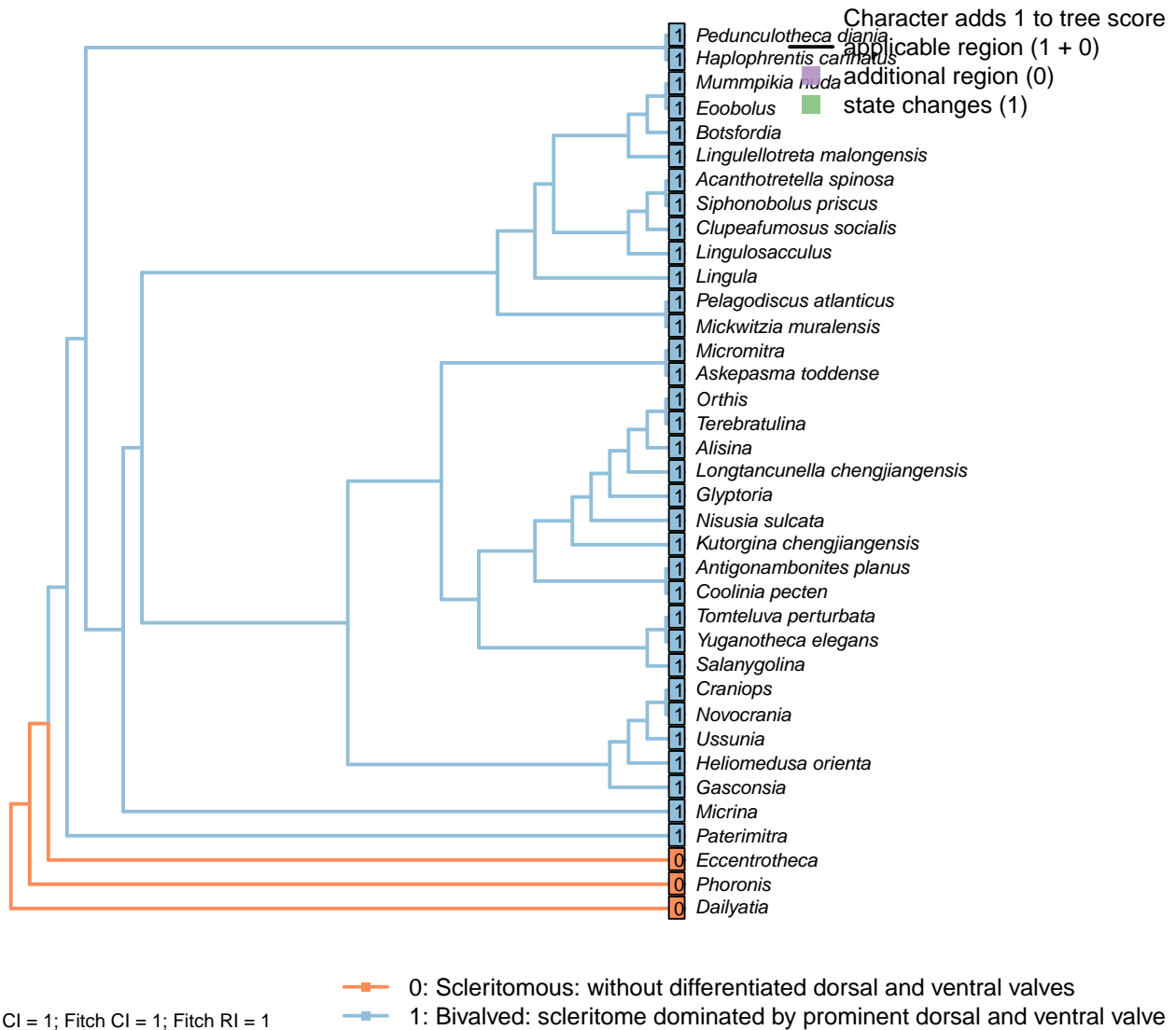
0: Absent

1: Present

Neomorphic character.

Plate-like (wider than tall) skeletal elements, whether mineralized or non-mineralized.  
 The definition deliberately excludes setae (which are taller than wide).

## 3.2 Sclerites: Bivalved [2]

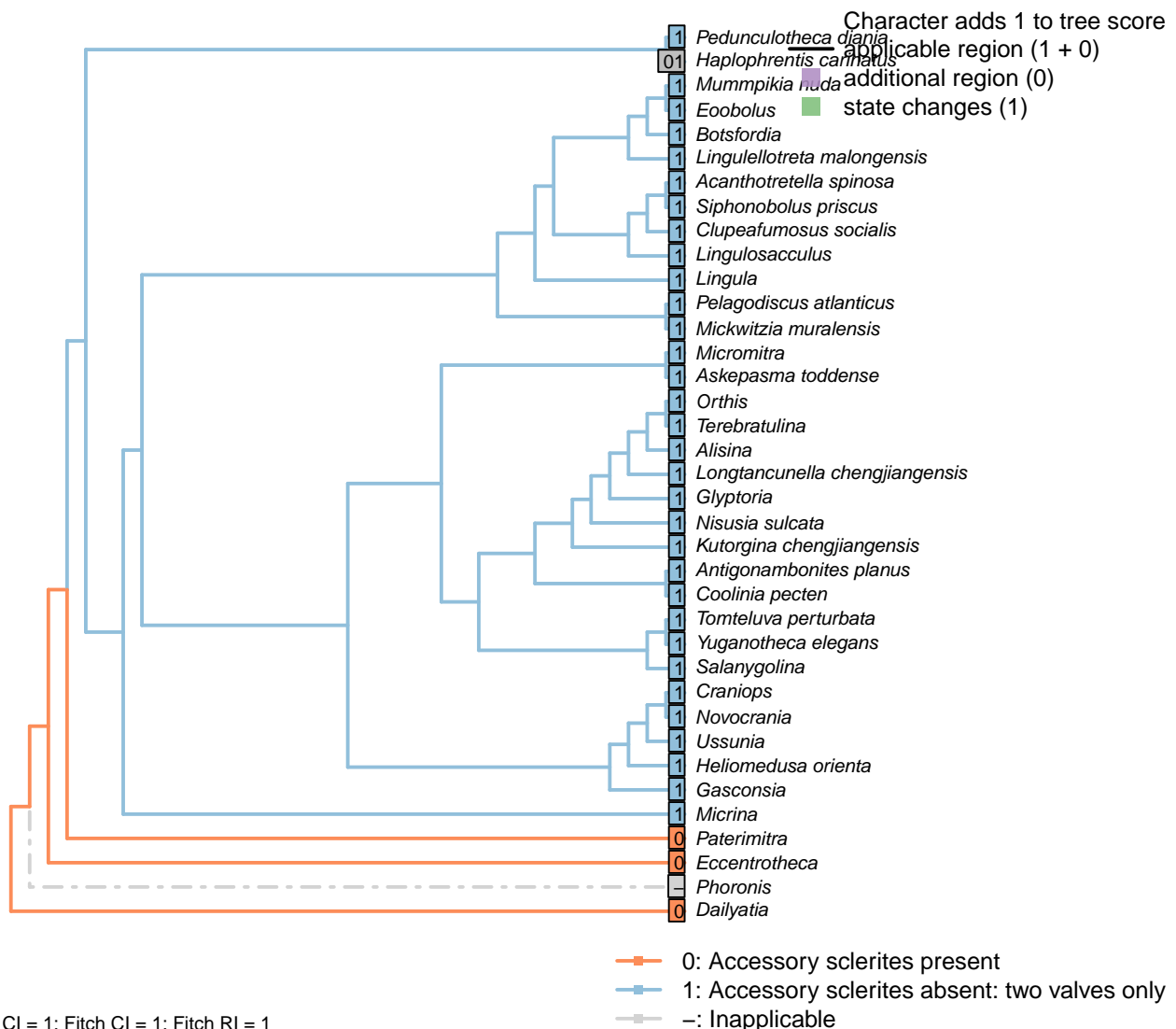


### Character 2: Sclerites: Bivalved

- 0: Scleritomous: without differentiated dorsal and ventral valves  
 1: Bivalved: scleritome dominated by prominent dorsal and ventral valve  
 Neomorphic character.

Scleritome dominated by prominent differentiated dorsal and ventral valves.

### [3] Accessory sclerites reduced



#### Character 3: Sclerites: Bivalved: Accessory sclerites reduced

0: Accessory sclerites present

1: Accessory sclerites absent: two valves only

Neomorphic character.

Taxa in the bivalved condition may retain sclerites as small additional elements, such as the L-elements of *Paterimitra* (Skovsted et al., 2015).

This character is treated as neomorphic, with accessory sclerites ancestrally present, recognizing the likely origin of brachiozoans (and Lophotrochozoans more generally) from a scleritomous organism.

Coded as inapplicable in taxa that lack multiple skeletal elements.

*Haplophrentis carinatus*: Coded as ambiguous to recognize the possibility that helens may correspond to L-elements of *Paterimitra* (Moysiuk et al., 2017).

*Paterimitra*: L-sclerites (Skovsted et al., 2009).

#### [4] Hinge line shape



#### Character 4: Sclerites: Bivalved: Hinge line shape

1: Astrophic

2: Strophic

Transformational character.

*Botsfordia*: Coded as dissociated in Williams *et al.* (1998), appendix 2.

*Craniops*: Astrophic: rounded posterior margin (see fig. 91 in Williams *et al.*, 2000).

*Gasconsia*: The straight posterior margin of *Gasconsia* contributes to an overall resemblance with the Chileids (?).

*Kutorgina chengjiangensis*: Williams *et al.* (2000, p. 208) consider the hinge of *Kutorgina* to be strophic, whereas Bassett *et al.* (2001) argue for an astrophic interpretation – whilst noting that the arrangement is prominently different from other astrophic taxa. We therefore code this taxon as ambiguous.

*Longtancunella chengjiangensis*: “*Longtancunella* has an oval to subcircular shell with a very short strophic

hinge line” – Zhang et al. (2011a).

*Mickwitzia muralensis*: non-strophic.

*Micrina*: See Holmer et al. (2008).

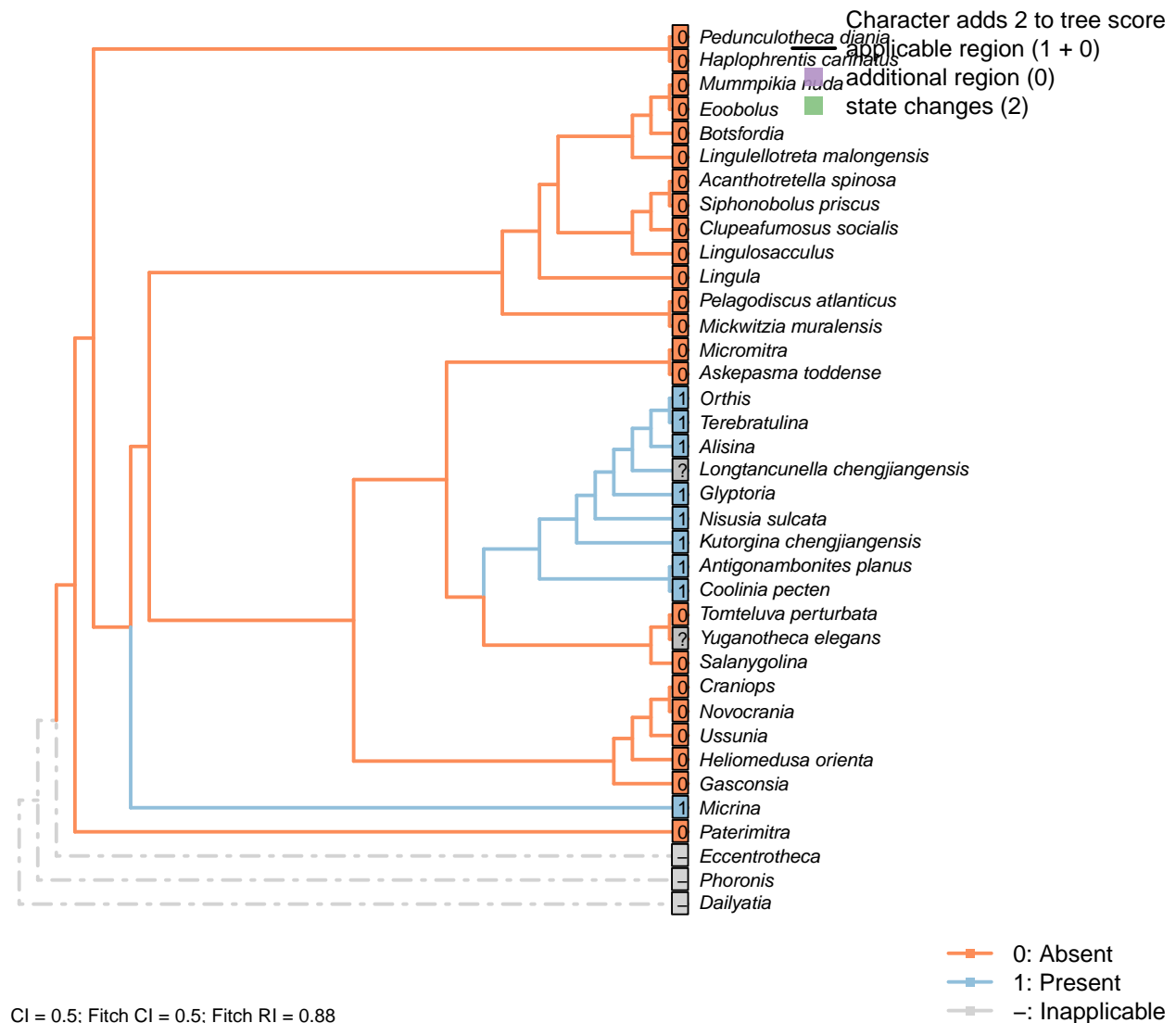
*Nisusia sulcata*: “The strophic, articulated shells of the Kutorginata rotated on simple hinge mechanisms that are different from those of other rhynchonelliforms” (Williams et al., 2000, p. 208).

*Novocrania*: Craniides have a strophic posterior valve edge (Williams et al., 2007, table 39 on p. 2853): *Novocrania*’s “dorsal posterior margin” is “straight” (Williams et al., 2000, p. 171).

*Tomteluva perturbata*: “Tomteluvic taxa all have a strongly ventribiconvex, astrophic shell with a unisulcate commissure” – Streng et al. (2016), p5.

*Yuganotheca elegans*: Not evident from fossil material; the possibility of a short strophic hinge line (as in *Longtancunella*) is difficult to discount.

## [5] Apophyses



0: Absent

1: Present

Neomorphic character.

Many brachiopods, in addition to *Micrina* and others, bear tooth-like structures or processes that articulate the two primary valves.

Caution must be applied before taxa are coded as “absent”, as teeth can be subtle and may be overlooked.

Kutorginata don't have teeth or dental sockets, but their shells are articulated by “two triangular plates formed by dorsal interarea, bearing oblique ridges on the inner sides” (Williams et al., 2000, p. 211); this simple hinge mechanism is different from other rhynchonelliforms (Williams et al., 2000, p.208), but serves an equivalent purpose and is thus potentially homologous. We thus code kutorginids as present, using a subsequent character to capture difference in tooth morphology.

*Alisina*: “Strophic articulation with paired, ventral denticles, composed of secondary shell” – definition of family Trematobolidae in Williams et al. (2000).

*Clupeafumosus socialis*: No articulating processes evident or reported by Topper et al. (2013a).

*Gasconsia*: “Articulatory structure comprising ventral cardinal socket and dorsal hinge plate [...] The shape of the shell probably correlates strongly with the unique type of articulation, which consists of a dorsal hinge plate that fits tightly into a cardinal socket in the ventral valve, with a concave homeodeltidium in the center of the ventral interarea” – Williams et al. (2000), p.184, concerning order Trimerellida.

*Kutorgina chengjiangensis*: “Articulation characterized by two triangular plates formed by dorsal interarea, bearing oblique ridges on the inner sides” – Williams et al. (2000), p. 211.

*Mickwitzia muralensis*: Not reported by or evident in Balthasar (2004).

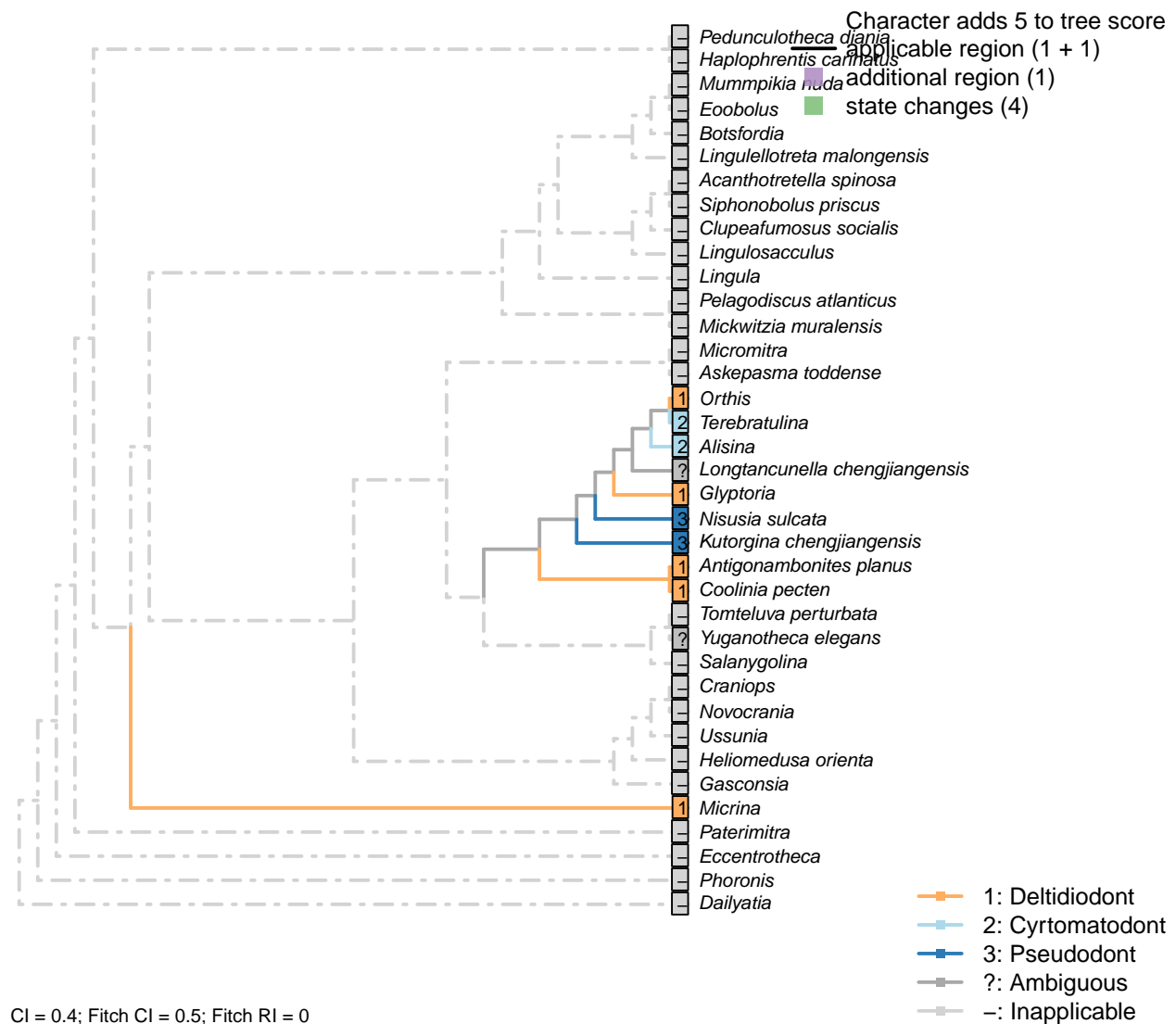
*Mummpikia nuda*: No articulation structures are evident; instead, the propareas are rotated inwards (Balthasar, 2008). The definition of Family Obolellidae in Williams et al. (2000) notes that articulation may be lacking or vestigial in the group.

*Nisusia sulcata*: Pseudodont articulation: teeth formed by distal lateral extensions from the ventral pseudodeltidium – Holmer et al. (2018a).

*Tomteluva perturbata*: Tomteluvids [...] lack articulation structures such as teeth and sockets (Streng et al., 2016).

*Ussunia*: “articulatory structures poorly developed” – Williams et al. (2000), p. 192.

## [6] Apophyses: Morphology



### Character 6: Sclerites: Bivalved: Apophyses: Morphology

- 1: Deltidiodont
- 2: Cyrtomatodont
- 3: Pseudodont
- Transformational character.

Deltidiodont teeth are simple hinge teeth developed by the distal accretion of secondary shell; Cyrtomatodont teeth are knoblike or hook-shaped hinge teeth developed by differential secretion and resorption of the secondary shell (fig. 322 in Williams et al., 2000).

Kutorginata (here represented by *Kutorgina* and *Nisusia*) don't have teeth (apophyses) or dental sockets, but their shells are articulated by "two triangular plates formed by dorsal interarea, bearing oblique ridges on the inner sides" (Williams et al., 2000, p. 211); this simple hinge mechanism is different from other rhynchonelliforms [Williams et al. (2000), p.208; table 13 character 30], and is described as a "pseudodont

articulation" (Holmer et al., 2018a).

*Antigonambonites planus*, *Glyptoria*: Coded as deltidiodont in Benedetto (2009).

*Kutorgina chengjiangensis*: "Articulation characterized by two triangular plates formed by dorsal interarea, bearing oblique ridges on the inner sides" – Williams et al. (2000), p. 211.

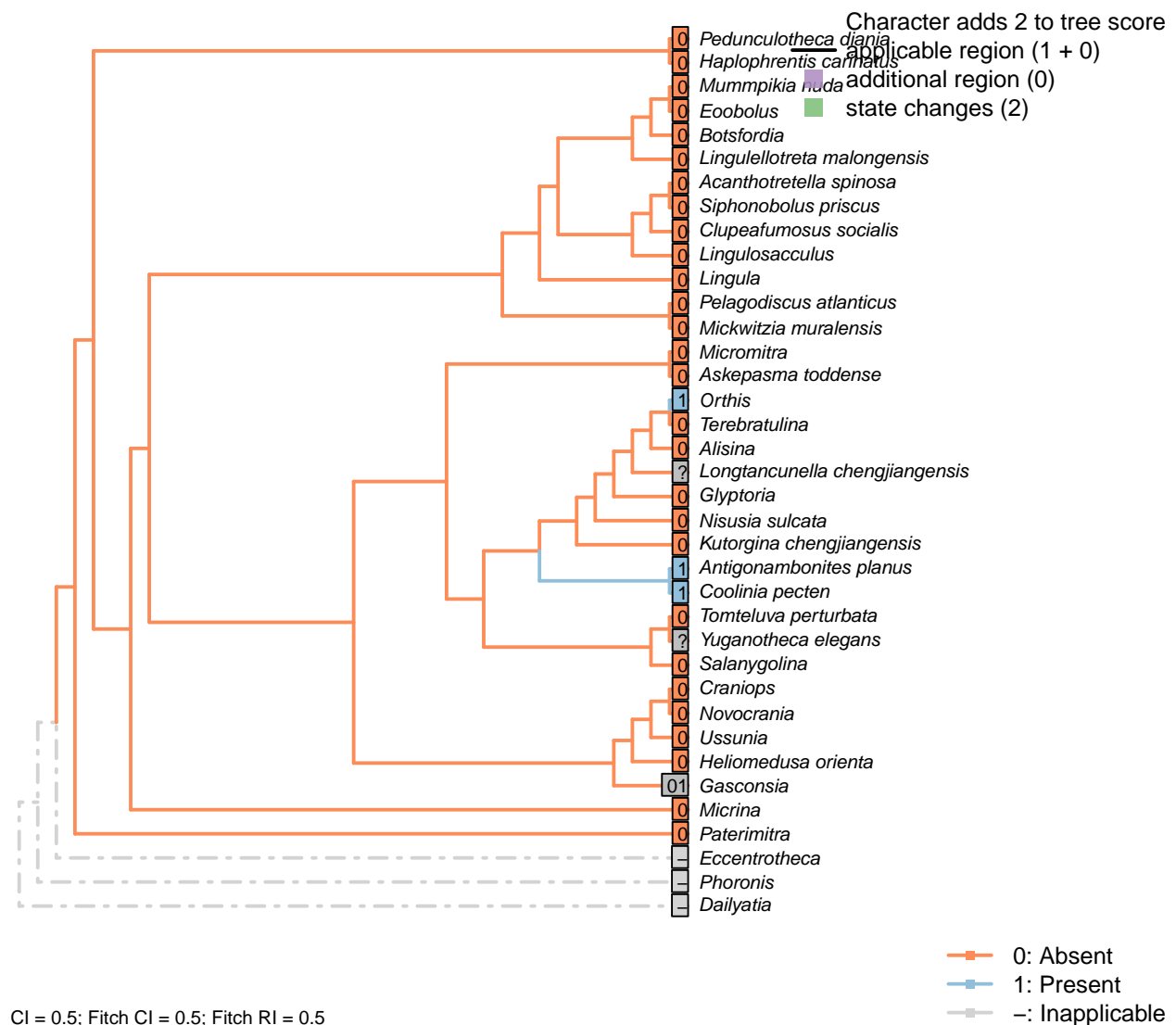
*Micrina*: The simple knob-like teeth of *Micrina* show no evidence of resprobtion or the hook-like shape that characterises Cyrtomatodont teeth.

*Nisusia sulcata*: The 'teeth' are formed by the distal lateral extensions from the ventral pseudodeltidium fitting into the 'sockets' on the inner side of the dorsal interarea (Holmer et al., 2018a). [Coded as "deltidiodont teeth absent" in Benedetto (2009)].

*Orthis*: Coded as deltidiodont (in *Eoorthis*) in Benedetto (2009).

*Terebratulina*: Cyrtomatodont – see fig. 322 in Williams et al. (2000).

## [7] Apophyses: Dental plates



0: Absent

1: Present

Neomorphic character.

Williams et al. (1997) (p362) write: “Teeth [...] are commonly supported by a pair of variably disposed plates also built up exclusively of secondary shell and known as dental plates (Fig. 323.1, 323.3).”

Dewing (2001) elaborates: “Dental plates are near-vertical, narrow sheets of shell tissue between the antero-median edge of the teeth and floor of the ventral valve. They are a composite structure, resulting from the growth of teeth over the ridge that bounds the ventral-valve muscle field.”

Williams et al. (2000) (p.201) write: “The denticles lack supporting structures in all Obolellida, but in Naukatida they are supported by an arcuate plate below the interarea, the anterise (Fig. 119.3a)”.

The anterise is conceivably homologous with the dental plates, thus the presence of either is coded “present” for this character.

*Antigonambonites planus*: Coded as present (well developed) in Benedetto (2009).

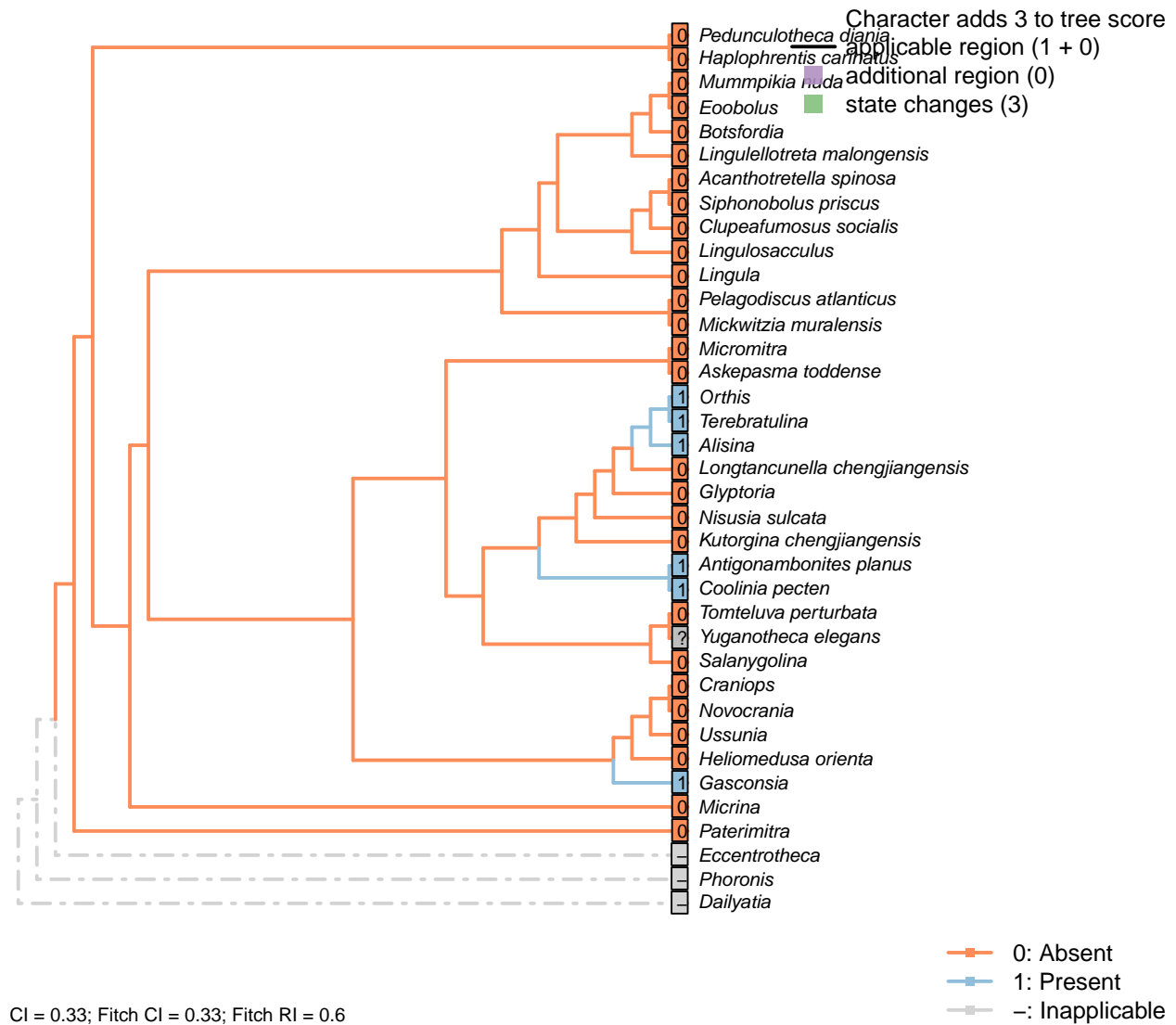
*Coolinia pecten*: Coded as present following Dewing (2001), who seems to use the term Strophomenoids to encompass *Coolinia*, and attests to the presence of dental plates.

*Gasconsia*: Coded ambiguous to reflect the possibility that the hinge plate in trimerellids is homologous to the dental plates of other taxa, and has replaced the teeth themselves as the primary articulatory mechanism (see Williams et al., 2000, p. 184, for details of the articulation).

*Glyptoria, Nisusia sulcata*: Coded as absent in Benedetto (2009).

*Orthis*: Coded as present (short and recessive, in *Eoorthis*) in Benedetto (2009).

## [8] Sockets



### Character 8: Sclerites: Bivalved: Sockets

0: Absent

1: Present

Neomorphic character.

Simplified from Bassett *et al.* (2001) character 16.

This character is independent of apophyses, as several taxa bear sockets without corresponding teeth; the function of these sockets is unknown.

See figs 323ff in Williams *et al.* (1997).

*Alisina*: “bearing sockets, bounded by low ridges” – Williams *et al.* (2000).

*Antigonambonites planus*: Coded as present in Benedetto (2009).

*Gasconsia*: “Articulatory structure comprising ventral cardinal socket and dorsal hinge plate” – Williams

et al. (2000), p. 184.

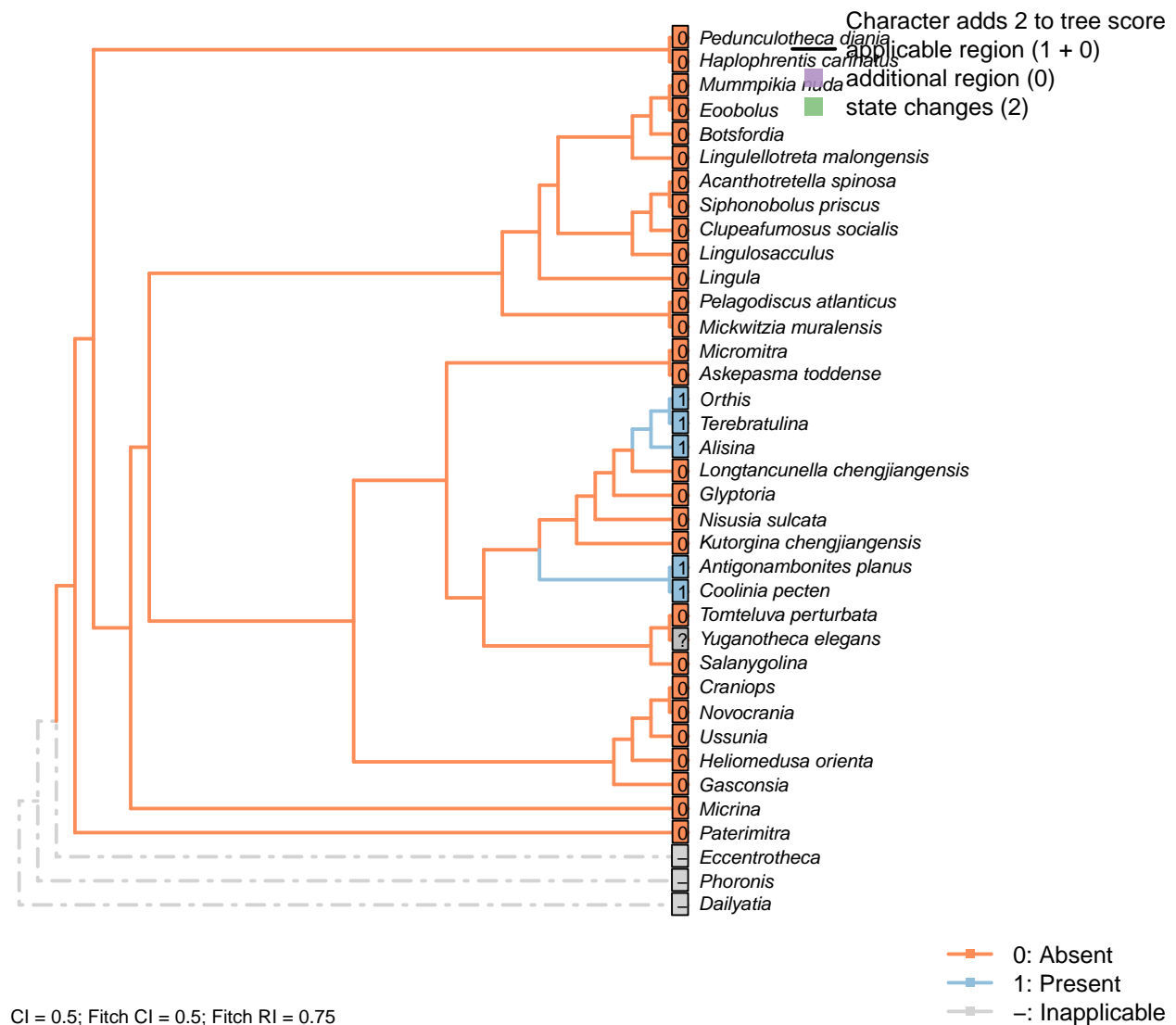
*Glyptoria, Nisusia sulcata*: Coded as absent in Benedetto (2009).

*Mickwitzia muralensis*: Not reported by or evident in Balthasar (2004).

*Tomteluva perturbata*: Tomteluvids [...] lack articulation structures such as teeth and sockets (Streng et al., 2016).

*Ussunia*: Following table 15 in Williams et al. (2000).

## [9] Socket ridges



### Character 9: Sclerites: Bivalved: Socket ridges

0: Absent

1: Present

Neomorphic character.

After Bassett *et al.* (2001) character 17. May be difficult to distinguish from a brachiophore (see Fig 323 in Williams *et al.*, 1997), so the two structures are not distinguished here.

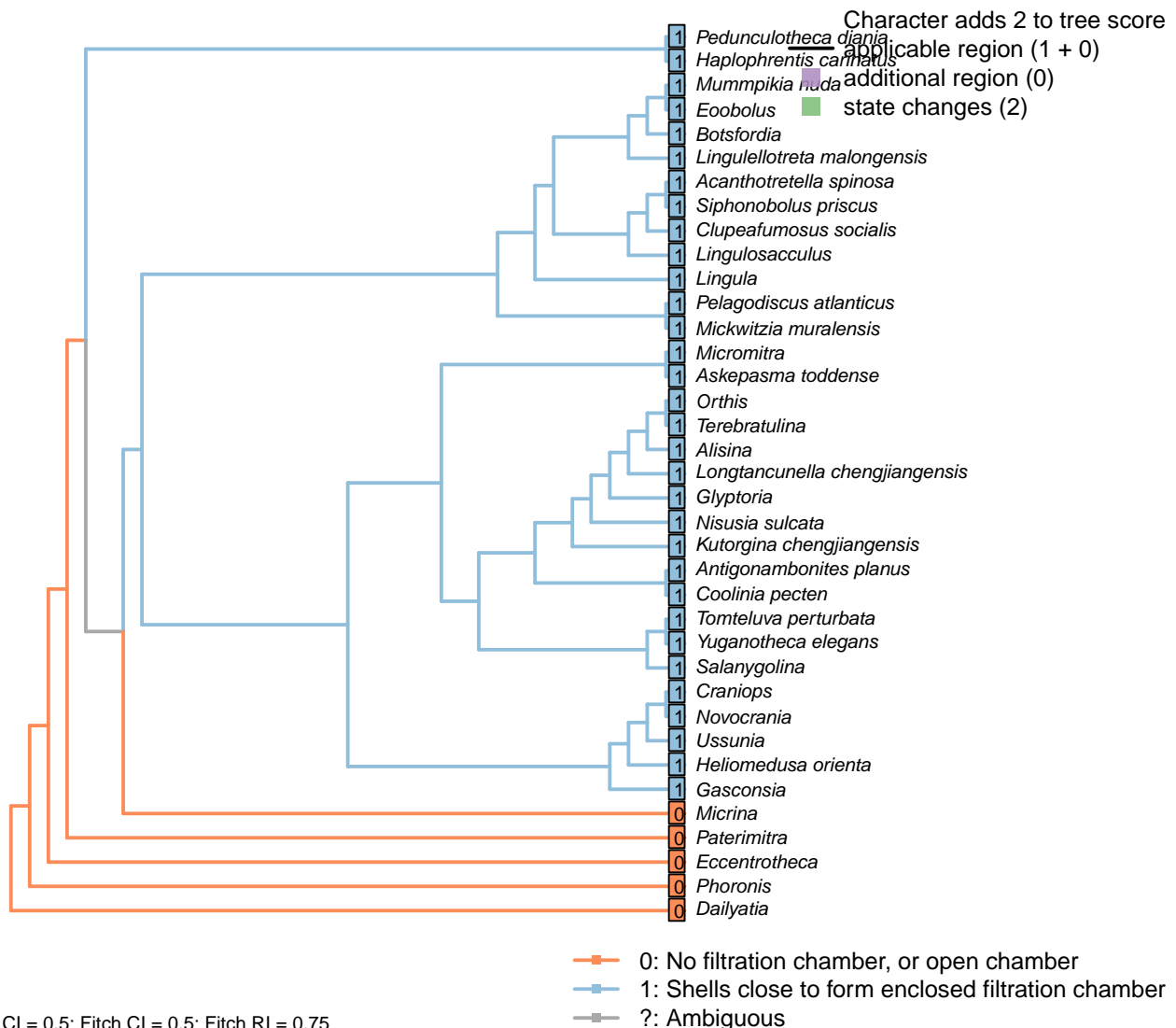
*Alisina*: “bearing sockets, bounded by low ridges” – Williams *et al.* (2000).

*Antigonambonites planus*: Coded as present in Benedetto (2009).

*Glyptoria*, *Nisusia sulcata*: Coded as absent in Benedetto (2009).

*Tomteluva perturbata*: Tomteluvids [...] lack articulation structures such as teeth and sockets (Streng *et al.*, 2016).

## [10] Enclosing filtration chamber



### Character 10: Sclerites: Bivalved: Enclosing filtration chamber

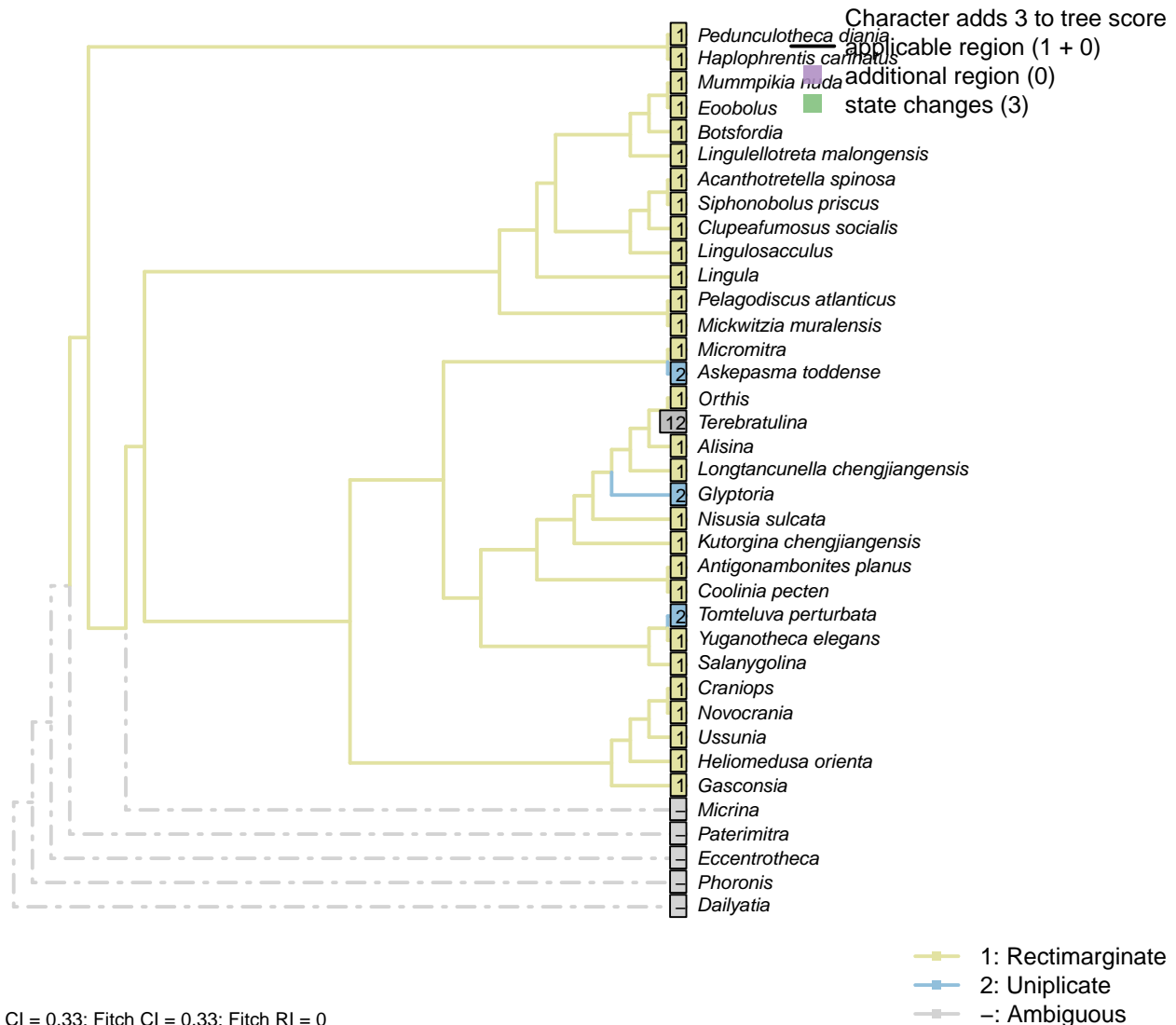
0: No filtration chamber, or open chamber

1: Shells close to form enclosed filtration chamber

Neomorphic character.

In crown-group brachiopods, the two primary shells close to form an enclosed filtration chamber. Further down the stem, taxa such as *Micrina* do not.

### [11] Commissure



#### Character 11: Sclerites: Bivalved: Commissure

- 1: Rectimarginate
  - 2: Uniplicate
  - 3: Sulcate
- Transformational character.

The anterior commissure can be rectimarginate (i.e. straight), uniplicate (i.e. median sulcus in ventral valve), or sulcate (with median sulcus in dorsal valve).

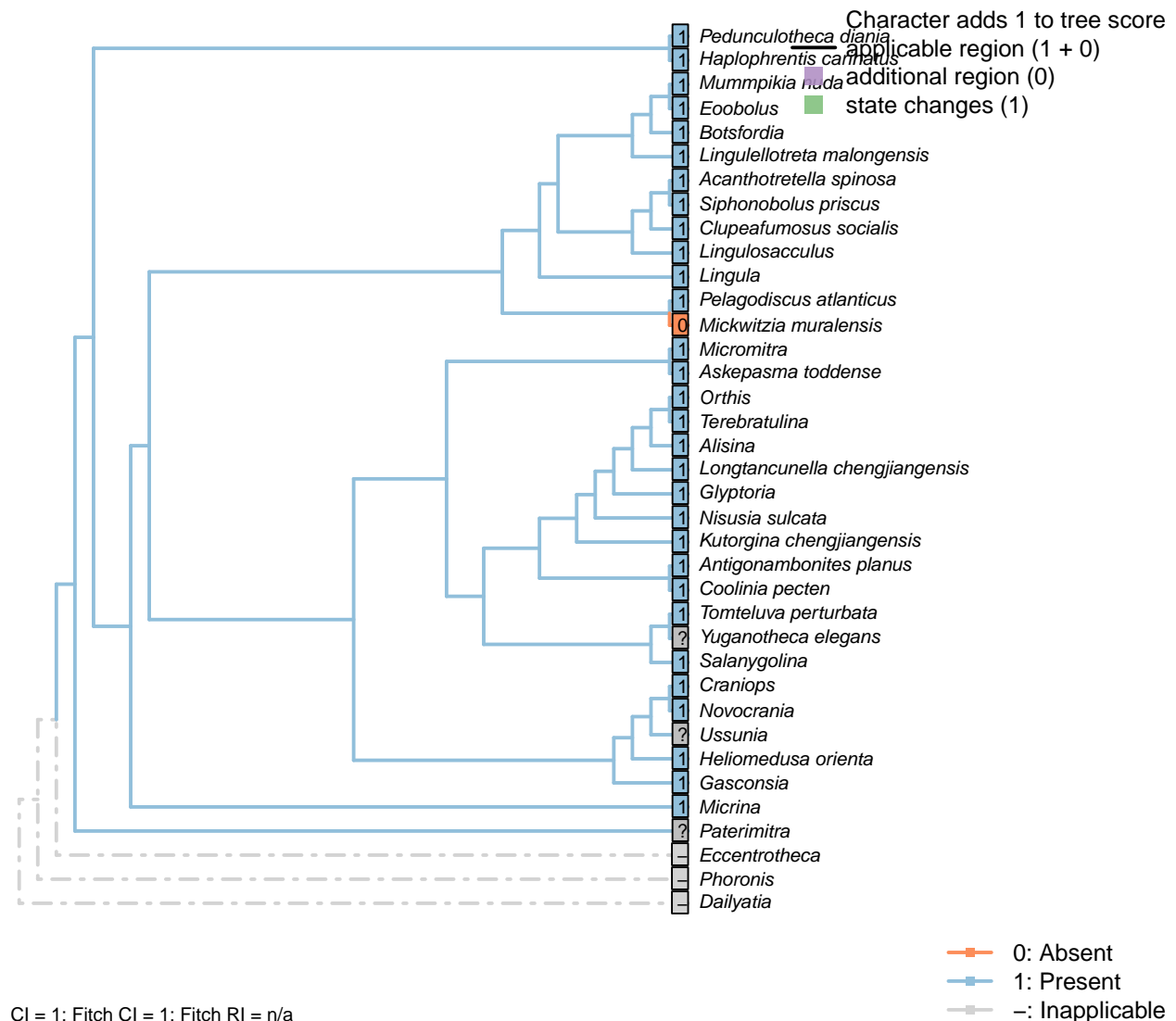
*Askepasma toddense*: “ventral valve weakly to moderately sulcate” (Topper et al., 2013b); a similar description is provided by Williams et al. (2000).

*Glyptoria*, *Kutorgina chengjiangensis*, *Micromitra*, *Salanygolina*: Following appendix 2 in Williams et al.

(1998).

*Terebratulina*: “Anterior commissure rectimarginate to uniplicate” – uniplicate in fig. 1425.1c of Williams *et al.* (2006).

## [12] Muscle scars: Ventral



### Character 12: Sclerites: Bivalved: Muscle scars: Ventral

0: Absent

1: Present

Neomorphic character.

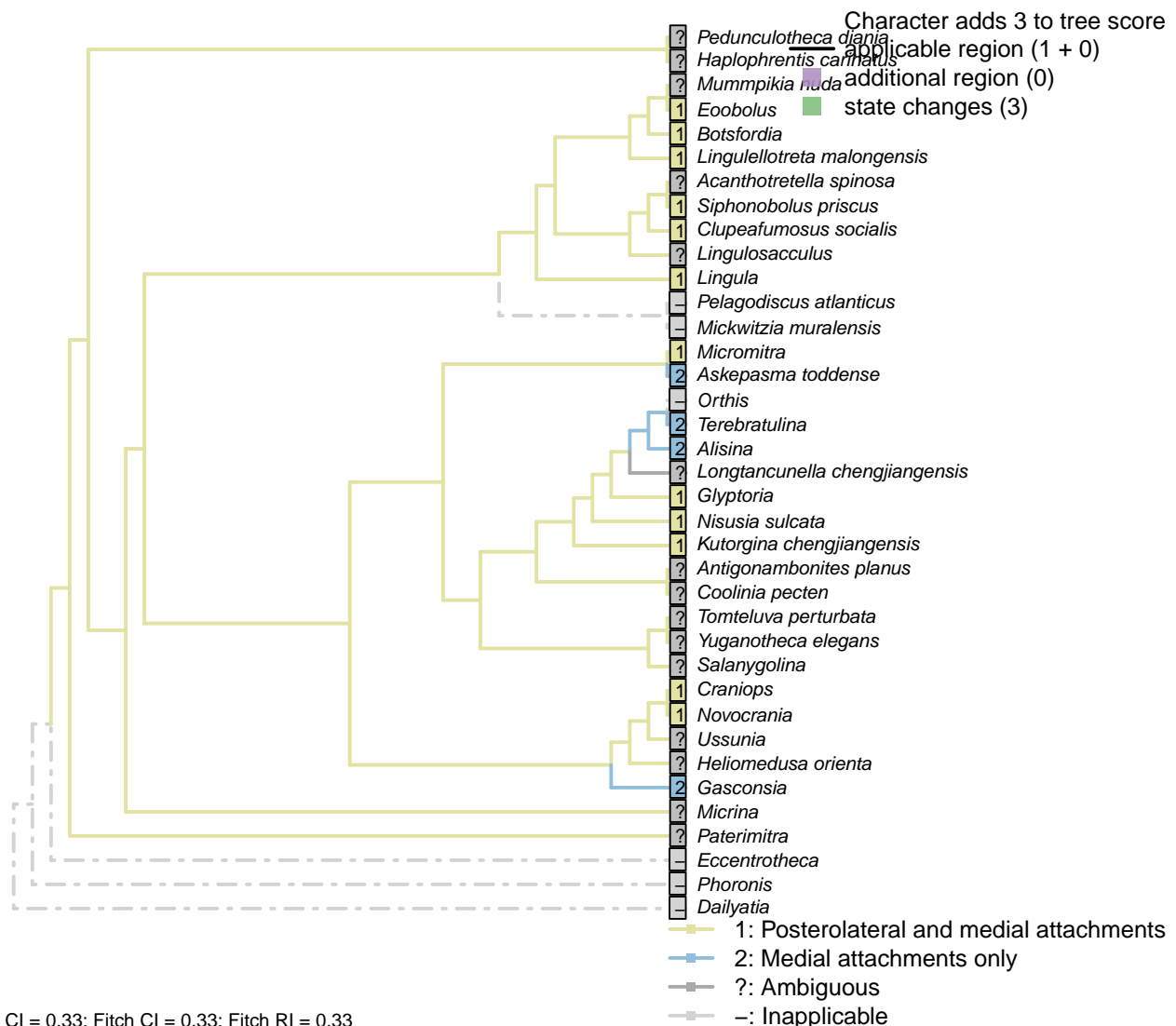
After Bassett *et al.* (2001) character 6.

*Alisina*: Muscle scars scored based on *Alisina comleyensis* (Bassett *et al.*, 2001).

*Mickwitzia muralensis*: Scars absent; instead, cones ornament shell's internal surface.

*Micrina*: Prominent ventral muscle scars – see e.g. Holmer *et al.* (2008), fig. 1f.

## [13] Muscle scars: Ventral: Position

**Character 13: Sclerites: Bivalved: Muscle scars: Ventral: Position**

1: Posterolateral and medial attachments

2: Medial attachments only

Transformational character.

Muscles can attach to the ventral valve posterolaterally to, as well as between, the *vascula lateralia* (Popov, 1992).

*Acanthotretella spinosa*: "Individual muscle scars cannot be distinguished" – Holmer and Caron (2006).

*Alisina*: Following reconstruction of Gorjansky & Popov (1986).

*Askepasma toddense*: Restricted to medial field, following the interpretation of the musculature presented by

Williams *et al.* (2000), fig. 81.

*Clupeafumosus socialis*: Coded following *Hadrotreta*, as illustrated in Popov (1992).

*Craniops*: See fig. 89 in Williams *et al.* (2000).

*Eoobolus*: The ‘laterals’ of Balthasar (2009, fig. 5) are situated almost upon the *vascula lateralia*; they are interpreted as sitting posterolateral to them.

*Gasconsia*: Musculature described in Hanken & Harper (1985).

*Glyptoria*: Posterolateral reflected by diductor attachments; see fig. 18.3.2 in Bassett *et al.* (2001).

*Kutorgina chengjiangensis*: Following situation in *Nisusia*; see fig. 18.2 in Bassett *et al.* (2001).

*Lingulellotreta malongensis*: See fig. 5 in Holmer *et al.* (1997).

*Micromitra*: Posteriomedial muscle field (Williams *et al.*, 1998, text-fig. 6) treated as equivalent to posterolateral muscles.

*Nisusia sulcata*: Posterolateral diductors (fig. 18.2 in Bassett *et al.*, 2001).

*Novocrania*: Posterior adductor muscles attach posterolaterally to ventral mantle canal (Robinson, 2014).

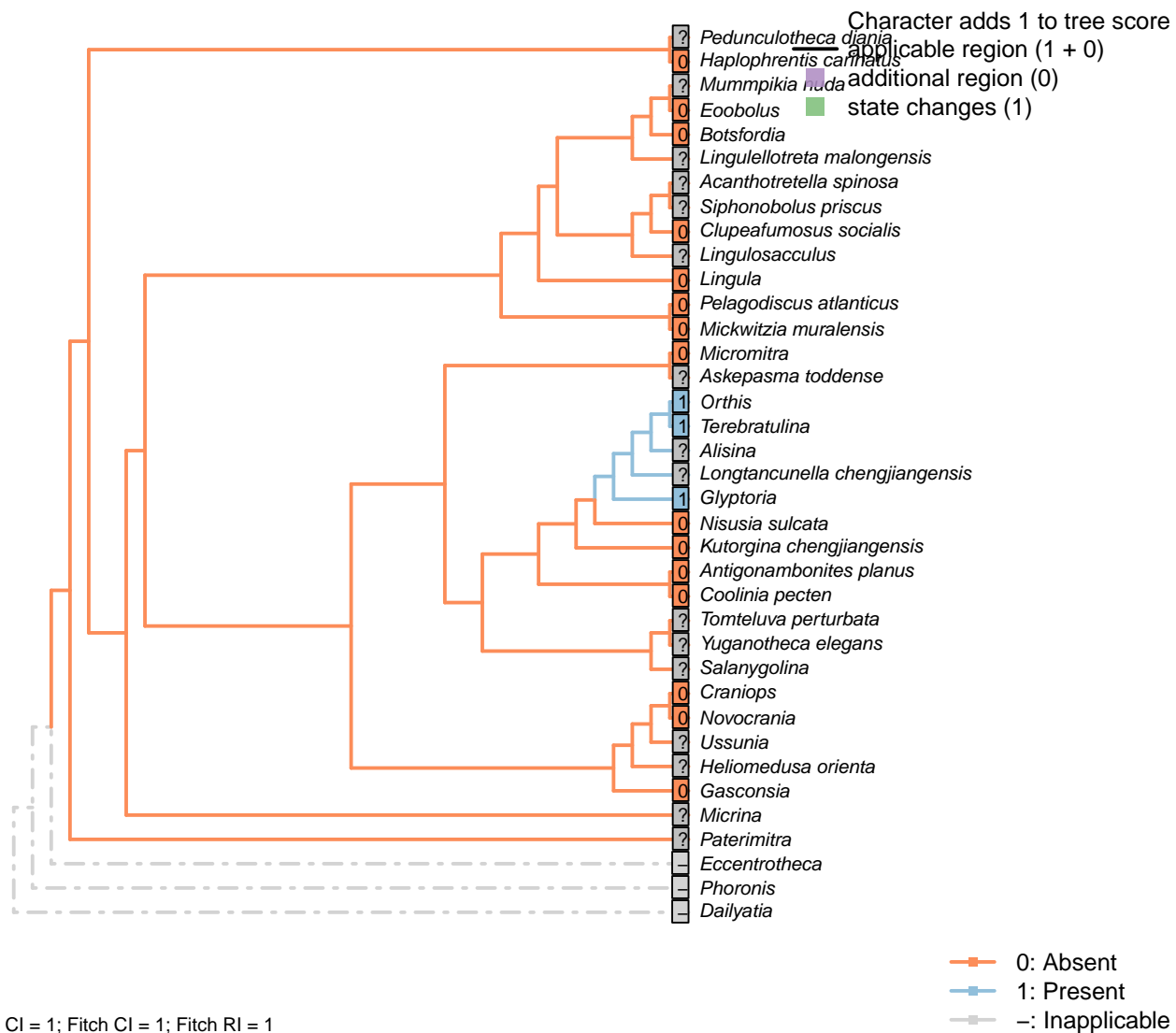
*Orthis*: Not applicable: *vascula lateralia* not comparable to those of other taxa.

*Pelagodiscus atlanticus*: Inapplicable as vascular system not directly equivalent to the canonical; see. fig 6b in Balthasar (2009).

*Salanygolina*: Ventral musculature not clearly constrained (Holmer *et al.*, 2009).

*Siphonobolus priscus*: Coded following general siphonotretid condition described by Popov (1992, p. 407).

## [14] Muscle scars: Adjustor

**Character 14: Sclerites: Bivalved: Muscle scars: Adjustor**

0: Absent

1: Present

Neomorphic character.

After Bassett *et al.* (2001) character 7.

This character is contingent on the presence of a pedicle. Extreme caution must be used in inferring an absent state, as adjustor scars can be extremely difficult to distinguish from the adductor scars.

*Alisina*: Muscle scars scored based on *Alisina comleyensis* (Bassett *et al.*, 2001). The presence of an adjustor is marked as not presently available, as it is not clear that a scar, if present, could be distinguished from the diminutive muscle scars present.

*Askepasma toddense*: Following the interpretation of the musculature presented by Williams *et al.* (2000),

fig. 81.

*Botsfordia*: Not described in Popov (1992).

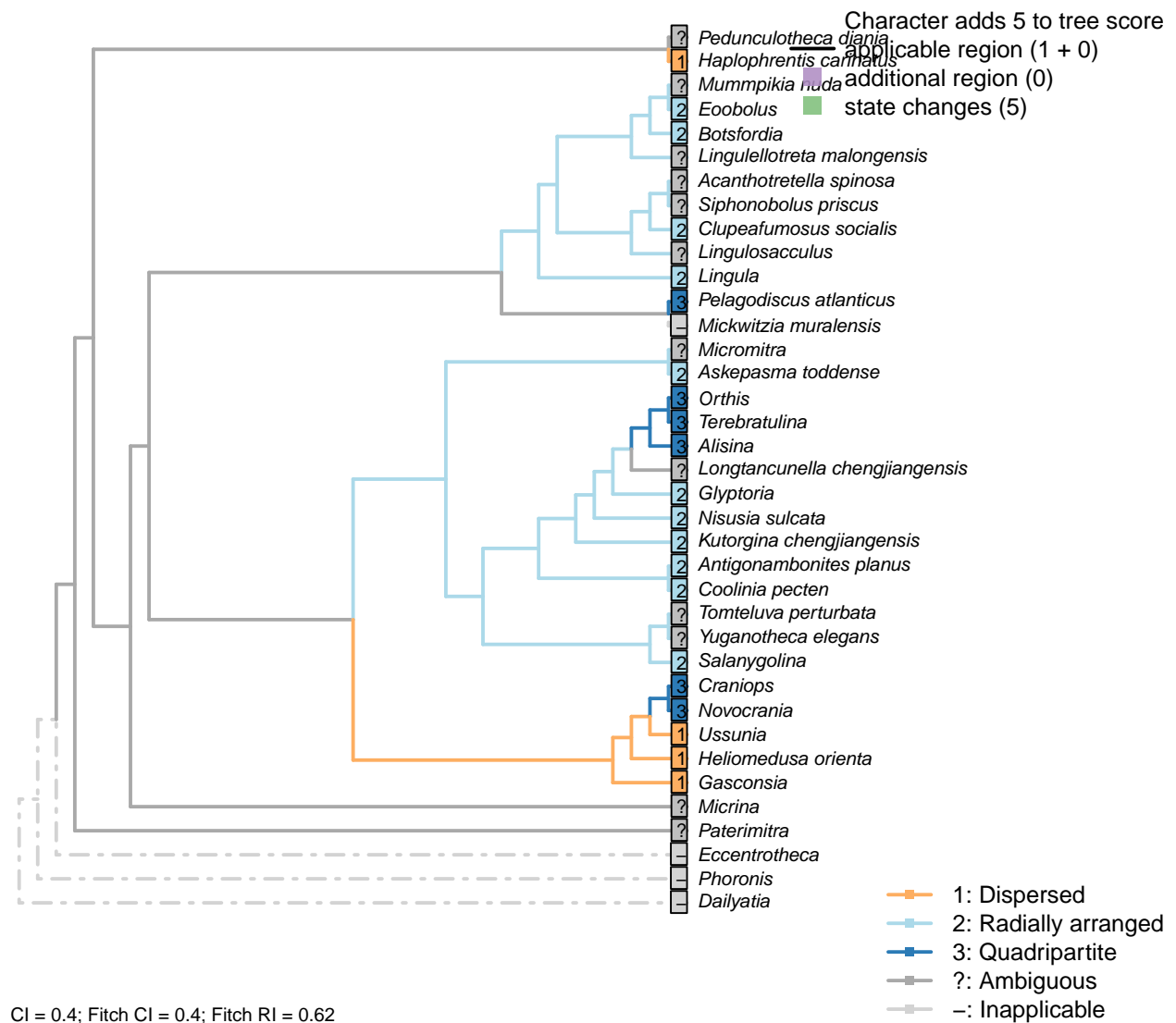
*Clupeafumosus socialis*: Not known in any acrotretid (Williams et al., 2000); not evident in *Clupeafumosus* (Topper et al., 2013a).

*Gasconsia*: No mention of an adjustor muscle in *Gasconsia* or Trimerellida more generally on pp. 184–185 of Williams et al. (2000), nor in discussion in Williams et al. (2007) (p. 2850). Coded as absent.

*Mickwitzia muralensis*: Scars absent; instead, cones ornament shell's internal surface.

*Siphonobolus priscus*: Ventral musculature poorly constrained (Williams et al., 2000; Popov et al., 2009).

## [15] Muscle scars: Dorsal adductors



### Character 15: Sclerites: Bivalved: Muscle scars: Dorsal adductors

1: Dispersed

2: Radially arranged

3: Quadripartite  
Transformational character.

After Bassett *et al.* (2001) character 8, and Williams *et al.* [Williams *et al.* (1996), character 35; 2000, p. 160, character 54]

In the dorsal valve, the anterior and posterior adductor scars of articulated brachiopods form a single (quadripartite) muscle field (Williams *et al.*, 2000, p. 201)

In contrast, the anterior and posterior scars of e.g. trimerellids have prominently separate attachment points, with anterior and posterior muscle fields clearly distinct, and coded as “dispersed”.

In e.g. kutorginates, adductor muscles are separated into left and right fields; the same is the case in lingulids, where there are more separate muscle groups and the left and right fields conspire to produce a radial arrangement; both of these configurations are scored as “radially arranged”.

*Alisina*: Following Williams *et al.* (2000) table 15 (their character 54).

*Antigonambonites planus*: Treatise.

*Askepasma toddense*: Separate left and right fields, so radially arranged – following the interpretation of the musculature presented by Williams *et al.* (2000), fig. 81.

*Botsfordia*: Following Williams *et al.* (1998), appendix 2.

*Clupeafumosus socialis*: Following reconstruction of *Hadrotreta* by Williams (2000), fig. 51, which exhibits distinct left and right fields.

*Coolinia pecten*: “radially arranged adductor scars” – Bassett and Popov (2017), p1.

*Gasconsia*: Following the coding of Williams *et al.* (2000), table 15.

*Glyptoria*: Scored as “dispersed” by Williams *et al.* (1998) ... but then so is *Kutorgina*, which Bassett *et al.* (2001) score as radial.

Williams *et al.* (2000) state, for superfamily Protorthida, “dorsal adductor scars probably linear”, which fits in the category of “radial” employed herein – so that’s what we follow.

*Haplophrentis carinatus*: Laterally dispersed, based on interpretation of Moysiuk *et al.* (2017), and consistent with general situation in hyoliths (see Dzik, 1980).

*Heliomedusa orienta*: Distinct anterior and posterior fields (Chen *et al.*, 2007); coded as “dispersed” by Williams *et al.* (2000) in table 15.

*Mickwitzia muralensis*: Scars absent; instead, cones ornament shell’s internal surface.

*Micromitra*: Williams *et al.* (1998) code as “dispersed”, but have a less divided scheme of character states and disagree with other sources in some codings (e.g. Bassett *et al.*, 2001, in Kutorginates). Williams *et al.* (2000) do not describe *Micromitra* musculature and we were unable to find any reliable description of the scars, so we code as “not presently available”.

*Novocrania*: Craniids scored as “open, quadripartite” by Williams *et al.* (1996).

*Pelagodiscus atlanticus*: Discinids scored as “open, quadripartite” by Williams *et al.* (1996).

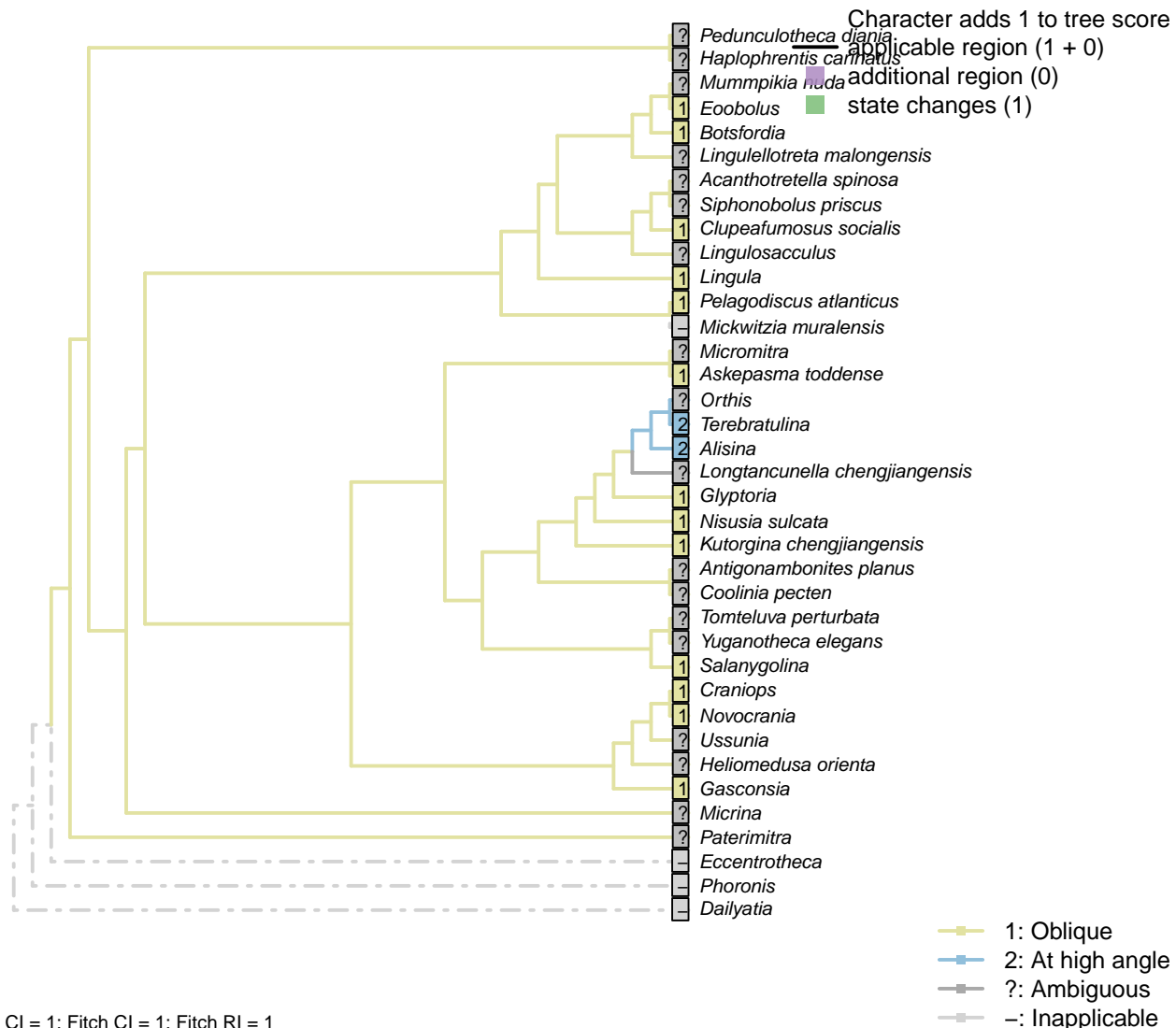
*Salanygolina*: “The dorsal valve of *Salanygolina* has a radial arrangement of adductor muscle scars and the scars of posteromedially placed internal oblique muscles, which are also characteristic of paterinates and chileates” – Holmer *et al.* (2009).

*Siphonobolus priscus*: Ventral musculature poorly constrained (Williams *et al.*, 2000; Popov *et al.*, 2009).

*Terebratulina*: Coded as “grouped, quadripartite” by Williams *et al.* (1996).

*Ussunia*: Following table 15 in Williams *et al.* (2000).

## [16] Muscle scars: Adductors: Position



### Character 16: Sclerites: Bivalved: Muscle scars: Adductors: Position

1: Oblique

2: At high angle

Transformational character.

Position of adductor muscles relative to commissural plane.

After Bassett *et al.* (2001) character 11.

*Askepasma toddense*: Following the interpretation of the musculature presented by Williams *et al.* (2000), fig. 81.

*Botsfordia*: Following description of Popov (1992).

*Coolinia pecten*: Not reported by Williams *et al.* (2000), nor Bassett & Popov (2017), nor explicitly by Dewing (2001).

*Eoobolus*: “*Eoobolus* should have anterior and posterior adductors and a variety of oblique muscles which

were probably arranged in criss-crossing pairs" – Balthasar (2009).

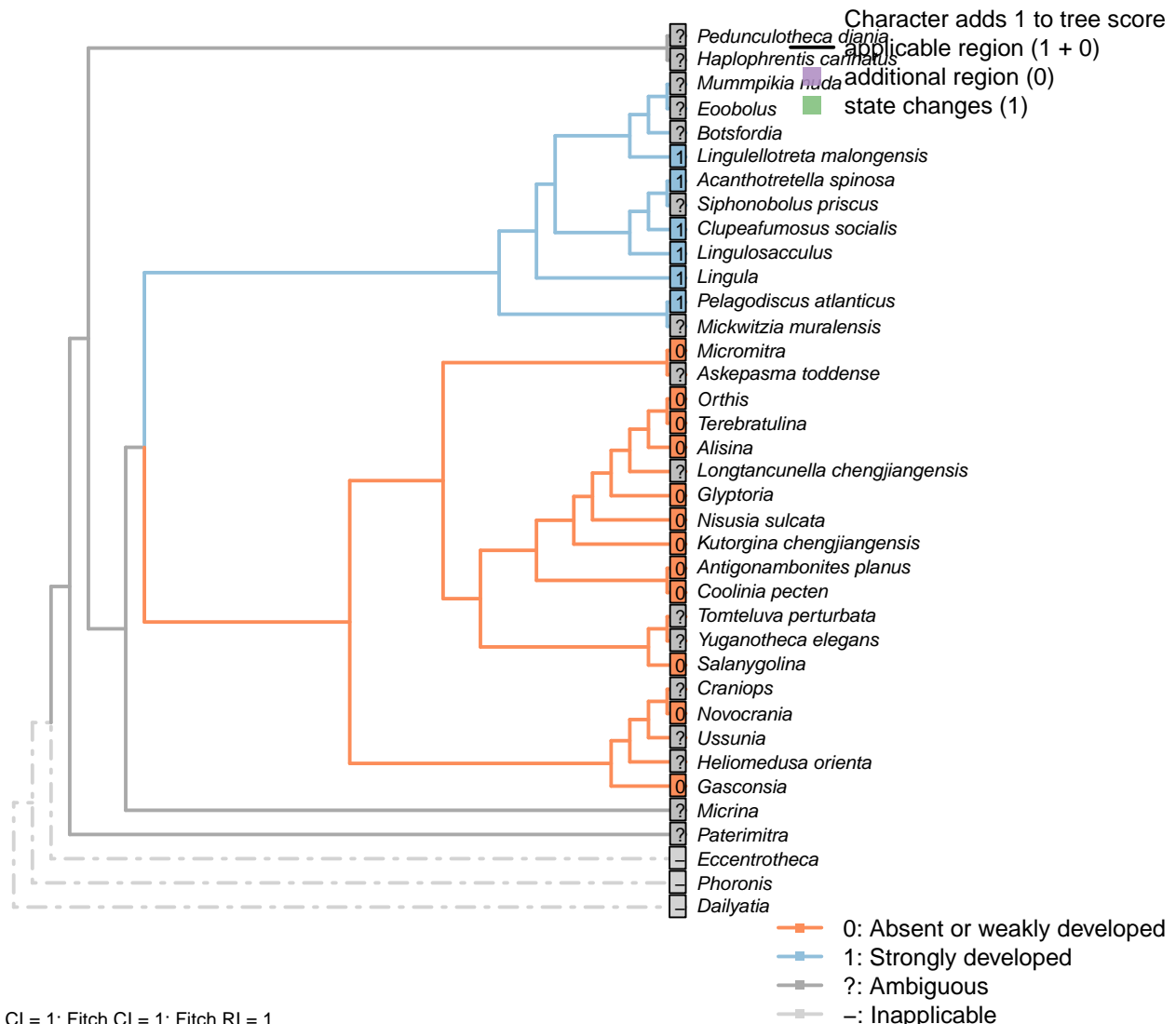
*Gasconsia*: See discussion under Trimerellida in Williams *et al.* (2000).

*Mickwitzia muralensis*: Scars absent; instead, cones ornament shell's internal surface.

*Pelagodiscus atlanticus*: Musculature considered essentially equivalent to *Lingula* by Williams *et al.* (2000), so *Lingula* coding followed here.

*Siphonobolus priscus*: Ventral musculature poorly constrained (Williams *et al.*, 2000; Popov *et al.*, 2009).

## [17] Muscle scars: Dermal muscles



### Character 17: Sclerites: Bivalved: Muscle scars: Dermal muscles

0: Absent or weakly developed

1: Strongly developed

Neomorphic character.

Based on character 11 in Zhang *et al.* (2014).

Well developed dermal muscles present in the body wall of recent lingulates, which are absent in all calcareous-

shelled brachiopods. These muscles are responsible for the hydraulic shell-opening mechanism, and possibly present in all organophosphatic-shelled brachiopods, with the possible exception of the paterinates (Williams et al., 2000, p. 32).

*Alisina, Antigonambonites planus, Gasconsia, Glyptoria, Nisusia sulcata, Orthis, Salanygolina:* According to the statement of Williams et al. (2000, p. 32) that these muscle are absent in all carbonate- shelled brachiopods.

*Askepasma tiddense:* According to the statement of Williams et al. (2000, p. 32) that the presence of these muscles in paterinates is uncertain.

*Botsfordia:* Implicitly taken as present in Popov (1992), though not marked in diagrams – suggesting not strongly developed.

*Clupeafumosus socialis:* This character is coded based on the score of Acrotreta in Zhang et al. (2014), and statement in Williams et al. (2000, P.32).

*Coolinia pecten:* According to the statement of Williams et al. (2000, p. 32) that these muscle are absent in all carbonate-shelled brachiopods.

*Eoobolus:* Not remarked upon by Balthasar (2009).

*Kutorgina chengjiangensis:* According to the statement of Williams et al. (2000, p. 32) that these muscle are absent in all carbonate- shelled brachiopods, and the coding for kutorginids in Zhang et al. (2014).

*Micromitra:* Williams et al. (2000, p. 32) are uncertain about the presence of these muscles in the paterinates. Zhang et al. (2014) code absence in Paterinida, but without specifying evidence; we follow their coding here.

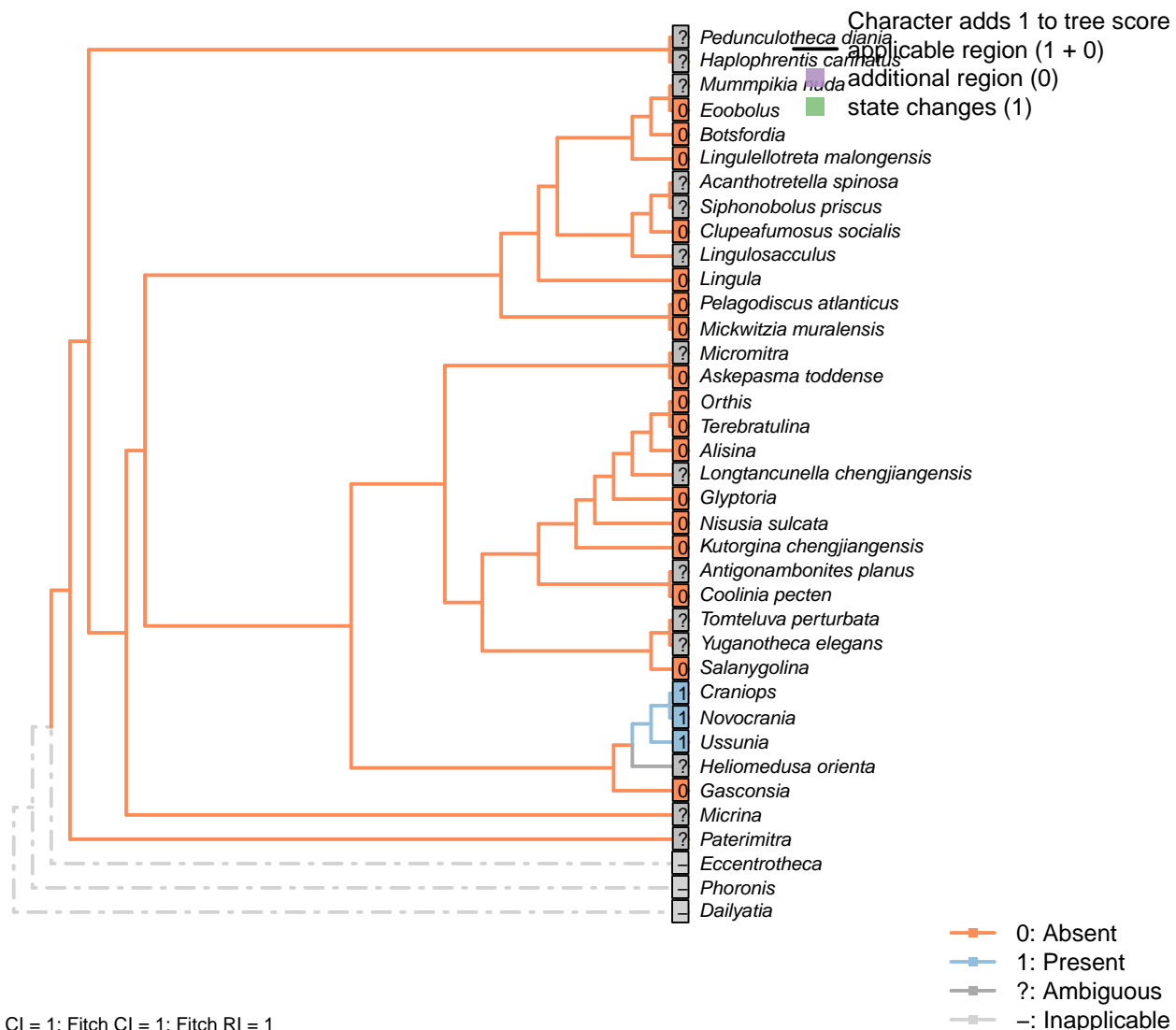
*Mummpikia nuda, Tomteluva perturbata:* Though Williams et al. (2000, p. 32) state that these muscles are absent in all carbonate-shelled brachiopods, their existence cannot be discounted with certainty in this taxon, which is therefore coded not presently available.

*Novocrania:* Following Zhang et al. (2014), and the statement of Williams et al. (2000) that such muscles are absent in all calcite-shelled brachiopods.

*Pelagodiscus atlanticus:* Musculature considered essentially equivalent to *Lingula* by Williams et al. (2000), so *Lingula* coding followed here.

*Siphonobolus priscus:* Ventral musculature poorly constrained (Williams et al., 2000; Popov et al., 2009).

*Terebratulina:* Williams et al. (2000, p. 32) state that these muscles are absent in all carbonate-shelled brachiopods.

[18] Muscle scars: Unpaired median (*levator ani*)**Character 18: Sclerites: Bivalved: Muscle scars: Unpaired median (*levator ani*)**

0: Absent

1: Present

Neomorphic character.

The *levator ani* is a diminutive unpaired medial muscle found in certain calcitic brachiopods [Williams et al. (2000); see fig. 89, character 34 in table 13].

*Alisina*, *Kutorgina chengjiangensis*, *Nisusia sulcata*: Following table 13 in Williams et al. (2000).

*Coolinia pecten*: Not reported in Dewing (2001).

*Craniops*: See fig. 90 in Williams et al. (2000).

*Gasconsia*: Williams et al. (2000) code an unpaired medial muscle scar as present in their table 13, but give no reference for this coding, which perhaps arises from their interpretation of the taxon as a trimerellid. Hanken and Harper (1985, p. 249 and text-fig. 2) explicitly identify a pair of central muscles, so we code a

*levator ani* as absent.

*Heliomedusa orienta*: Poor preservation of minor muscle scars noted by Chen *et al.* (2007).

*Mickwitzia muralensis*: Scars absent; instead, cones ornament shell's internal surface.

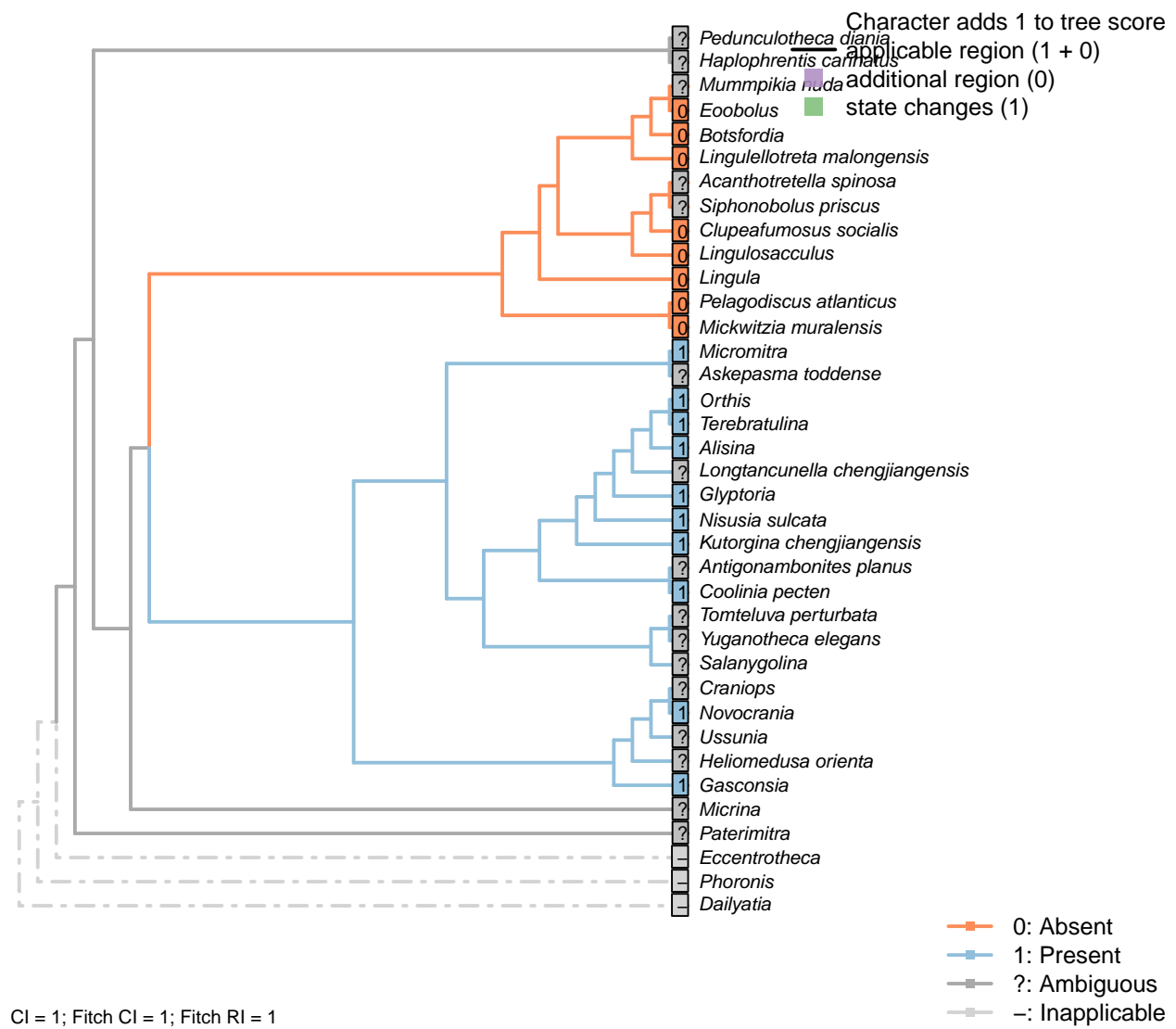
*Novocrania*: Following table 13 in Williams *et al.* (2000) (for *Novocrania*).

*Pelagodiscus atlanticus*: Musculature considered essentially equivalent to *Lingula* by Williams *et al.* (2000), so *Lingula* coding followed here.

*Siphonobolus priscus*: Ventral musculature poorly constrained (Williams *et al.*, 2000; Popov *et al.*, 2009).

*Ussunia*: Following table 15 in Williams *et al.* (2000).

## [19] Muscle scars: Dorsal diductor



CI = 1; Fitch CI = 1; Fitch RI = 1

### Character 19: Sclerites: Bivalved: Muscle scars: Dorsal diductor

0: Absent

1: Present

Neomorphic character.

After Bassett *et al.* (2001) character 9.

*Acanthotretella spinosa*: Not observable in *Acanthotretella* itself, so coded as ambiguous – though it is likely based on the anticipated phylogenetic affinities of *Acanthotretella* that the muscles are absent.

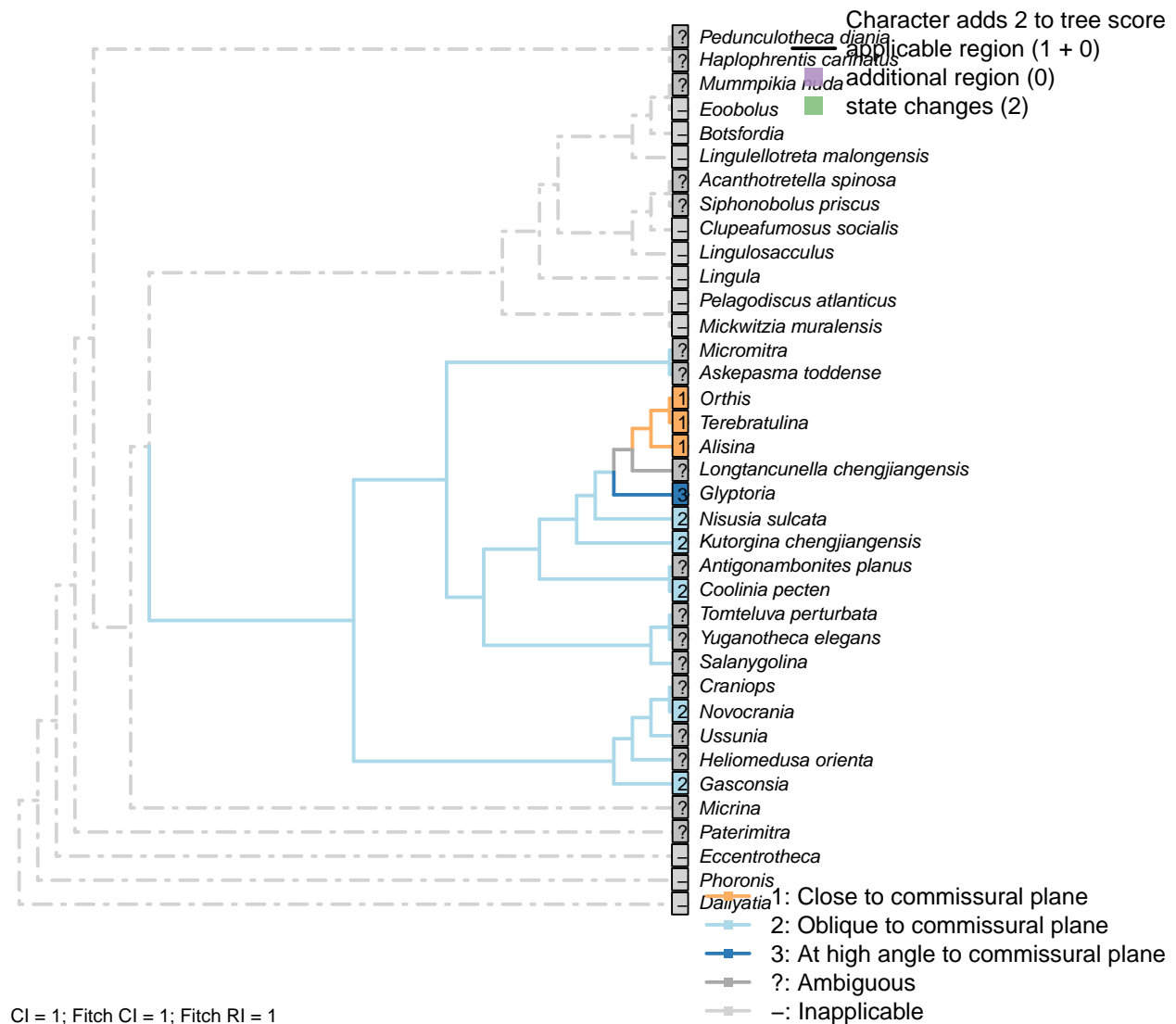
*Askepasma toddense*: Not reconstructed in the interpretation of the musculature presented by Williams *et al.* (2000), fig. 81, but presence cannot be confidently excluded.

*Clupeafumosus socialis*: Not reported by Topper *et al.* (2013a), nor reconstructed in generic acrotretid by Williams *et al.* (2000).

*Gasconsia*: Internal oblique muscles serve as diductors.

*Siphonobolus priscus*: Ventral musculature poorly constrained (Williams *et al.*, 2000; Popov *et al.*, 2009).

## [20] Muscle scars: Dorsal diductor: Position



Character 20: Sclerites: Bivalved: Muscle scars: Dorsal diductor: Position

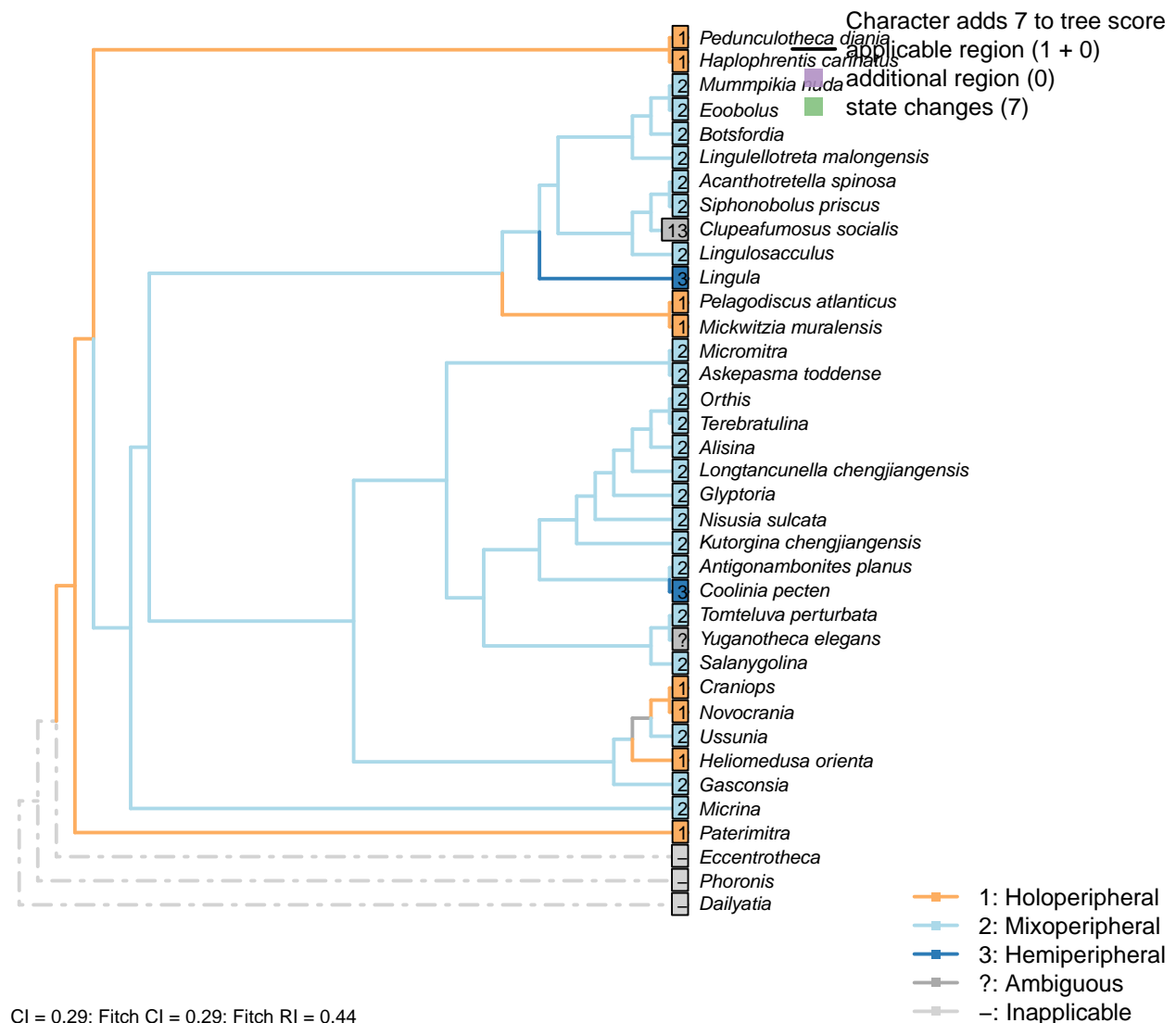
- 1: Close to commissural plane
  - 2: Oblique to commissural plane
  - 3: At high angle to commissural plane
- Transformational character.

After Bassett *et al.* (2001) character 10.

*Siphonobolus priscus*: Ventral musculature poorly constrained (Williams *et al.*, 2000; Popov *et al.*, 2009).

### 3.3 Sclerites: Dorsal valve

#### [21] Growth direction



#### Character 21: Sclerites: Dorsal valve: Growth direction

- 1: Holoperipheral
- 2: Mixoperipheral

3: Hemiperipheral  
Transformational character.

See Fig. 284 in Williams *et al.* (1997).

The growth direction dictates the attitude of the cardinal area relative to the hinge, which does not therefore represent an independent character.

Crudely put, if, viewed from a dorsal position, the umbo falls within the outer margin of the shell, growth is holoperipheral; if it falls outside the margin, it is mixoperipheral; if it falls exactly on the margin, it is hemiperipheral.

*Clupeafumosus socialis*: Appears hemiperipheral in fig. 3 in Topper *et al.* (2013a), though bordering on holoperipheral, so scored as ambiguous.

*Craniops*: “both valves with growth holoperipheral” – Williams *et al.* (2000) p164.

*Heliomedusa orienta*: “holoperipheral growth in dorsal valve” – Williams *et al.* (2007).

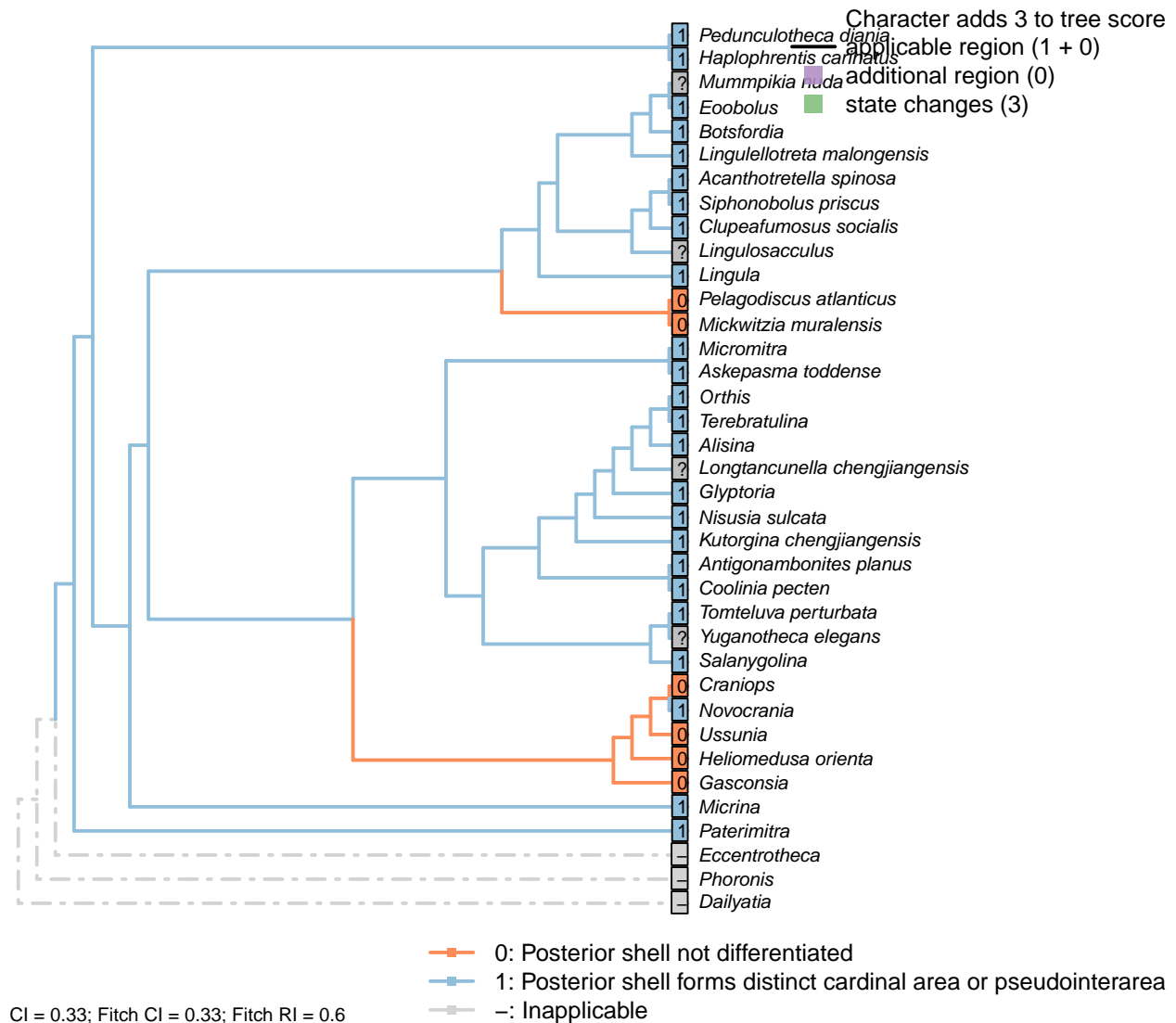
The insinuation from Zhang *et al.* (2009) is that Chen *et al.* (2007) misidentify the dorsal valve as the ventral valve.

*Micrina*: See Holmer *et al.* (2008).

*Paterimitra*: S2 and L sclerites are clearly holoperipheral. See Larsson *et al.* (2014), fig. 2.

*Ussunia*: Following description of order in Williams *et al.* (2000).

## [22] Posterior surface: Differentiated



### Character 22: Sclerites: Dorsal valve: Posterior surface: Differentiated

- 0: Posterior shell not differentiated
- 1: Posterior shell forms distinct cardinal area or pseudointerarea
- Neomorphic character.

In shells that grow by mixoperipheral growth, the triangular area subtended between each apex and the posterior ends of the lateral margins is termed the cardinal area. In shells with holoperipheral growth, a flattened surface on the posterior margin of the valve is termed a pseudointerarea (paraphrasing Williams et al., 1997).

In order for this character to be independent of a shell's growth direction, we do not distinguish between a "cardinal area", "interarea" or "pseudointerarea".

*Acanthotretella spinosa*: Pseudointerarea present, following Siphonotretidae coding in Williams et al. (2000), table 6.

*Alisina*, *Antigonambonites planus*, *Coolinia pecten*, *Glyptoria*, *Kutorgina chengjiangensis*, *Orthis*, *Salany-*

*golina*, *Tomteluva perturbata*: Cardinal area (interarea) present.

*Askepasma toddense*: Well-defined pseudointerarea (Williams et al., 2000, p153).

*Botsfordia*: “dorsal pseudointerarea vestigial, divided by median groove” – Williams et al. (2000).

*Clupeafumosus socialis*: Pseudointerarea present; figured by Topper et al. (2013a), fig. 3j.

*Craniops*: “Only some craniopsids (Lingulapholis, Pseudopholidops [not *Craniops*]) have well-developed pseudointerareas.” – Williams et al. (2000).

*Gasconsia*: Absent: the dorsal (branchial) pseudointerarea of *G. schucherti* is “reduced or obsolete”; that of *G. worsleyi* “short, virtually obsolete” (Hanken and Harper, 1985).

*Haplophrentis carinatus*: A very short pseudointerarea appears to be present (Moysiuk et al., 2017).

*Heliomedusa orienta*: Pseudointerarea in ventral valve, but not dorsal valve (Williams et al., 2000, 2007).

*Lingula*, *Lingulellotreta malongensis*: Pseudointerarea present, following Williams et al. (2000), table 6.

*Lingulosacculus*: Unclear from fossil material.

*Longtancunella chengjiangensis*: Zhang et al. (2011a) note that “all evidence of a pseudointerarea is lacking”, but the two-dimensional preservation style of Chengjiang material makes details of dorsal valve difficult to distinguish, and the possibility of a diminutive pseudointerarea cannot be excluded with total confidence.

*Mickwitzia muralensis*: Shell flat.

*Micrina*: = Sellate sclerite duplicature (Holmer et al., 2008).

*Micromitra*: “Dorsal pseudointerarea usually well defined, low, anacline to catacline” – Williams et al. (2000).

*Mummpikia nuda*: “Information on the dorsal interarea is inconclusive [...] no obvious interarea is recognisable; whether or not this is the primary state or a taphonomic artefact is difficult to assess” – Balthasar (2008), p. 276.

*Nisusia sulcata*: Cardinal area (interarea) present – with reference to Holmer et al. (2018a).

*Novocrania*, *Paterimitra*, *Pedunculotheca diania*: Pseudointerarea.

*Pelagodiscus atlanticus*: Absent, following entry for Discinidae in Williams et al. (2000), table 6.

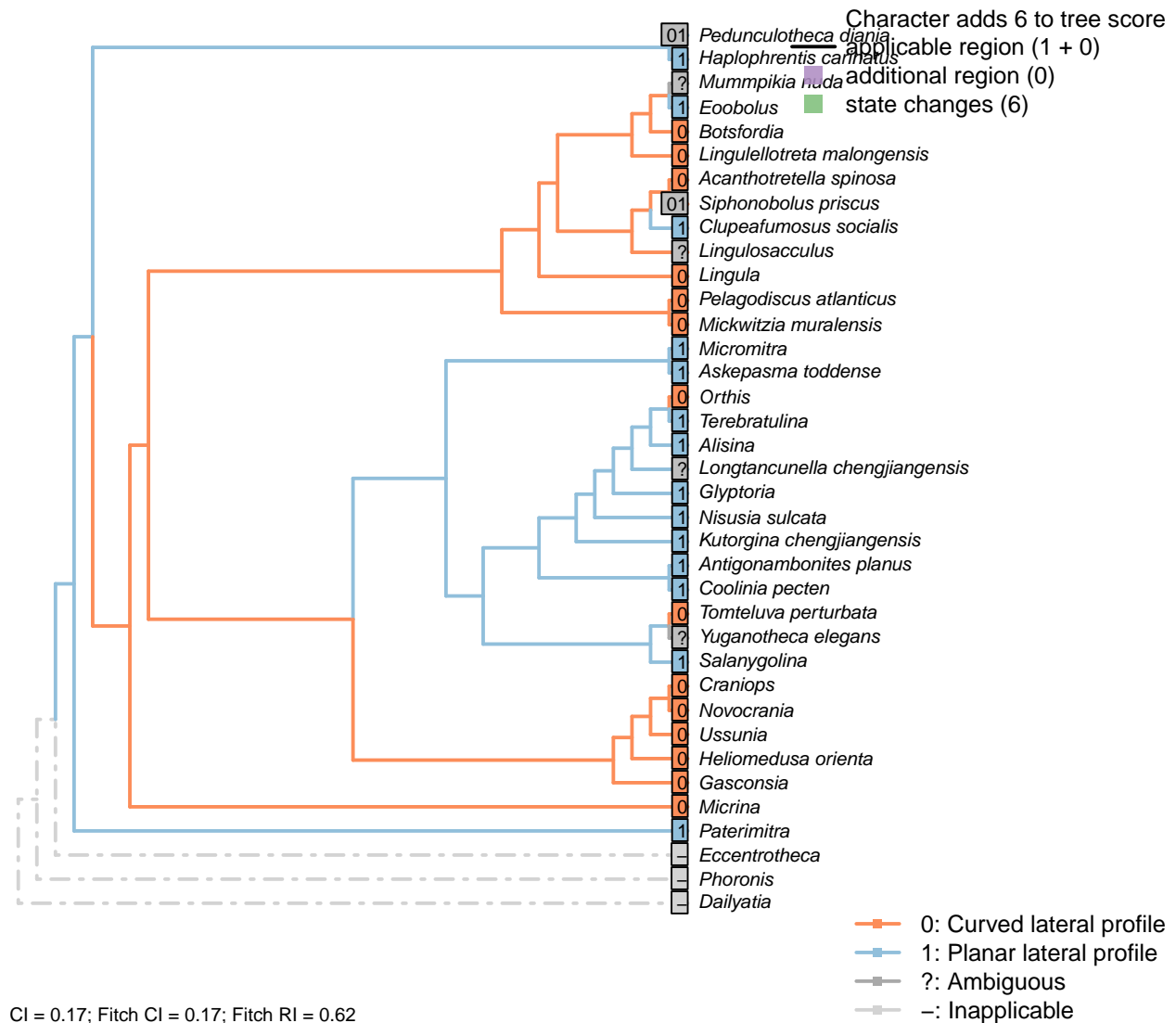
*Siphonobolus priscus*: “Dorsal pseudointerarea weakly anacline, undivided, elevated above the valve floor” – Popov et al. (2009).

*Terebratulina*: Interarea present.

*Ussunia*: Following table 15 in Williams et al. (2000).

*Yuganotheca elegans*: A differentiated region is not obvious in fossil material or its reconstruction (Zhang et al., 2014), but the two-dimensional preservation style of Chengjiang material makes details of dorsal valve difficult to distinguish, and the possibility of a diminutive pseudointerarea cannot be excluded with confidence.

### [23] Differentiated posterior surface: Morphology



#### Character 23: Sclerites: Dorsal valve: Differentiated posterior surface: Morphology

- 0: Curved lateral profile
- 1: Planar lateral profile
- Neomorphic character.

It is possible for a cardinal area or pseudointerarea to be distinct from the anterior part of the shell, yet to remain curved in lateral profile.

Taking an undifferentiated posterior margin as primitive, the primitive condition is curved – flattening of the posterior margin represents an additional modification that can only occur once the posterior margin is differentiated.

*Botsfordia*: “Curved pseudointerarea” – Skovsted et al. (2017).

*Clupeafumosus socialis*: Truncated but essentially planar surface; see e.g. p196 of Topper et al. (2013a).

*Eoobolus*: Essentially planar; see Balthasar (2009), fig. 4a.

*Gasconsia*, *Heliomedusa orienta*, *Mickwitzia muralensis*, *Pelagodiscus atlanticus*, *Ussunia*: Posterior surface

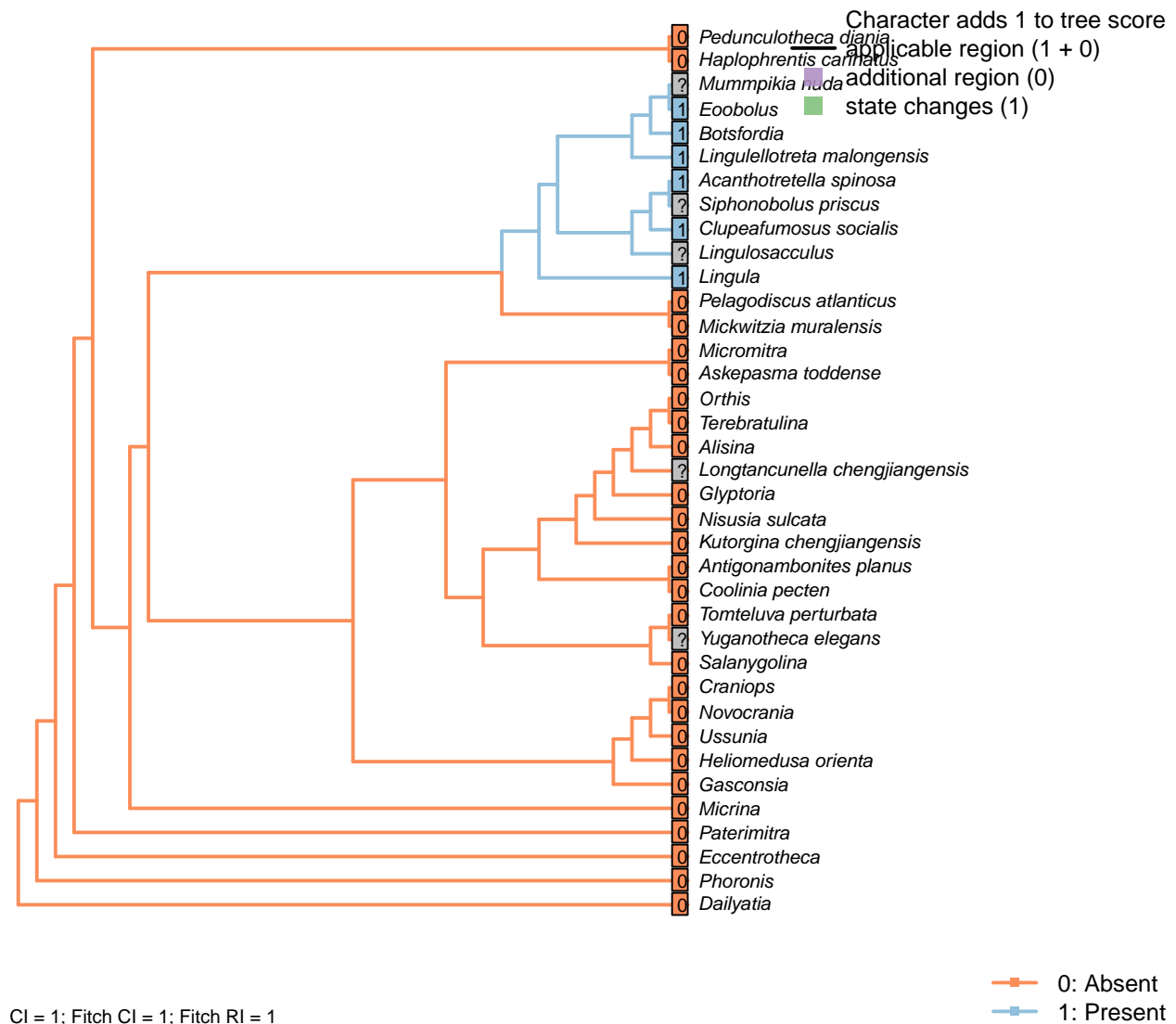
cannot be flat if it is not differentiated.

*Micromitra*: Essentially straight; see fig. 3.7 in Ushatinskaya (2016).

*Pedunculotheca diana*: Difficult to evaluate based on present material, given low nature of valve and compressed preservation.

*Siphonobolus priscus*: The short interarea appears planar (see for example Popov et al. 2009 fig. 6A), but its short length makes it difficult to establish whether slight curvature is present.

## [24] Posterior surface: Medial groove



### Character 24: Sclerites: Dorsal valve: Posterior surface: Medial groove

0: Absent

1: Present

Neomorphic character.

Following character 29 in Williams *et al.* (2000), table 9 (which relates to pseudointerarea).

*Acanthotretella spinosa*: The dorsal pseudointerarea is poorly preserved, but appears to have a median groove

(Holmer and Caron, 2006).

*Botsfordia*: “dorsal pseudointerarea vestigial, divided by median groove” – Williams et al. (2000).

*Clupeafumosus socialis*: Present; figured by Topper et al. (2013a), fig. 3j.

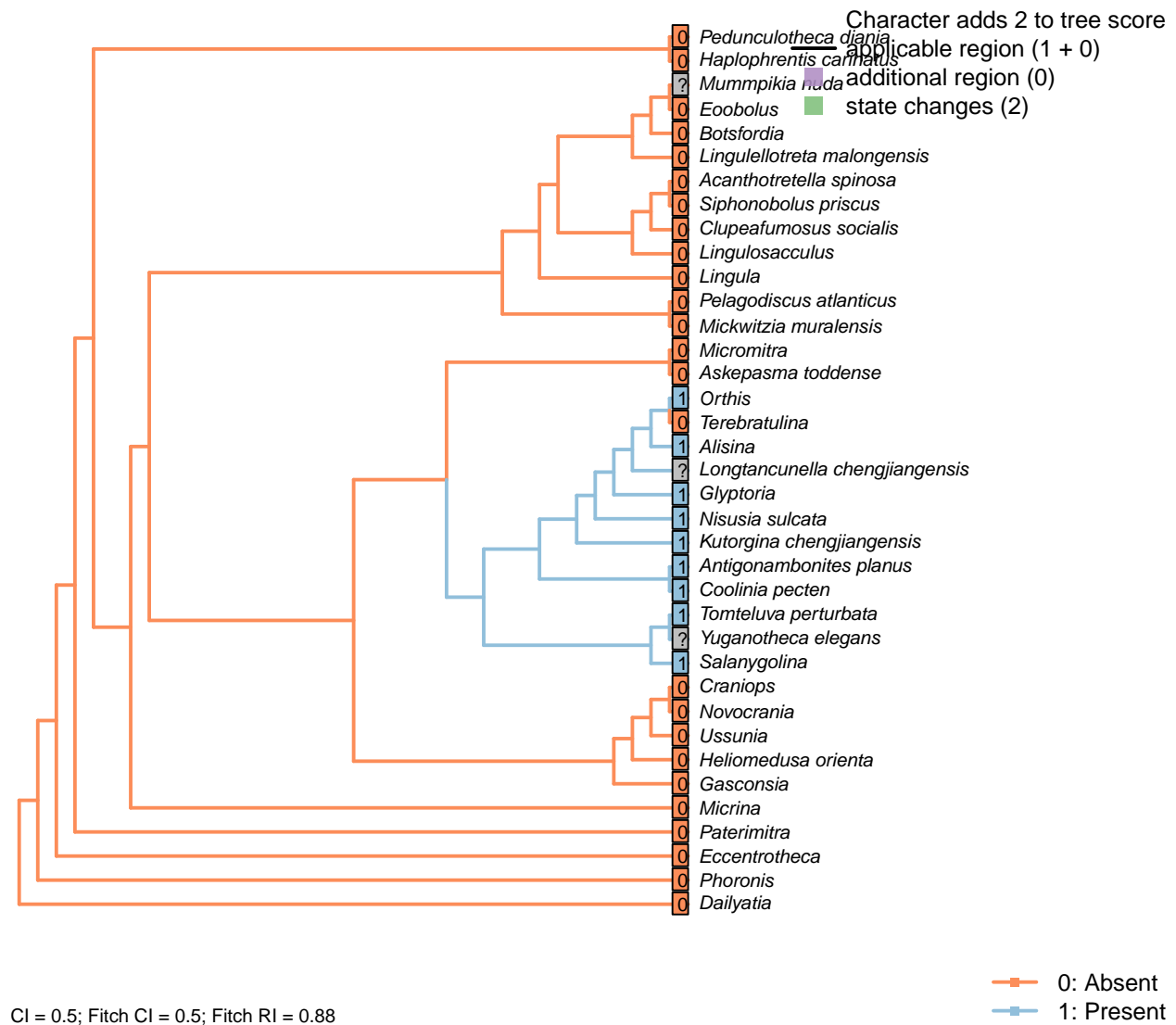
*Eoobolus*: Prominent medial groove (Balthasar, 2009).

*Heliomedusa orienta*: “A posteriorly protruding dorsal pseudointerarea with no median groove and no flexure lines” – Chen et al. (2007).

*Lingulellotreta malongensis*: Dorsal pseudointerarea with wide, concave median groove and short propareas” – Williams et al. (2000).

*Siphonobolus priscus*: The dorsal pseudointerarea of *S. priscus* is undivided (Popov et al., 2009), but in other species it is divided by a “wide, poorly defined median groove” (Williams et al., 2000). Coded, therefore, as polymorphic.

## [25] Posterior surface: Notothyrium



0: Absent

1: Present

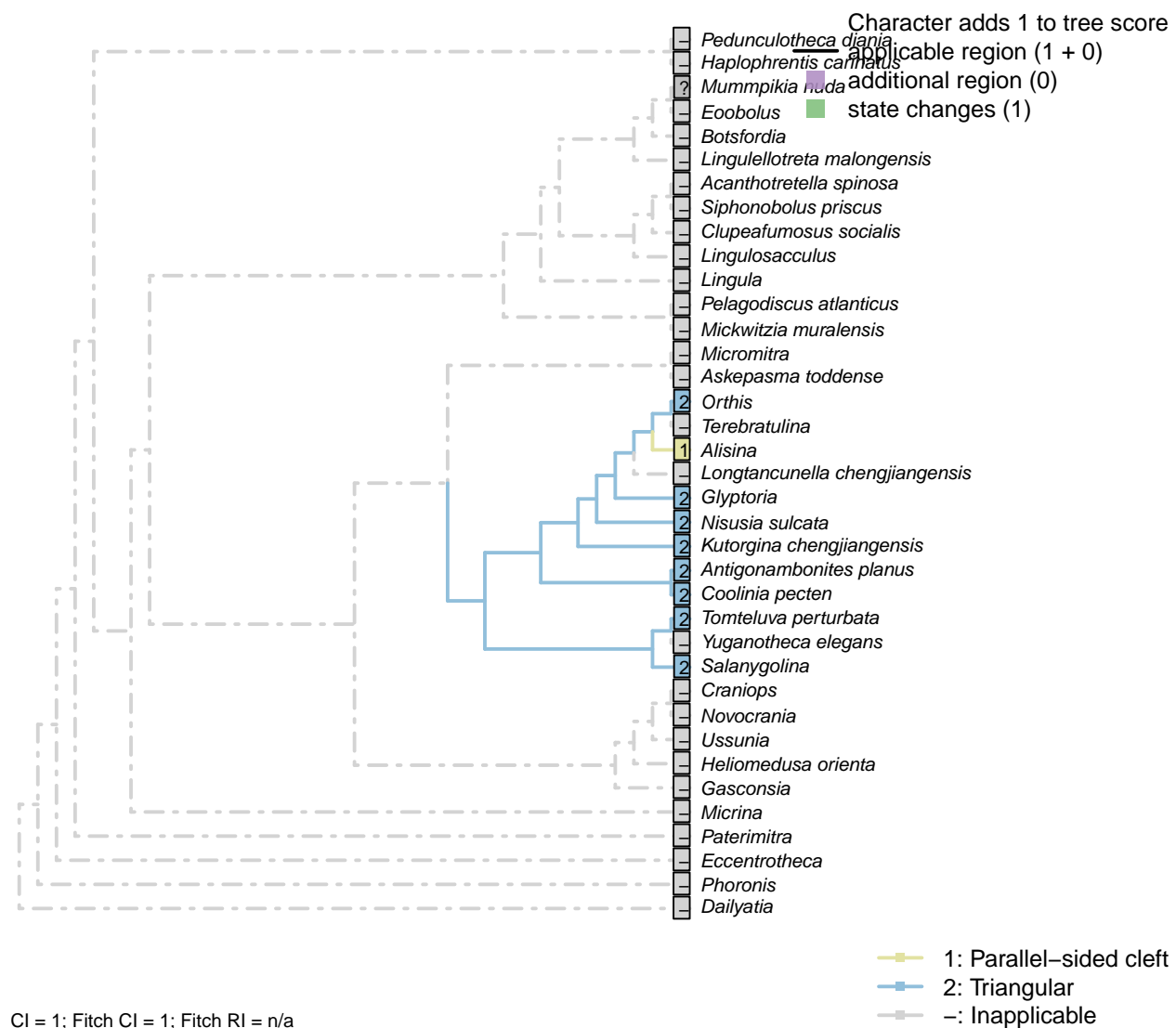
Neomorphic character.

A notothyrium is an opening in an interarea that accommodates the pedicle, and may be filled with plates.

*Botsfordia*: Following Williams et al. (1998), appendix 2.

*Longtancunella chengjiangensis*: No evidence or report of an opening at the hinge line in fossil material in Zhang et al. (2007c) or Zhang et al. (2011a).

## [26] Posterior surface: Notothyrium: Shape



### Character 26: Sclerites: Dorsal valve: Posterior surface: Notothyrium: Shape

1: Parallel-sided cleft

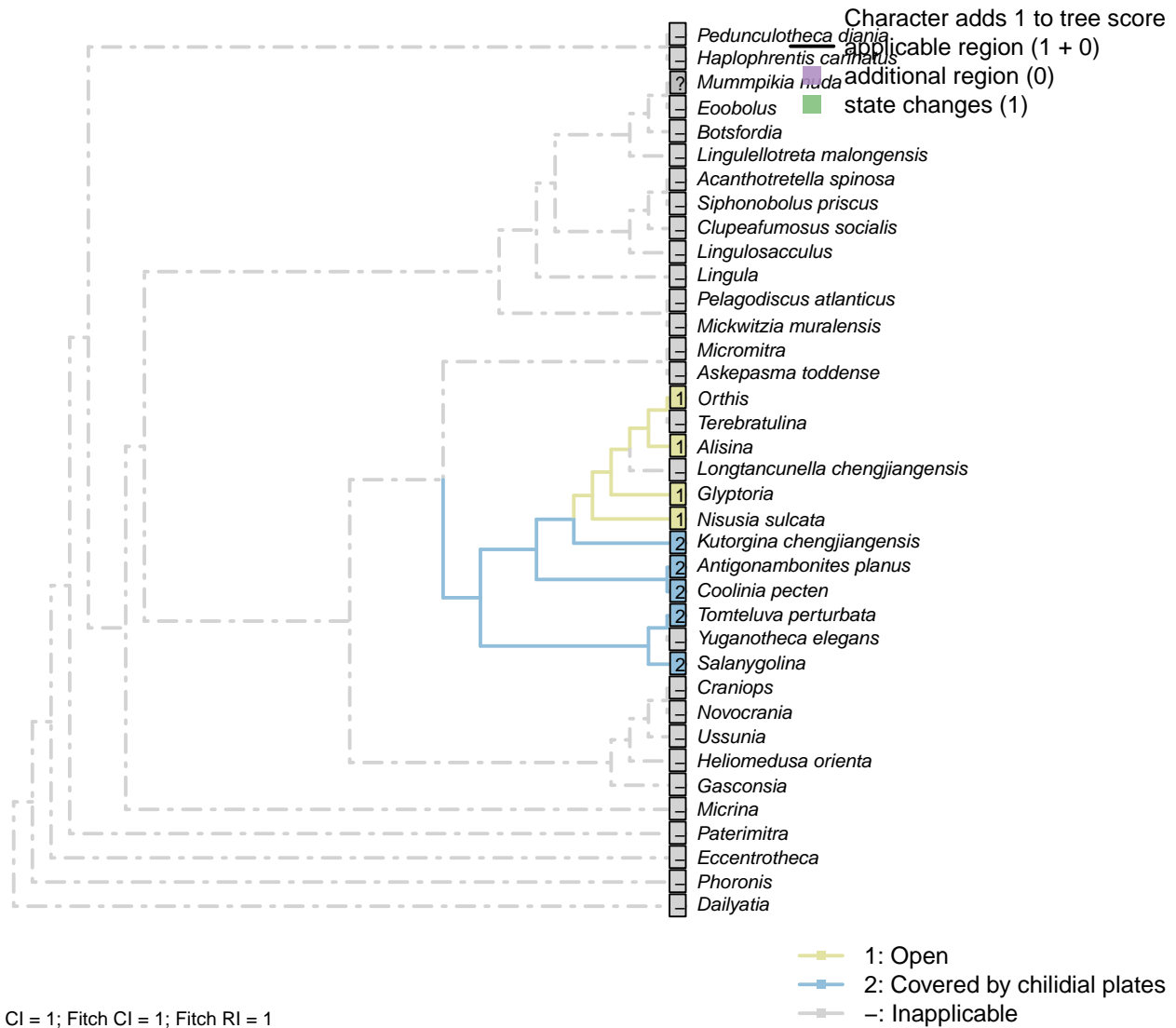
2: Triangular

Transformational character.

A notothyrium is an opening in an interarea that accommodates the pedicle, and may be filled with plates.

A simplification of character 5 in Bassett et al. (2001).

### [27] Posterior surface: Notothyrium: Chilidial plates



#### Character 27: Sclerites: Dorsal valve: Posterior surface: Notothyrium: Chilidial plates

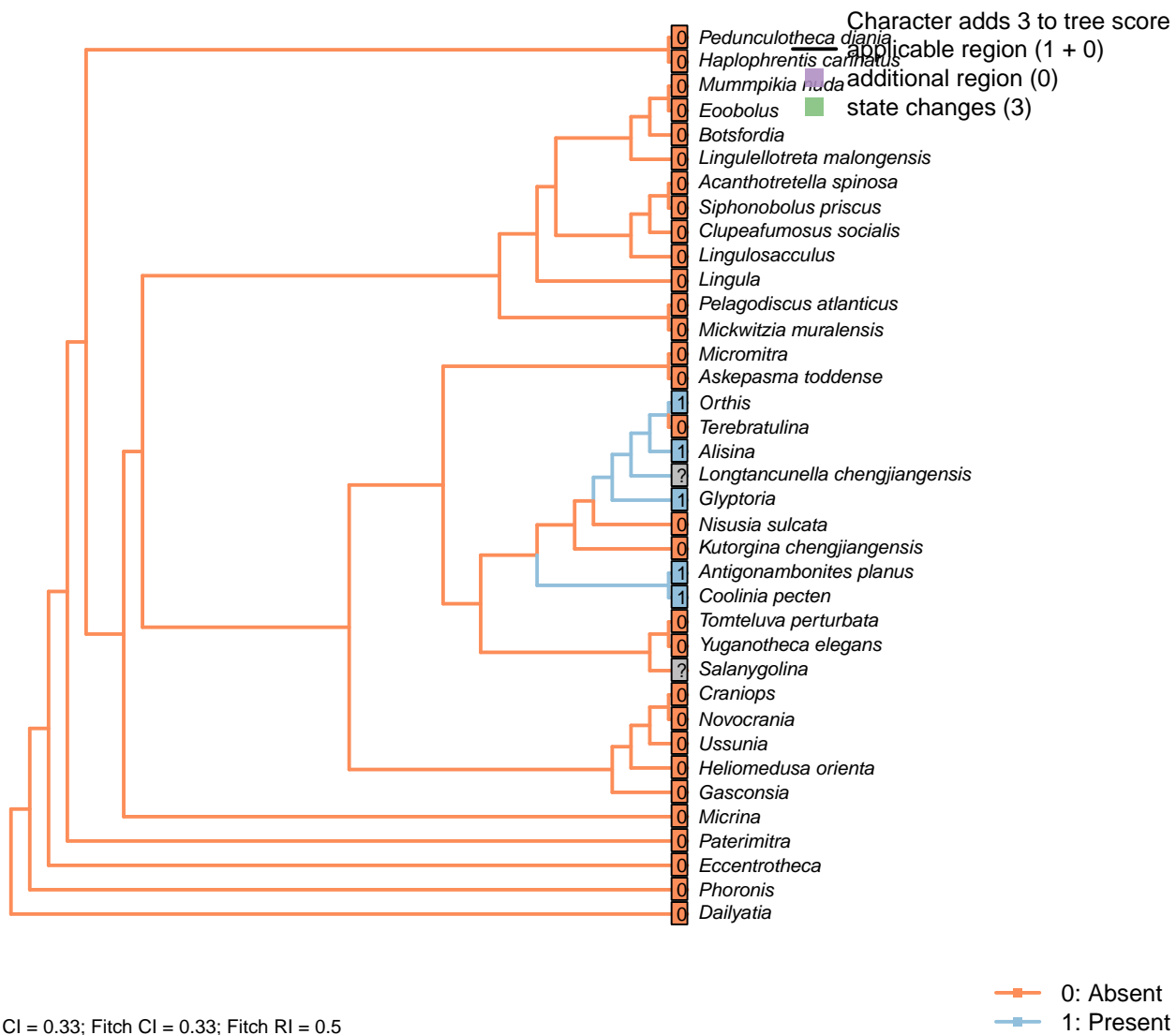
- 1: Open
- 2: Covered by chilidial plates
- Transformational character.

A notothyrium may be open or covered by a chilidium or two chilidial plates.

No included taxa exhibit more than one chilidial plate.

Transformational as it is not self-evident whether the ancestral taxon had an open or closed notothyrium.

## [28] Notothyrial platform



### Character 28: Sclerites: Dorsal valve: Notothyrial platform

0: Absent

1: Present

Neomorphic character.

After Bassett *et al.* (2001) character 12.

The presence or absence of a notothyrial platform, which often serves as an attachment point for the diductors in a similar fashion to the cardinal processes, is independent of the presence of a notothyrium.

*Alisina*, *Glyptoria*: Bassett *et al.* (2001) score as present in Table 18.1.

*Coolinia pecten*: Referred to as the “posterior platform” in Dewing (2001).

*Kutorgina chengjiangensis*: “Dorsal diductor scars impressed on floor of notothyrial cavity”: Williams *et al.* (2000), regarding Kutorginata.

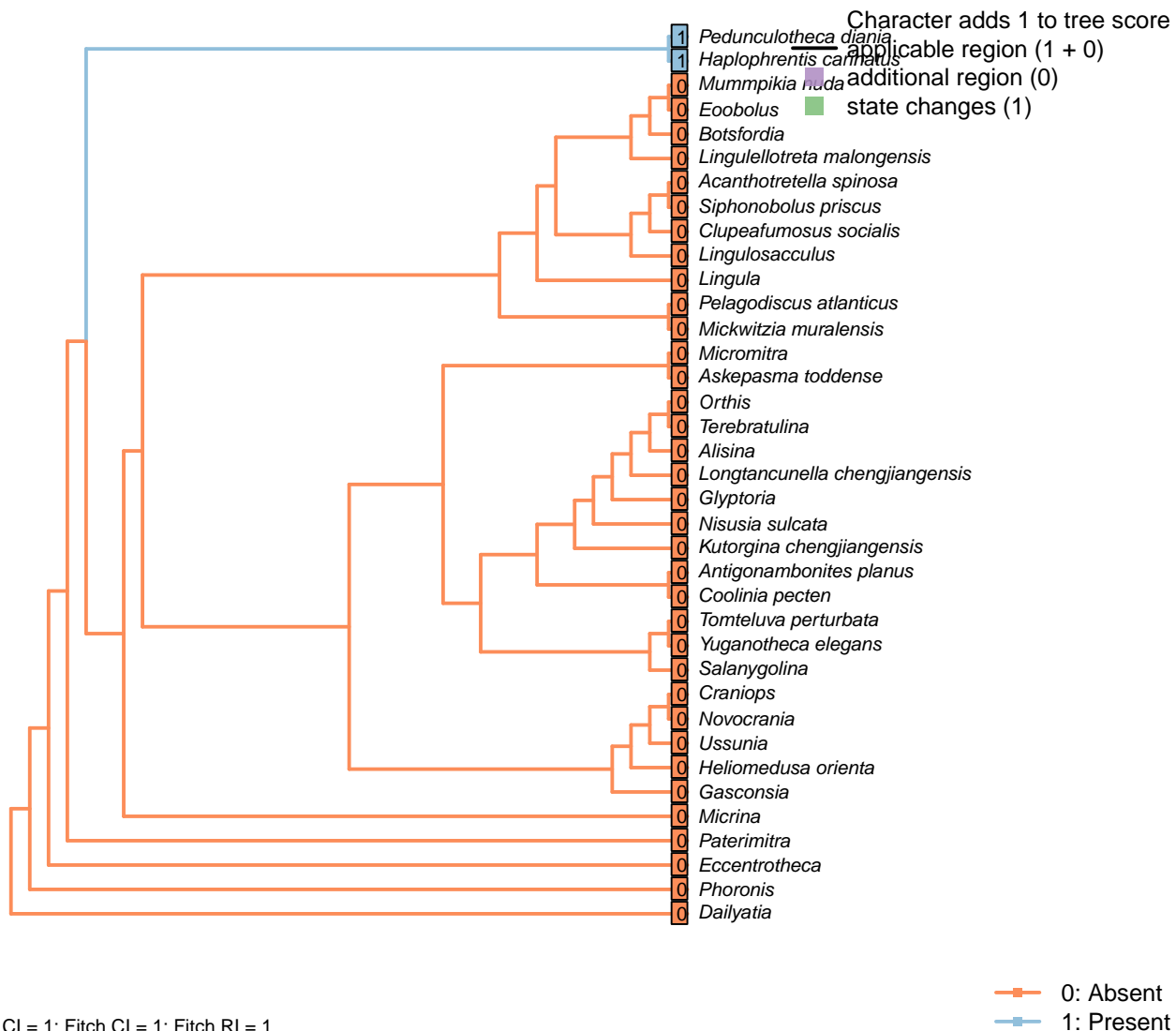
Bassett *et al.* (2001) score as absent in Table 18.1.

*Nisusia sulcata*: Bassett *et al.* (2001) score as absent in Table 18.1.

"Dorsal diductor scars impressed on floor of notothyrial cavity": Williams et al. (2000), regarding *Kutorginata*.

*Ussunia*: "Visceral platforms absent in both valves" – Williams et al. (2000), p. 192.

## [29] Cardinal shield



### Character 29: Sclerites: Dorsal valve: Cardinal shield

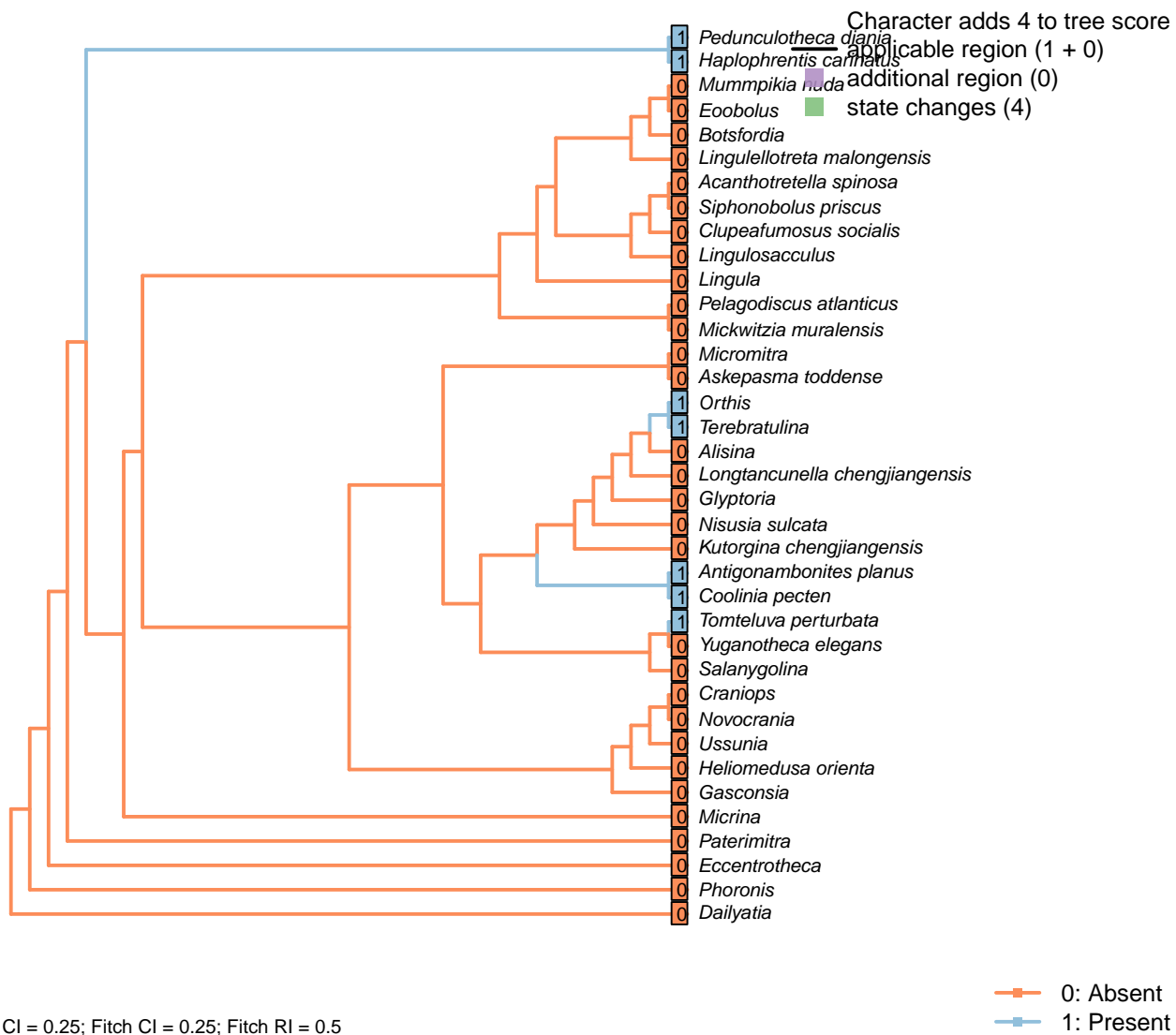
0: Absent

1: Present

Neomorphic character.

A prominent platform in the hyolith operculum. With no obvious sites for muscle attachment, it is unlikely to be homologous to the notothyrial platform.

## [30] Cardinal processes

**Character 30: Sclerites: Dorsal valve: Cardinal processes**

0: Absent

1: Present

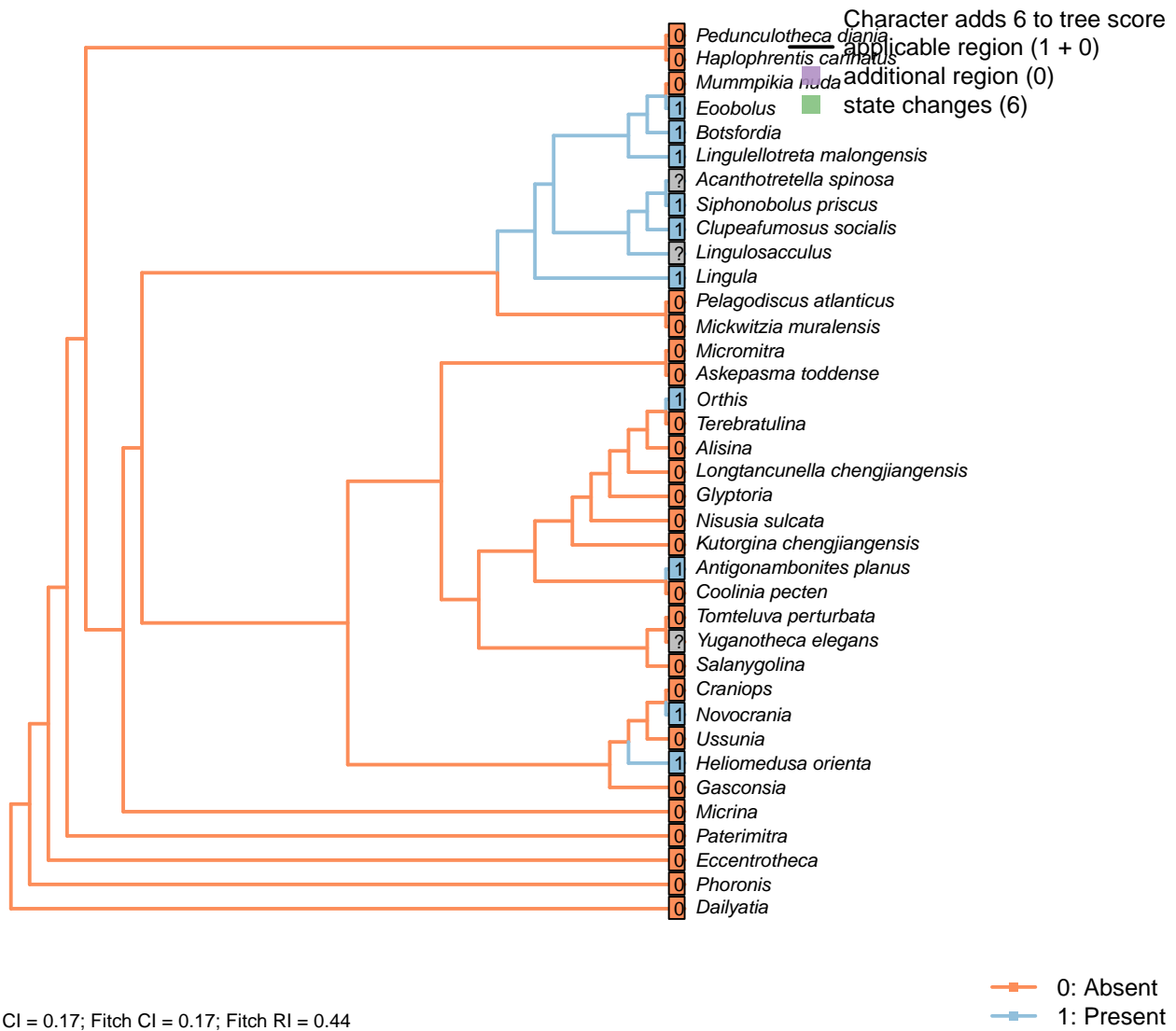
Neomorphic character.

After Bassett *et al.* (2001) character 13.

Cardinal processes are unlikely to be homologous with the notothyrial platform, even if their function is similar.

*Clupeafumosus socialis*: Not reported by Topper *et al.* (2013a).*Longtancunella chengjiangensis*: Not evident, and ought arguably to be discernable if present given the quality of preservation.

### [31] Medial septum



#### Character 31: Sclerites: Dorsal valve: Medial septum

0: Absent

1: Present

Neomorphic character.

The dorsal valve of many taxa exhibits a septum or process (or myophragm) along the medial line. See character 25 in Benedetto (2009).

*Acanthotretella spinosa*: Not described by Holmer & Caron (2006), but an unannotated linear feature corresponds to the position of a median septum. Without detailed study of the specimen, we opt to score this as ambiguous.

*Antigonambonites planus*: Weakly developed septum evident in internal cast: Williams et al. (2000), fig. 508.2e.

*Botsfordia*: “dorsal interior with narrow anterior projection extending to midvalve, bisected by median ridge”

– Williams et al. (2000).

*Clupeafumosus socialis*: Prominent process evident (Topper et al., 2013a).

*Eoobolus*: A “median projection” is present (fig. 4g in Balthasar, 2009).

*Glyptoria*: Neither evident nor reported in Williams et al. (2000).

*Heliomedusa orienta*: Reported on ‘ventral’ valve by Chen et al. (2007); we consider their ‘ventral’ valve to be the dorsal valve.

The structure is unambiguously figured (e.g. fig. 5.1 in Chen et al., 2007), contra its coding as absent in Williams et al. (2000) and its lack of mention in Williams et al. (2007) or Zhang et al. (2009).

*Kutorgina chengjiangensis*: Absent – fig. 129.1f in Williams et al. (2000).

*Lingulellotreta malongensis*: Very weakly developed but seemingly present between muscle scars in *Lingulellotreta*, more prominent in *Aboriginella* (also Lingulellotretidae) (Williams et al., 2000, fig. 34).

*Lingulosacculus*: It is not possible to determine, based on the material presented in Balthasar & Butterfield (2009), whether the anterior projection of the visceral area in the dorsal valve corresponds to a medial septum in the underlying shell.

*Mummpekia nuda*: See pl. 2 panel 6 in Balthasar (2008).

*Nisusia sulcata*: Fig. 125 in Williams et al. (2000).

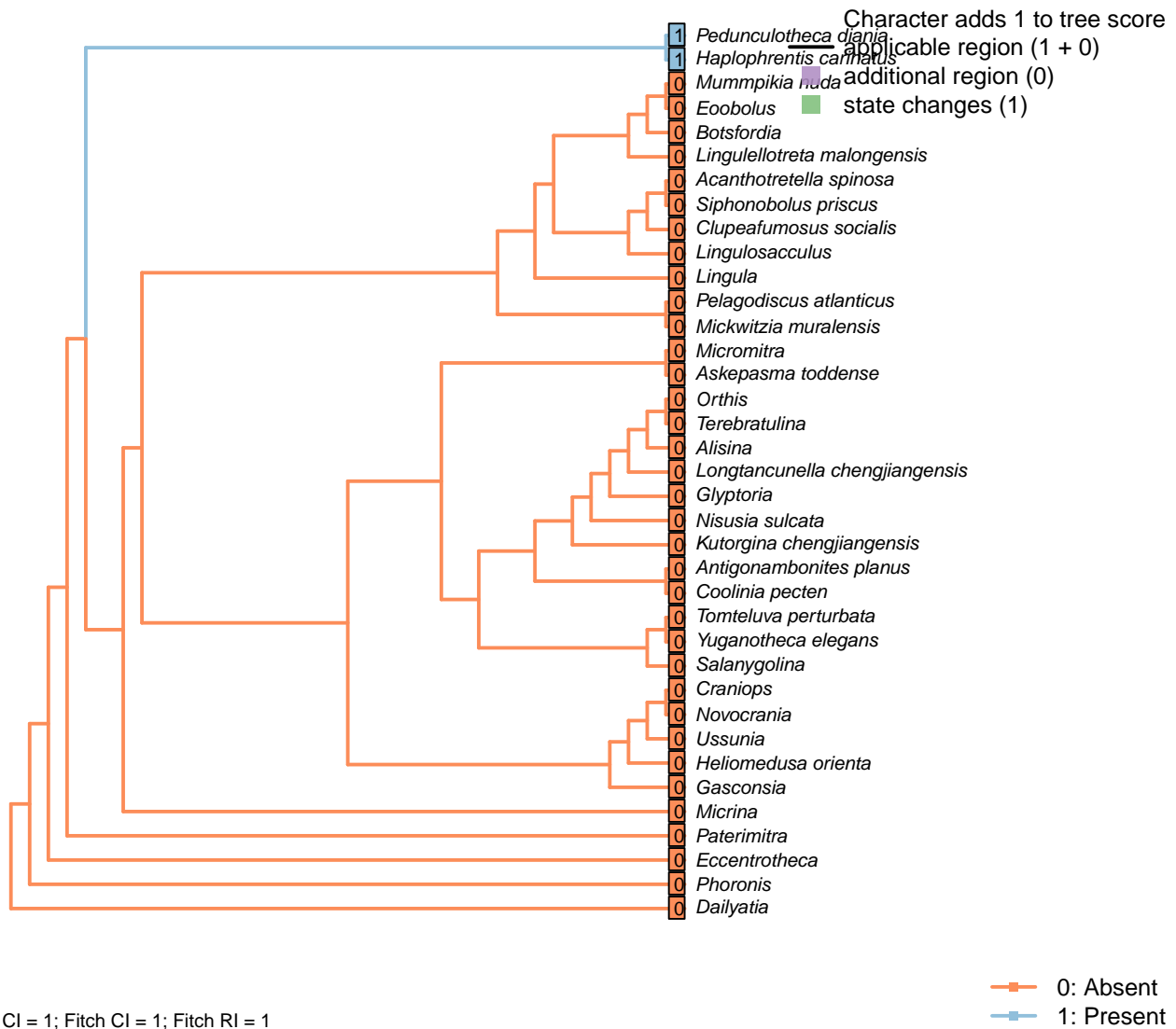
*Novocrania*: Median process evident: Williams et al. (2000) fig. 100.2a, d.

*Orthis*: Short medial process (“low median ridge”, p. 724) present in dorsal valve; see Fig. 523.3b in Williams et al. (2000).

*Siphonobolus priscus*: “Dorsal interior [...] bisected by a short median ridge.” – Popov et al. (2009).

*Ussunia*: Following char 42 in table 15 in Williams et al. (2000).

## [32] Clavicles



### Character 32: Sclerites: Dorsal valve: Clavicles

0: Absent

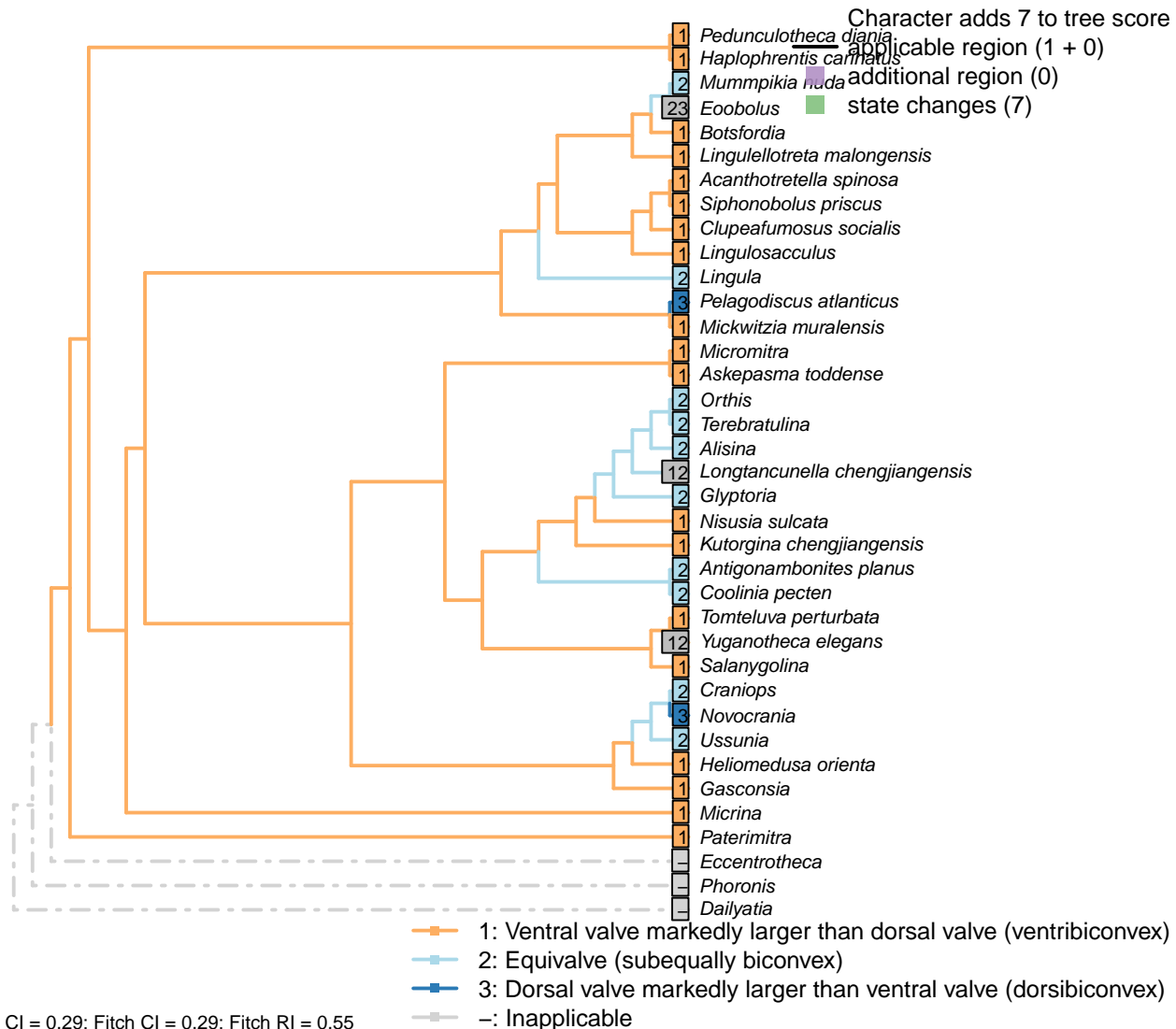
1: Present

Neomorphic character.

Prominent symmetrical ridges on the inner surface of the hyolith operculum.

### 3.4 Sclerites: Ventral valve

#### [33] Relative size



#### Character 33: Sclerites: Ventral valve: Relative size

- 1: Ventral valve markedly larger than dorsal valve (ventribiconvex)
  - 2: Equivalve (subequally biconvex)
  - 3: Dorsal valve markedly larger than ventral valve (dorsibiconvex)
- Transformational character.

In many brachiopods, the valves are closely similar in size; in others, the ventral valve is markedly larger than the dorsal, on account of being more convex. Marginal cases are treated as ambiguous for the relevant

states.

*Antigonambonites planus*: Broadly equivalve – see Williams *et al.* (2000) fig. 508.2c.

*Botsfordia*: After table 8 in Williams *et al.* (2000).

*Craniops*: “Shell subequally biconvex” – Williams *et al.* (2000).

*Eoobolus*: “*Eoobolus* is biconvex”, but in his amended diagnosis, Balthasar (2009) described it as “shell inequivaled, dorsibiconvex”.

*Gasconsia*: Convexiplane (Williams *et al.*, 2000, p. 187).

*Heliomedusa orienta*: Ventral valve larger than the dorsal valve (Zhang *et al.*, 2009, p. 659).

*Kutorgina chengjiangensis*: Ventral valve larger (see Williams *et al.*, 2000, fig. 125.).

*Longtancunella chengjiangensis*, *Yuganotheca elegans*: The ventral valve is somewhat, but not markedly, larger than the dorsal; as such, this character is coded ambiguous for equivalve/ventral valve larger.

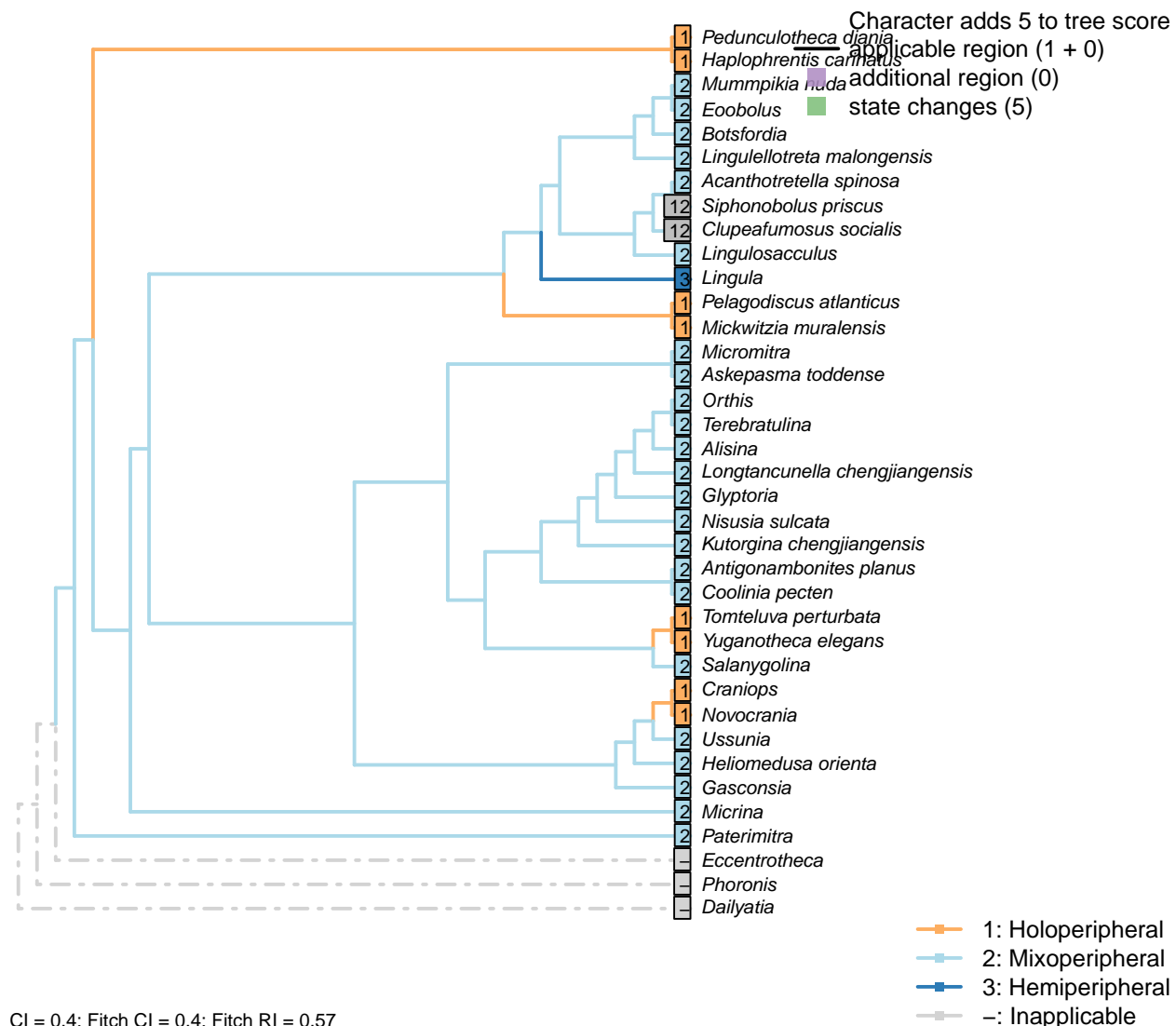
*Mummpikia nuda*: Aside from hinge, valves similar in convexity and size (Balthasar, 2008).

*Nisusia sulcata*: Ventral valve larger (see Williams *et al.*, 2000, fig. 126.).

*Siphonobolus priscus*: Ventribiconvex (Popov *et al.*, 2009).

*Ussunia*: Subequally biconvex (Williams *et al.*, 2000, p. 192).

## [34] Growth direction

**Character 34: Sclerites: Ventral valve: Growth direction**

- 1: Holoperipheral
  - 2: Mixoperipheral
  - 3: Hemiperipheral
- Transformational character.

See Fig. 284 in Williams *et al.* (1997) for depiction of terms.

The growth direction dictates the attitude of the cardinal area relative to the hinge, which does not therefore represent an independent character.

Crudely put, if, viewed from a dorsal position, the umbo falls within the outer margin of the shell, growth is holoperipheral; if it falls outside the margin, it is mixoperipheral; if it falls exactly on the margin, it is hemiperipheral.

*Clupeafumosus socialis*: Inferred from Topper *et al.* (2013a).

*Heliomedusa orienta*: Williams *et al.* (2000, 2007) reconstruct mixoperipheral growth in the ventral valve [though Chen *et al.* (2007) reconstruct the valves the other way round, i.e. it is the ventral valve that grows

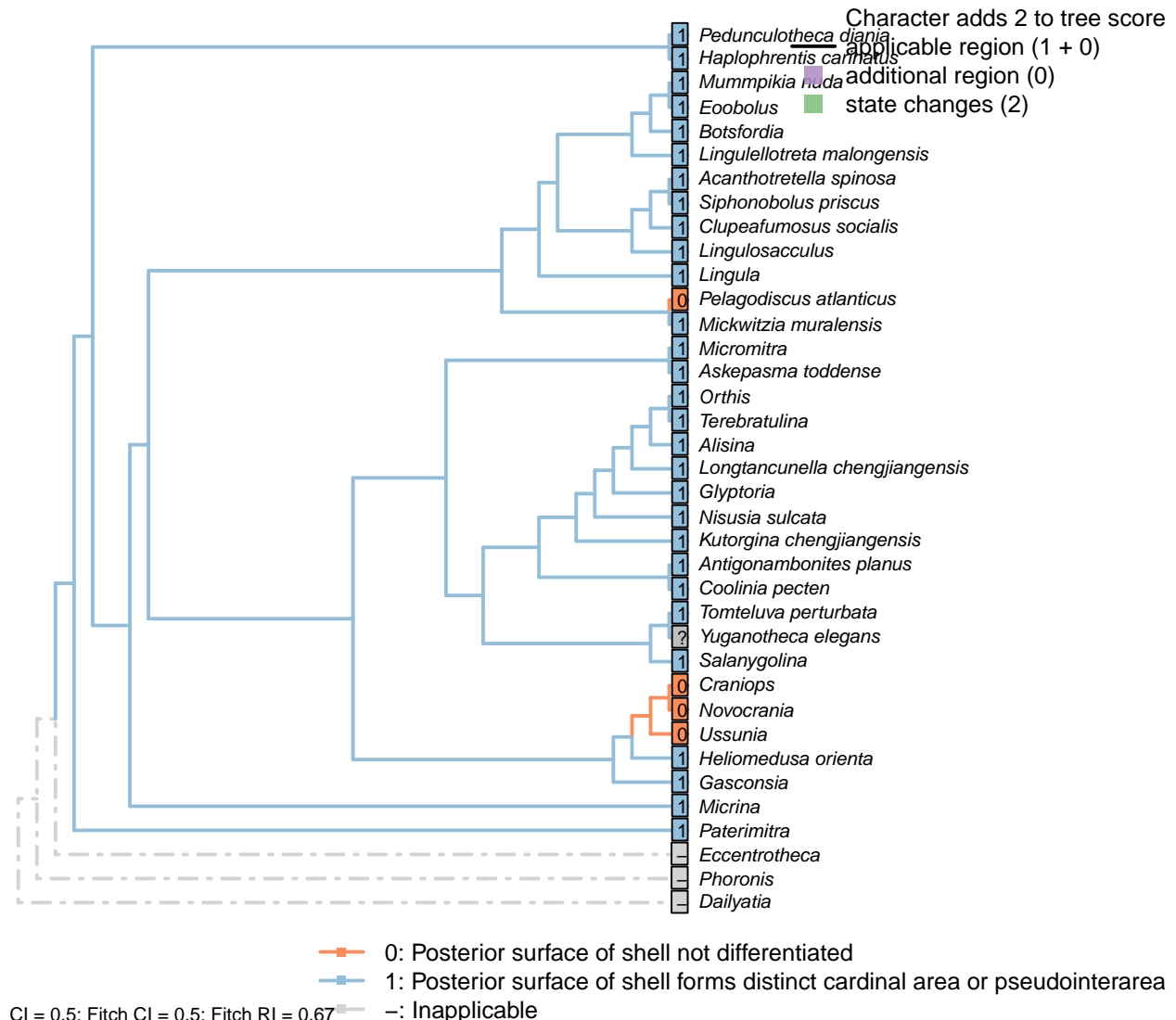
holoperipherally, and the dorsal mixoperipherally].

*Paterimitra*: The apical flange notwithstanding, the umbo of the S1 sclerite is posterior of the hinge line and the posterior edge of the lateral plate – see Larsson et al. (2014), fig. 2a, c.

*Siphonobolus priscus*: Initially holoperipheral (Popov et al., 2009, p. 159), then on the brink of being mixoperipheral in adulthood, so coded as polymorphic.

*Ussunia*: Following description of order in Williams et al. (2000).

### [35] Posterior surface: Differentiated



#### Character 35: Sclerites: Ventral valve: Posterior surface: Differentiated

0: Posterior surface of shell not differentiated

1: Posterior surface of shell forms distinct cardinal area or pseudointerarea

Neomorphic character.

In shells that grow by mixoperipheral growth, the triangular area subtended between each apex and the posterior ends of the lateral margins is termed the cardinal area. In shells with holoperipheral growth, a

flattened surface on the posterior margin of the valve is termed a pseudointerarea (paraphrasing Williams et al., 1997).

In order for this character to be independent of a shell's growth direction, we do not distinguish between a "cardinal area", "interarea" or "pseudointerarea".

*Alisina, Antigonambonites planus, Coolinia pecten, Glyptoria, Kutorgina chengjiangensis, Nisusia sulcata, Orthis, Salamygolina, Tomteluva perturbata*: Interarea present.

*Clupeafumosus socialis*: Described by Topper et al. (2013a).

*Gasconsia*: The region corresponding to the ventral (pseudo)interarea is described as a "trimerellid ventral cardinal area" by Williams et al. (2000, p.162), who code both an interarea and a pseudointerarea as absent in trimerellids.

*Heliomedusa orienta*: Zhang et al. (2009) report a moderate to somewhat developed ventral pseudointerarea, confirmed by Williams et al. (2007).

*Lingulosacculus*: The conical valve is interpreted as the ventral valve with an extended pseudointerarea.

*Longtancunella chengjiangensis*: Though "all evidence of a pseudointerarea is lacking" – Zhang et al. (2011a) – the region of the shell between the strophic hinge line and the colleplax (fig. 2 in Zhang et al., 2011a) is distinct from the rest of the shell; the ends of the strophic hinge line are marked by prominent nicks in the shell margin. *Longtancunella* is therefore coded as having a differentiated posterior surface.

*Mickwitzia muralensis*: Termed an interarea by Balthasar (2004).

*Mummpikia nuda*: Balthasar (2008) interprets a pseudointerarea as being present – e.g. p273, "Of particular interest is the vault that bridges the most anterior portion of the ventral pseudointerarea and raises it above the visceral platform"; "This pattern is reversed in the ventral valves of *M. nuda*, where the anterior projection of the pedicle groove is raised above the valve floor whereas the lateral parts of pseudointerarea are not".

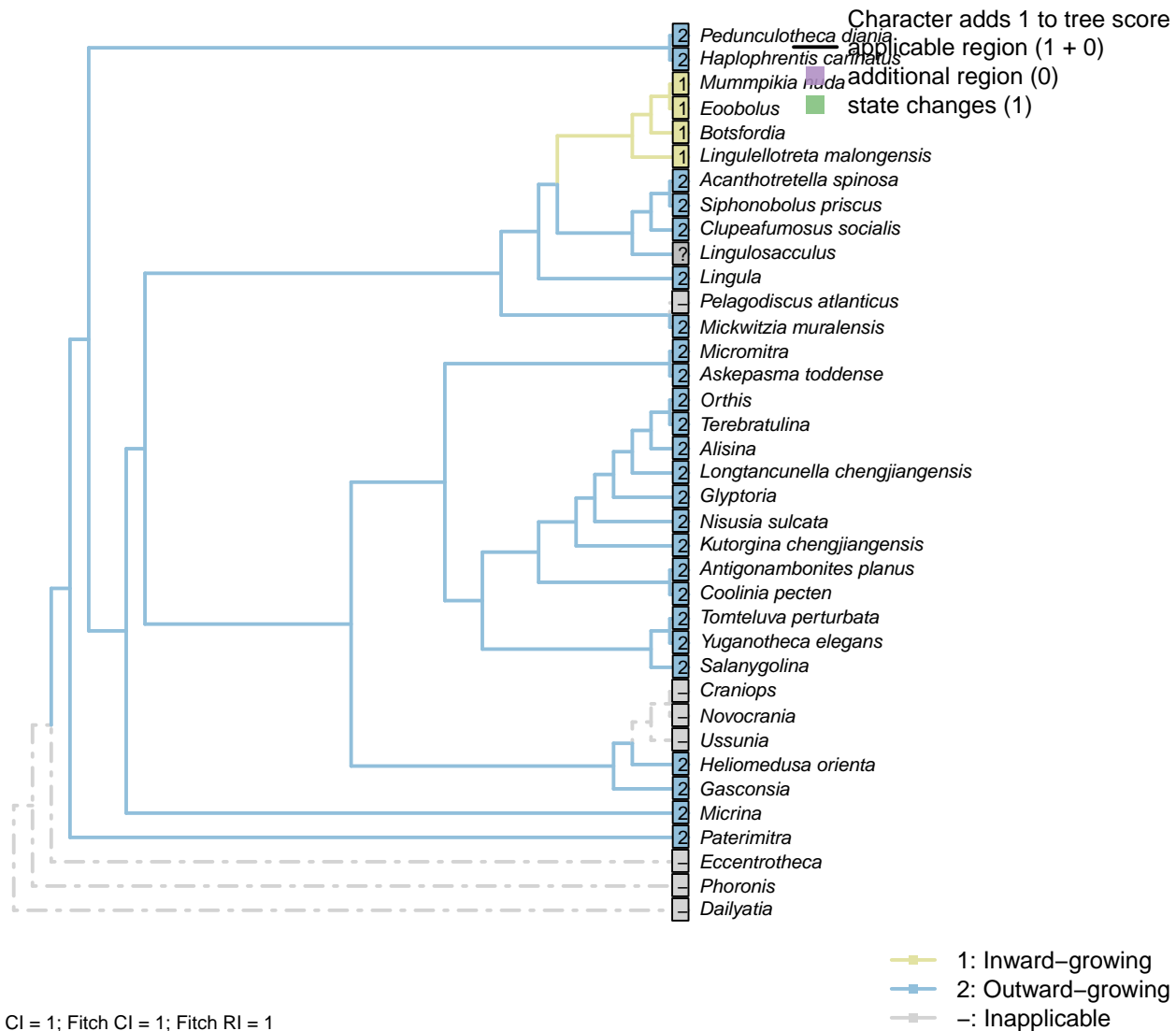
*Paterimitra*: Triangular notch and subapical flange.

*Siphonobolus priscus*: "Ventral pseudointerarea, low, undivided, poorly defined" – Williams et al. (2000).

*Terebratulina*: Interarea.

*Ussunia*: Following char 17 in table 15 in Williams et al. (2000).

### [36] Posterior margin growth direction



#### Character 36: Sclerites: Ventral valve: Posterior margin growth direction

- 1: Inward-growing
- 2: Outward-growing
- Transformational character.

Balthasar (2008) notes an inward-growing posterior margin of the pseudointerarea as potentially linking *Mummpikia* with the linguliform brachiopods.

Coded as inapplicable in taxa without a differentiated posterior margin: the posterior margin can only grow

inwards if it is differentiated from the anterior margin; else the entire shell would grow in on itself.

*Botsfordia*: Inward-growing; see Skovsted & Holmer (2005), pl. 4.

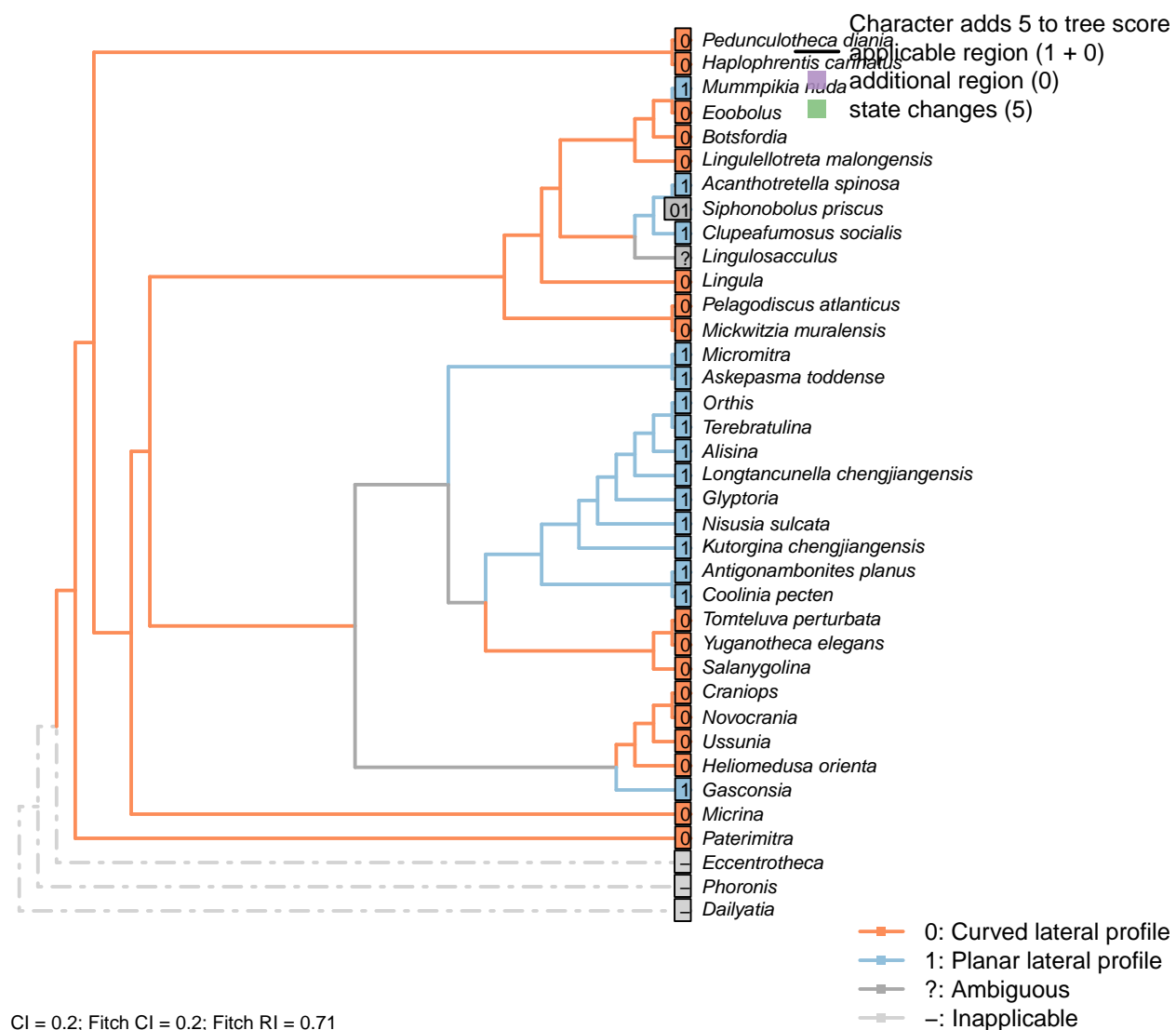
*Clupeafumosus socialis*: See Topper *et al.* (2013a).

*Eoobolus*: See for example Skovsted & Holmer (2005), pl. 3.

*Lingulellotreta malongensis*: Transverse cross section of ventral pseudointerarea concave.

*Mummpikia nuda*: Balthasar (2008) interprets an inward-growing posterior margin of the pseudointerarea – e.g. p273, “Of particular interest is the vault that bridges the most anterior portion of the ventral pseudointerarea and raises it above the visceral platform [...] An inward-growing posterior margin is otherwise known only from the pseudointerareas of linguliform brachiopods”.

### [37] Posterior surface: Planar



#### Character 37: Sclerites: Ventral valve: Posterior surface: Planar

0: Curved lateral profile

1: Planar lateral profile

Neomorphic character.

It is possible for a cardinal area or pseudointerarea to be distinct from the anterior part of the shell, yet to remain curved in lateral profile.

Taking an undifferentiated posterior margin as primitive, the primitive condition is curved – flattening of the posterior margin represents an additional modification that can only occur once the posterior margin is differentiated.

A flat and triangular interarea links *Mummpikia* with the Obolellidae (Balthasar, 2008) – but all included taxa have triangular interareas, so this is not listed as a separate character.

*Acanthotretella spinosa*: ventral pseudointerareas are most similar to those found within the Order Siphonotretida.

*Botsfordia*: See Skovsted & Holmer (2005), pl. 3, fig. 14.

*Clupeafumosus socialis*: “Ventral pseudointerarea is gently procline and is flat in lateral profile”. — (Topper et al., 2013a).

*Eoobolus*: Some curvature retained.

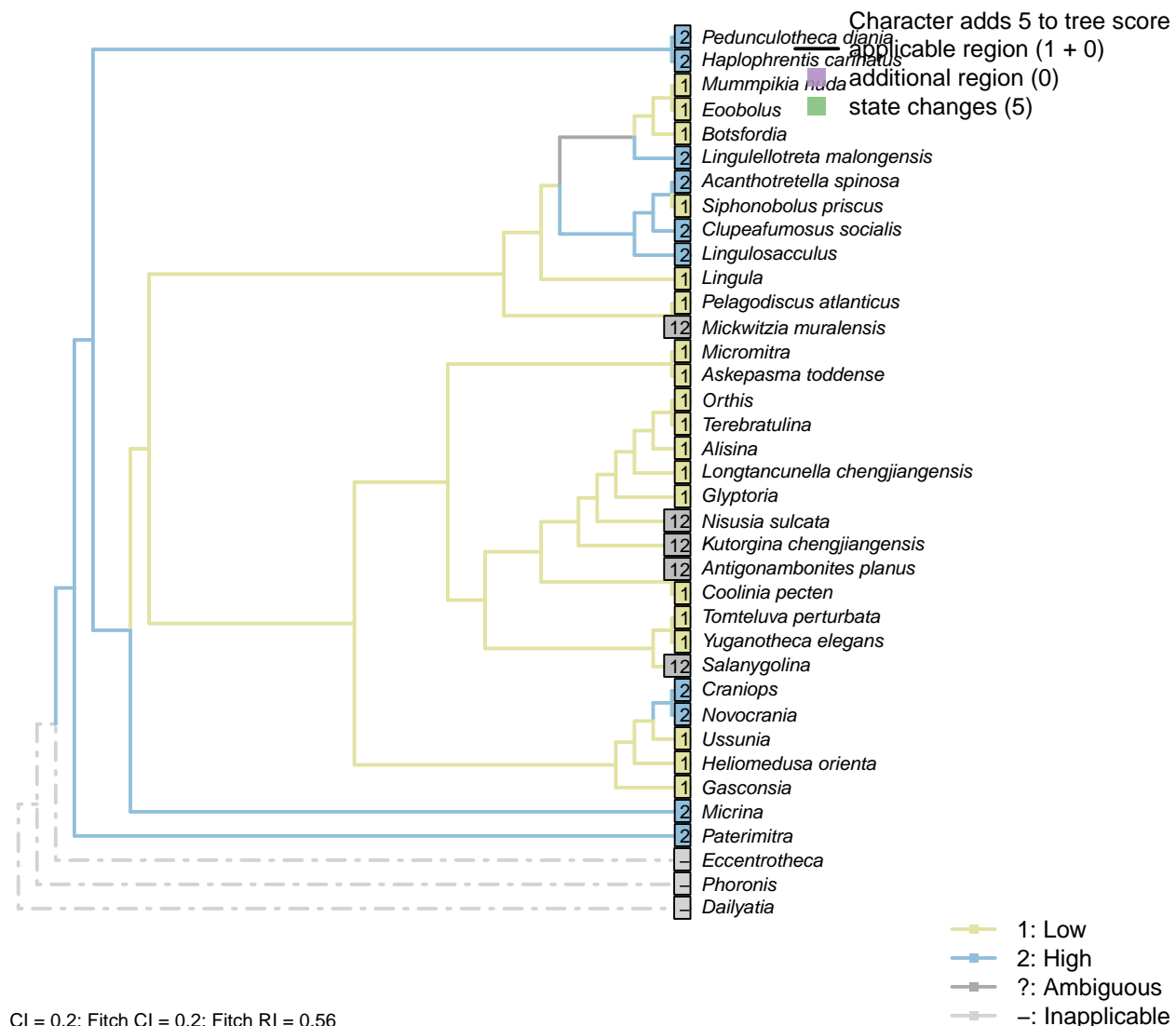
*Lingulellotreta malongensis*: Transverse cross section of ventral pseudointerarea concave.

*Longtancunella chengjiangensis*: Flattened, reflecting the strophic hinge line.

*Micromitra*: Essentially planar; see fig. 6 in Ushatinskaya (2016).

*Siphonobolus priscus*: ‘Almost’ planar – see Popov et al. (2009, fig. 4). Coded as ambiguous.

## [38] Posterior surface: Extent



## Character 38: Sclerites: Ventral valve: Posterior surface: Extent

1: Low

2: High

Transformational character.

Distinguishes taxa whose ventral valve is essentially flat from those that are essentially conical.

*Antigonambonites planus*: Though scored High in data matrix of Benedetto (2009), this taxon (see Williams et al., 2000, fig. 508) does not express the deeply conical ventral valve that this character is intended to reflect. It is charitably coded as ambiguous.

*Clupeafumosus socialis*: Entire valve length – see schematic in Williams et al. (1997), fig. 286.

*Coolinia pecten*: See fig. 485 in Williams et al. (2000).

*Gasconsia*: “ventral cardinal interarea low, apsacline, with narrow, poorly defined homeodeltidium” – Williams et al. (2000), p. 186.

*Kutorgina chengjiangensis*: This taxon (see Williams et al., 2000, fig. 129; Popov, 1992, fig. 1) comes close

to expressing the deeply conical ventral valve that this character is intended to reflect, though this is not always so pronounced (e.g. Williams et al., 2000, fig. 125). It is therefore coded as ambiguous.

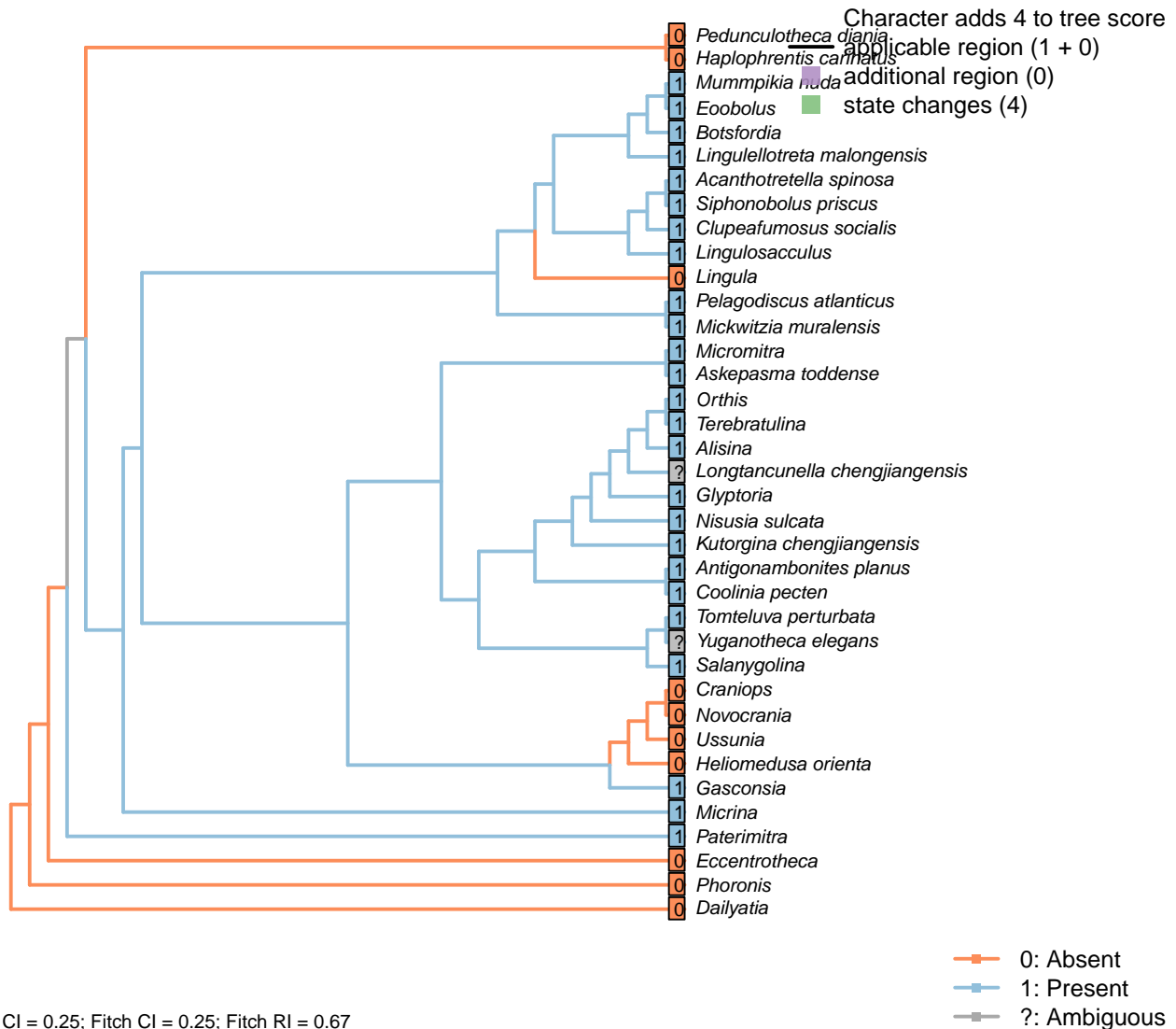
*Mickwitzia muralensis*: Often not prominently high (Skovsted and Holmer, 2003; Balthasar, 2004), though in some cases (e.g. Butler et al., 2015) the ventral valve approaches the conical shape that this character is intended to capture. Coded as polymorphic.

*Nisusia sulcata*: Scored as high in data matrix of Benedetto (2009), and depicted as such in Williams et al. (2000, fig. 125) and Popov (1992, fig. 1); but not high in all specimens (e.g. Williams et al., 2000, fig. 126). It is therefore coded as polymorphic.

*Orthis*: Scored ‘Low’ for *Eoorthis* by Benedetto (2009); assumed same in *Orthis*.

*Salanygolina*: Whereas Williams et al. (2000, p. 156) describe the ventral pseudointerarea as high, the shell lacks the deeply conical aspect that this character is intended to capture; we thus code the taxon as ambiguous.

### [39] Posterior surface: Delthyrium



Character 39: Sclerites: Ventral valve: Posterior surface: Delthyrium

0: Absent

1: Present

Neomorphic character.

A delthyrium is an opening in an interarea or pseudointerarea that accommodates the pedicle, and may be filled with plates.

The homology of the pedicle in the pseudointerarea of obolellids and botsfordiids with the umbonal pedicle foramen of acrotretids was proposed by Popov (1992), and seemingly corroborated by observations of Ushatinskaya & Korovnikov (2016), who note that the propareas of the *Botsfordia* ventral valve sometimes merge to form an elongate teardrop-shaped pedicle foramen.

*Acanthotretella spinosa*: Origin modelled on *Siphonobolus*.

*Askepasma toddense*: Homeodeltidium absent (Williams et al., 2000, p. 153); deltidium is open (see Topper et al., 2013b, fig. 4).

*Botsfordia*: The homology of the triangular notch or groove in the pseudointerarea with the umbonal pedicle foramen of acrotretids was proposed by Popov (1992), and seemingly corroborated by observations of Ushatinskaya & Korovnikov (2016), who note that the propareas of the *Botsfordia* ventral valve sometimes merge to form an elongate teardrop-shaped pedicle foramen.

*Clupeafumosus socialis*: Following Popov (1992), the larval delthyrium is sealed in adults by outgrowths of the posterolateral margins of the shell.

*Eoobolus*: See for example fig. 5 in Balthasar (2009).

*Glyptoria*: “Delthyrium and notothyrium open, wide” – Cooper (1976).

*Longtancunella chengjiangensis*: Unclear: a narrow ridge that may correspond to a pseudodeltidium evident in fig 2a and sketched in fig. 2c is not discussed in the text of Zhang et al. (2011a), so the delthyrial region is coded as ambiguous.

*Mickwitzia muralensis*: A delthyrium is present in young individuals (Balthasar, 2004).

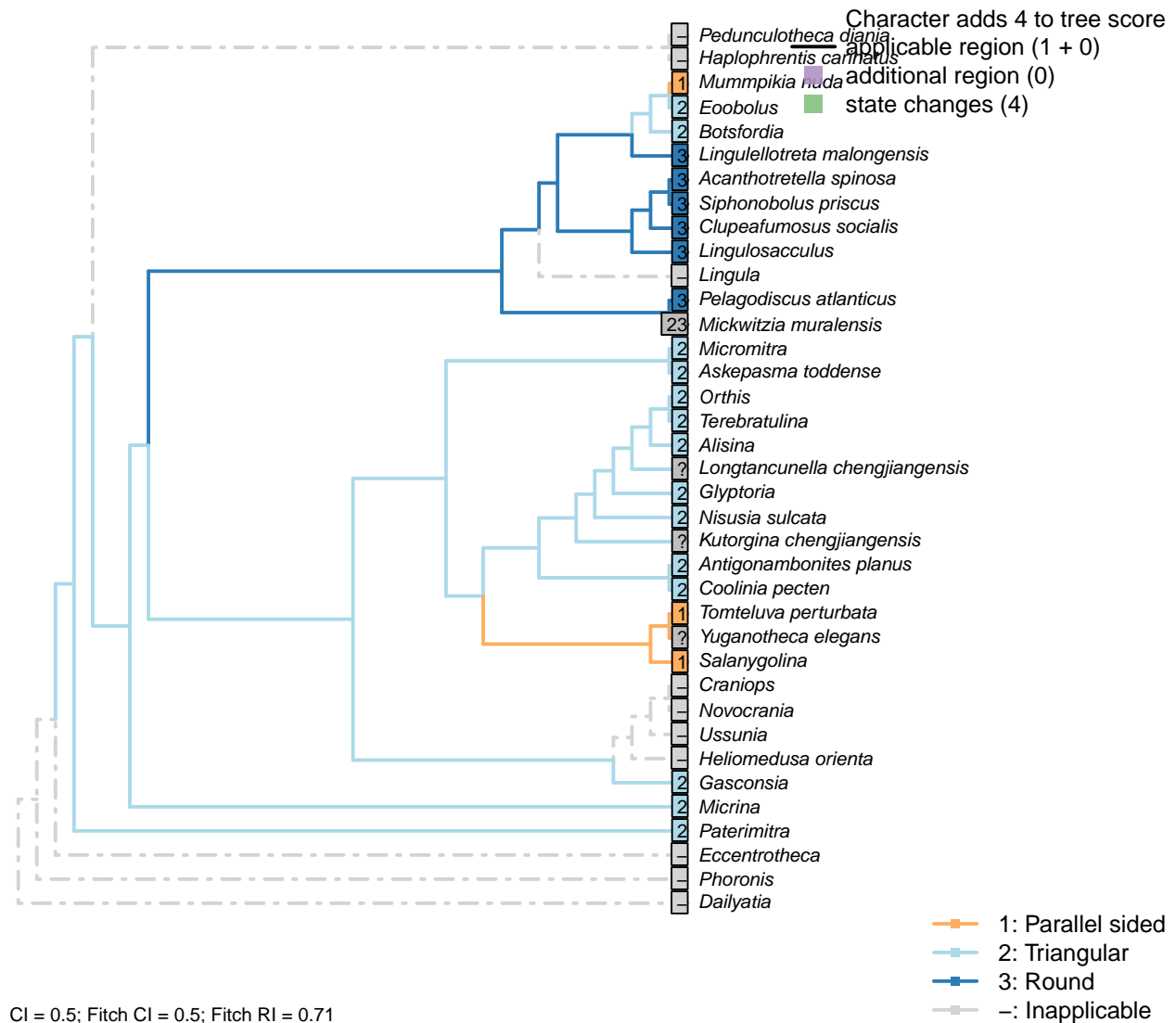
*Micrina*: Opening inferred by Holmer et al. (2008).

*Pelagodiscus atlanticus*: The listrum (pedicle opening) is interpreted as originating via a similar mechanism to that of acrotretids (Popov, 1992), and hence corresponding to a basally sealed delthyrium.

*Siphonobolus priscus*: Ontogeny presumed to resemble that of acrotretids.

*Yuganotheca elegans*: Details of the hinge region are unclear due to the flattened and overprinted nature of fossil preservation.

### [40] Posterior surface: Delthyrium: Shape



#### Character 40: Sclerites: Ventral valve: Posterior surface: Delthyrium: Shape

1: Parallel sided

2: Triangular

3: Round

Transformational character.

A parallel-sided delthyrium links *Mummpikia* with the Obolellidae (Balthasar, 2008).

Following Popov (1992), the larval delthyrium of acrotretids and allied taxa is understood to be sealed in adults by outgrowths of the posterolateral margins of the shell. The resultant round or teardrop-shaped foramen corresponds to the delthyrium.

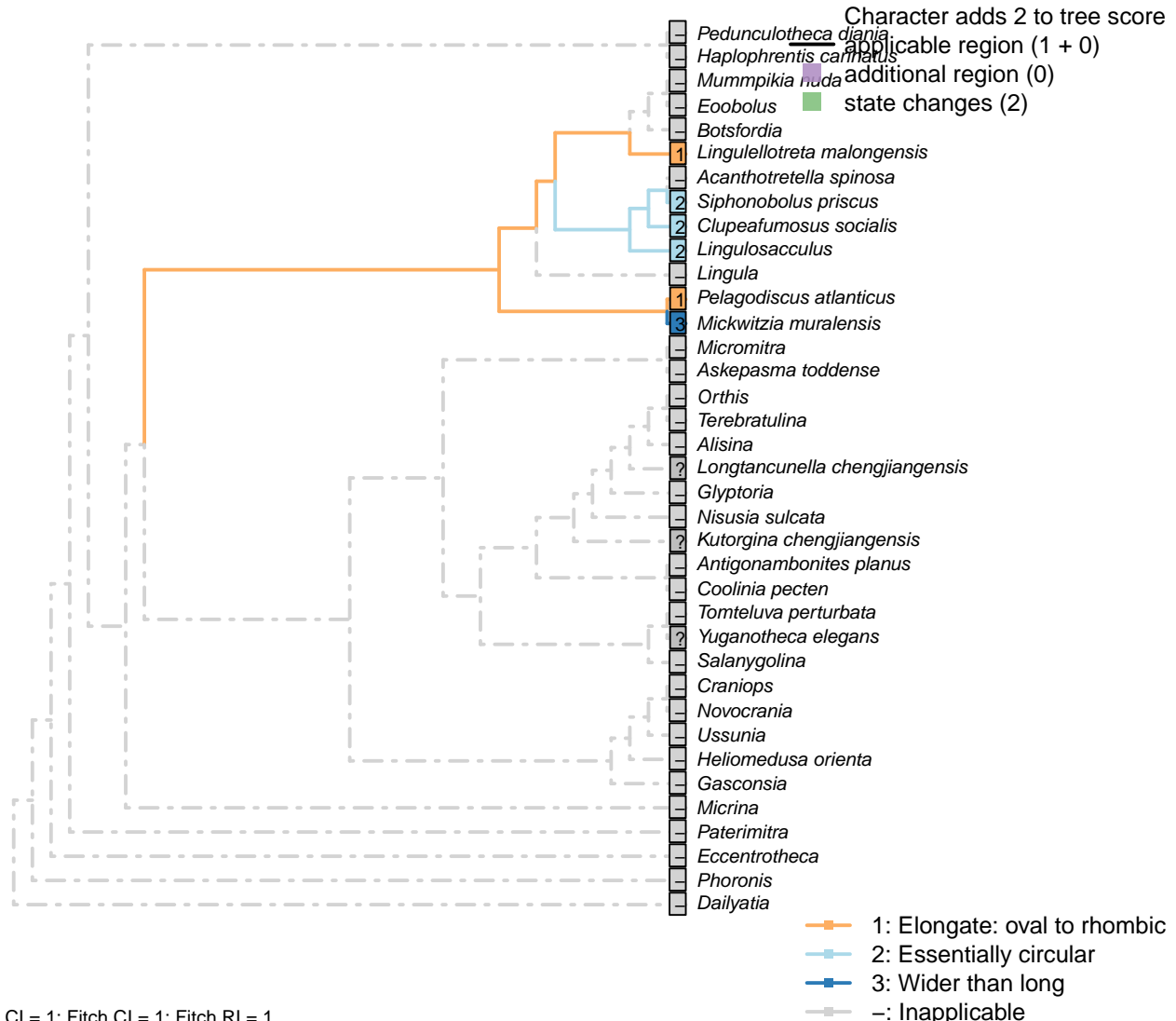
*Askepasma toddense*: Prominently triangular (see Topper et al., 2013b, fig. 2).

*Clupeafumosus socialis*: Following the model of Popov (1992).

*Mickwitzia muralensis*: An opening is incorporated at the base of the homeodeltidium when the organism switches from early to late maturity (fig. 10 in Balthasar, 2004). This opening is conceivably homologous

with the pedicle foramen of acrotretid brachiopods and their ilk. To reflect this possible homology, *Mickwitzia* is coded as polymorphic (triangular/round).

#### [41] Posterior surface: Delthyrium: Shape: Aspect of rounded opening



#### Character 41: Sclerites: Ventral valve: Posterior surface: Delthyrium: Shape: Aspect of rounded opening

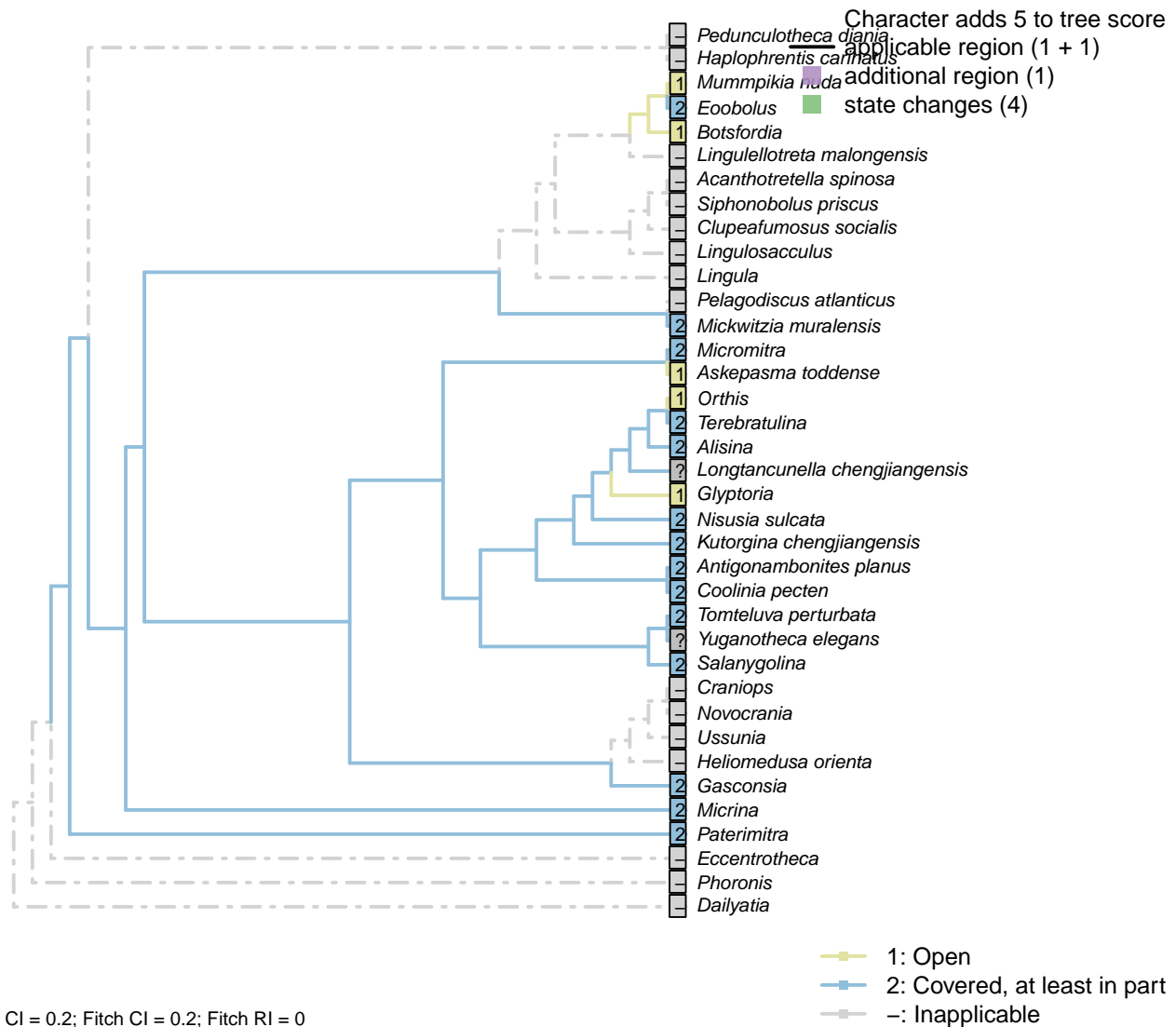
- 1: Elongate: oval to rhombic
- 2: Essentially circular
- 3: Wider than long
- Transformational character.

Chen *et al.* (2007) propose that an oval to rhombic foramen characterises the discinids [and *Heliomedusa*, though the foramen in this taxon has since been reinterpreted by Zhang *et al.* (2009) as an impression of internal tissue].

*Lingulellotreta malongensis*: Oval (Williams *et al.*, 2000).

*Mickwitzia muralensis*: Wider than long: see fig. 10 in Balthasar (2004).

## [42] Posterior surface: Delthyrium: Cover



### Character 42: Sclerites: Ventral valve: Posterior surface: Delthyrium: Cover

1: Open

2: Covered, at least in part

Transformational character.

An open delthyrium links *Mummpikia* with the Obolellidae (Balthasar, 2008).

The delthyrial opening can be covered by one or more deltidial plates, or a pseudodeltitium.

Inapplicable in taxa with a round delthirum (generated by overgrowth of the delthyrial opening by postero-

lateral parts of the shell, per Popov, 1992).

*Askepasma toddense*: Open (Topper et al., 2013b).

*Botsfordia*: See pl. 3 fig. 15 in Skovsted & Holmer (2005).

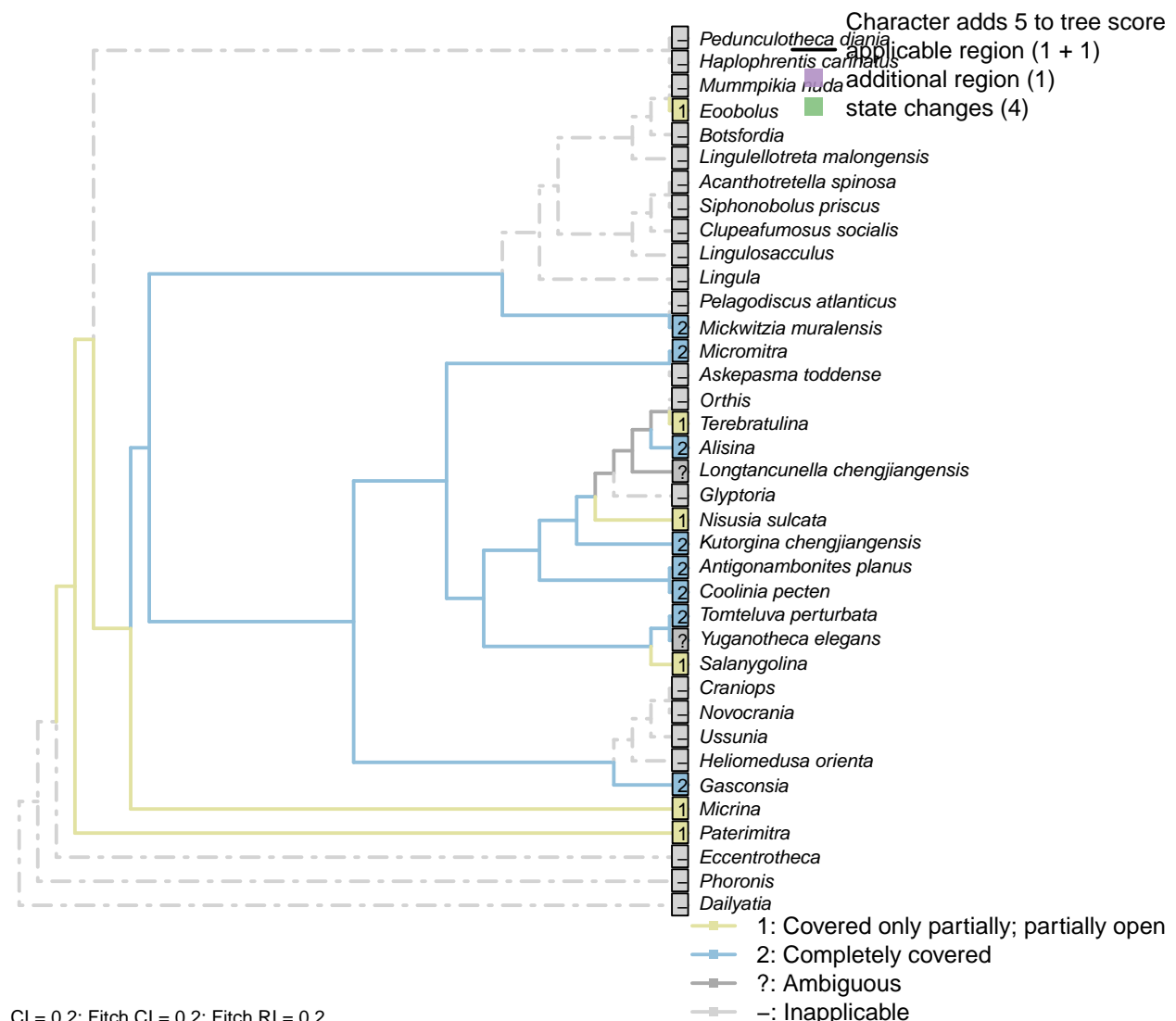
*Coolinia pecten*: A convex pseudodeltidium completely covers the delthyrium in *Coolinia*.

*Glyptoria*: Coded as open by Williams *et al.* (1998).

*Nisusia sulcata*: “Covered only apically by a small convex pseudodeltitium” – Holmer et al. (2018a).

*Paterimitra*: Covered by subaical flange, in part.

### [43] Posterior surface: Delthyrium: Cover: Extent



#### Character 43: Sclerites: Ventral valve: Posterior surface: Delthyrium: Cover: Extent

1: Covered only partially; partially open

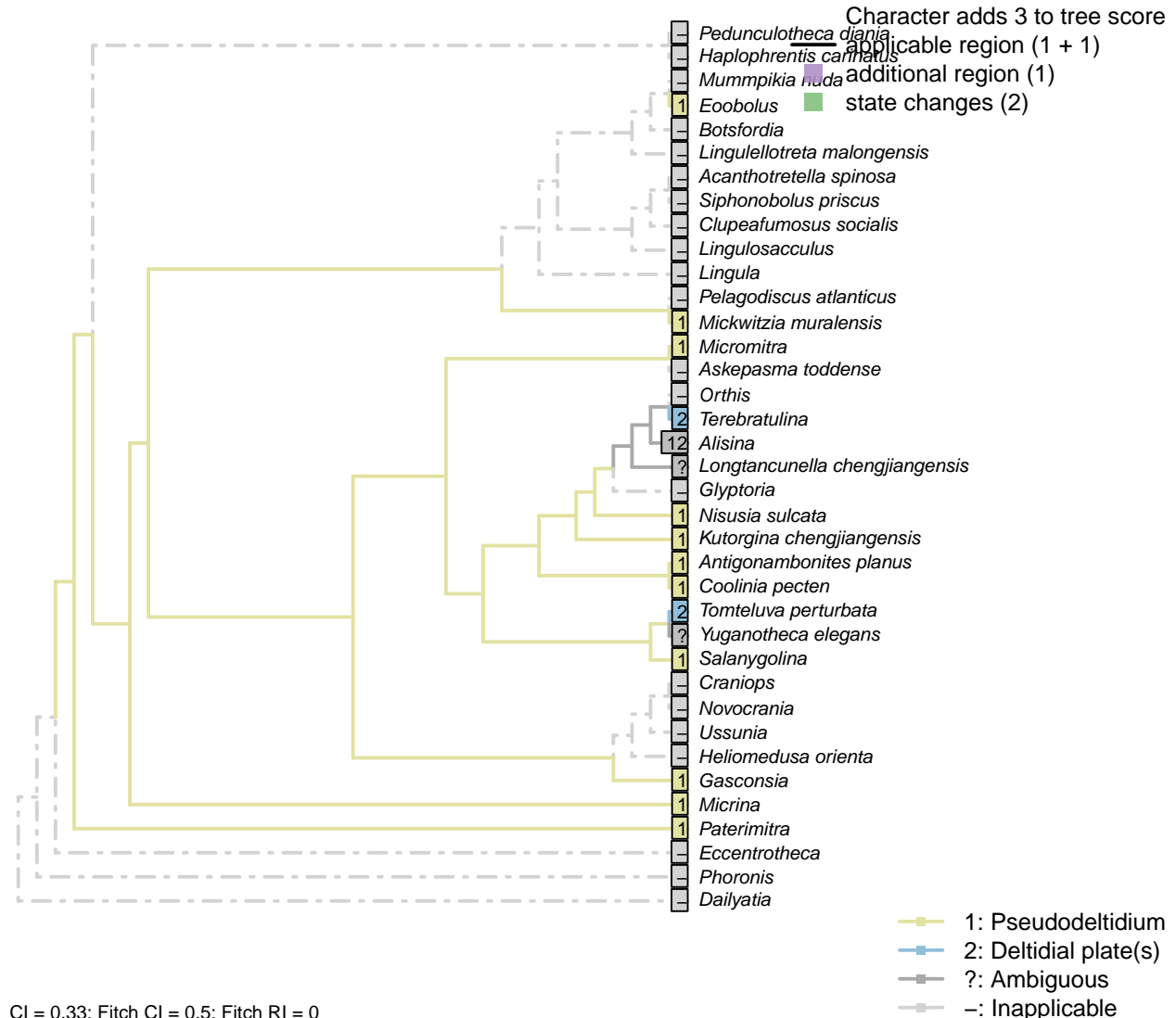
2: Completely covered

Transformational character.

*Micrina*: Remains somewhat open.

*Nisusia sulcata*: A well-defined pseudo-deltidium [...] closes only the apical part of the delthyrium (Rowell and Caruso, 1985).

#### [44] Posterior surface: Delthyrium: Cover: Identity



CI = 0.33; Fitch CI = 0.5; Fitch RI = 0

**Character 44: Sclerites: Ventral valve: Posterior surface: Delthyrium: Cover: Identity**

- 1: Pseudodeltidium
- 2: Deltidial plate(s)
- Transformational character.

This character has the capacity for further resolution (one or more deltidial plates), but this is unlikely to affect the results of the present study.

The pseudodelthyrium is also referred to as a homeodeltidium.

*Alisina*: Stated as “concave pseudodeltidium with median plication” – Williams et al. (2000)  
Coded as “Pseudodeltidium: Covered by concave plate” by Bassett et al. (2001).

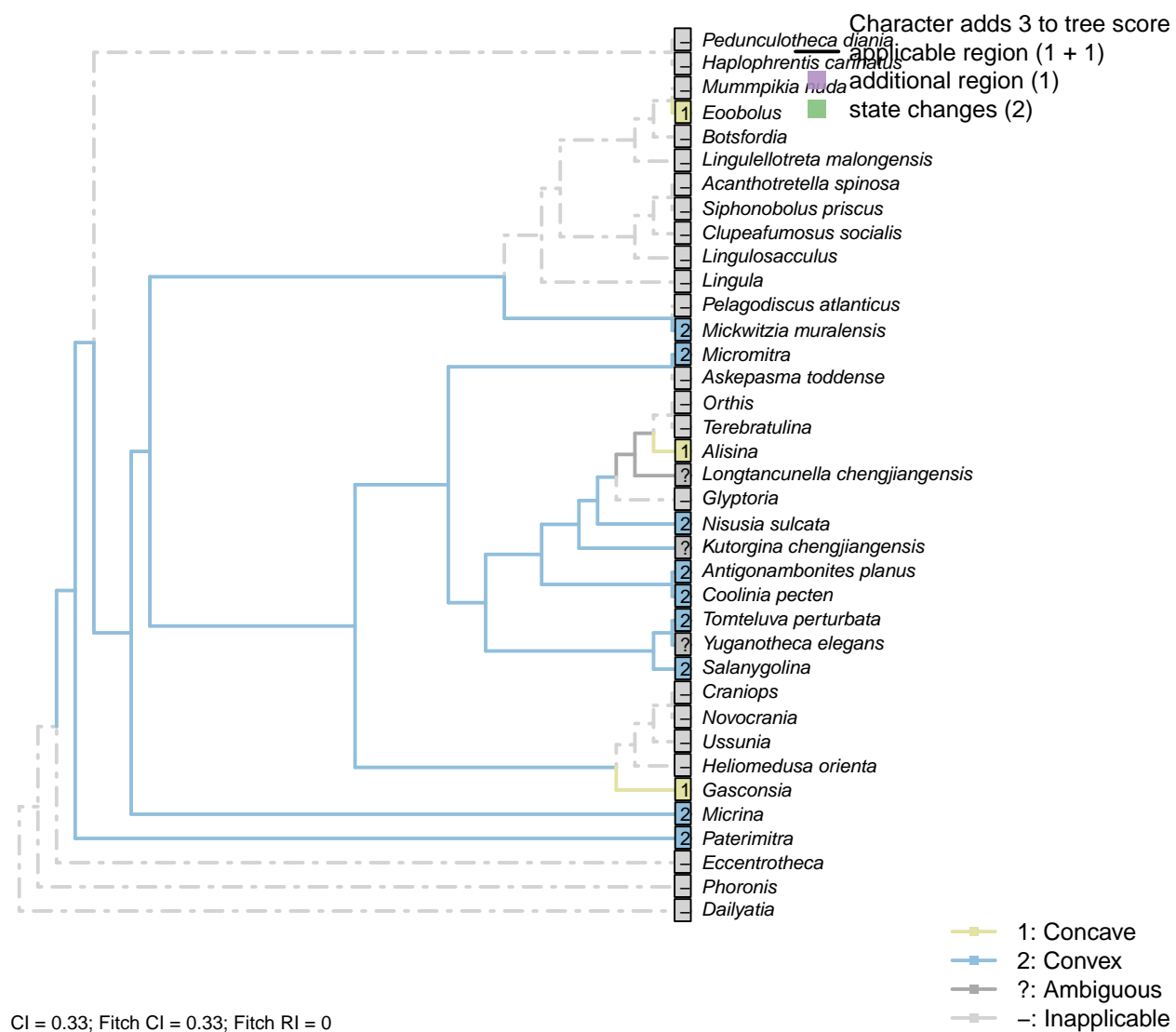
*Askepasma toddense*: No pseudodeltidium (Williams et al., 2000, p. 153).

*Lingulellotreta malongensis*: The subapical flange of the *Paterimitra* S1 sclerite has been homologised with the ventral homeodeltidium of *Micromitra* (Larsson et al., 2014).

*Mickwitzia muralensis*: Termed a homoedeltidium by Balthasar (2004).

*Micrina*: “Ventral valve convex with apsacline interarea bearing delthyrium, covered by a convex pseudodeltidium” – Holmer et al. (2008).

#### [45] Posterior surface: Delthyrium: Pseudodeltidium: Shape



Character 45: Sclerites: Ventral valve: Posterior surface: Delthyrium: Pseudodeltidium: Shape

- 1: Concave
- 2: Convex
- Transformational character.

A ridge-like (i.e. convex) pseudodeltidium unites *Salanygolina* with *Coolinia* and other Chileata (Holmer et al., 2009, p. 6).

*Alisina*: “concave pseudodeltidium with median plication” – Williams et al. (2000)  
Coded as “Pseudodeltidium: Covered by concave plate” by Bassett et al. (2001).

*Antigonambonites planus*: Convex (Williams et al., 2000, fig. 508).

*Gasconsia*: *Gasconsia* possesses narrow concave homeodeltidium, but absent pseudodeltidium.

*Kutorgina chengjiangensis*: Difficult to determine based on material presented in Zhang et al. (2007b), or indeed for other species in the genus (e.g. Williams et al., 2000; Skovsted and Holmer, 2005; Holmer et al., 2018b).

*Mickwitzia muralensis*: Convex (see Balthasar, 2004, fig. 4B).

*Micrina*: Convex deltoid (Holmer et al., 2008).

*Micromitra*: Gently convex (see Williams et al., 2000, fig. 83.3).

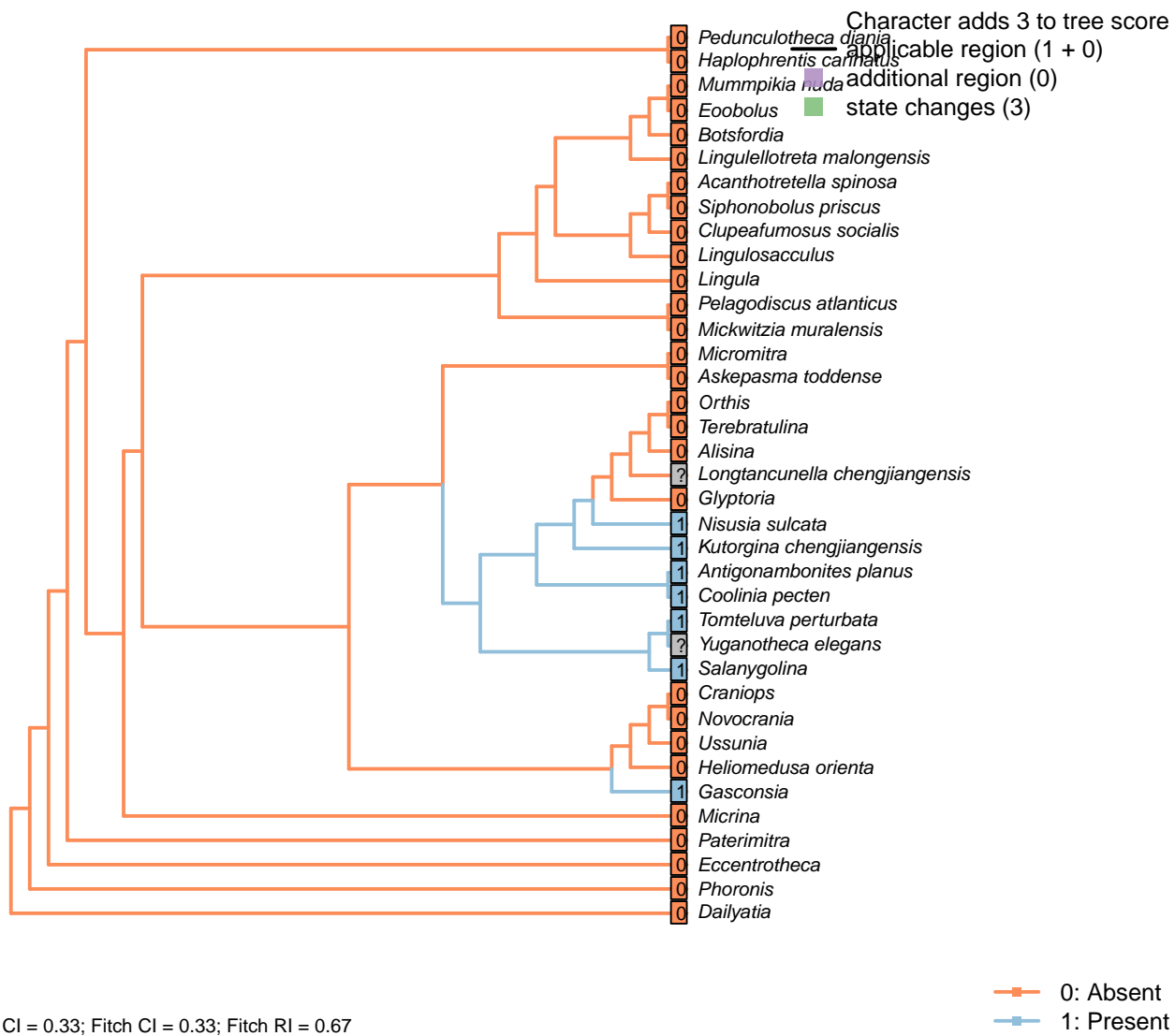
*Nisusia sulcata*: Convex in *Nisusia* (see Rowell and Caruso, 1985, fig. 8.4).

*Paterimitra*: Gently convex (see Williams et al., 2000, fig. 83.1).

*Salanygolina*: “The presence of [...] a narrow delthyrium covered by a convex pseudodeltidium, places Salanygolinidae outside the Class Paterinata and strongly suggests affinity to the Cambrian Chileida” – Holmer et al. (2009), p. 9.

*Tomteluva perturbata*: Convex (Streng et al., 2016).

## [46] Posterior surface: Delthyrium: Pseudodeltidium: Hinge furrows



**Character 46: Sclerites: Ventral valve: Posterior surface: Delthyrium: Pseudodeltidium: Hinge furrows**

0: Absent

1: Present

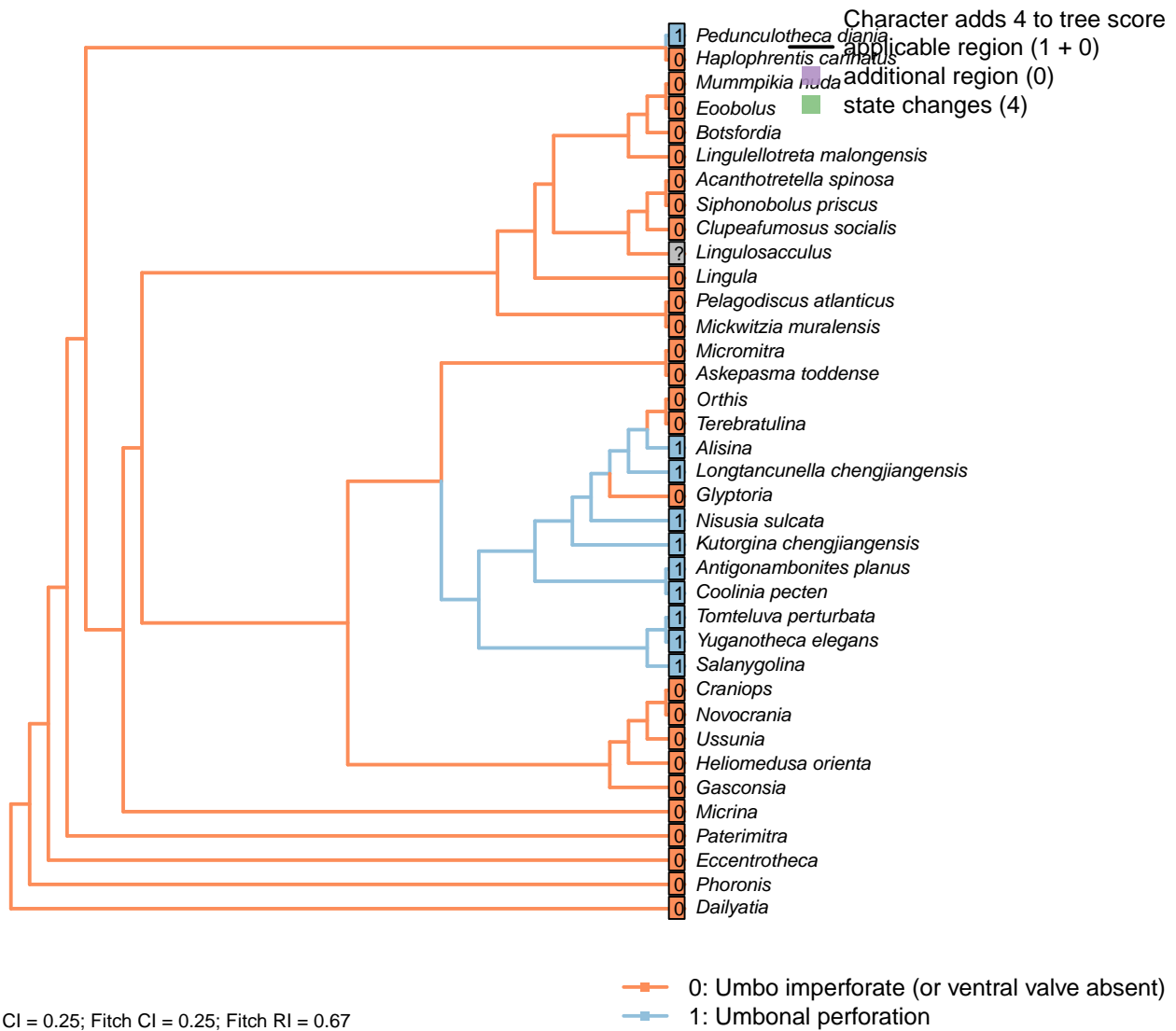
Neomorphic character.

After Bassett *et al.* (2001) character 18, "Hinge furrows on lateral sides of pseudodeltidium".

*Acanthotretella spinosa*, *Askepasma toddense*, *Clupeafumosus socialis*, *Dailyatia*, *Eccentrotheca*, *Glyptoria*, *Haplophrentis carinatus*, *Heliomedusa orienta*, *Lingula*, *Lingulellotreta malongensis*, *Lingulosacculus*, *Micrina*, *Micromitra*, *Mummpikia nuda*, *Novocrania*, *Orthis*, *Paterimitra*, *Pedunculotheca diania*, *Pelagodiscus atlanticus*, *Phoronis*, *Terebratulina*: Absent due to inapplicability of neomorphic character.

*Salanygolina*: The presence of this feature is impossible to determine based on the available material.

## [47] Umbonal perforation



### Character 47: Sclerites: Ventral valve: Umbonal perforation

0: Umbo imperforate (or ventral valve absent)

1: Umbonal perforation

Neomorphic character.

Certain taxa, particularly those with a colleplax, exhibit a perforation at the umbo of the ventral valve. This opening is sometimes associated with a pedicle sheath, which emerges from the umbo of the ventral valve without any indication of a relationship with the hinge.

In contrast, the pedicle of acrotretids and similar brachiopods is situated on the larval hinge line, but is later surrounded by the posterolateral regions of the growing shell to become separated from the hinge line, and encapsulated in a position close to (or with resorption of the benthic shell, at) the umbo (see Popov, 1992, pp. 407–411 and fig. 3 for discussion). In some cases, an internal pedicle tube attests to this origin – potentially corresponding to the pedicle groove of lingulids. As such, the pedicle foramen of acrotretids and allies is not originally situated at the umbo; it is instead understood to represent a basally sealed delthyrium.

*Clupeafumosus socialis*: The presumed pedicle foramen reported by Topper *et al.* (2013a) is at the ventral

valve umbo. No evidence of an internal pedicle tube is present, but we follow Popov (1992) in inferring the encapsulation of the pedicle foramen.

*Dailyatia*: The B and C sclerites of *Dailyatia* bear small umbonal perforations (Skovsted et al., 2015), but these are not considered to be homologous with the ventral valve, so this character is coded as inapplicable – though the possibility that the perforations are equivalent is intriguing.

A1 sclerites typically have a pair of perforations, which are conceivably equivalent to the setal tubes of *Micrina* (Holmer et al., 2011). The A1 sclerite of *D. bacata* has a structure that is arguably similar to the ‘colleplax’ of *Paterimitra*. But the homology of any of these structures to the umbonal aperture of brachiopods is difficult to establish.

*Eccentrotheca*: The sclerites of *Eccentrotheca* form a ring that surrounds the inferred attachment structure; the attachment structure does not emerge from an aperture within an individual sclerite. Thus no feature in *Eccentrotheca* is judged to be potentially homologous with the apical perforation in bivalved brachiopods.

*Heliomedusa orienta*: There is “compelling evidence to demonstrate that the putative pedicle illustrated by Chen et al. (2007, Figs. 4, 6, 7) in fact is the mold of a three-dimensionally preserved visceral cavity.” – Zhang et al. (2009).

*Lingulosacculus*: The apical termination of the fossil is unknown.

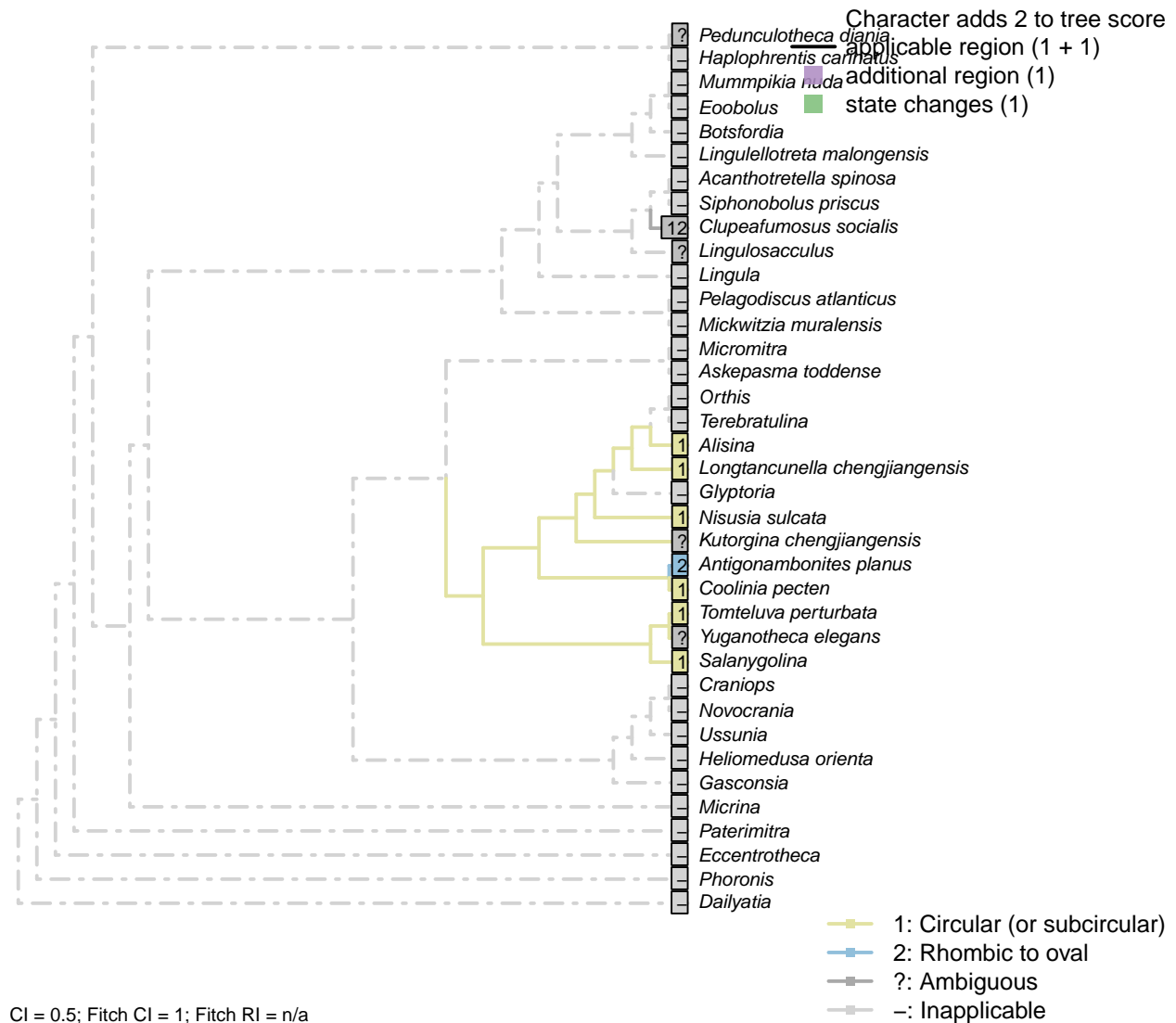
*Mickwitzia muralensis*: The umbo itself is imperforate (Balthasar, 2004).

*Paterimitra*: The presumed pedicle foramen is an opening between the S1 and S2 sclerites, neither of which are perforated (Skovsted et al., 2009).

*Siphonobolus priscus*: Prominent subcircular perforation at umbo associated with an internal pedicle tube (Popov et al., 2009), thus presumed to share an origin with the acrotretid pedicle foramen.

*Tomteluva perturbata*: Streng et al. (2016) observe “an internal tubular structure probably representing the ventral end of the canal within the posterior wall of the pedicle tube”, but do not consider this tomteluvid tube to be homologous with the pedicle tube of acrotretids and their ilk, stating (p. 274) that it appears to be unique within Brachiopoda.

### [48] Umbonal perforation: Shape



#### Character 48: Sclerites: Ventral valve: Umbonal perforation: Shape

1: Circular (or subcircular)

2: Rhombic to oval

Transformational character.

*Acanthotretella spinosa*: Too small to observe given quality of preservation (Holmer and Caron, 2006).

*Alisina*: Seemingly circular (Zhang et al., 2011b).

*Antigonambonites planus*: Based on p.92, fig.4B.

*Clupeafumosus socialis*: Taller than wide in some cases, but very nearly circular in others; see Topper *et al.* (2013a).

*Coolinia pecten*: Bassett and Popov write “a dominant feature of the ventral umbo is a sub-oval perforation about 270 µm long and 250 µm wide”: the width and height of this structure are almost identical, and we

score it as (sub) circular.

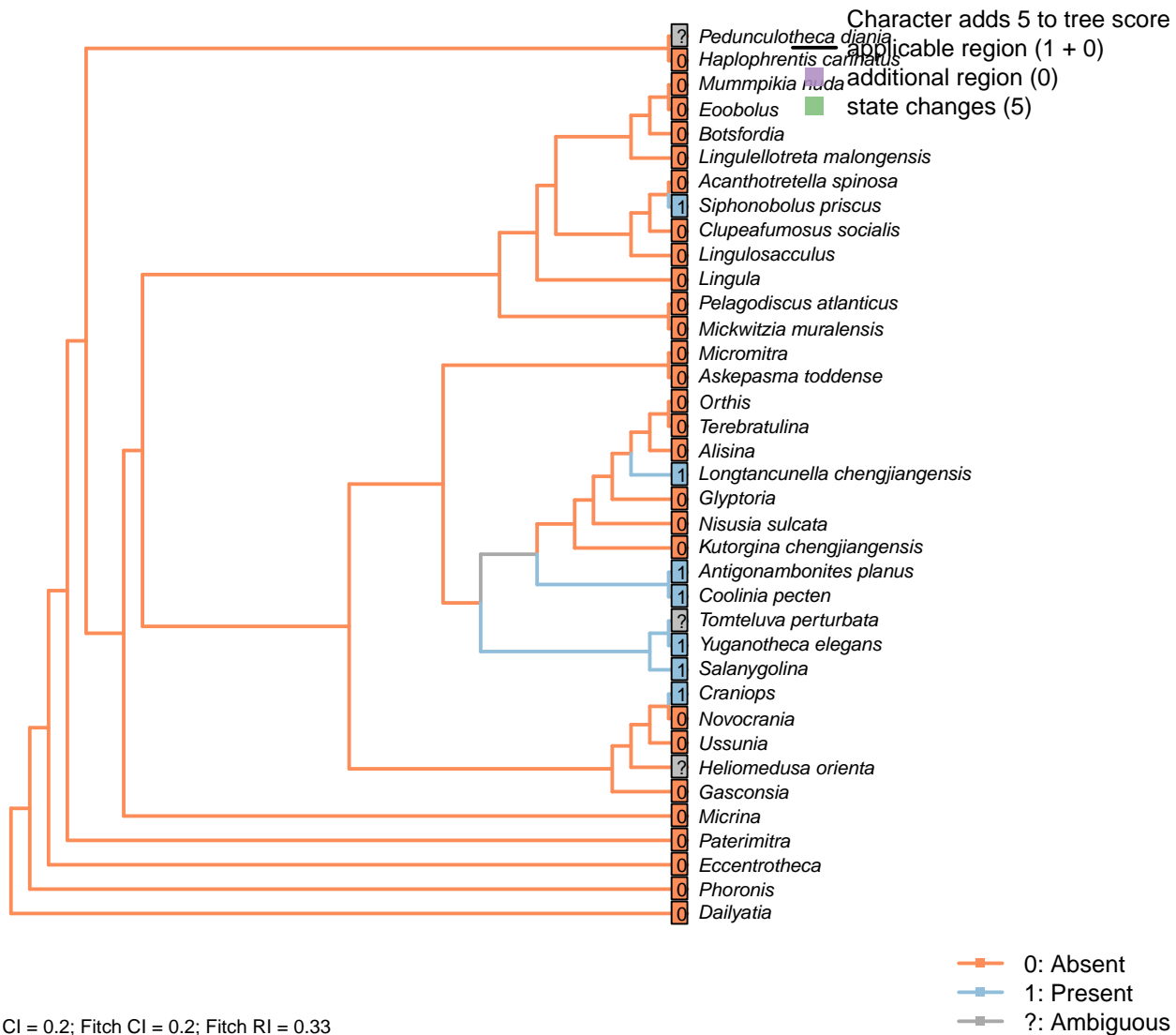
*Heliomedusa orienta*: Rhombic to oval – seen as evidence for a discinid affinity (Chen et al., 2007).

*Kutorgina chengjiangensis*: The exact size and shape of the apical perforation is obscured by the emerging pedicle.

*Nisusia sulcata*: “close to circular” (Holmer et al., 2018a).

*Salanygolina*: Essentially circular (Holmer et al., 2009, fig. 4).

#### [49] Colleplax, cicatrix or pedicle sheath



CI = 0.2; Fitch CI = 0.2; Fitch RI = 0.33

#### Character 49: Sclerites: Ventral valve: Colleplax, cicatrix or pedicle sheath

0: Absent

1: Present

Neomorphic character.

In certain taxa, the umbo of the ventral valve bears a colleplax, cicatrix or pedicle sheath; Bassett *et al.* (2008) consider these structures as homologous.

*Botsfordia*: Following Williams *et al.* (1998), appendix 2.

*Clupeafumosus socialis*: Not reported by Topper *et al.* (2013a).

*Craniops*: *Paracraniops* is “externally similar to *Craniops*, but lacking cicatrix” – indicating that *Craniops* bears a cicatrix (Williams *et al.*, 2000). Also coded as present in their table 15.

*Heliomedusa orienta*: A cicatrix was reconstructed by Jin and Wang (1992) (figs 6b, 7), but has not been reported by later authors; possibly, as with the ‘pedicle foramen’ of Chen *et al.* (2007), this structure represents internal organs rather than a cicatrix proper (Zhang *et al.*, 2009); as such it has been recorded as ambiguous.

*Kutorgina chengjiangensis*: The umbonal region of kutorginides “clearly lacks a pedicle sheath” (Holmer *et al.*, 2018b).

*Lingulellotreta malongensis*: The pedicle is identified as such (rather than a pedicle sheath) by the internal pedicle tube.

*Longtancunella chengjiangensis*: A ring-like structure surrounding the pedicle is interpreted as a colleplax (Zhang *et al.*, 2011a), though the authors make no comparison with the pedicle capsule exhibited by extant terebratulids (see Holmer *et al.*, 2018a).

*Micrina*: Absent in *Micrina* (Holmer *et al.*, 2011).

*Pedunculotheca diana*: The flat apical termination of juvenile individuals possibly functioned as colleplax for attachment, but may simply represent the brepthic shell; we treat it as ambiguous to reflect this potential homology.

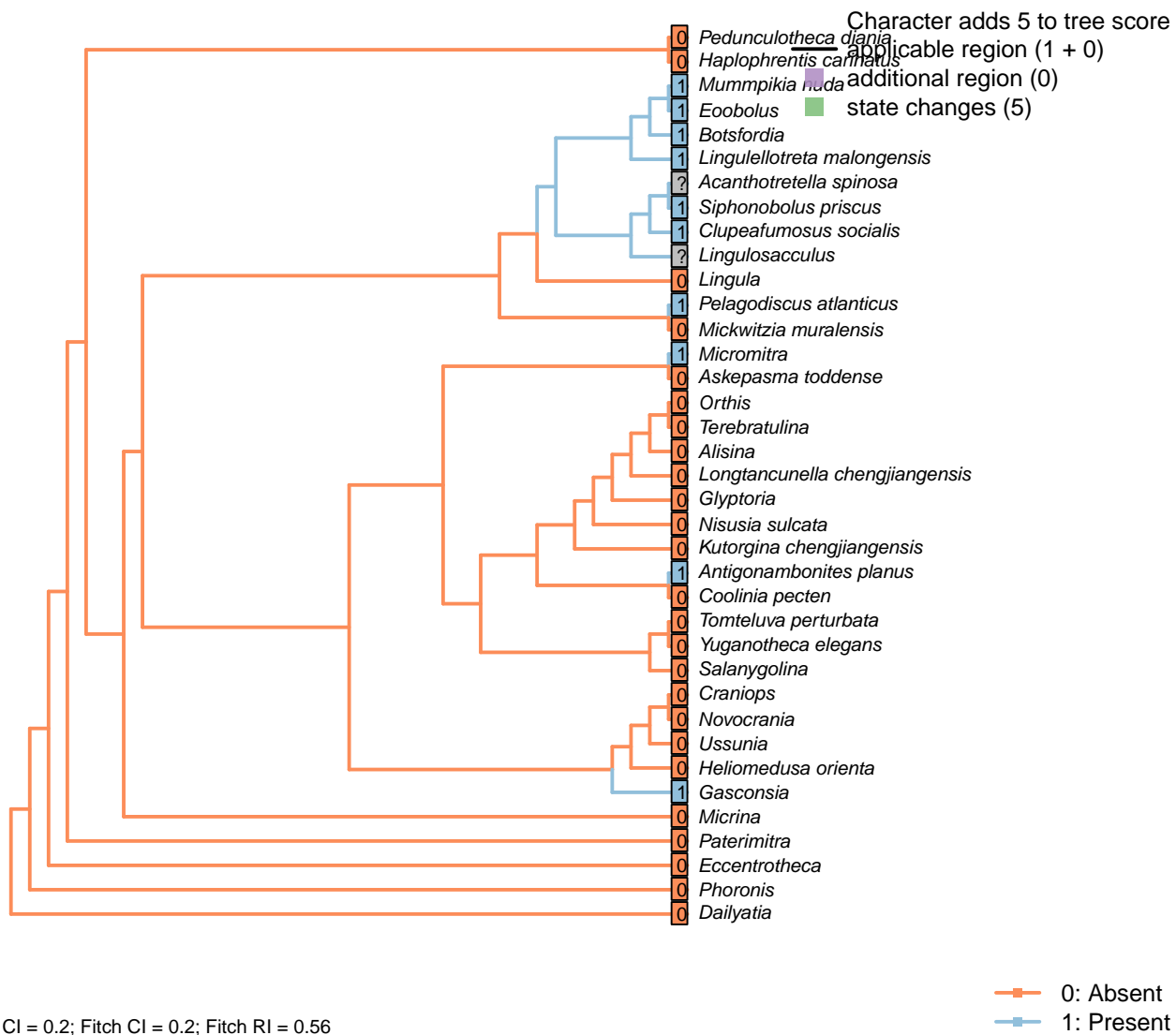
*Siphonobolus priscus*: Coded as present in view of the attachment scar, which has been considered homologous with the “adult colleplax and foramen with attachment pad” in *Salanygolina* (Popov *et al.*, 2009).

*Tomteluva perturbata*: The internal canal associated with the pedicle is unique to the tomteluvids, and has an uncertain identity (Streng *et al.*, 2016). It could conceivably correspond to an internalized pedicle sheath or an equivalent structure, so this feature is coded as ambiguous here.

*Ussunia*: Following table 15 in Williams *et al.* (2000).

*Yuganotheca elegans*: The median collar or conical tube is conceivably homologous with the pedicle sheath.

## [50] Median septum



## Character 50: Sclerites: Ventral valve: Median septum

0: Absent

1: Present

Neomorphic character.

Chen *et al.* (2007) observe a median septum in what they interpret as the ventral valve of *Heliomedusa*, and the ventral valve of *Discinisca*, which they propose points to a close relationship.

*Acanthotretella spinosa*: Carbonaceous preservation confounds the identification of internal shell structures;

it is possible that this feature is present, but not observable in the Burgess Shale material.

*Botsfordia*: Following Williams et al. (1998), appendix 2.

*Clupeafumosus socialis*: A short medial ridge (septum) is present in the ventral valve (Topper et al., 2013a).

*Eoobolus*: Prominent median septum (fig. 4d, e in Balthasar, 2009).

*Gasconsia*: Evident in moulds of ventral valve; see Watkins (2002).

*Glyptoria*: Neither evident nor reported in Williams et al. (2000).

*Haplophrentis carinatus*: The carina of *H. carinatus* is an angular elevation of the ventral valve surface, rather than a septum growing inward on the interior of shell.

*Helomedusa orienta*: Reported on ‘ventral’ valve by Chen et al. (2007); we consider the ‘ventral’ valve to be the dorsal valve.

*Lingulellotreta malongensis*: Medial septum visible in ventral valve in Williams et al. (2000), fig. 34.1c.

*Micromitra*: Ventral ridge characteristic of *Micromitra* (Skovsted and Peel, 2010).

*Mummpikia nuda*: “Some specimens also reveal that the vault had a slight median septum, which is now visible as a notch or a groove dividing the right from the left part” – Balthasar (2008).

*Novocrania*: Valve thin and often unmineralized.

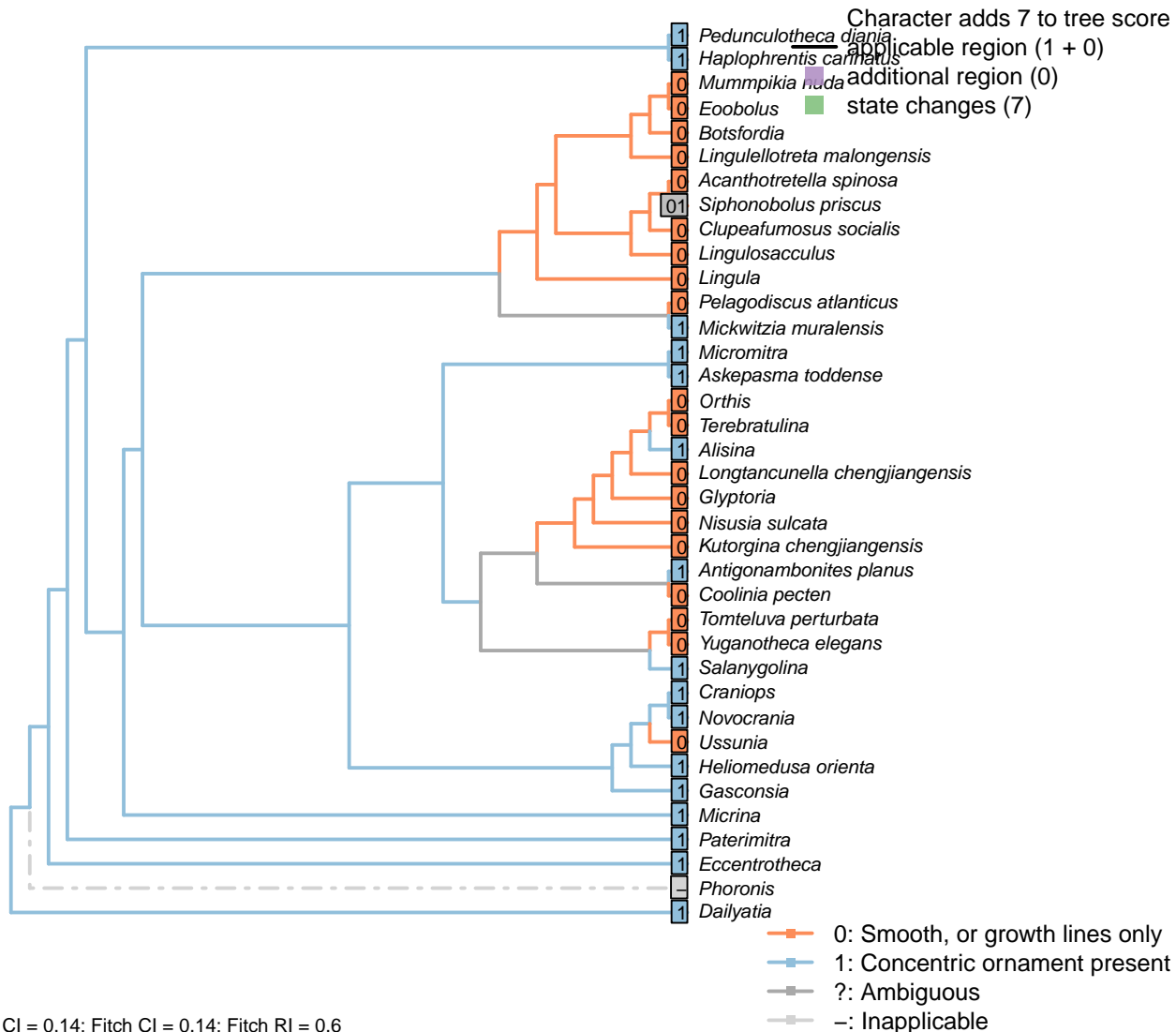
*Pelagodiscus atlanticus*: Described as present in *Discinisca* by Chen et al. (2007); assumed present also in *Pelagodiscus*.

*Siphonobolus priscus*: Present; see Popov et al. (2009), fig. 5J.

*Ussunia*: Following char. 42 in table 15 in Williams et al. (2000).

## 3.5 Sclerites: Ornament

### [51] Concentric ornament



#### Character 51: Sclerites: Ornament: Concentric ornament

- 0: Smooth, or growth lines only
- 1: Concentric ornament present
- Neomorphic character.

After character 11 in Williams *et al.* (1998).

*Askepasma toddense*, *Glyptoria*, *Kutorgina chengjiangensis*, *Micromitra*, *Salanygolina*: Following appendix 2 in Williams *et al.* (1998).

*Botsfordia*: Following Williams *et al.* (1998), appendix 2.

Pustules are arranged along concentric growth lines (Skovsted and Holmer, 2005), so are not treated as a

distinct ornamentation.

*Eccentrotheca*: More or less concentric ridges occur on *Eccentrotheca* sclerites (Skovsted et al., 2011).

*Haplophrentis carinatus*: A series of regularly spaced concentric ridges adorn both valves (Moysiuk et al., 2017); these are more pronounced than mere growth lines.

*Helomedusa orienta*: The ornament on shell exterior is described as concentric fila (Chen et al., 2007, P.43), and also scored as it in Williams *et al.* (2000, pp.160–163).

*Mickwitzia muralensis*: Symmetric fila.

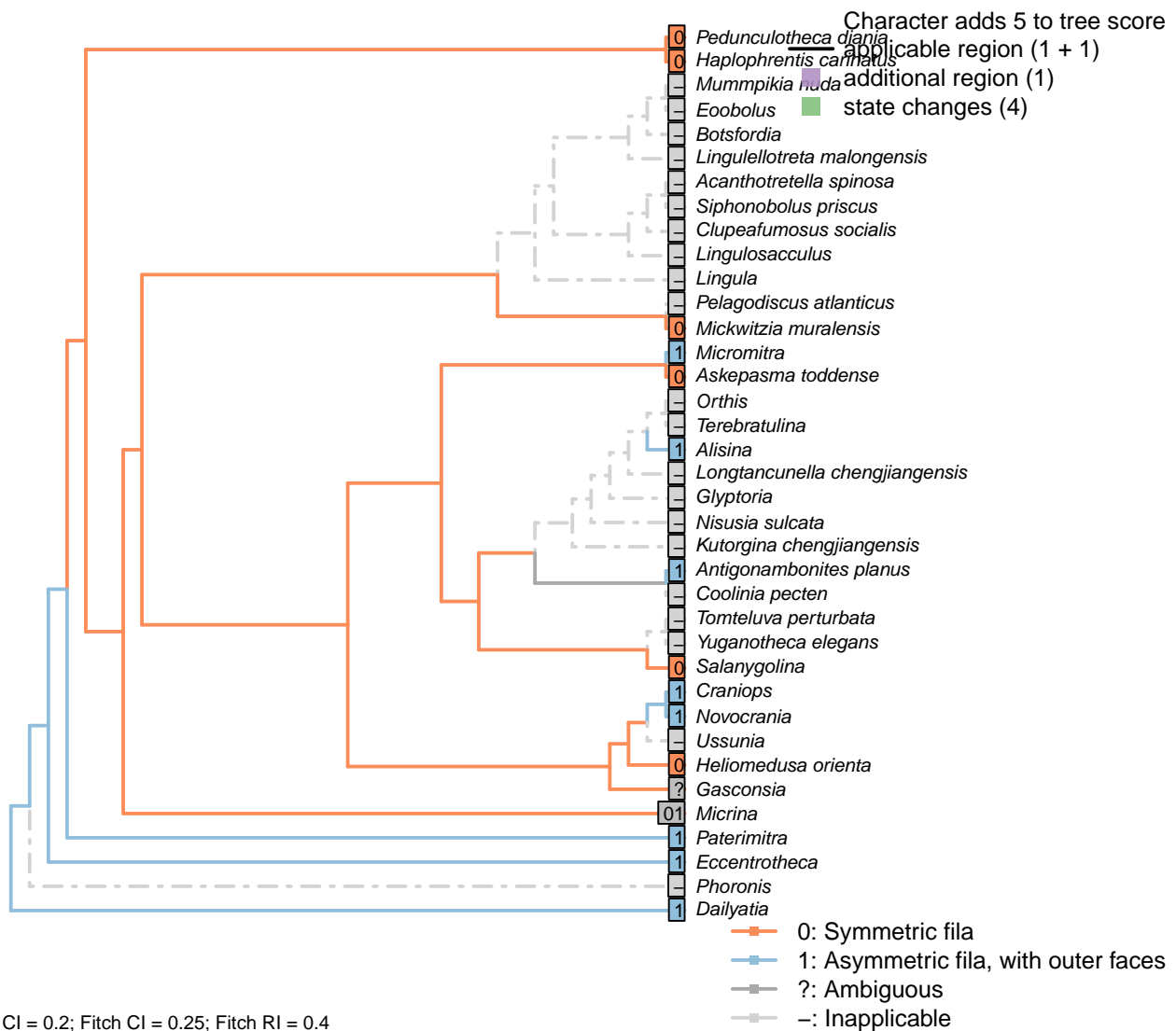
*Novocrania*: Irregular ridges externally (Williams et al., 2000).

*Pedunculotheca diana*: A series of regularly spaced concentric ridges adorn the ventral valve; comparatively less regular lines ornament the operculum.

*Pelagodiscus atlanticus*: Only growth lines evident (Williams et al., 2000).

*Terebratulina*: Single ridge evident in Williams *et al.* (2006) fig. 1425.1a interpreted as interruption of growth rather than inherent feature, so coded as absent (i.e. smooth).

## [52] Concentric ornament: Symmetry



### Character 52: Sclerites: Ornament: Concentric ornament: Symmetry

- 0: Symmetric fila
- 1: Asymmetric fila, with outer faces
- Neomorphic character.

After character 11 in Williams *et al.* (1998).

*Alisina*: Seemingly asymmetric (Williams *et al.*, 2000, fig. 122.3c; Zhang *et al.*, 2011b, Fig. 1).

*Askepasma toddense*, *Glyptoria*, *Kutorgina chengjiangensis*, *Micromitra*, *Salanygolina*: Following appendix 2

in Williams *et al.* (1998).

*Dailyatia*: Clear asymmetry (Skovsted *et al.*, 2015).

*Eccentrotheca*: Ornament, such as it is, is asymmetric, with prominent outer faces (Skovsted *et al.*, 2011).

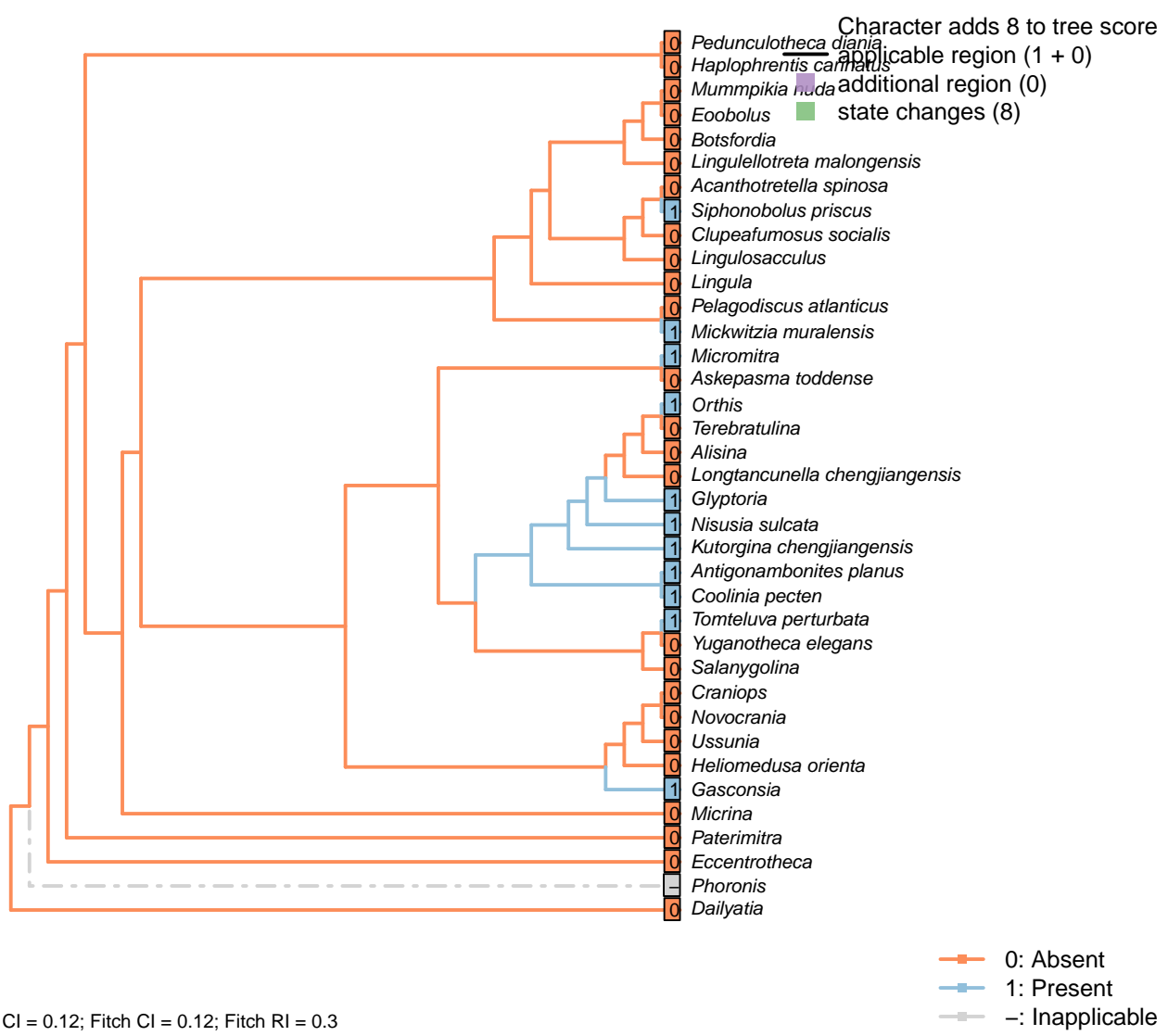
*Heliomedusa orienta*: See fig. 1715 in Williams *et al.* (2007).

*Mickwitzia muralensis*: Symmetric fila (Balthasar, 2004).

*Micrina*: No obvious asymmetry, even if not obviously symmetric either (Holmer *et al.*, 2008). Coded as ambiguous.

*Novocrania*: Clear outer faces (Williams *et al.*, 2000, fig. 100.2b).

## [53] Radial ornament



CI = 0.12; Fitch CI = 0.12; Fitch RI = 0.3

### Character 53: Sclerites: Ornament: Radial ornament

0: Absent

1: Present

Neomorphic character.

Ridges radiating from umbo, i.e. ribs.

*Askepasma toddense*: "Ornament of irregularly developed, concentric growth lamellae; microornamentation of irregularly arranged, polygonal pits" – Williams et al. (2000), p153; figs on p.155.

*Botsfordia*: Following Williams et al. (1998), Appendix 2.

*Eoobolus*: Very faint costellae in some specimens but coded absent.

*Gasconsia*: "Ornament of indistinct low radial ribs" – Williams et al. (2000, p167).

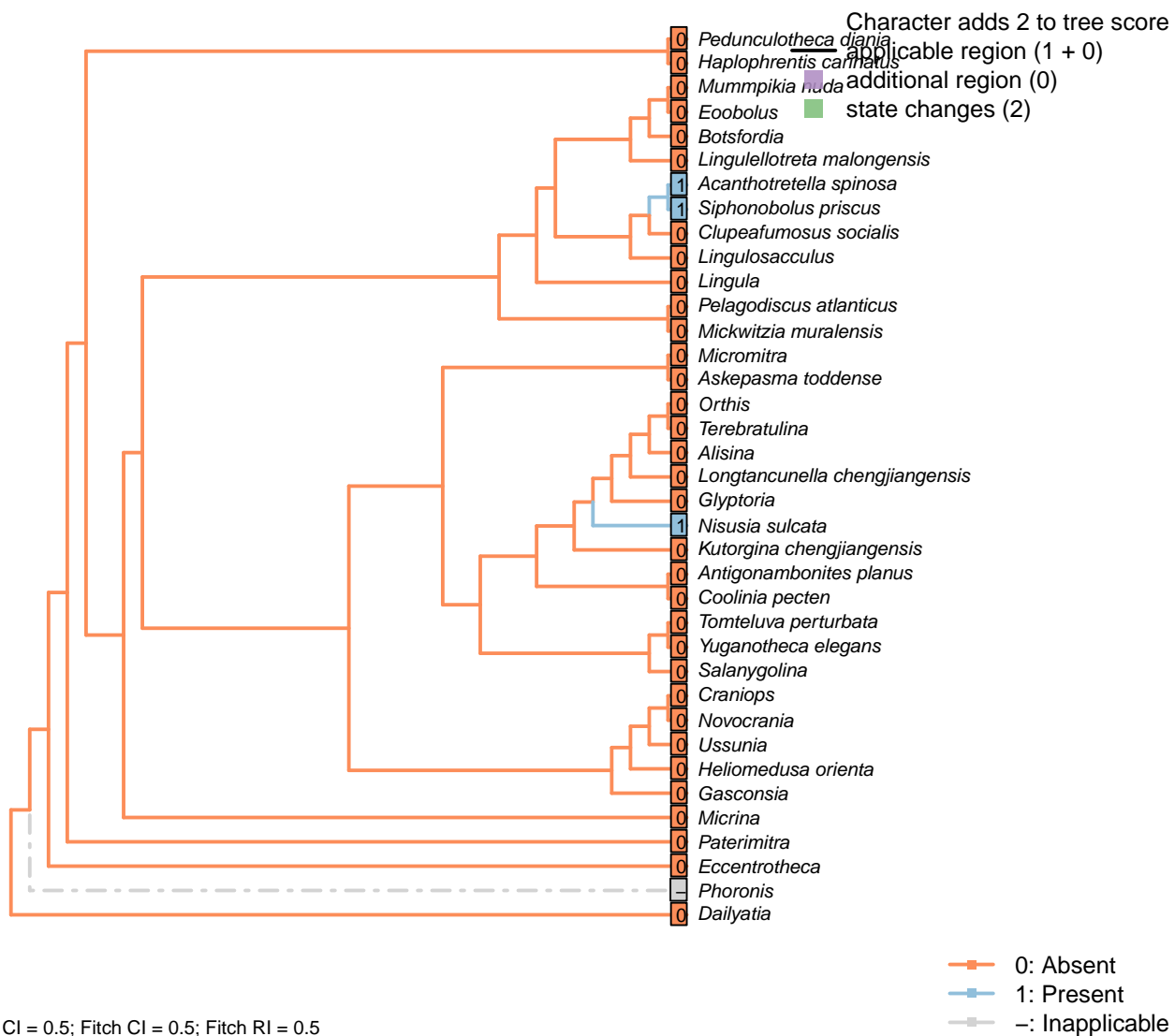
*Glyptoria*: "Coarsely costate" – Williams et al. (2000, p710).

*Heliomedusa orienta*: See fig. 1715 in Williams et al. (2007).

*Siphonobolus priscus*: "Indistinct radial ribs accentuated by radial rows of tubercles" – Popov et al. (2009).

*Ussunia*: Unornamented.

## [54] Shell-penetrating spines



CI = 0.5; Fitch CI = 0.5; Fitch RI = 0.5

#### Character 54: Sclerites: Ornament: Shell-penetrating spines

0: Absent

1: Present

Neomorphic character.

Mineralized or partly mineralized spines are observed in *Heliomedusa* and *Acanthotretella*.

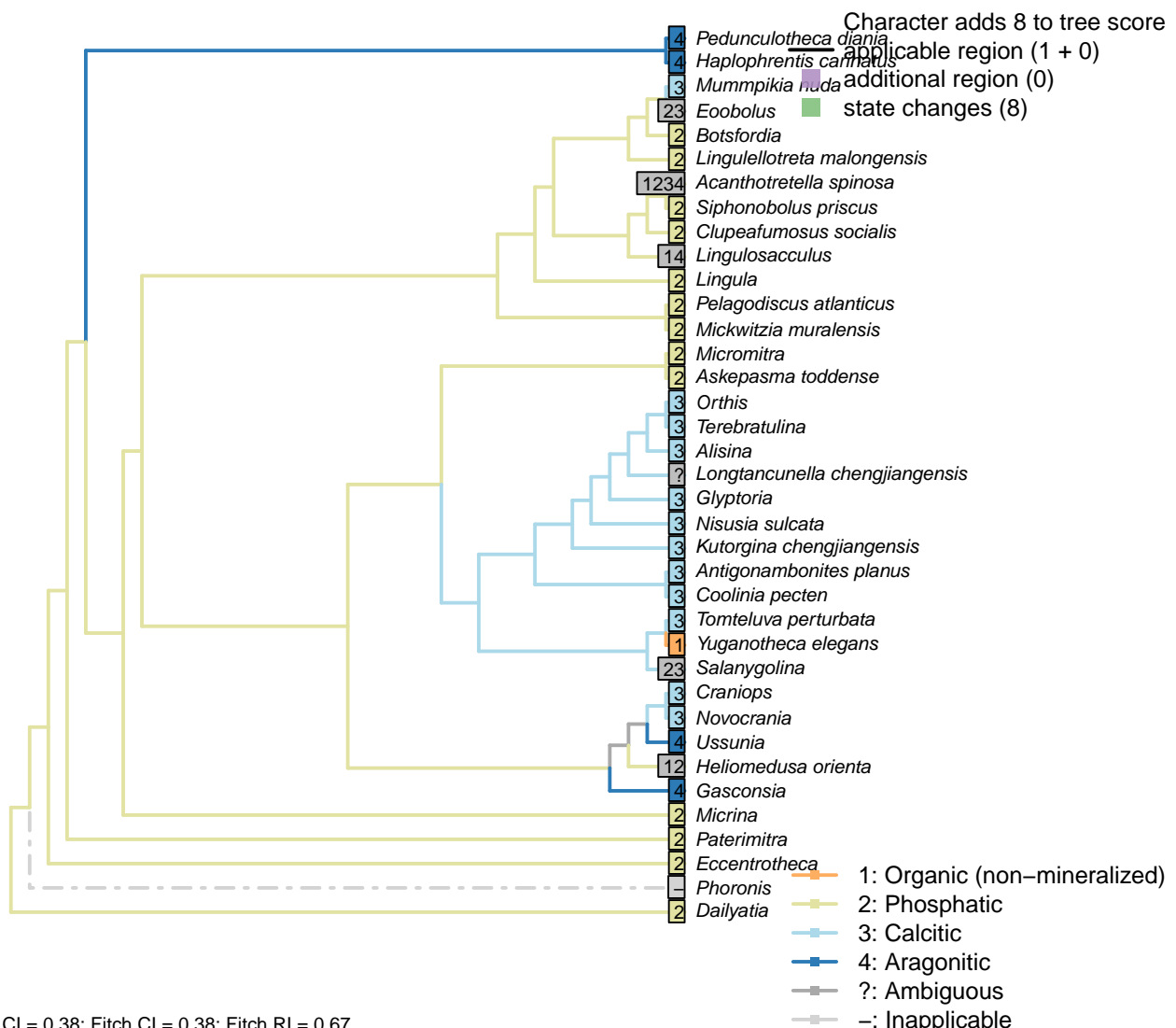
*Glyptoria*: Neither evident nor reported in Williams *et al.* (2000).

*Heliomedusa orienta*: The ‘spines’ reported by Chen *et al.* (2007) are pyritized spinelike setae – see pp. 2580–2590 in Williams *et al.* (2007).

*Nisusia sulcata*: Bears numerous small, hollow spines (Williams *et al.*, 2000).

## 3.6 Sclerites: Composition

### [55] Mineralogy



**Character 55: Sclerites: Composition: Mineralogy**

- 1: Organic (non-mineralized)
  - 2: Phosphatic
  - 3: Calcitic
  - 4: Aragonitic
- Transformational character.

*Acanthotretella spinosa*: Holmer & Caron (2006) note the absence of brittle breakage, interpreted as indicating the absence of a material mineralized component to the shells. The preservation is strikingly different from that of other Burgess Shale brachiopods, ruling out a primarily calcitic or phosphatic composition. The two-dimensional nature of the preservation also differs from that of co-occurring aragonitic taxa (hyoliths; Holmer and Caron, 2006, p. 273), indicating that any mineralization was minor at best.

Holmer & Caron (2006, p. 286) suggest that it is more likely that a (minor) mineral component was present than that it was not, though without providing an uncontested rationale. To be as conservative as possible, we therefore code this taxon as ambiguous.

*Clupeafumosus socialis*: Phosphatic – hence the conventional placement within Linguliformea.

*Craniops*: Shell calcitic.

*Eoobolus*: “the original shell of *Eoobolus* contained small calcareous grains that were incorporated into organic-rich layers alongside apatite” (Balthasar, 2007).

*Gasconsia*: Confirmed in Trimerella by Balthasar et al. (2011).

*Heliomedusa orienta*: “Shell originally organophosphatic, but may generally have been poorly mineralized” – Williams et al. (2007) – cf. ibid, p. 2889, “These strong similarities to discinoids in soft-part anatomy imply that the *Heliomedusa* shell was chitinous or chitinophosphatic, not calcareous.”

*Lingulellotreta malongensis*: Coded as phosphatic by Zhang et al. (2014), but with no explanation. Cracks within shells of Chengjiang specimens (e.g. Zhang et al., 2007a, fig. 3) demonstrate that the shells were originally mineralized, but not the identity of the original biomineral. This said, phosphatized material from Kazakhstan (Holmer et al., 1997) is attributed to the same species; presuming this phosphate to be original and the material to be conspecific, *L. malongensis* is coded as having phosphatic shells.

*Lingulosacculus*: The absence of relief in *Lingulosacculus* rules out a phosphatic or calcitic composition, but co-occurring (and presumably aragonitic) hyolithids are preserved in the same fashion. Its constitution was thus either organic or aragonitic (Balthasar and Butterfield, 2009).

*Longtancunella chengjiangensis*: “The original composition of the shell cannot be determined with certainty”, though it was “most probably entirely soft and organic” – Zhang et al. (2011a).

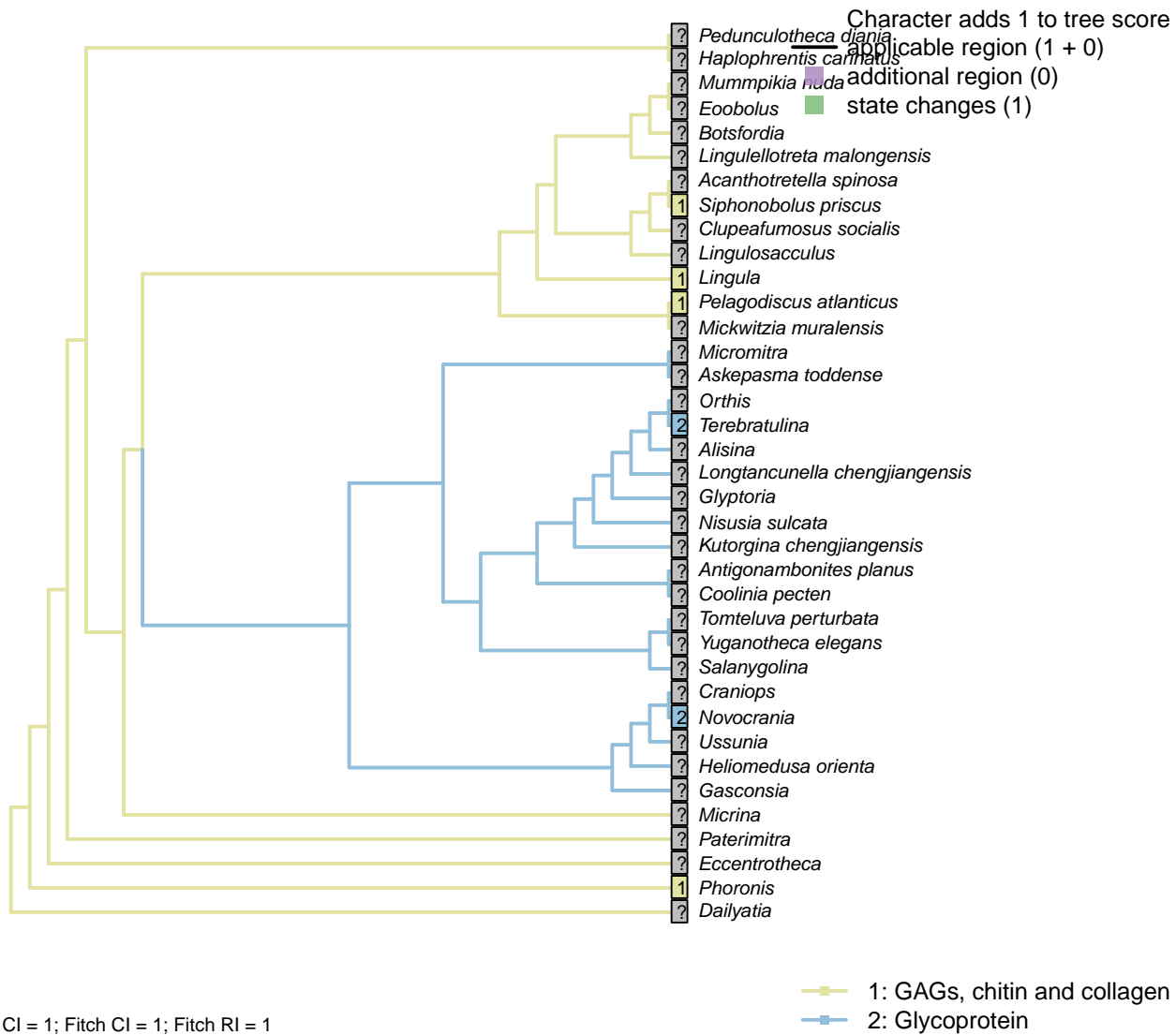
*Mickwitzia muralensis*: Calcite and silica deemed diagenetic by Balthasar (2004).

*Mummikia nuda*: Identified as calcareous by preservational criteria, and description “primary calcitic shells of *M. nuda*” (Balthasar, 2008).

*Novocrania*: Ventral valve uncalcified in extant forms or sometimes thin (Williams et al., 2000), but coded as calcitic as calcite-mineralizing pathways are present.

*Salanygolina*: Original mineralogy unknown, but known to be mineralised and anticipated to be phosphatic (Holmer et al., 2009).

## [56] Cuticle or organic matrix



### Character 56: Sclerites: Composition: Cuticle or organic matrix

1: GAGs, chitin and collagen

2: Glycoprotein

Transformational character.

Williams *et al.* (1996) identify glycoprotein-based organic scaffolds as distinct from those comprising glycosaminoglycans (GAGs), chitin and collagen. This character can only be scored for extant taxa.

*Lingula*: Coded as GAGs, chitin and collagen in lingulids by Williams *et al.* (1996).

*Novocrania*: Coded as glycoprotein for craniids by Williams *et al.* (1996).

*Pelagodiscus atlanticus*: Coded as GAGs, chitin and collagen in discinids by Williams *et al.* (1996).

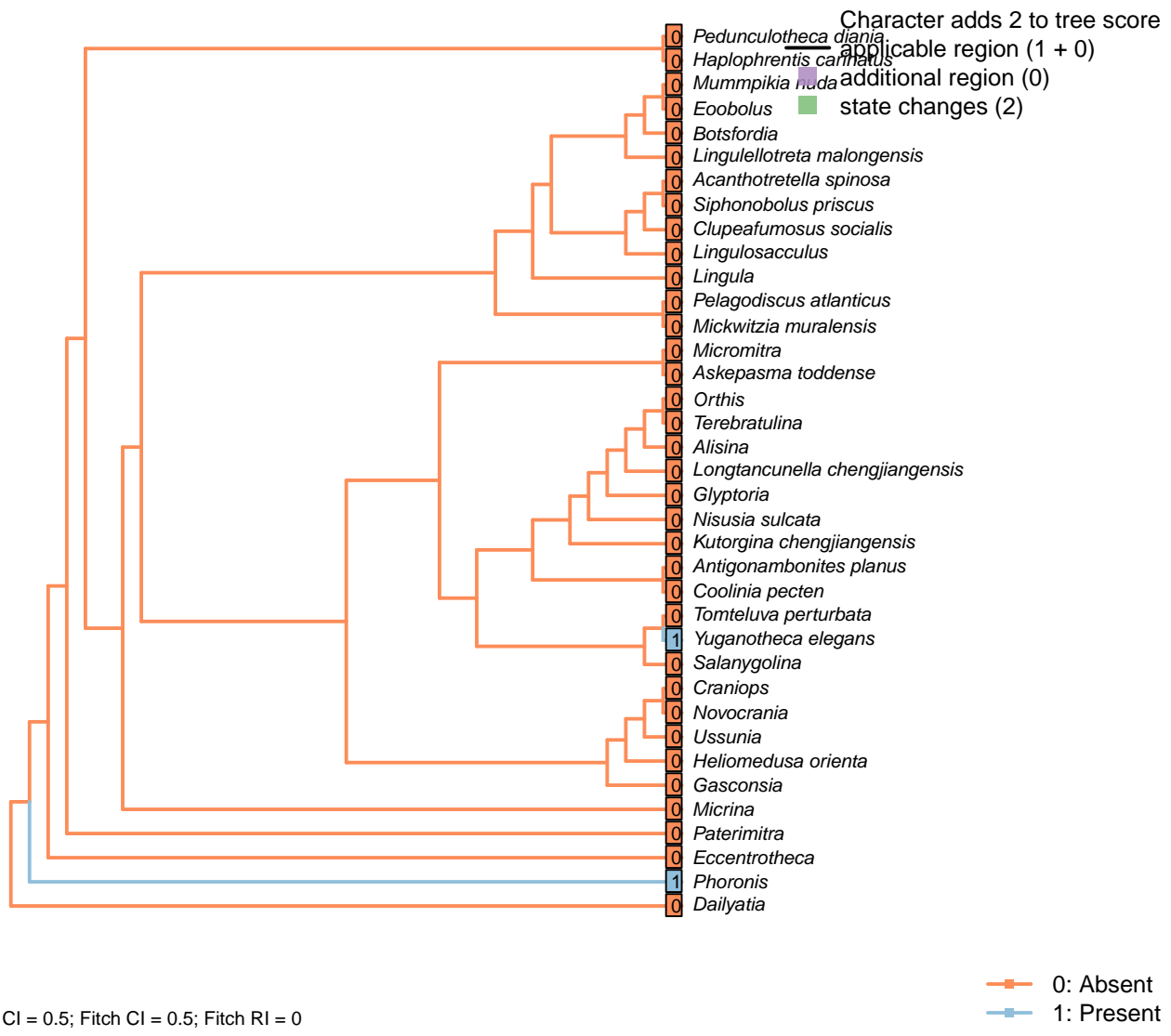
*Phoronis*: “The presence of sulphated glycosaminoglycans (GAGs) in the chitinous cuticle of *Phoronis* (Hermann, 1997, p. 215) would suggest a link with linguliforms, as GAGs are unknown in rhynchonelliform shells (Fig. 1891, 1896)” – Williams *et al.* (2007), p. 2830.

*Siphonobolus priscus*: Lenticular chambers in siphonotretid shells interpreted as degraded GAG residue

(Williams et al., 2004).

*Terebratulina*: Coded as glycoprotein for terebratulids by Williams *et al.* (1996).

## [57] Incorporation of sedimentary particles



**Character 57: Sclerites: Composition: Incorporation of sedimentary particles**

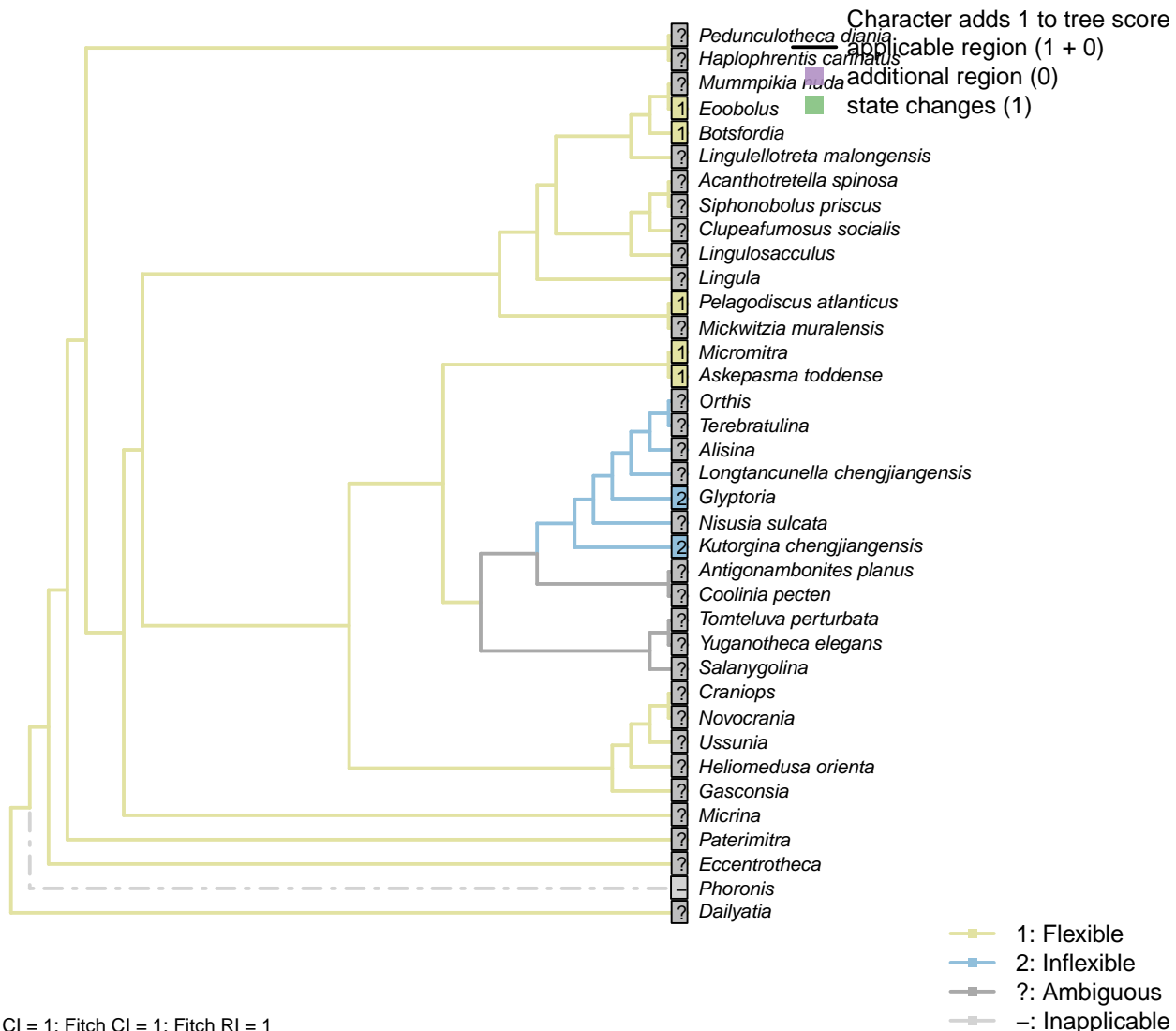
0: Absent

1: Present

Neomorphic character.

Phoronids and *Yuganotheca* agglutinate particles into their sclerites.

## [58] Periostracum: Flexibility



### Character 58: Sclerites: Composition: Periostracum: Flexibility

1: Flexible

2: Inflexible

Transformational character.

Following character 9 in Williams *et al.* (1998); see their p228–230 for a discussion of how this might be inferred from fossil material.

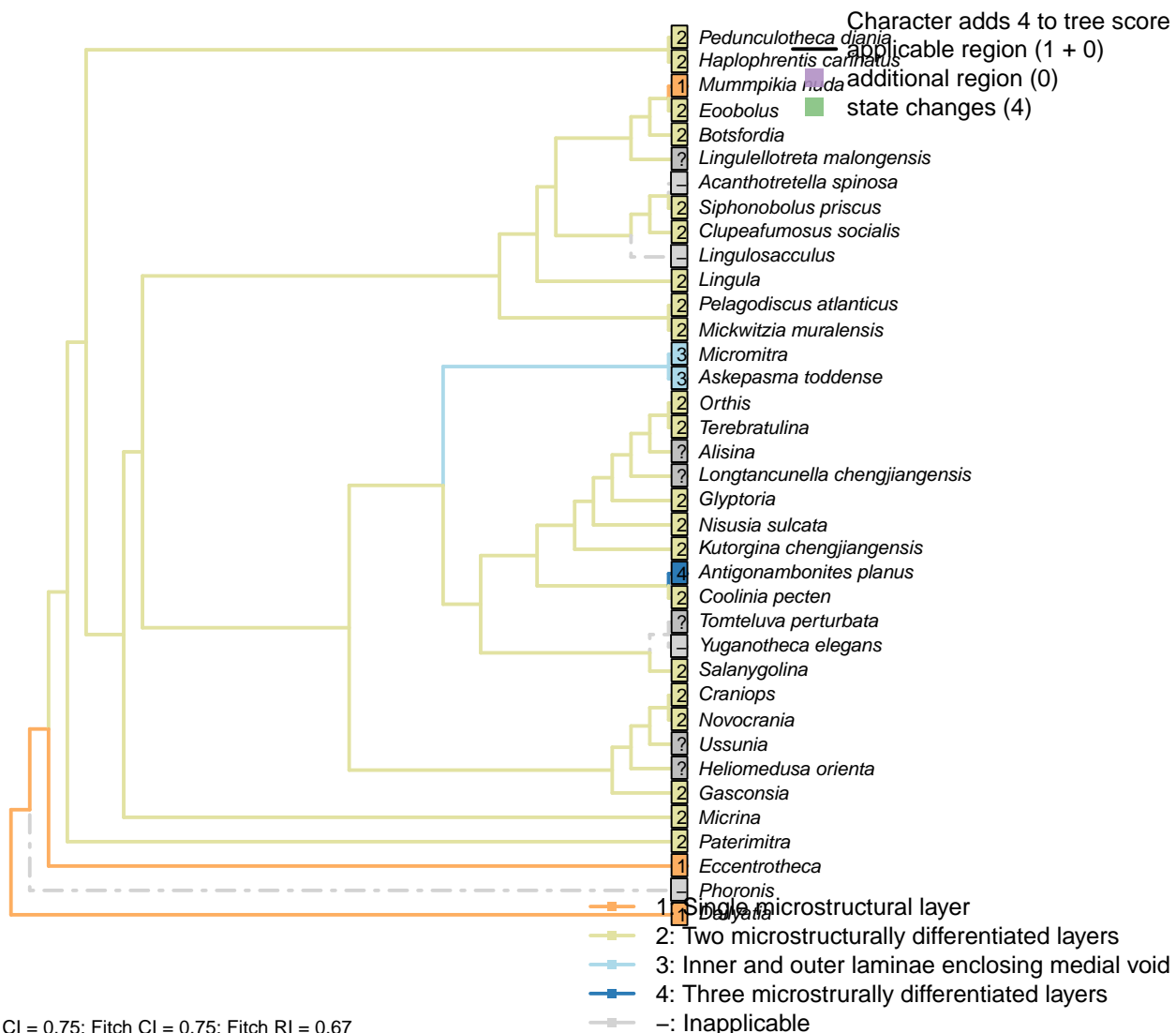
*Askepasma toddense*, *Glyptoria*, *Kutorgina chengjiangensis*, *Micromitra*: Following appendix 2 in Williams *et al.* (1998).

*Botsfordia*, *Eoobolus*: Coded as flexible in Williams *et al.* (1998), Appendix 2.

*Pelagodiscus atlanticus*: Flexible (Williams *et al.*, 1998).

*Salanygolina*: Coded as uncertain in appendix 2 in Williams *et al.* (1998).

## [59] Microstructure: Layers

**Character 59: Sclerites: Composition: Microstructure: Layers**

- 1: Single microstructural layer
  - 2: Two microstructurally differentiated layers
  - 3: Inner and outer laminae enclosing medial void
  - 4: Three microstrurally differentiated layers
- Transformational character.

Hyolith conchs comprise two mineralized layers of fibrous bundles. Bundles are measure 5–15 µm across; their constituent fibres are each 0.1–1.0 µm wide. In the inner layer, the fibres are transverse; in the outer layer, the bundles are inclined towards the umbo, becoming longitudinal on the outermost margin.

Obolellids comprise a single laminated mineralogical layer (Balthasar, 2008). Shell-penetrating canals are not considered as contributing to the mineralogical microstructure and are coded separately.

Coded as non-additive as there is no clear necessity to pass through the brachiopod-like construction: the three layers could arise by the addition of a void to a single pre-existing layer, for example.

Inapplicable in taxa with a non-mineralized shell.

*Botsfordia*: “Composed of a thin primary layer and a laminate secondary shell exhibiting baculate shell structure” – Skovsted & Holmer (2005), with reference to Skovsted and Holmer (2003).

*Clupeafumosus socialis*: General acrotretid structure taken from Zhang *et al.* (2016).

*Eoobolus*: “*Eoobolus* shells exhibit the general characteristics of modern linguliform shells, i.e. they were composed of alternating sets of organic and apatite-rich layers that were separated by thin sheets of recalcitrant organic layers.” – Balthasar (2007).

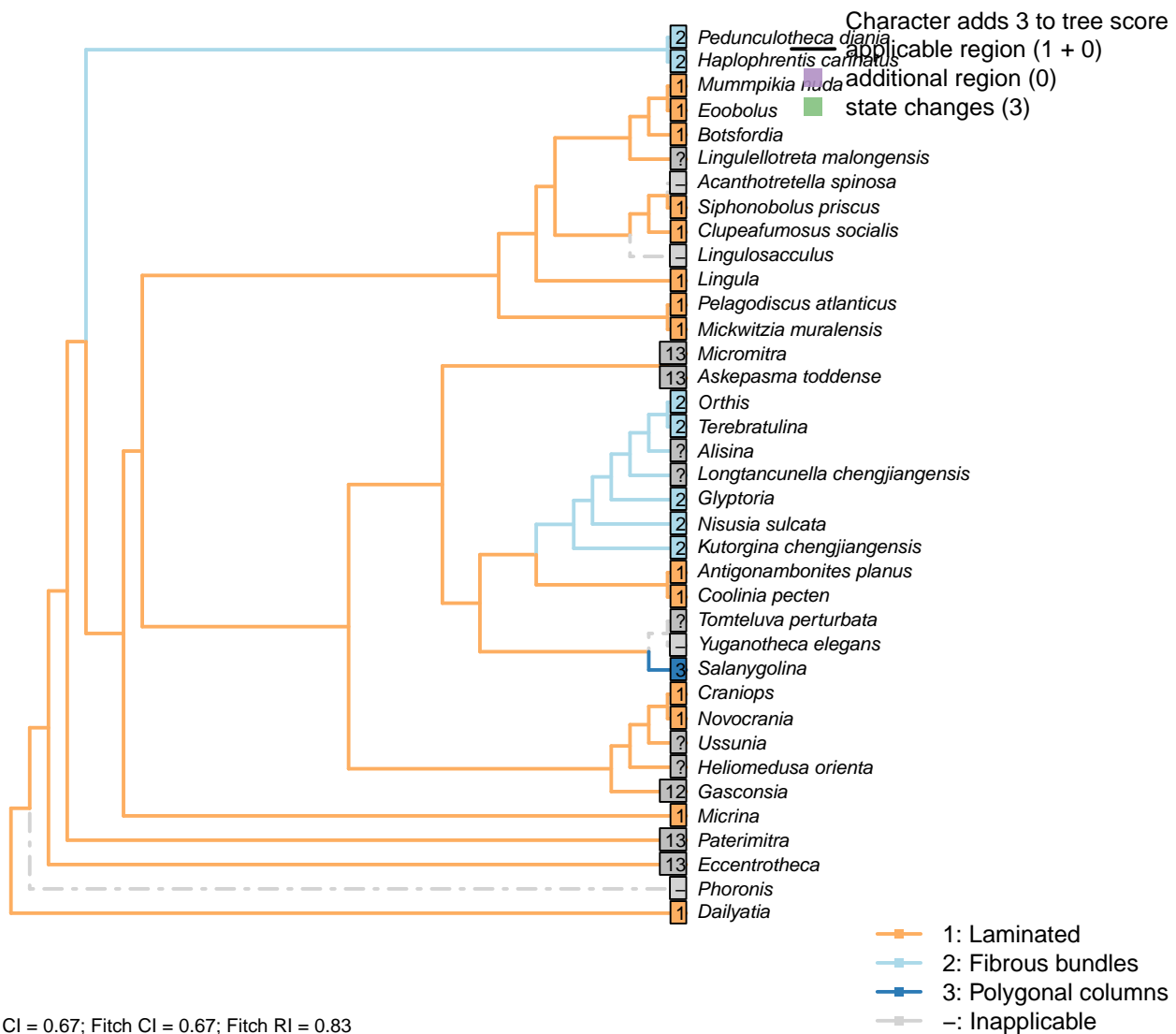
*Haplophrentis carinatus*: Assumed to be equivalent to the hyoliths described by Kouchinsky (2000).

*Mickwitzia muralensis*: “the shell structure of *Mickwitzia* [...] is closely similar to the columnar shell of linguliform acrotretoid brachiopods as well as to the linguloid *Lingulellotreta*, in that it has slender columns in the laminar succession” – Williams *et al.* (2007).

*Micrina*: Identical to *Mickwitzia* and more derived linguliforms (Holmer *et al.*, 2011).

*Siphonobolus priscus*: “Orthodoxly secreted primary and secondary layers” – Williams *et al.* (2004).

## [60] Microstructure: Crystal format

**Character 60: Sclerites: Composition: Microstructure: Crystal format**

- 1: Laminated
  - 2: Fibrous bundles
  - 3: Polygonal columns
- Transformational character.

Hyolith conchs comprise two mineralized layers of fibrous bundles. Bundles measure 5–15 µm across; their constituent fibres are each 0.1–1.0 µm wide. In the inner layer, the fibres are transverse; in the outer layer, the bundles are inclined towards the umbo, becoming longitudinal on the outermost margin.

Obolellids comprise a single laminated mineralogical layer (Balthasar, 2008). Shell-penetrating canals are not considered as contributing to the mineralogical microstructure and are coded separately.

The pervasive (not just superficial) polygonal structures in *Paterimitra* are distinct, and characterize *Askepasma*, *Salanygolina*, *Eccentrotheca* and *Paterimitra* (Larsson et al., 2014).

Williams *et al.* (2000) identify cross-bladed laminae as diagnostic of Strophomenata, with the exception of

some older groups that contain fibres or laminar laths.

*Antigonambonites planus*: Shell structure of this taxon is laminated, rather than fibrous as previously considered.

*Botsfordia*: “Composed of a thin primary layer and a laminate secondary shell exhibiting baculate shell structure” – Skovsted & Holmer (2005), with reference to Skovsted and Holmer (2003).

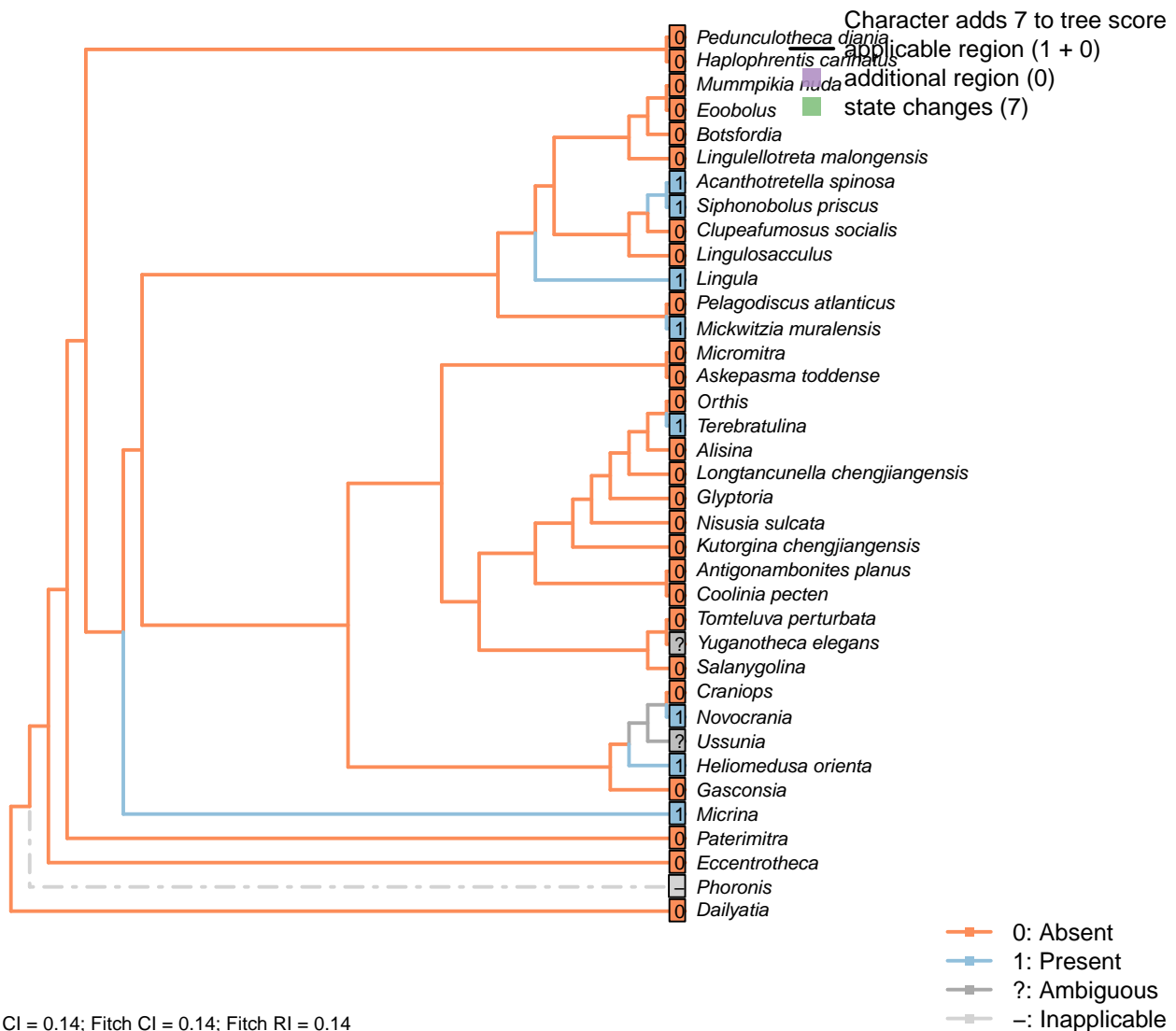
*Craniops*: “with calcitic or possibly aragonitic inarticulated shells with laminar (tabular) secondary layers” (Williams et al., 2000).

*Haplophrentis carinatus*: Inferred from other hyolithids (e.g. Moore and Porter, 2018).

*Pedunculotheca diania*: Assumed to be fibrous by analogy with the allotheconomorph orthothecid described by Kouchinsky (2000).

*Siphonobolus priscus*: Prominent laminations; see Williams et al. (2004).

## [61] Microstructure: Punctae



Character 61: Sclerites: Composition: Microstructure: Punctae

0: Absent

1: Present

Neomorphic character.

Punctae are 10–20 µm wide canals created by multicellular extensions of the outer epithelium. They penetrate the full depth of the shell.

Balthasar (2008) writes:

“Vertical shell penetrating structures, such as punctae, pseudopunctae, extropunctae and canals, are common in many groups of brachiopods and are distinguished based on their geometry and size (Williams et al., 1997). Punctae are 10–20 µm wide and represent multicellular extensions of the outer epithelium (Owen and Williams, 1969). Pseudopunctae and extropunctae are similar in diameter but, instead of canals, are vertical stacks of conical deflections of individual shell layers (Williams and Brunton, 1993). None of these three types of vertical shell structure, all of which are confined to calcitic-shelled brachiopods, compares with the much smaller canals (< 1 µm in diameter) of *M. nuda*. The only type of vertical structure that fits the size and nature of the canals of the Mural obolellids are the canals of linguliform brachiopods, which range in width from 180 to 740 nm and are occupied by proteinaceous strands in extant taxa (Williams et al., 1992, 1994, 1997). In contrast to obolellid canals, however, linguliform canals are not known to penetrate the entire shell but terminate in organic-rich layers (Williams et al., 1997). Based on these considerations it would, therefore, be misleading to call obolellid shells punctate (they are as much “punctate” as acrotretids or other linguliforms); rather their shell structure should be called canaliculate (Williams et al., 1997).”

*Craniops*: “impunctate”.

*Haplophrentis carinatus*: The tubules within the centre of the bundles of hyolith shells (Kouchinsky, 2000) are c. 10 µm wide, making them an order of magnitude larger than the canals that characterize lingulid valves, and a similar scale to punctae. This said, they have only been reported in a putative allathecid, so the presence of equivalent structures in hyolithids has never been demonstrated.

*Heliomedusa orienta*: ‘Identical’ to those in *Mickwitzia* – see Williams et al. (2007).

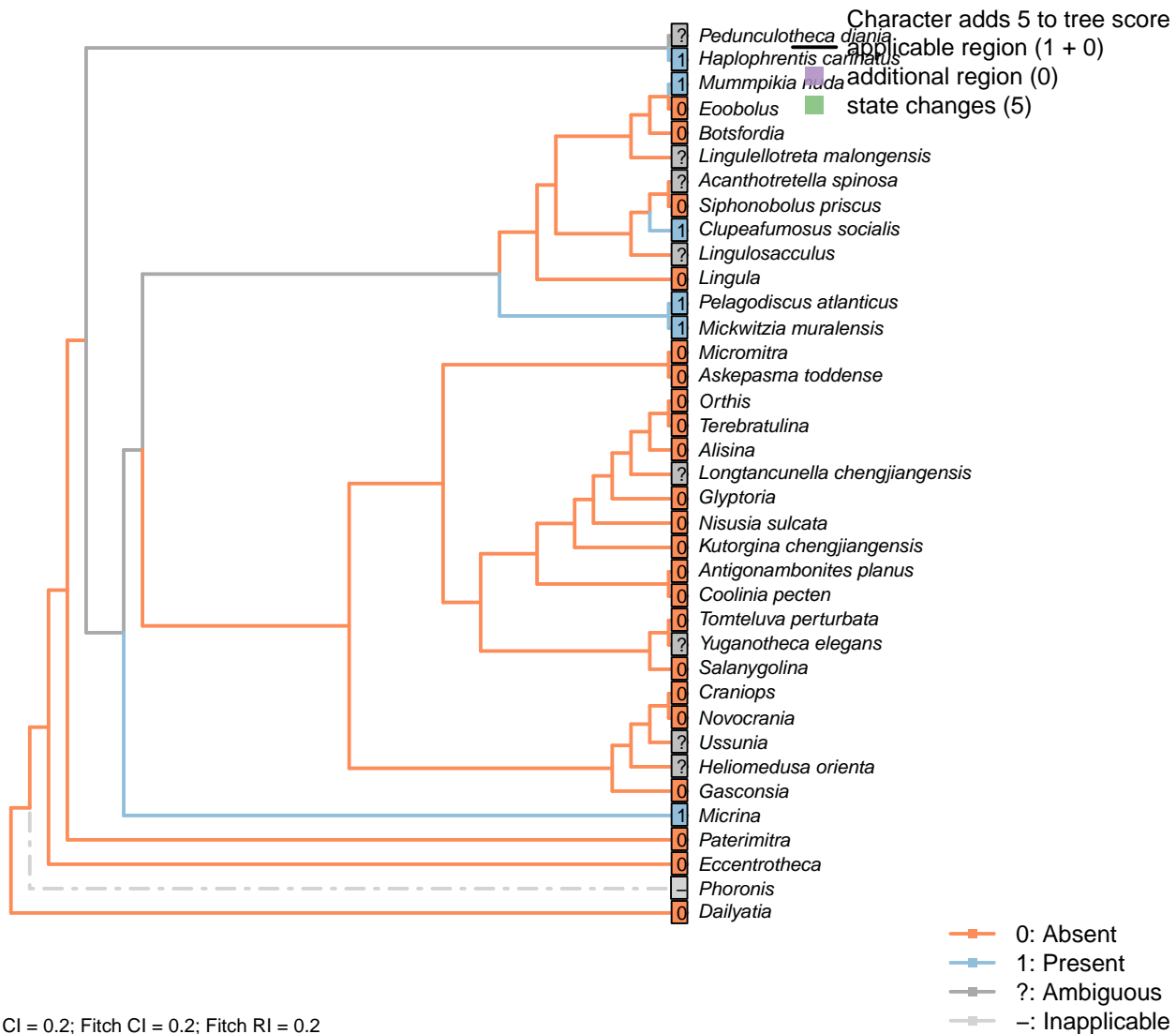
*Mickwitzia muralensis*: Coded as present to reflect that the chambers contained setae; following Carlson in Williams et al. (2007), the punctae may or may not be homologous as punctae, but are likely homologous as shell perforations; both these perforations and those of *Micrina* were associated with setae, even if their equivalence bay be with juvenile vs adult setal structures in modern brachiopods (Balthasar, 2004, p. 397).

*Mummpikia nuda*: “Vertical shell penetrating structures, such as punctae, pseudopunctae, extropunctae and canals, are common in many groups of brachiopods and are distinguished based on their geometry and size (Williams et al., 1997). Punctae are 10–20 µm wide and represent multicellular extensions of the outer epithelium (Owen and Williams, 1969). [...] None of these three types of vertical shell structure, all of which are confined to calcitic-shelled brachiopods, compares with the much smaller canals (< 1 µm in diameter) of *M. nuda*. The only type of vertical structure that fits the size and nature of the canals of the Mural obolellids are the canals of linguliform brachiopods, which range in width from 180 to 740 nm and are occupied by proteinaceous strands in extant taxa (Williams et al., 1992, 1994; Williams et al., 1997).” – Balthasar (2008).

*Siphonobolus priscus*: The ‘canals’ through the shell have a diameter of c. 20 µm (Williams et al., 2004, text-fig. 2a), falling within the definition of punctae used herein.

*Terebratulina*: Endopunctae are relatively large canals, diameter vary greatly from 5–20 m.

## [62] Microstructure: Canals



### Character 62: Sclerites: Composition: Microstructure: Canals

0: Absent

1: Present

Neomorphic character.

A caniculate microstructure occurs in lingulids; canals are narrower (< 1 µm) than punctae, may branch, and do not fully penetrate the shell, terminating just within the boundaries of a microstructural layer. See Williams et al. (1997), p303ff, and Balthasar (2008), p273, for discussion.

Tubules described in hyoliths by Kouchinsky (2000) measure around 10 µm in diameter, making them an order of magnitude wider than lingulid canals.

This said, Balthasar (2008) considers the tubules within the columnar shell microstructure of *Mickwitzia* cf. *occidens* (1–3 µm wide, Skovsted and Holmer, 2003), acrotretides (1 µm wide, see Holmer, 1989, Zhang et al. (2016)) and lingulellotretids (100 nm wide, Cusack et al., 1999) as equivalent to lingulid canals.

*Micrina* exhibits both punctae and canals (Harper et al., 2017), challenging Carlson's contention (in Williams

et al., 2007) that the structures are potentially homologous as shell perforations.

*Botsfordia*: Not evident in section presented by Skovsted & Holmer (2003).

*Clupeafumosus socialis*: Acrotretid laminae bear characteristic columns (e.g. Zhang et al., 2016).

Balthasar (2008) considers these columns as homologous with tubules within the columnar shell microstructure *Mummpikia*, *Mickwitzia* and lingulellotretids.

*Haplophrentis carinatus*: Zhang et al. (2018) have reported um-scale canals, replicated in phosphate, within the shell of the hyolithid *Paramicrocornus*; as shell microstructure is not preserved in *Haplophrentis*, this latter taxon is taken as a model.

*Longtancunella chengjiangensis*: Preservational resolution not sufficient to evaluate.

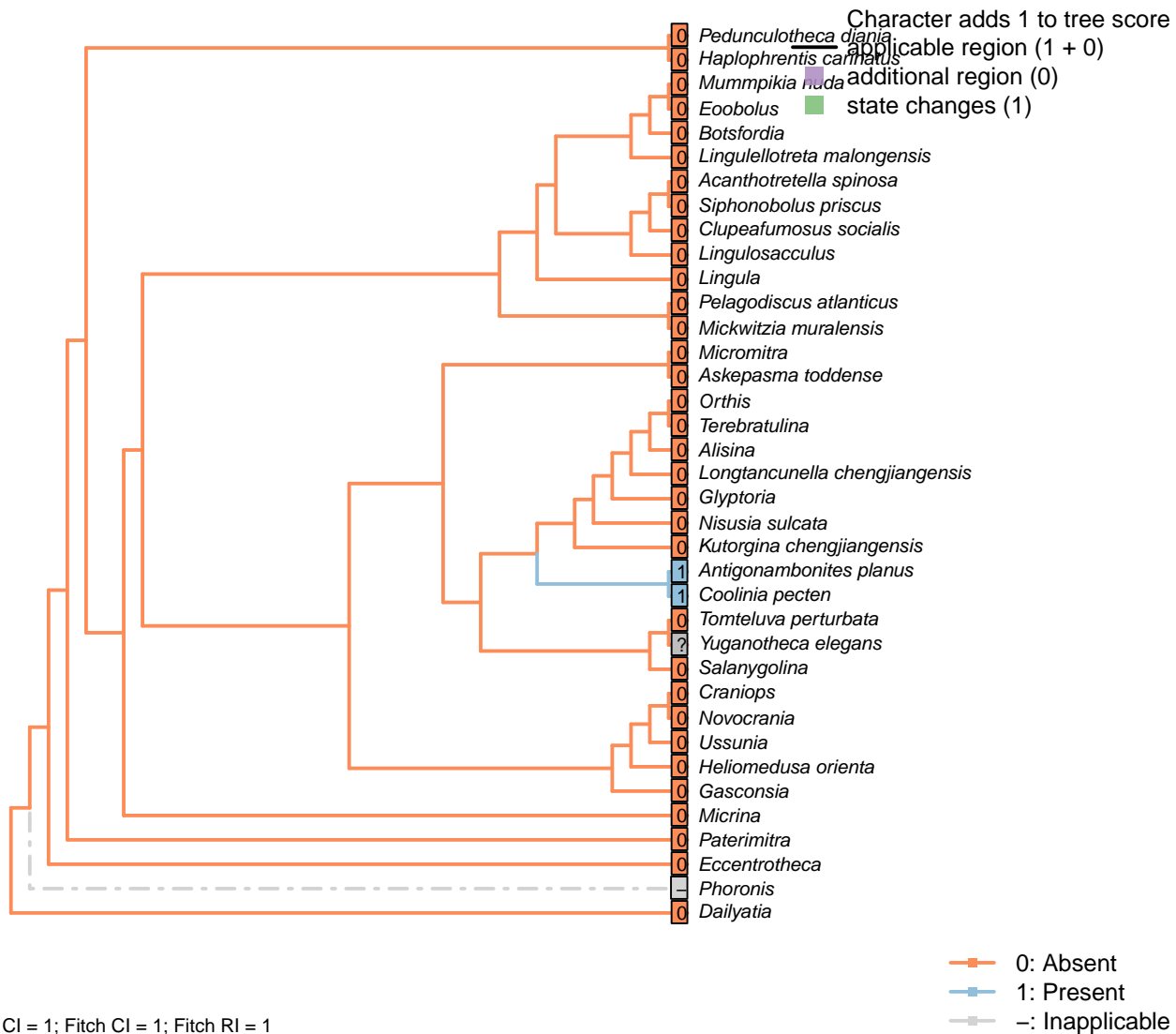
*Mickwitzia muralensis*: Coded as present to reflect similarity of columnar microstructure remarked on by, among others, Balthasar (2008); Williams et al. (2007); Skovsted & Holmer (2003).

*Micrina*: Acrotretid laminae bear characteristic columns (e.g. Zhang et al., 2016); a similar fabric has been reported, and assumed homologous, in *Micrina* (Butler et al., 2012).

A similar columnar shell microstructure also occurs in the closely related *Mickwitzia* (Balthasar, 2008).

*Siphonobolus priscus*: The ‘canals’ through the shell have a diameter of c. 20 µm (Williams et al., 2004, text-fig. 2a), falling within the definition of punctae (rather than canals) used herein.

### [63] Microstructure: Pseudopunctae



#### Character 63: Sclerites: Composition: Microstructure: Pseudopunctae

0: Absent

1: Present

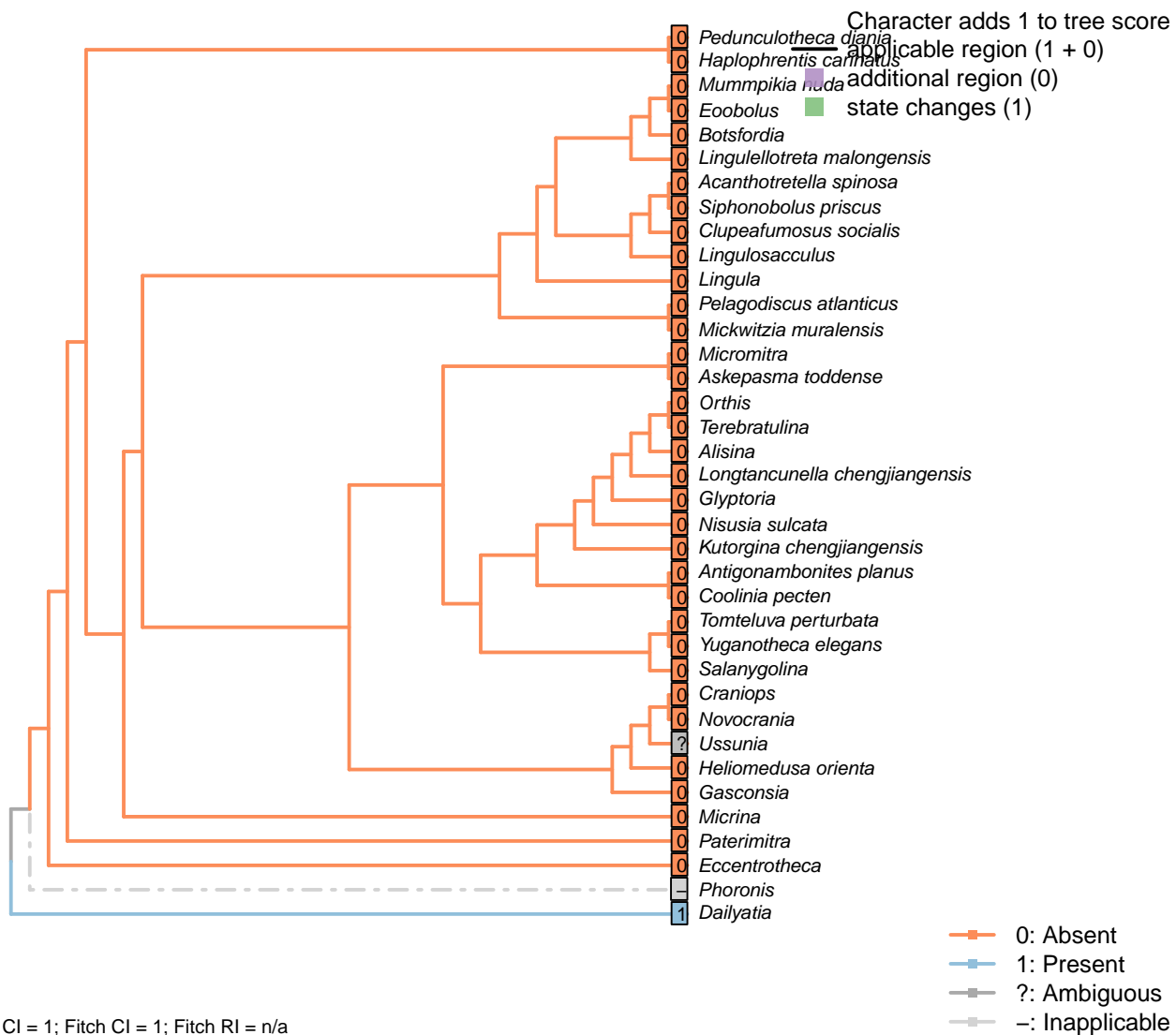
Neomorphic character.

Pseudopunctae are not punctae, but deflections of shell laminae. They characterise Strophomenata in particular.

*Antigonambonites planus*, *Glyptoria*, *Nisusia sulcata*: Scored absent in data matrix of Benedetto (2009).

*Orthis*: Scored absent (in *Eoorthis*) in data matrix of Benedetto (2009).

## [64] Microstructure: External polygonal ornament

**Character 64: Sclerites: Composition: Microstructure: External polygonal ornament**

0: Absent

1: Present

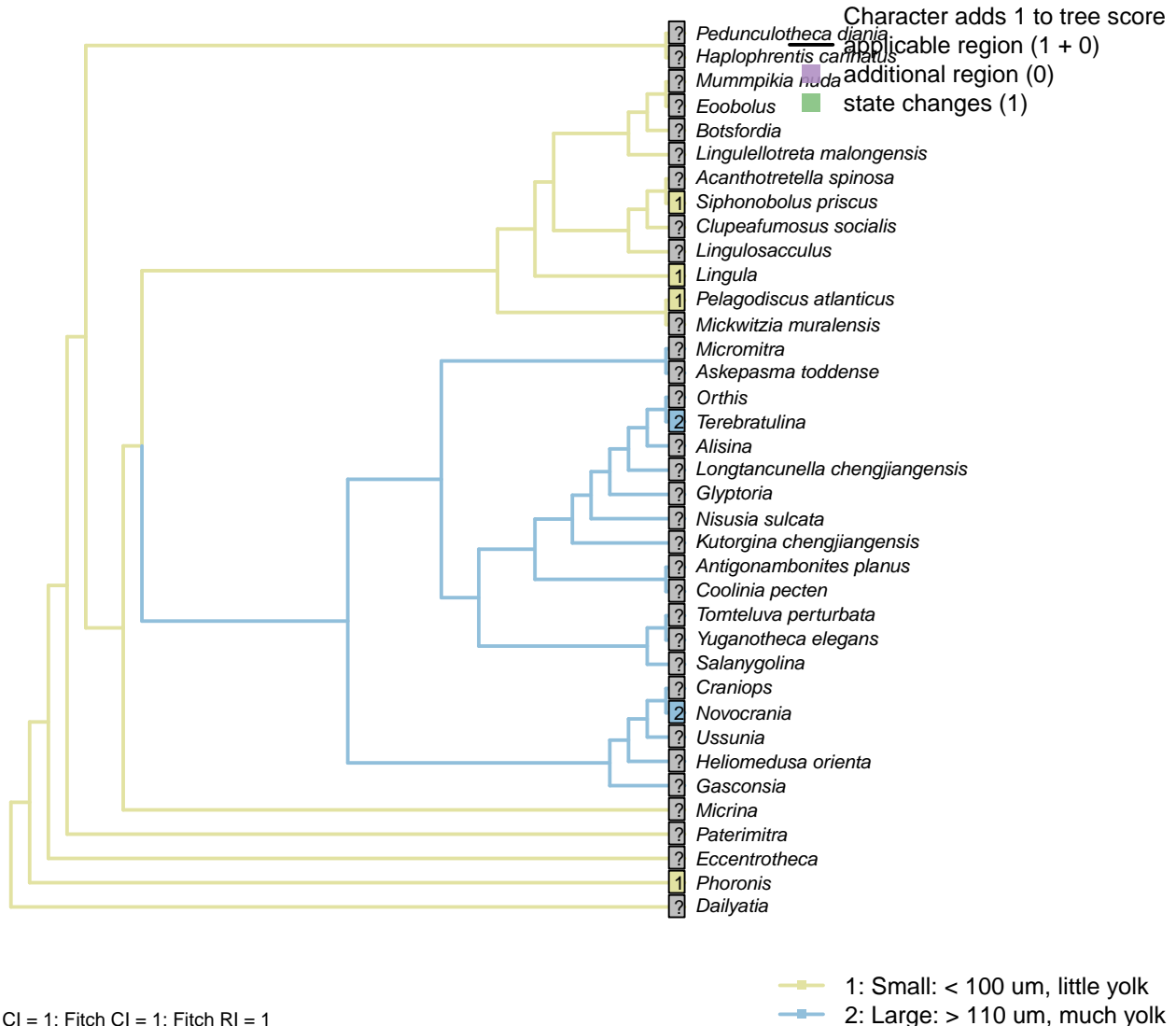
Neomorphic character.

Regular polygonal compartments, around 10 µm in diameter, characterise *Paterimitra*. Walls between compartments have the cross-section of an anvil. An external polygonal structure (possible imprints of epithelial tissue) occurs in *Dailyatia*, but it is a surface pattern, which is different from the polygonal prisms in the body wall of other paterinid-like groups.

*Clupeafumosus socialis*: The polygonal ornament reported in acrotretids by Zhang *et al.* (2016) is on the internal surface of the shell.

### 3.7 Gametes

[65] Egg size



#### Character 65: Gametes: Egg size

1: Small: < 100 um, little yolk

2: Large: > 110 um, much yolk

Transformational character.

Following Carlson (1995), character 7. This character is only possible to code in extant taxa. It is not considered independent of Carlson's character 11, number of gametes released per spawning, as it is possible to produce more small eggs than large eggs – thus this latter character is not reproduced in the present study. The same goes for Carlson's character 12, gamete dispersal mode; brooders will tend to brood large eggs.

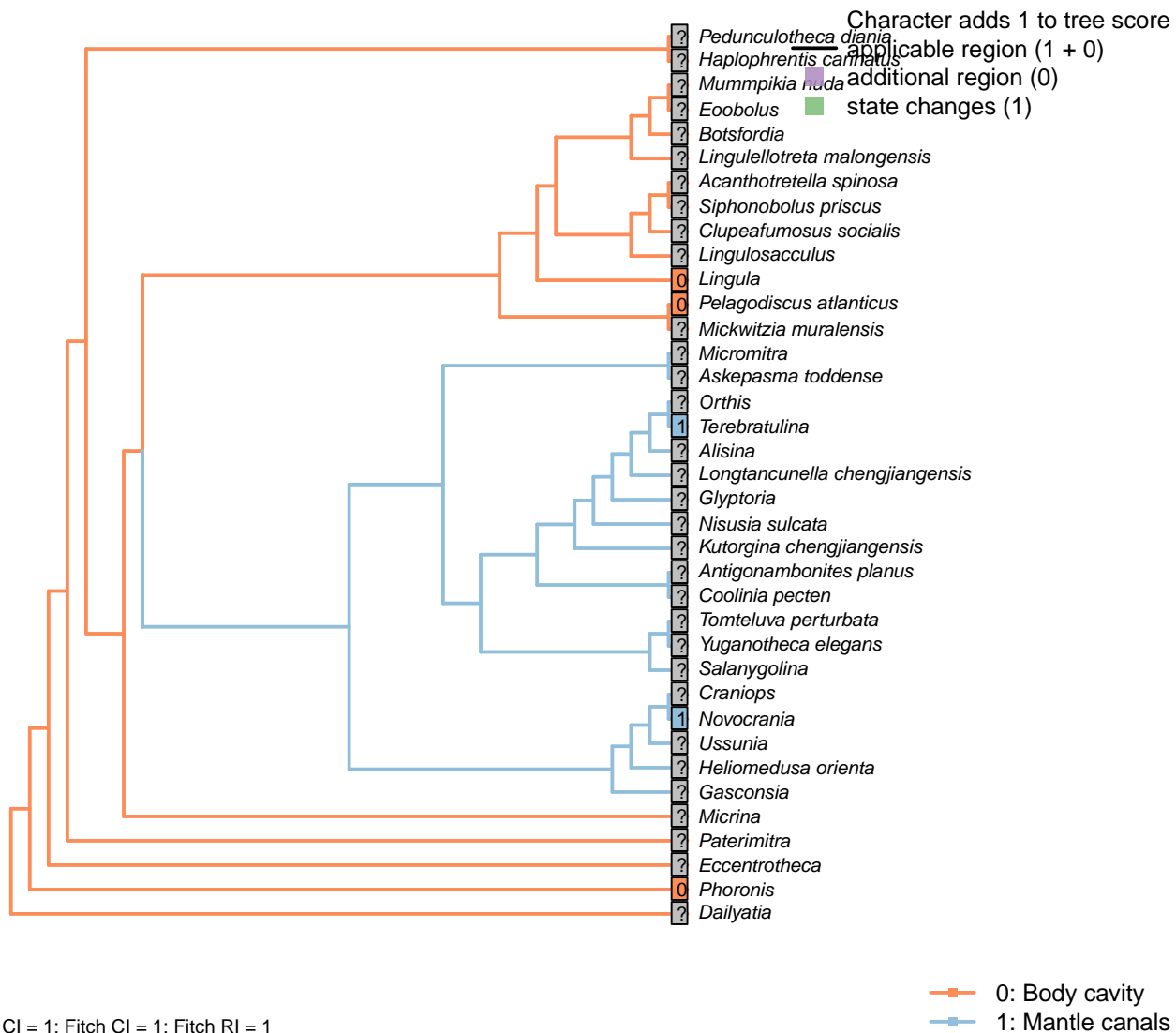
*Lingula, Novocrania, Pelagodiscus atlanticus, Terebratulina*: Following coding for class in Carlson (1995) appendix 1, character 7.

*Phoronis*: *Phoronis* has planktotrophic larvae. indicating a small egg size (Ruppert et al., 2004). Carlson

(1995) codes phoronids as polymorphic, as some members of the phylum have eggs of each size.

*Siphonobolus priscus*: “the ventral brespic valve [was] 50 µm across, [which] is close to the known lower limit of the brachiopod egg size” – Popov et al. (2009).

## [66] Site of maturation



### Character 66: Gametes: Site of maturation

0: Body cavity

1: Mantle canals

Neomorphic character.

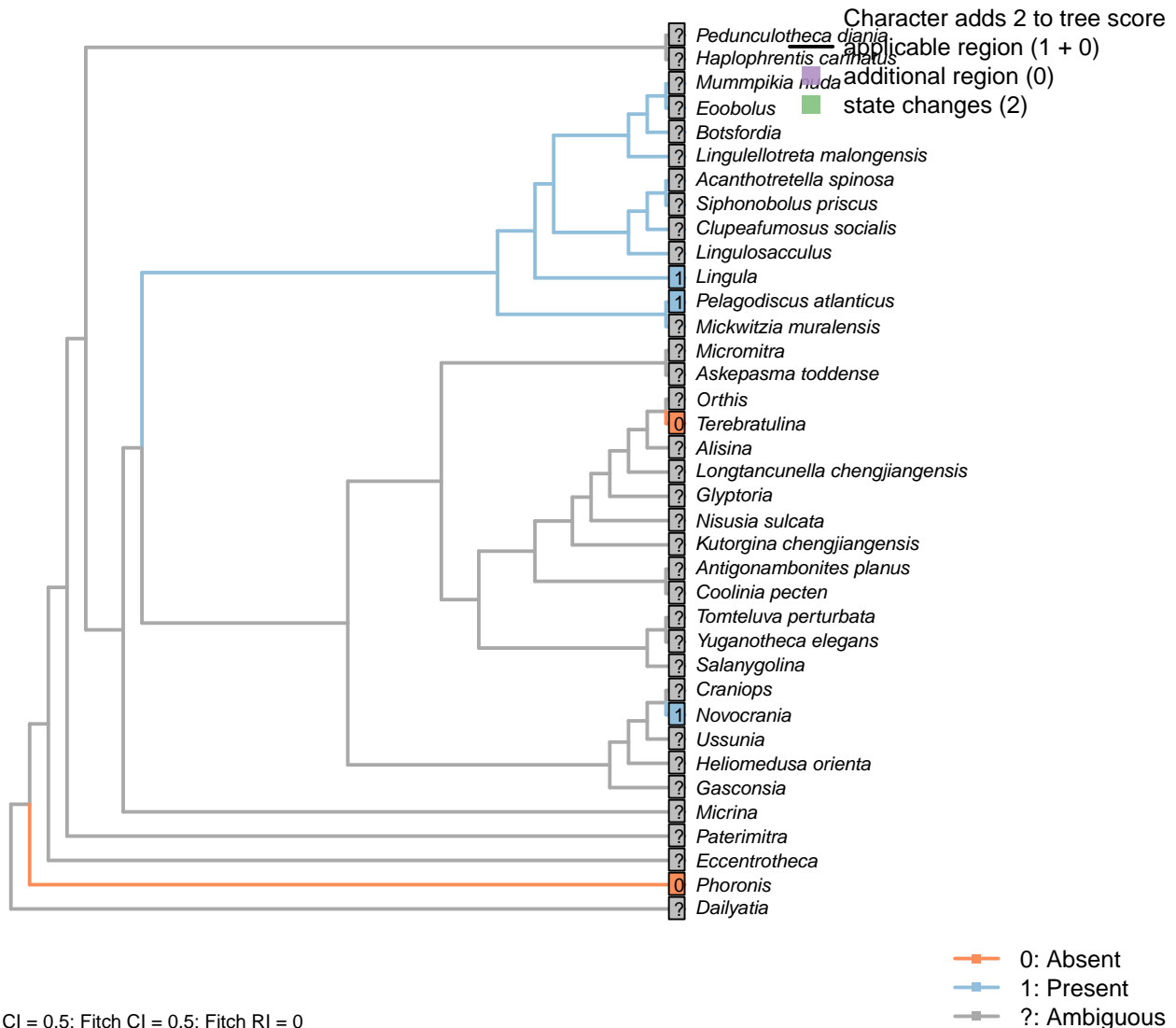
After Carlson (1995), character 9. Only possible to code in extant taxa. Mantle canals is considered the derived state, as it represents a migration from the body cavity, where gametes are produced.

*Lingula*, *Novocrania*, *Pelagodiscus atlanticus*, *Terebratulina*: Following Hodgson & Reunov (1994).

*Phoronis*: Following coding for class in Carlson (1995) Appendix 1, character 9.

### 3.8 Gametes: Spermatozoa

[67] Nucleus: Broad anterior invagination



**Character 67: Gametes: Spermatozoa: Nucleus: Broad anterior invagination**

0: Absent

1: Present

Neomorphic character.

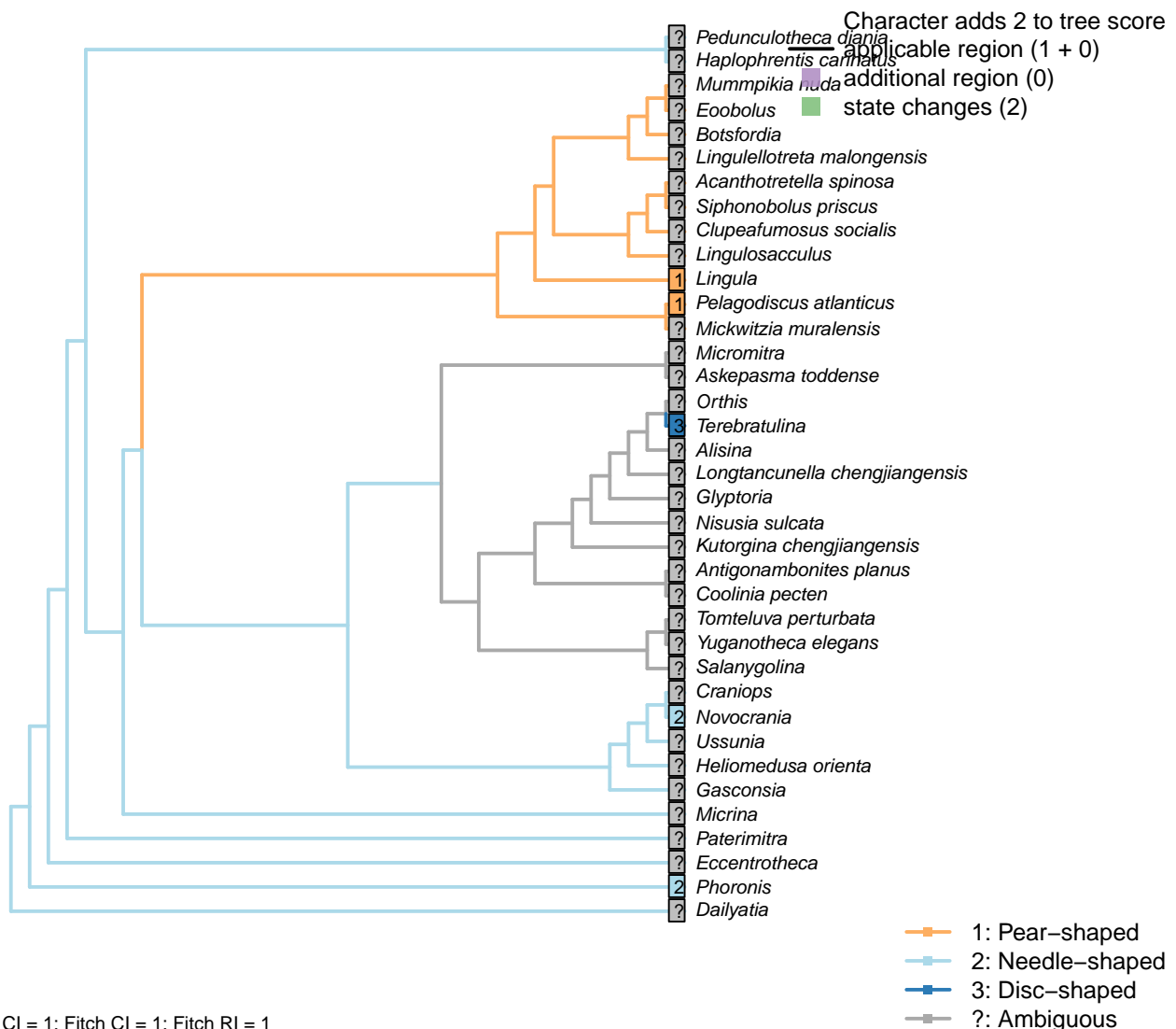
Following discussion in Hodgson and Reunov (1994).

*Pelagodiscus atlanticus*: Following *Discinisca tenuis*, described in Hodgson & Reunov (1994).

*Phoronis*: Nucleus “almost round”: Reunov and Klepal (2004).

*Terebratulina*: Hodgson and Reunov (1994).

## [68] Acrosome: Shape



## Character 68: Gametes: Spermatozoa: Acrosome: Shape

1: Pear-shaped

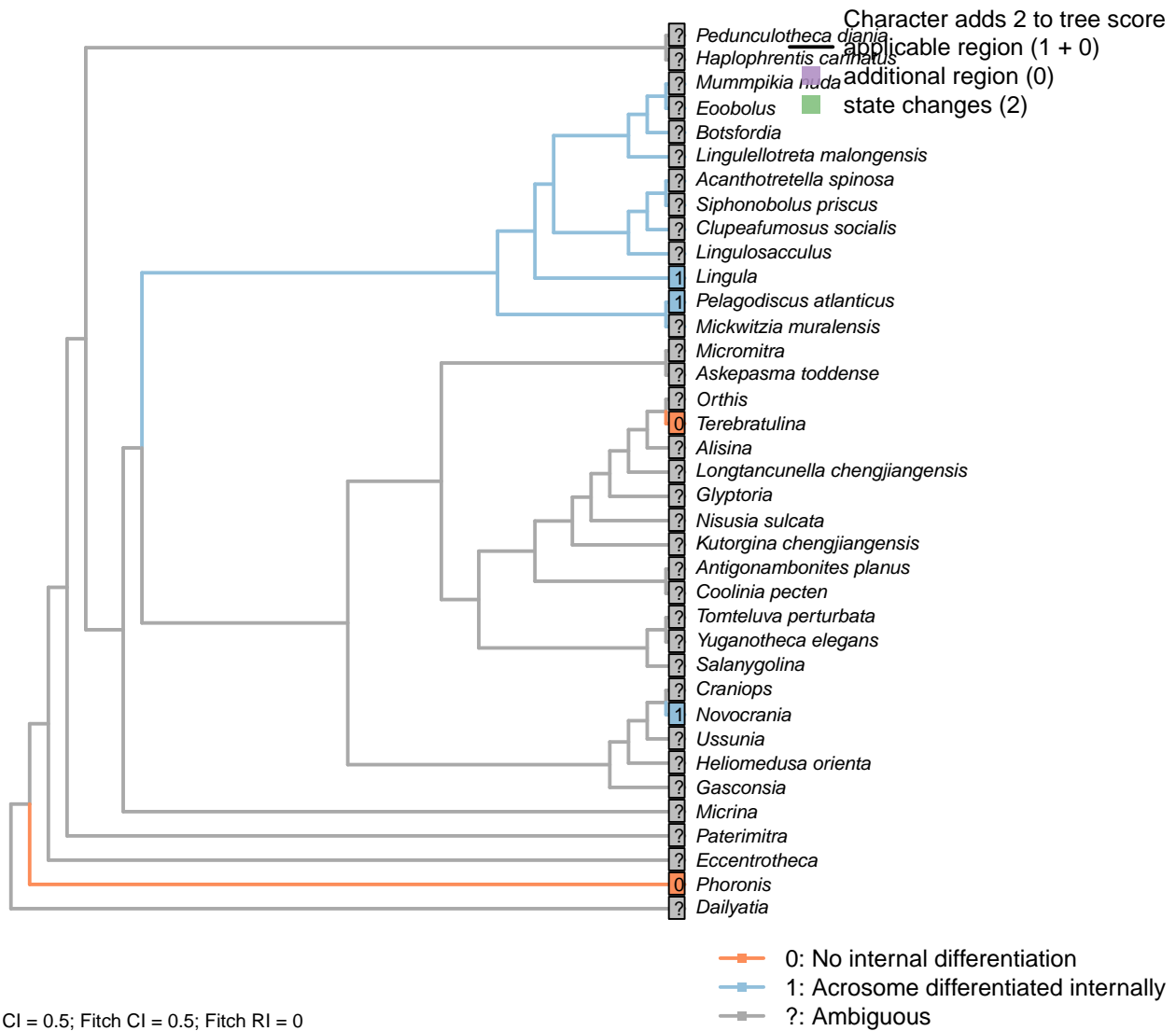
2: Needle-shaped

3: Disc-shaped

Transformational character.

*Lingula*: Pear-shaped (Fukumoto, 2003).*Novocrania*: Needle-shaped (Afzelius and Ferraguti, 1978).*Pelagodiscus atlanticus*: Pear-shaped (Hodgson and Reunov, 1994).*Phoronis*: Needle-shaped (Reunov and Klepal, 2004).*Terebratulina*: Disc-shaped (in *Kraussina*) (Hodgson and Reunov, 1994).

### [69] Acrosome: Differentiated internally



#### Character 69: Gametes: Spermatozoa: Acrosome: Differentiated internally

- 0: No internal differentiation
- 1: Acrosome differentiated internally
- Neomorphic character.

Hodgson and Reunov (1994) describe the *Discinisca* acrosome as having “an electron-lucent centre and an electron-dense outer region”, and state that this trait is characteristic of inarticulate brachiopods.

*Lingula*: Clear differentiation of marginal area (Fukumoto, 2003).

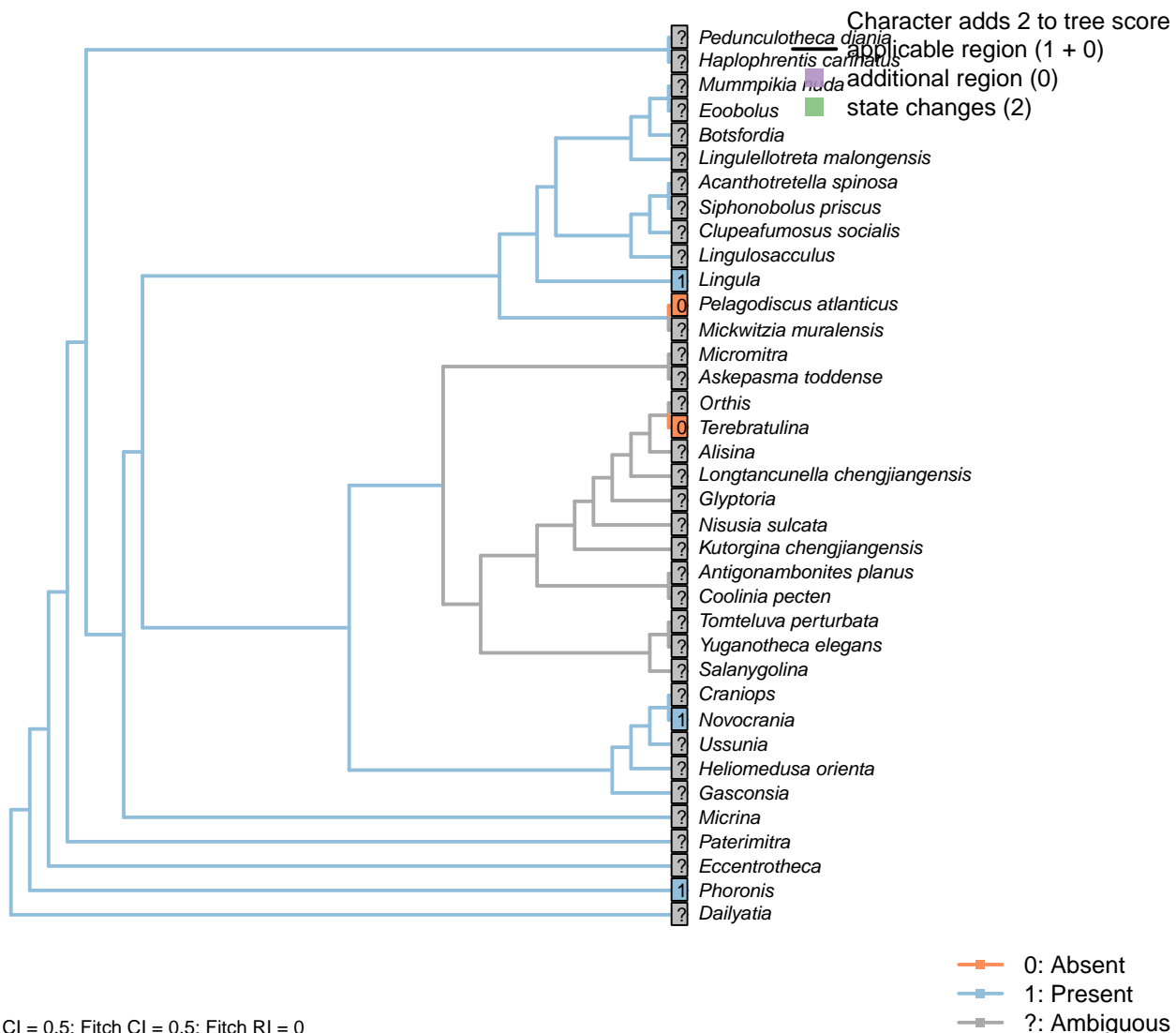
*Novocrania*: “Along the inner and outer margins there are periodically banded layers, and between them there is a less dense layer” – Afzelius and Ferraguti (1978).

*Pelagodiscus atlanticus*: Following *Discinisca tenuis*, described in Hodgson & Reunov (1994).

*Phoronis*: Acrosome-like structure; no internal division or surrounding membrane, with possibility that much of the acrosome is secondarily lost (Reunov and Klepal, 2004).

*Terebratulina*: Following Hodgson & Reunov (1994).

## [70] Acrosome: Sub-acrosomal space

**Character 70: Gametes: Spermatozoa: Acrosome: Sub-acrosomal space**

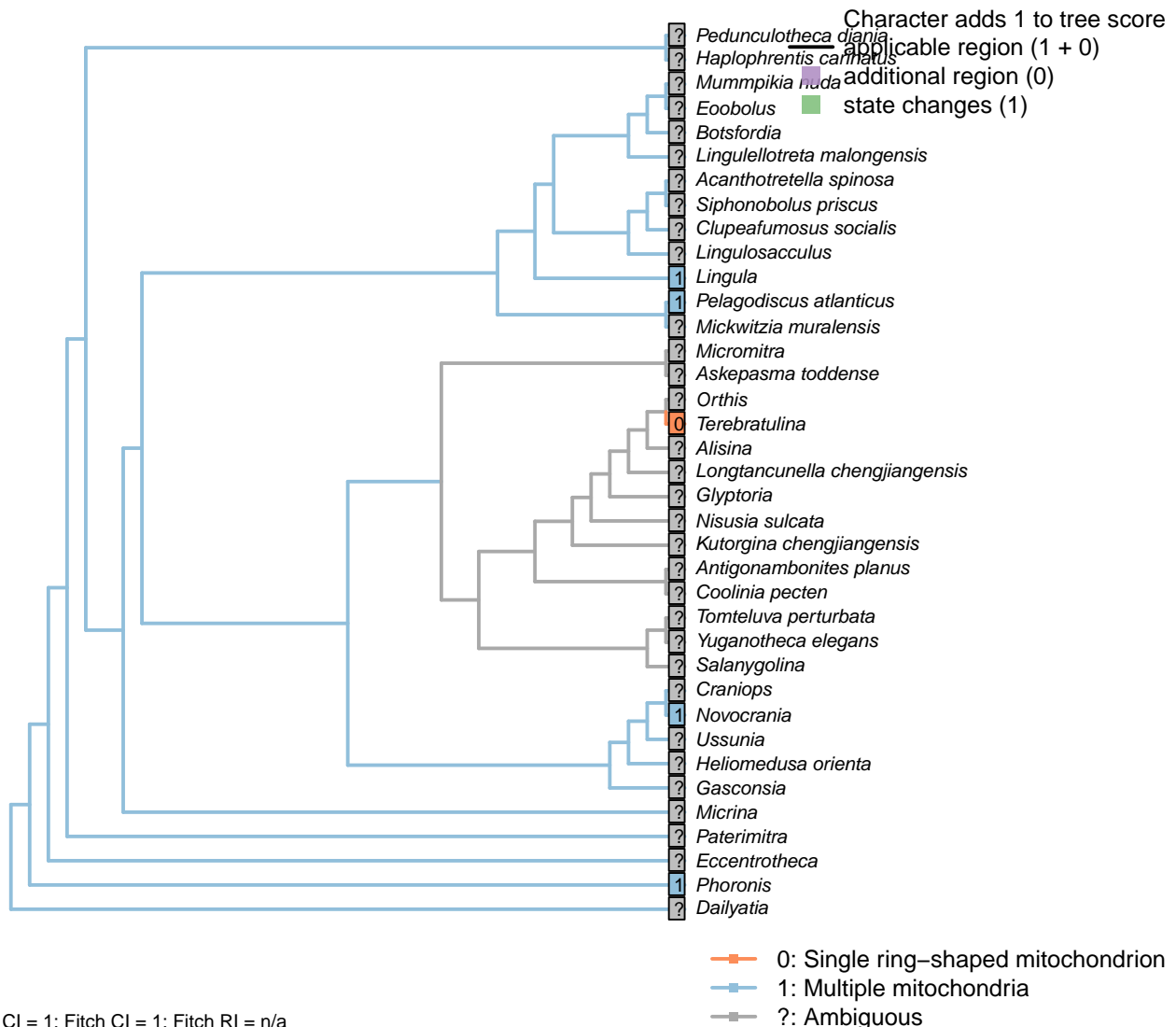
0: Absent

1: Present

Neomorphic character.

*Lingula*: Filled with sub-acrosomal substance (Fukumoto, 2003).*Novocrania*: Prominent (Afzelius and Ferraguti, 1978).*Pelagodiscus atlanticus*: Subacrosomal material (in *Discinisca*) but no subacrosomal space (Hodgson and Reunov, 1994).*Phoronis*: The filament-like acrosome continues backwards as a tube-like structure (Franzen and Ahlfors, 1980, summarized in Jamieson (1991)).*Terebratulina*: No subacrosomal material, let alone a subacrosomal space (e.g. Hodgson and Reunov, 1994).

## [71] Mid-piece

**Character 71: Gametes: Spermatozoa: Mid-piece**

- 0: Single ring-shaped mitochondrion
- 1: Multiple mitochondria
- Neomorphic character.

Following Hodgson & Reunov (1994).

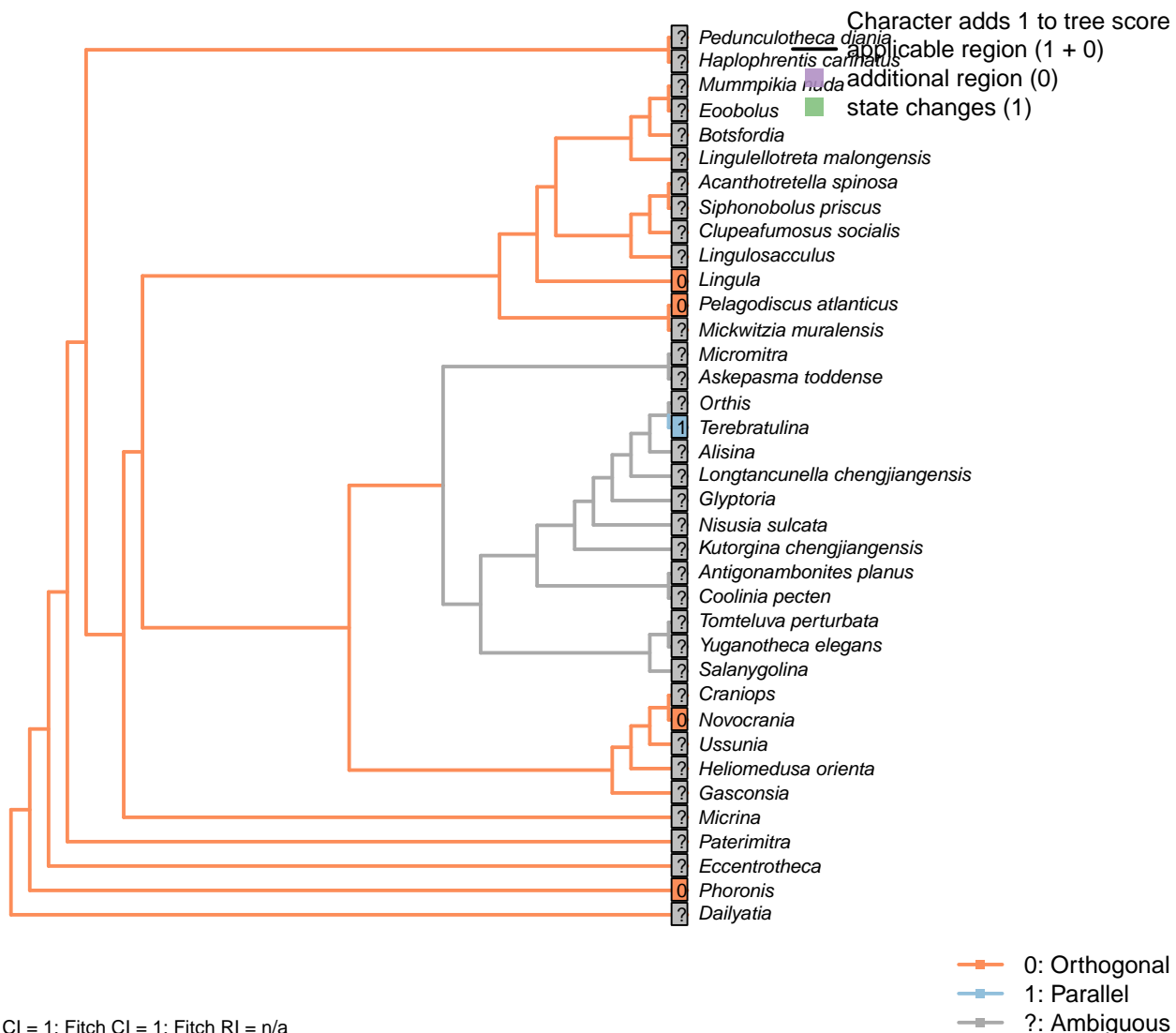
*Lingula*, *Terebratulina*: Following Hodgson & Reunov (1994).

*Novocrania*: Four mitochondria (Afzelius and Ferraguti, 1978).

*Pelagodiscus atlanticus*: Following *Discinisa tenuis*, described in Hodgson & Reunov (1994).

*Phoronis*: The mitochondria fuse in the middle stage of spermiogenesis to become a pair of mitochondria (Reunov and Klepal, 2004).

## [72] Centrioles

**Character 72: Gametes: Spermatozoa: Centrioles**

0: Orthogonal

1: Parallel

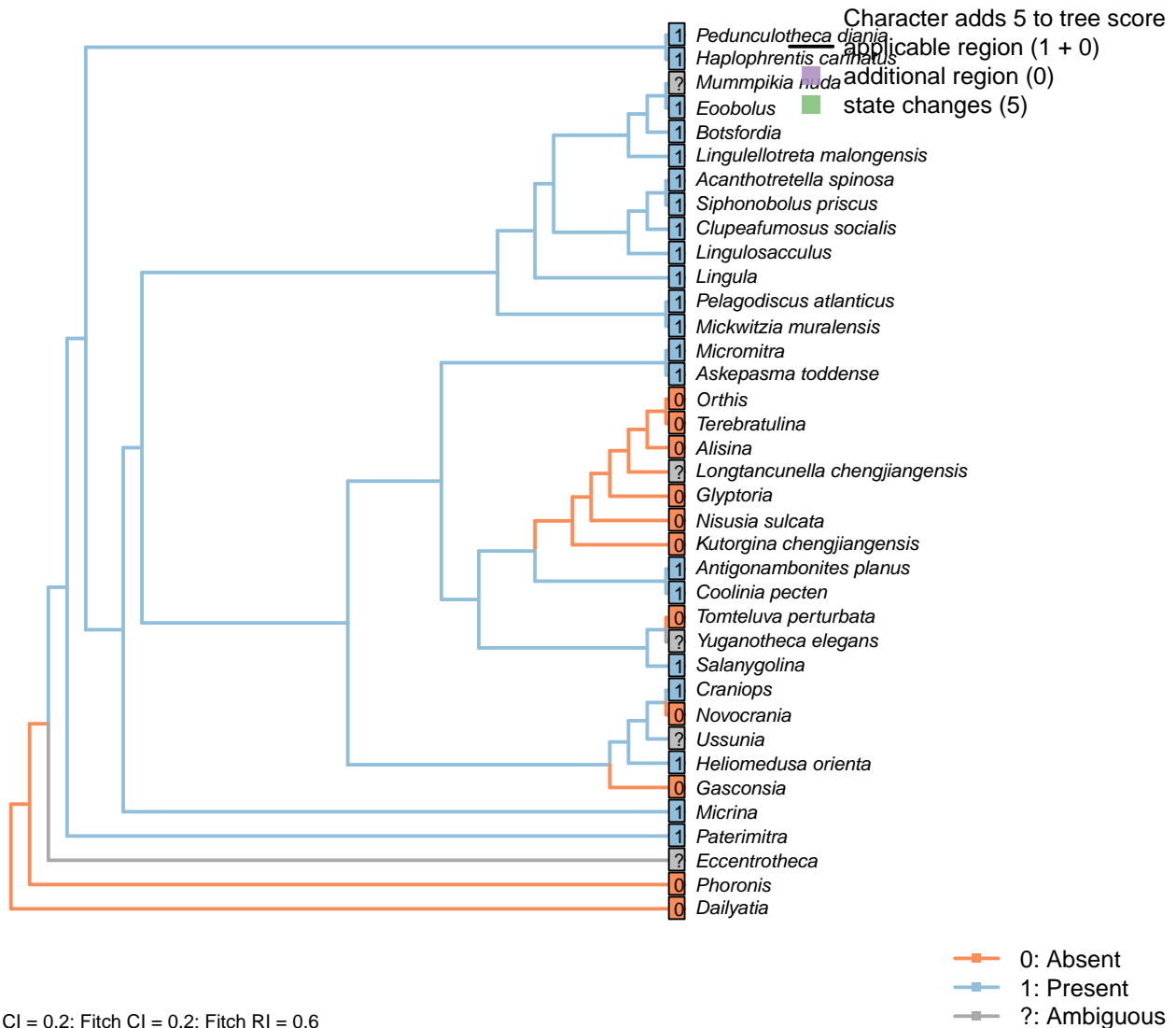
Neomorphic character.

Following Hodgson and Reunov (1994).

*Lingula, Terebratulina*: Following Hodgson & Reunov (1994).*Novocrania*: Two orthogonal centrioles (Afzelius and Ferraguti, 1978).*Pelagodiscus atlanticus*: Following *Discinisa tenuis*, described in Hodgson & Reunov (1994).*Phoronis*: Only one centriole in spermatozoon (Reunov and Klepal, 2004, p. 7), but centrioles are perpendicularly oriented in spermatogonia (*ibid.*, p. 2).

### 3.9 Brephic shell

[73] Embryonic shell



#### Character 73: Brephic shell: Embryonic shell

0: Absent

1: Present

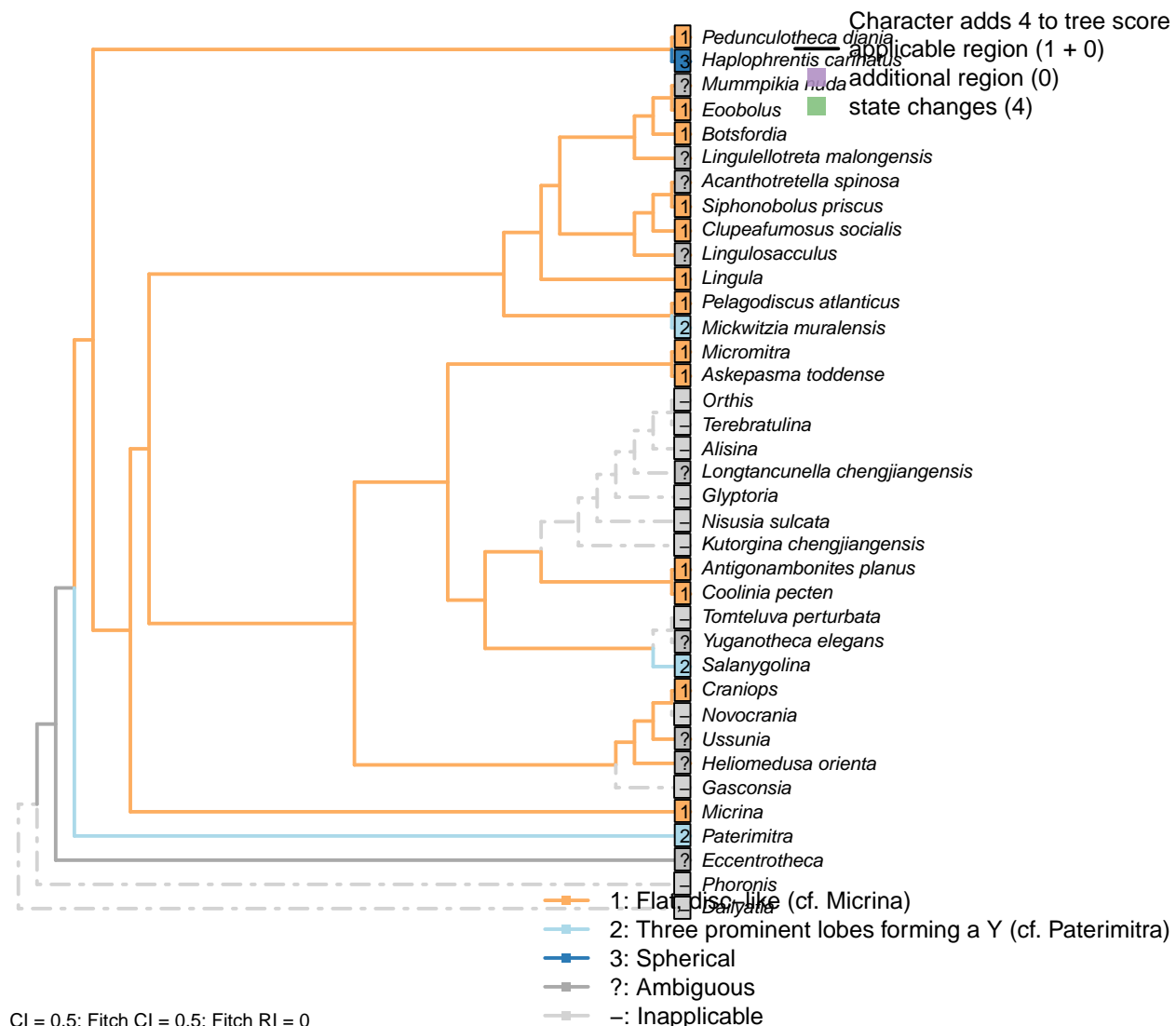
Neomorphic character.

The embryonic shell or protegulum is secreted by the embryo immediately before hatching.

*Clupeafumosus socialis*: Described by Topper *et al.* (2013a).

*Novocrania*: Shell not secreted until after metamorphosis (Popov *et al.*, 2010).

## [74] Morphology



### Character 74: Brephic shell: Morphology

- 1: Flat, disc-like (cf. *Micrina*)
  - 2: Three prominent lobes forming a Y (cf. *Paterimitra*)
  - 3: Spherical
- Transformational character.

The brephic shell is the shell possessed by the young organism (see Ushatinskaya and Korovnikov, 2016, and references therein for discussion of terminology).

*Micrina* resembles linguliforms (Holmer et al., 2011): in both, the brephic mitral shell has one pair of setal sacs enclosed by lateral lobes, whereas the brephic ventral shell has two lateral setal tubes.

*Paterimitra* and *Salanygolina* have “identical” ventral brephic shells (Holmer et al., 2011), resembling the shape of a ship’s propeller.

*Haplophrentis* is coded following typical hyoliths, which have a spherical brephic shell; *Pedunculotheca*’s, in

contrast, is seemingly cap-shaped.

*Askepasma toddense*: Renoid – see fig. 4B3 in Topper et al. (2013b).

*Clupeafumosus socialis*: The flat larval shell of *Clupeafumosus* resembles that of *Micrina* in outline (Topper et al., 2013a; cf. Holmer et al., 2011).

*Coolinia pecten*: See fig. 3 in Bassett and Popov (2017).

*Craniops*: The embryonic shell is more or less circular in outline – see Freeman and Lundelius (1999), fig. 6A.

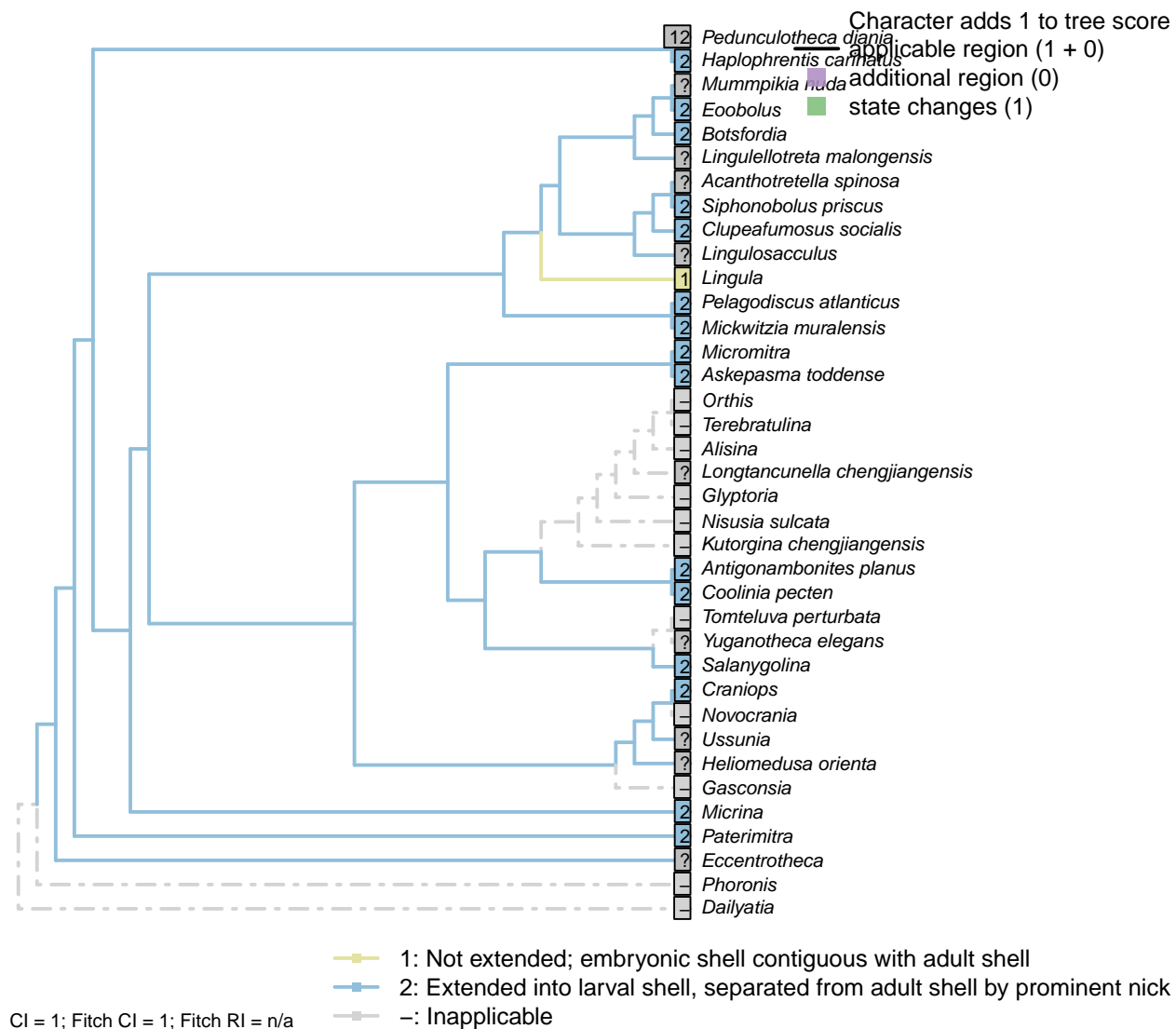
*Lingula*: See fig. 159 in Williams et al. (1997).

*Mickwitzia muralensis*: Trifoliate appearance results from prominent attachment rudiment and bunching of setal sacs (Balthasar, 2009).

*Micromitra*: Subtriangular – essentially round.

*Pelagodiscus atlanticus*: See e.g. fig 169 in Williams et al. (1997).

## [75] Embryonic shell extended in larvae

**Character 75: Brephic shell: Embryonic shell extended in larvae**

- 1: Not extended; embryonic shell contiguous with adult shell
- 2: Extended into larval shell, separated from adult shell by prominent nick
- Transformational character.

Many taxa add to their embryonic shell (the protegulum possessed by the embryo upon hatching) during the larval phase of their life cycle. The shell that exists at metamorphosis, marked by a halo or nick point, is variously termed the “first formed shell”, “metamorphic shell” or “larval shell” (Bassett and Popov, 2017).

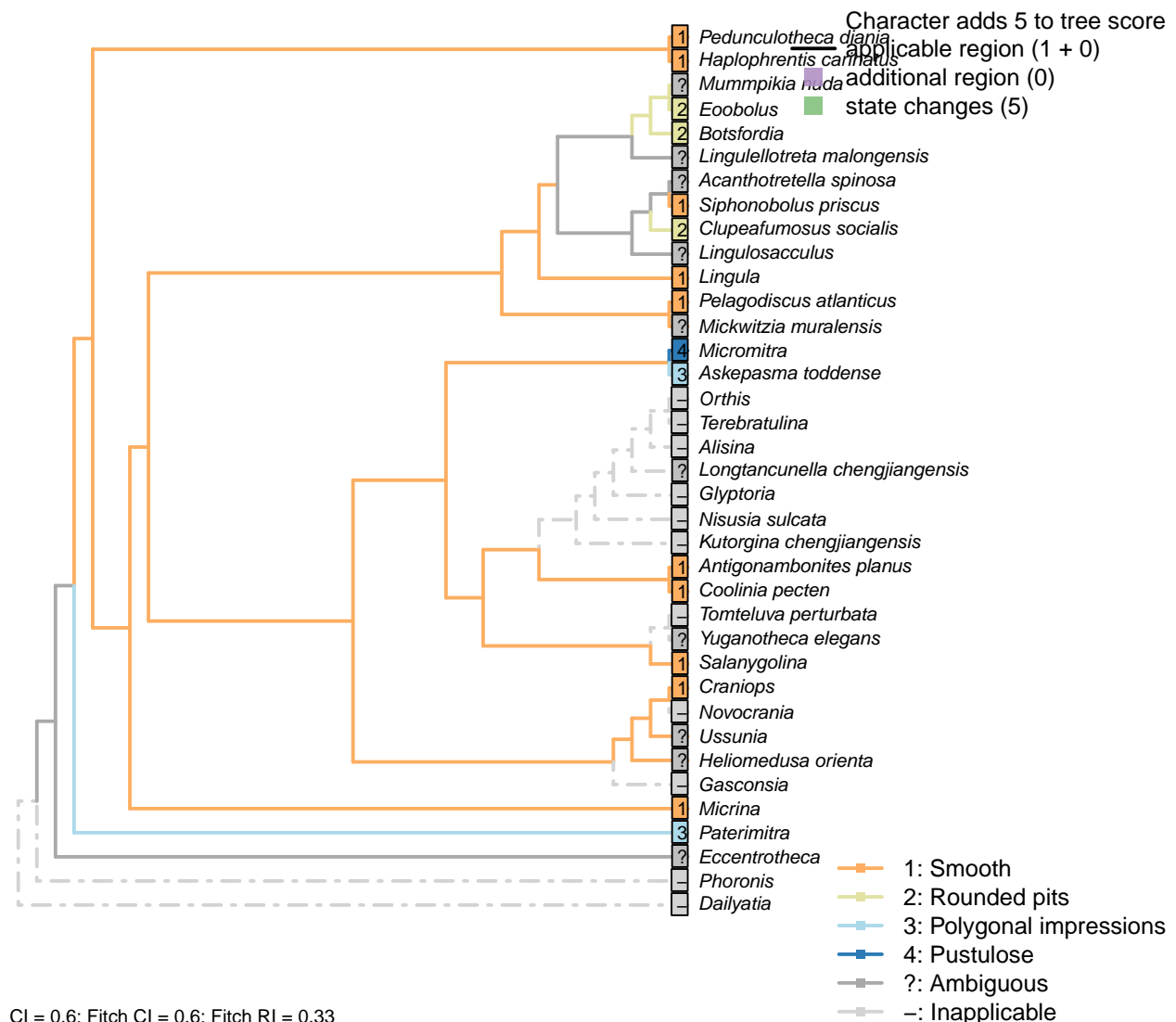
*Clupeafumosus socialis*: Described by Topper *et al.* (2013a).

*Craniops*: Prominent nick; see Freeman and Lundelius (1999), fig. 6A.

*Eoobolus*: Nick point indicated by arrows in fig. 1 of Balthasar (2009).

*Pedunculotheca diana*: The flattened region at the umbo of the ventral valve in smaller specimens conceivably represents an embryonic shell, though it may alternatively represent a cicatrix or colleplax-like structure.

## [76] Surface ornament



Pitting of the larval shell characterises acrotretids and their relatives. Pustules occur on Paterinidae. See

Character 3 in Williams *et al.* (2000) tables 5–6.

*Askepasma toddense*: Indented with hexagonal pits (Williams *et al.*, 1998, appendix 2).

*Eoobolus*: Pitted (Williams *et al.*, 2000, table 8).

*Lingula*, *Pelagodiscus atlanticus*: Smooth, following family-level codings of Williams *et al.* (2000), table 6.

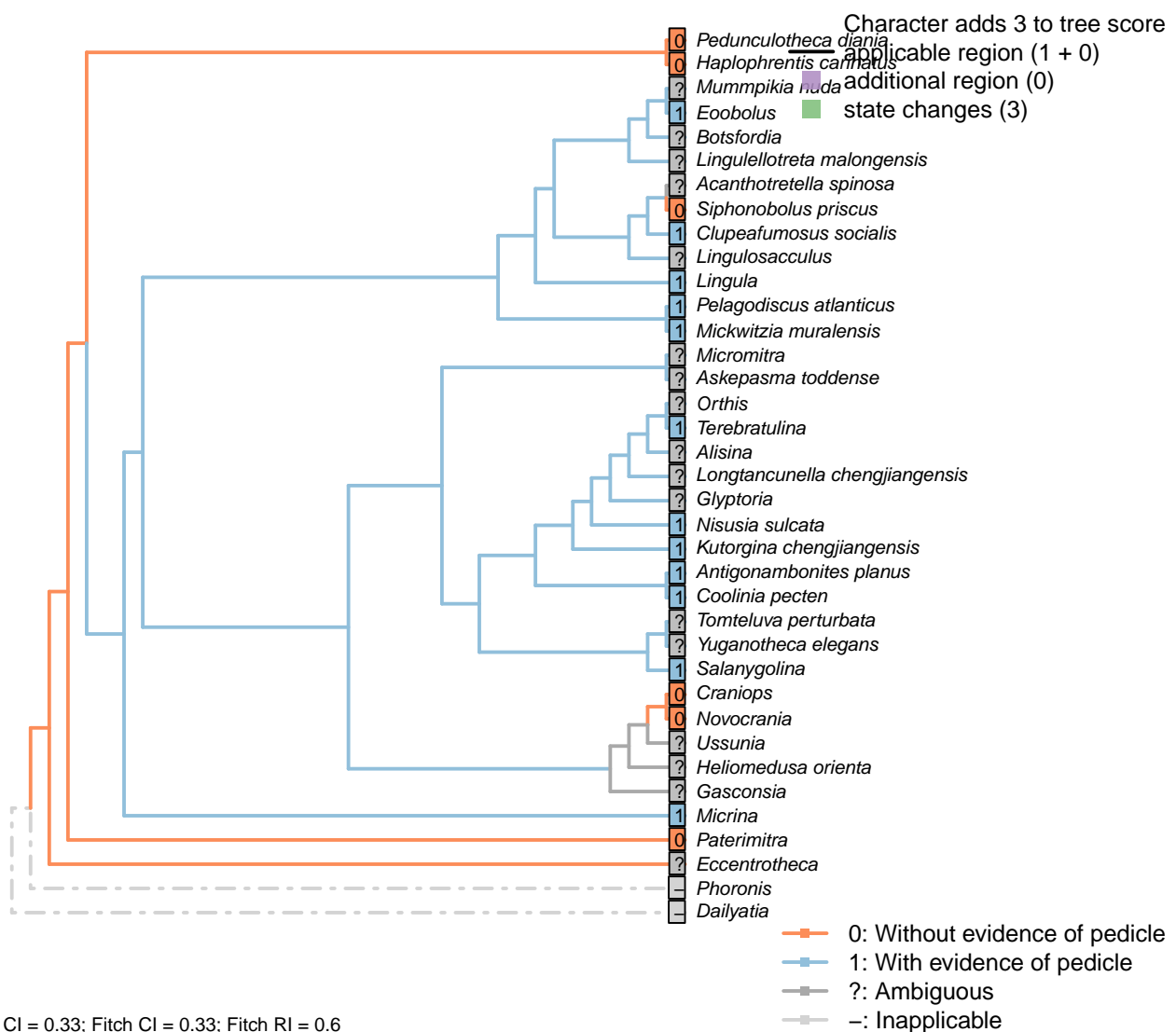
*Micrina*: Smooth (Holmer *et al.*, 2011).

*Micromitra*: Pustulose in Paterinidae (Williams *et al.*, 2000, table 6).

*Paterimitra*: Polygonal texture present (Holmer *et al.*, 2011), as in the adult shell.

*Salanygolina*: Smooth (Holmer *et al.*, 2009).

## [77] Larval attachment structure



### Character 77: Brephic shell: Larval attachment structure

0: Without evidence of pedicle

1: With evidence of pedicle

Neomorphic character.

Embryonic shells of *Micrina* and certain linguliforms exhibit a transversely folded posterior extension that speaks of the original presence of a pedicle in the embryo.

This is independent of the presence of an adult pedicle, which may arise after metamorphosis.

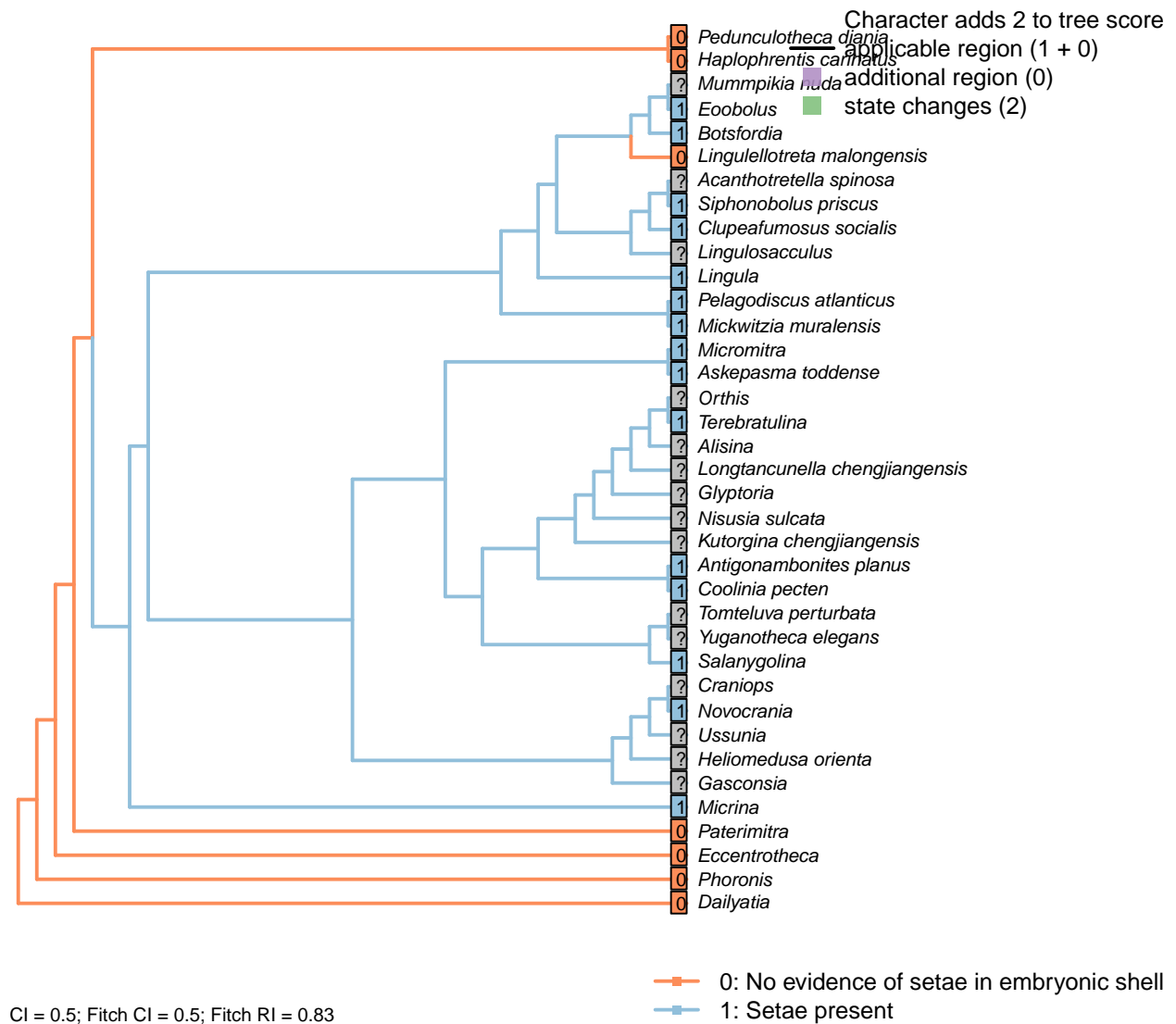
*Clupeafumosus socialis*: The larval shell embraces the pedicle foramen, suggesting a larval attachment. See fig. 4 of Topper *et al.* (2013a).

*Eoobolus*: Lobe related to the attachment rudiment (Balthasar, 2009, fig. 2).

*Mickwitzia muralensis*: Note the posterior lobe related to the attachment rudiment in fig. 2 of Balthasar (2009).

*Siphonobolus priscus*: Interpreted as having planktotrophic (and thus non-attached) larvae (Popov *et al.*, 2009).

## [78] Setulose



Character 78: Bivalve shell: Setulose

- 0: No evidence of setae in embryonic shell  
 1: Setae present  
 Neomorphic character.

The protogulum of *Micrina* is penetrated with canals that were originally associated with setae, a character that it has in common with linguliforms (Holmer et al., 2011).

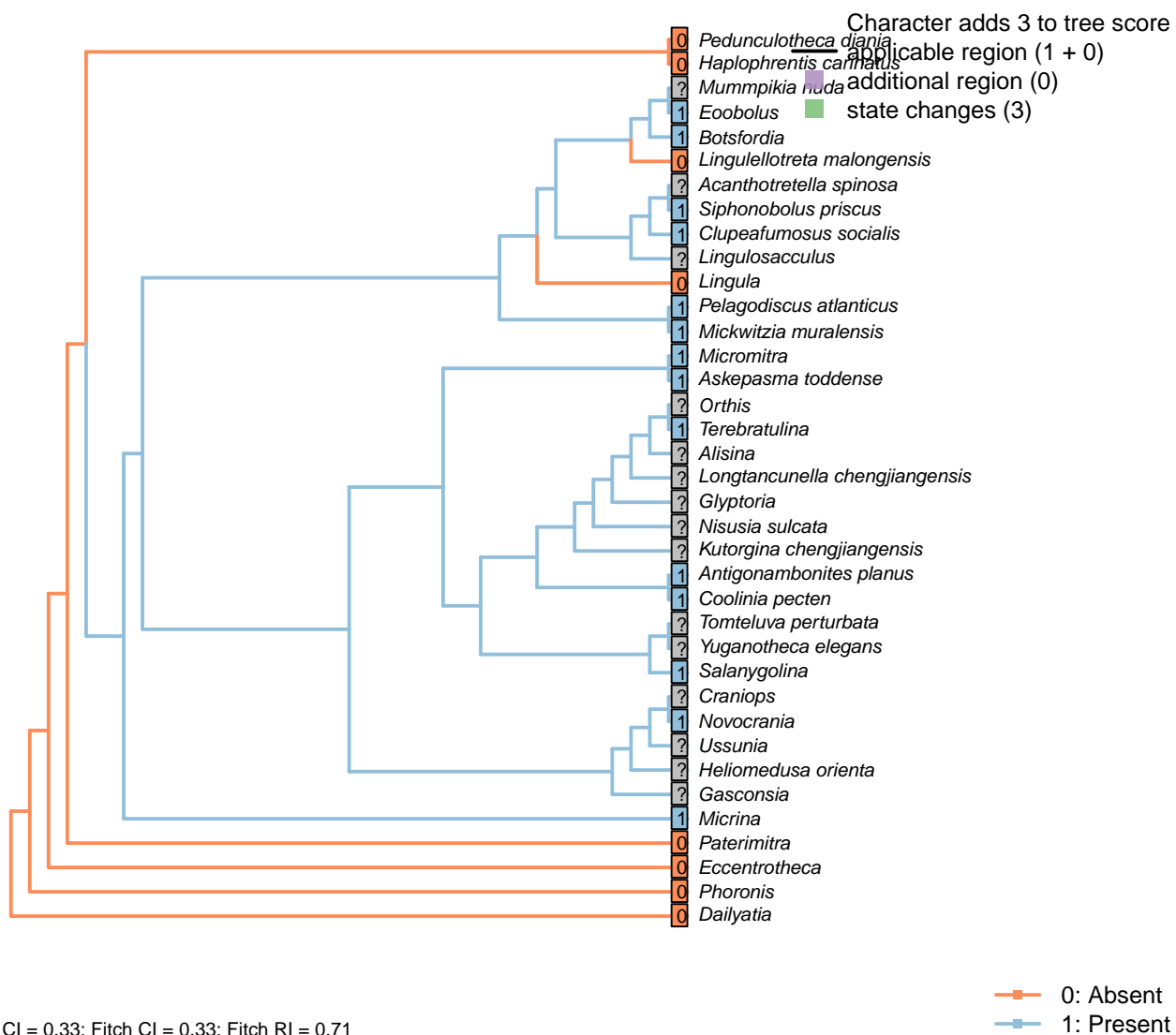
*Botsfordia*: “One specimen shows fine capillae running laterally from the posterior tubercles on the dorsal valve (Pl. 3, fig. 5b). This is possibly the imprints of setae.” – Ushatinskaya and Korovnikov (2016).

*Clupeafumosus socialis*: Setal bundles interpreted as present in acrotretids by Ushatinskaya (2016).

*Lingulellotreta malongensis*: Familial character: larval shell smooth (williams et al., 2000, p.72).

*Mickwitzia muralensis*: Four setal sacs.

### 3.10 Brephic shell: Setal sacs [79]



0: Absent

1: Present

Neomorphic character.

Setal sacs are recognizable as raised lumps on the juvenile shell (see Bassett and Popov, 2017).

*Micrina* and linguliforms have setal sacs on their mitral/dorsal embryonic shell, whereas these are absent in *Paterimitra* (Holmer et al., 2011).

*Botsfordia*: A single pair of low tubercles are (Ushatinskaya and Korovnikov, 2016, state “may be”) located in the middle region of the dorsal and the ventral biphthic valve; these are interpreted as a single pair of setal sacs, with the identity of the (dorsally unpaired) tubercles uncertain.

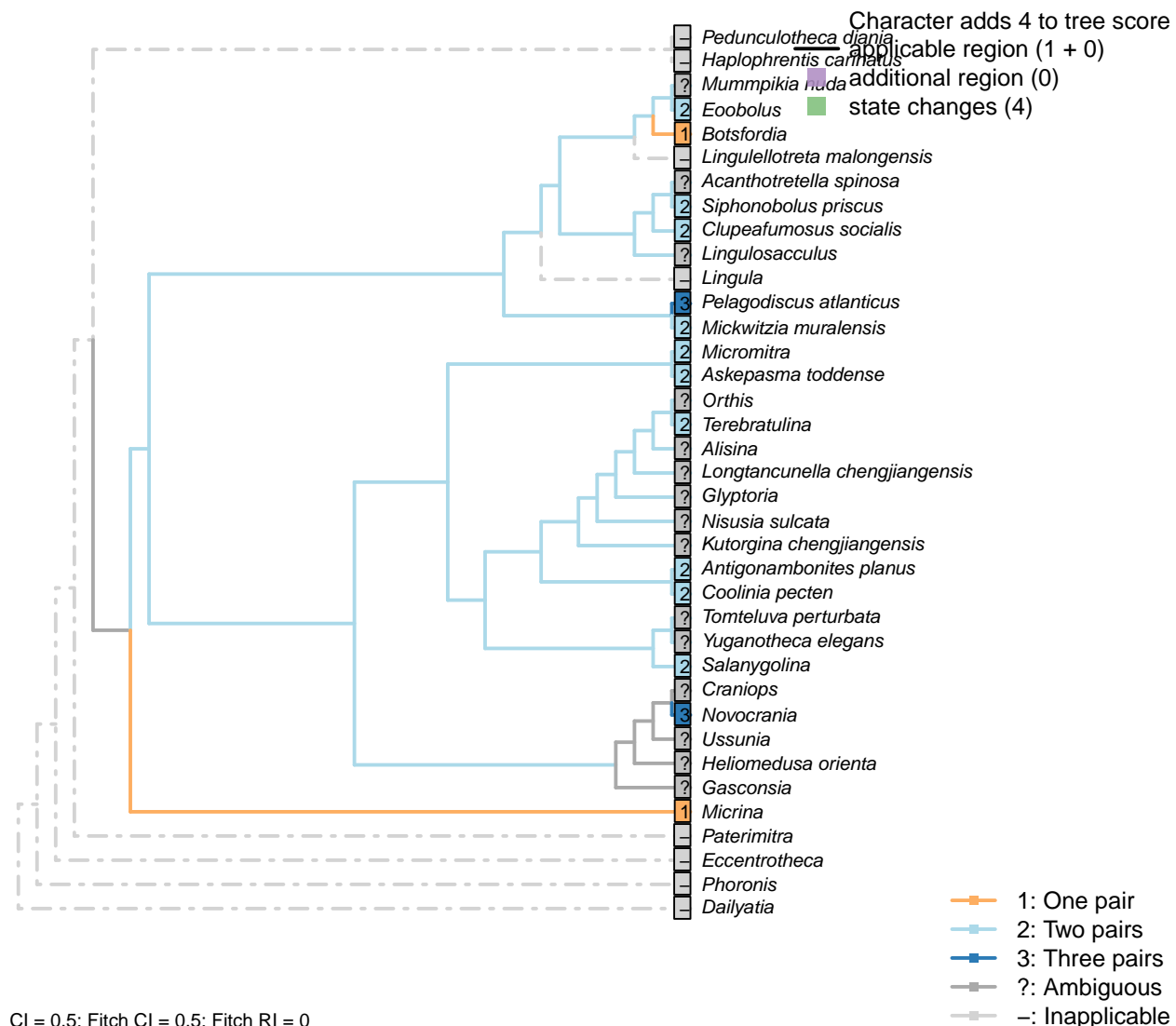
*Clupeafumosus socialis*: Setal bundles interpreted as present in acrotretids by Ushatinskaya (2016).

*Lingula*: Lingulids’ larval setae are not arranged in bundles (Carlson, 1995).

*Lingulellotreta malongensis*: Familial character: larval shell smooth (williams et al., 2000, p.72).

*Novocrania*, *Pelagodiscus atlanticus*: Three pairs (Carlson, 1995).

## [80] Number

**Character 80: Brephic shell: Setal sacs: Number**

1: One pair

2: Two pairs

3: Three pairs

Transformational character.

Two pairs on e.g. *Coolina*; one on e.g. *Micrina*.

*Botsfordia*: “larval shell with one to three apical tubercles in ventral valve and two in dorsal valve” (Williams et al., 2000) – if these correspond to setal sacs, then we interpret this as equivalent to one pair.

*Clupeafumosus socialis*: Two pairs identified in acrotretids by Ushatinskaya (2016).

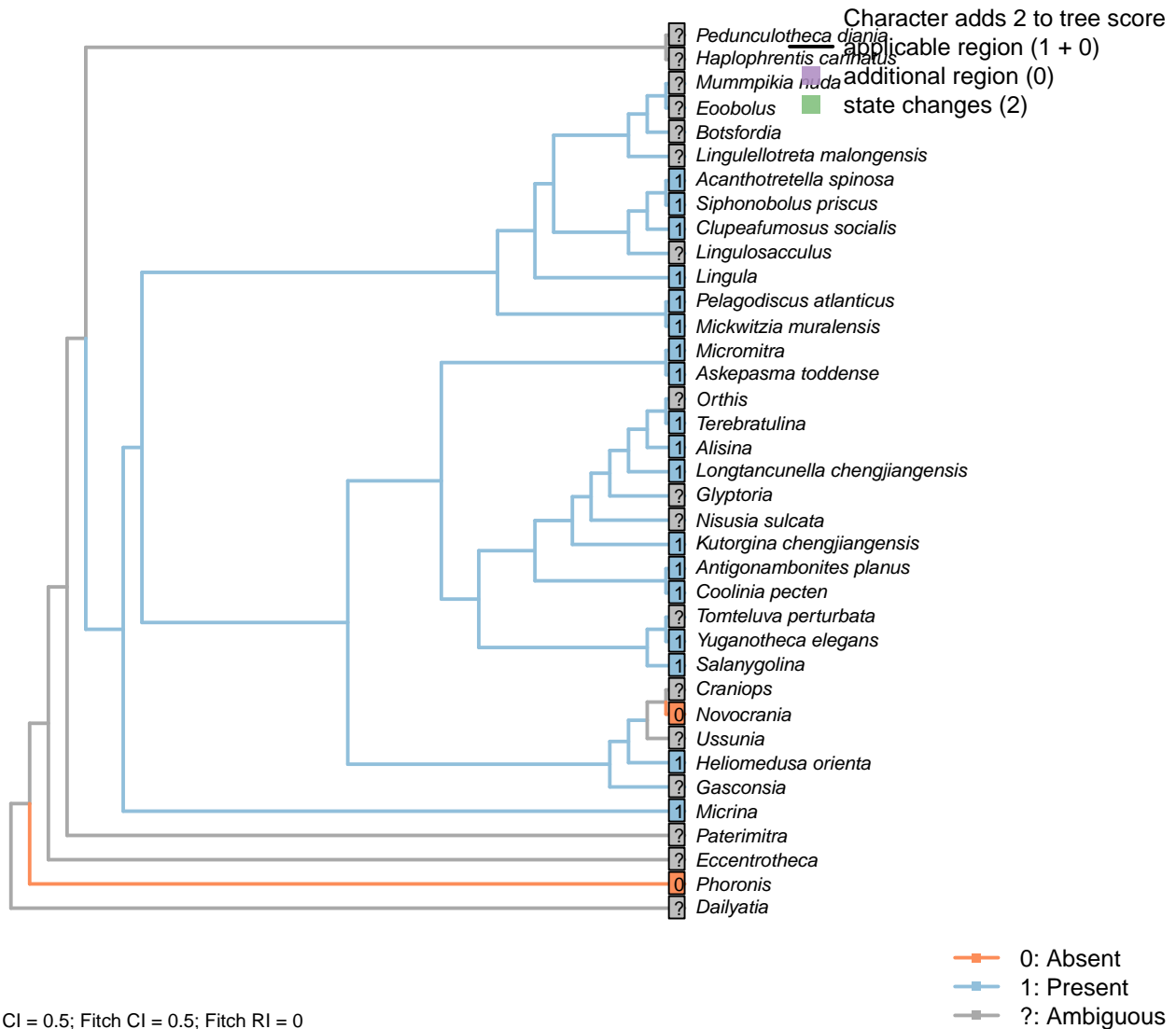
*Mickwitzia muralensis*: See fig. 2 in Balthasar (2009).

*Novocrania*, *Pelagodiscus atlanticus*: Three pairs (Carlson, 1995).

*Siphonobolus priscus*: Two pairs of setal sacs (Popov et al., 2009).

### 3.11 Setae

#### [81] Present in adults



#### Character 81: Setae: Present in adults

0: Absent

1: Present

Neomorphic character.

Although preservation of setae (in adults) is exceptional, their presence can be inferred from shelly material (see Holmer and Caron, 2006).

*Acanthotretella spinosa*: Note that the setae do not obviously emerge from tubes, leading Holmer and Caron to question their homology with the setae of other taxa (*Helio-medusa*, *Mickwitzia*).

Both valves of *Acanthotretella* were covered by long spine-like and shell penetrating setae. The setae of *A.*

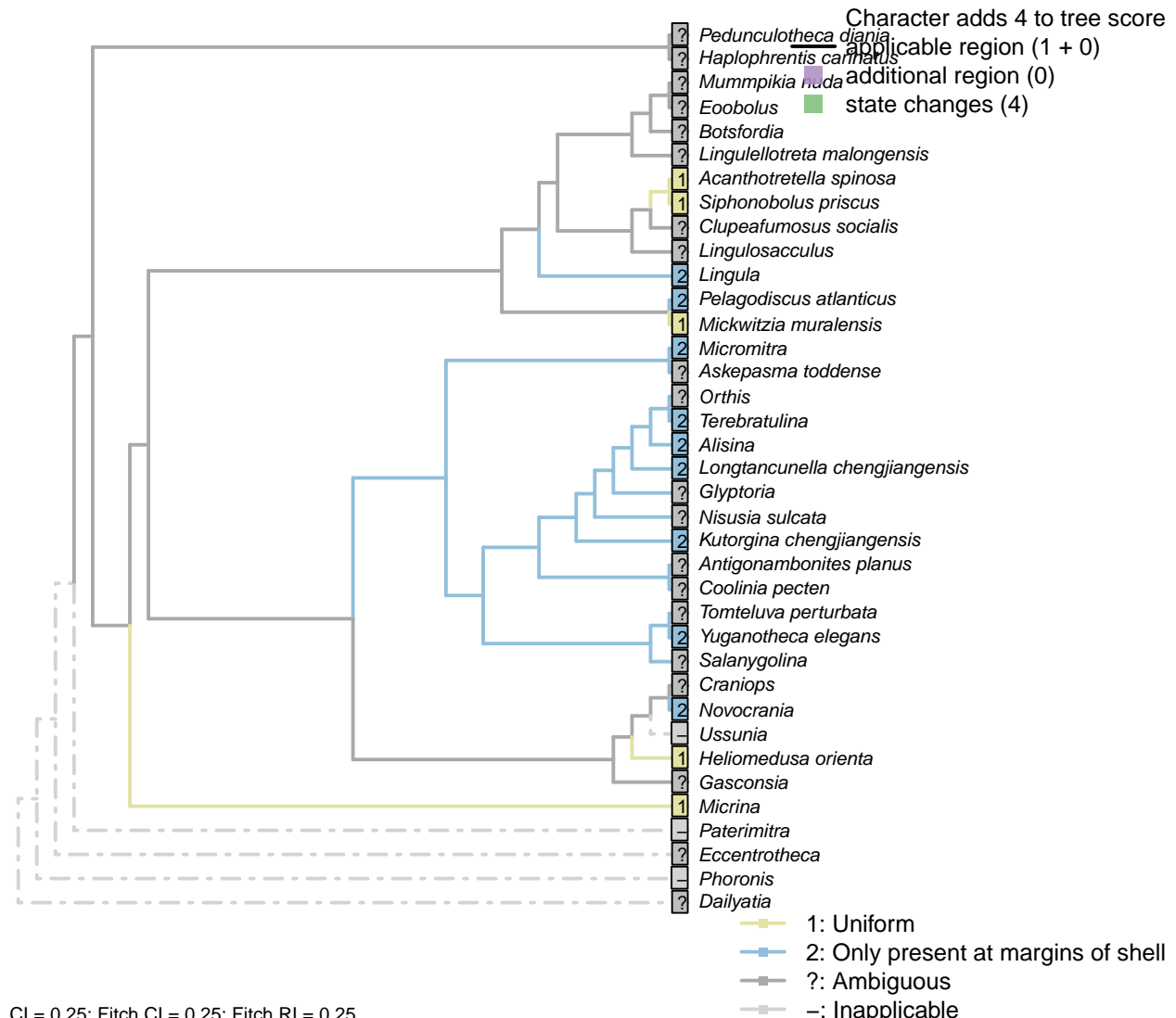
*decaius* are usually preserved along anterior and anterolateral margins (Hu et al., 2010).

*Clupeafumosus socialis*: Setal bundles interpreted as present in acrotretids by Ushatinskaya (2016).

*Novocrania*: “Adult craniids are without setae (a feature shared with the thecideides, the shells of which are also cemented).” – Williams et al. (2007).

*Siphonobolus priscus*: Phosphatised setae emerge from hollow spines (Popov et al., 2009).

## [82] Distribution



### Character 82: Setae: Distribution

1: Uniform

2: Only present at margins of shell

Transformational character.

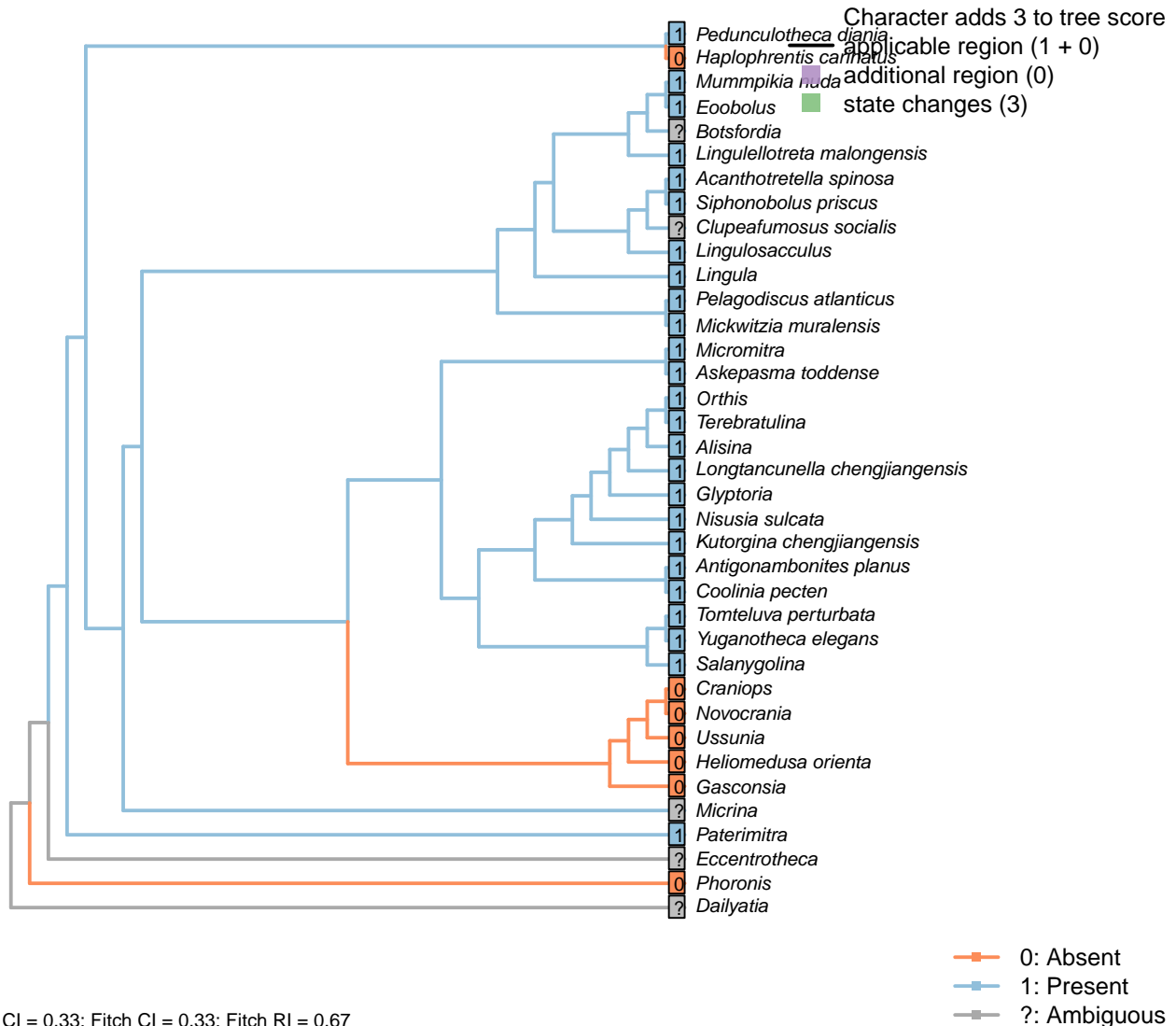
Setae penetrate the valves of many brachiopods. In certain taxa, they are apparent only at the margins of the valves, in association with the commissure, being reduced or lost over the surface of the shell.

*Eccentrotheca*: Skovsted et al. (2011) assumed the setae may have been present along the margin of the

adapical opening, but there is no fossil evidence.

*Heliomedusa orienta*: Throughout the shell – see Williams et al. (2007) – causing the pustulose appearance remarked upon by Chen et al. (2007).

### 3.12 Pedicle [83]



#### Character 83: Pedicle

0: Absent

1: Present

Neomorphic character.

The brachiopod pedicle is a fleshy protuberance that emerges from the posterior part of the body wall – as denoted in fossil taxa by its occurrence between the dorsal and ventral valves.

It is important to distinguish the pedicle from the “pedicle sheath”, a tubular extension of the umbo that grows by accretion from an isolated portion of the ventral mantle. For discussion see Holmer et al. (2018b)

and Bassett and Popov (2017).

*Acanthotretella spinosa*: The attachment structure of *Acanthotretella* originates at the margin of the dorsal and ventral valves; although it emerges from the umbo of the ventral valve, the presence of an internal pedicle tube betrays its identity as a pedicle, rather than a pedicle sheath.

The pedicle of *Acanthotretella* emerges from a short extension of the umbo of the ventral valve. This extension is contiguous with the valve and presumably grew by accretion; its position and continuity with the valve suggest its interpretation as a pedicle sheath that is superseded as an attachment structure. On the other hand, its continuity with the internal pedicle tube suggests that it may represent an independent organ.

*Botsfordia*: Pedicle foramen was not necessarily occupied by a pedicle (though it presumably was).

*Clupeafumosus socialis*: A pedicle was presumably present, but only the foramen is preserved.

*Craniops*: Attached apically by cementation.

*Heliomedusa orienta*: “It seems unlikely that *H. orienta* possessed a pedicle that attached it to the soft seafloor, like most other Chengjiang brachiopods.” ...

“The putative pedicle illustrated by Chen *et al.* (2007, Figs 4, 6, 7) in fact is the mold of a three-dimensionally preserved visceral cavity” – Zhang *et al.* (2009).

*Lingulosacculus*: The absence of a pedicle is inferred from the absence of an internal pedicle tube, and the absence of a pedicle at the hinge.

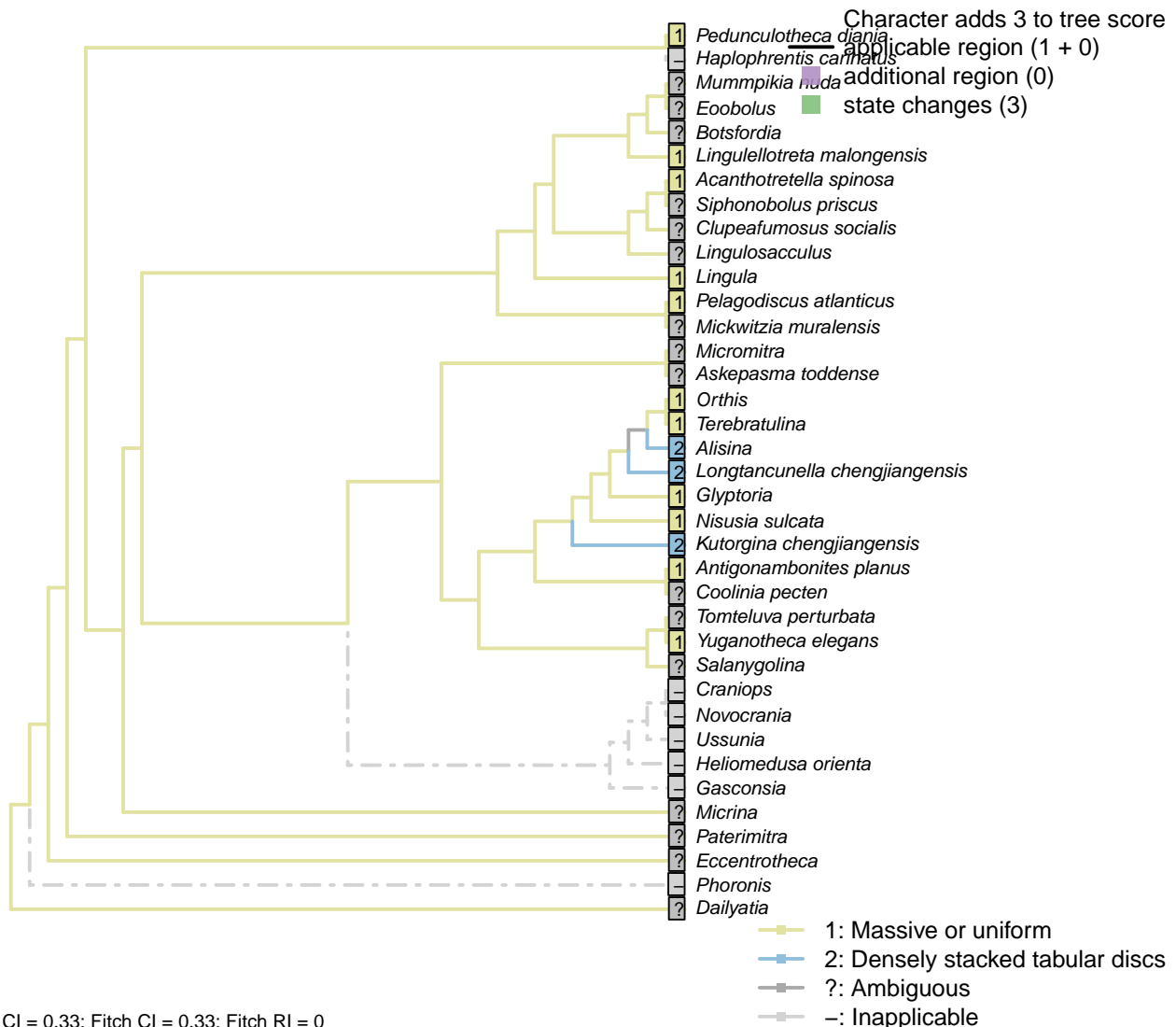
*Mickwitzia muralensis*: An attachment structure is inferred based on the presence of an opening (Balthasar, 2004); this is assumed to have been homologous with the brachiopod pedicle.

*Nisusia sulcata*: Has a pedicle, rather than a pedicle sheath as in *Kutorgina* (Holmer *et al.*, 2018a,b).

*Paterimitra*: “*Paterimitra* is interpreted to have attached to hard substrates via a pedicle that emerged through the small posterior opening” – Skovsted *et al.* (2009).

*Siphonobolus priscus*: Presumed present, based on ventral foramen with colleplax.

## [84] Constitution

**Character 84: Pedicle: Constitution**

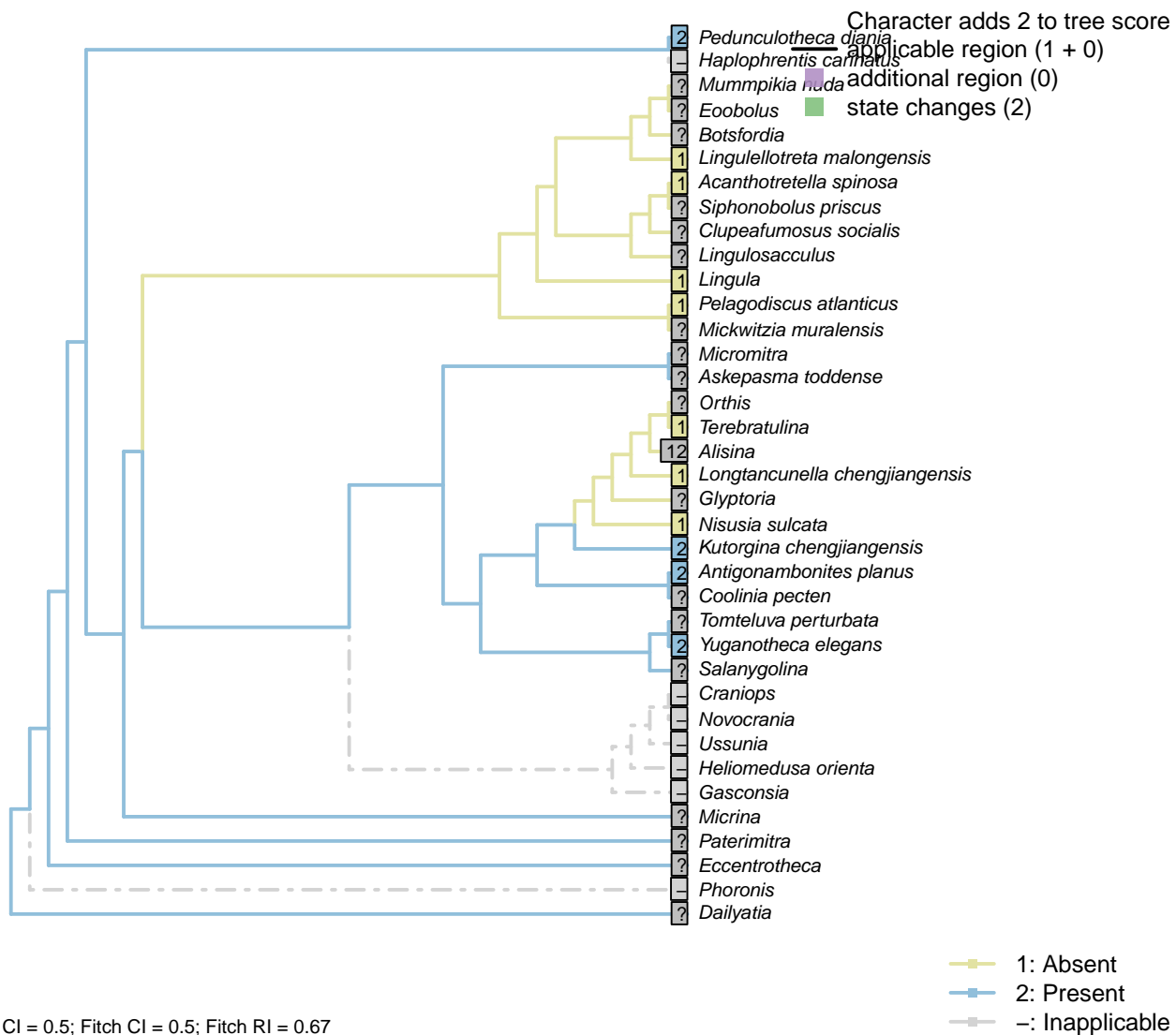
- 1: Massive or uniform
- 2: Densely stacked tabular discs
- Transformational character.

The pedicle of certain chengjiang rhynchonelliforms comprises “densely stacked, three dimensionally preserved, tabular discs” (Holmer et al., 2018a).

This contrasts with the uniform (‘massive’) pedicles of living taxa.

*Terebratulina*: Extant rhynchonellid pedicles are massive, consisting of a thick outer chitinous cuticle, a pedicle epithelium, and a core composed of collagen fibres and cartilage-like connective tissue (Holmer et al., 2018a).

## [85] Biomineralization



### Character 85: Pedicle: Biomineralization

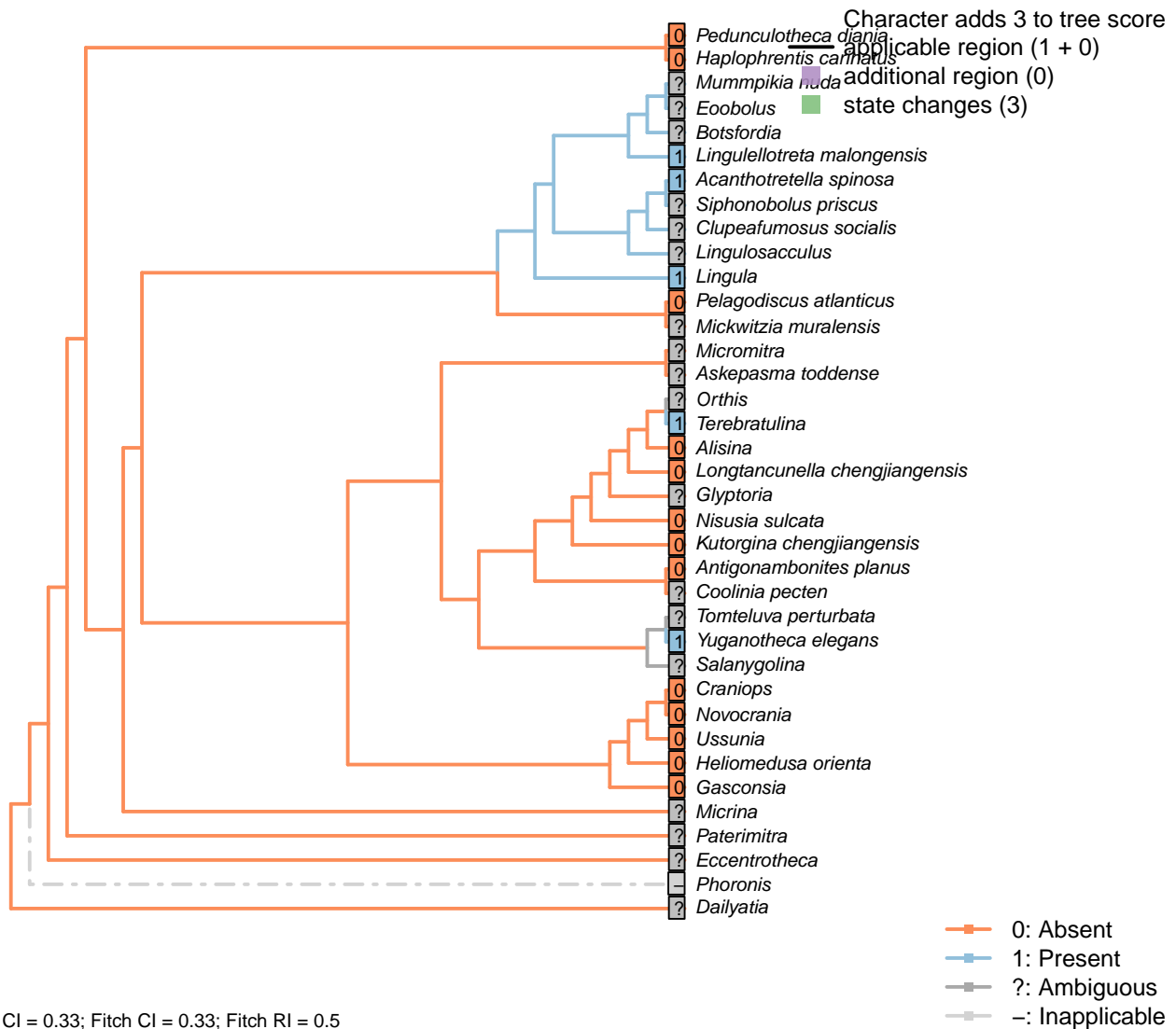
1: Absent

2: Present

Transformational character.

The pedicle of strophomenates such as *Antigonambonites* is biomineralized (Holmer et al., 2018a).

## [86] Bulb

**Character 86: Pedicle: Bulb**

0: Absent

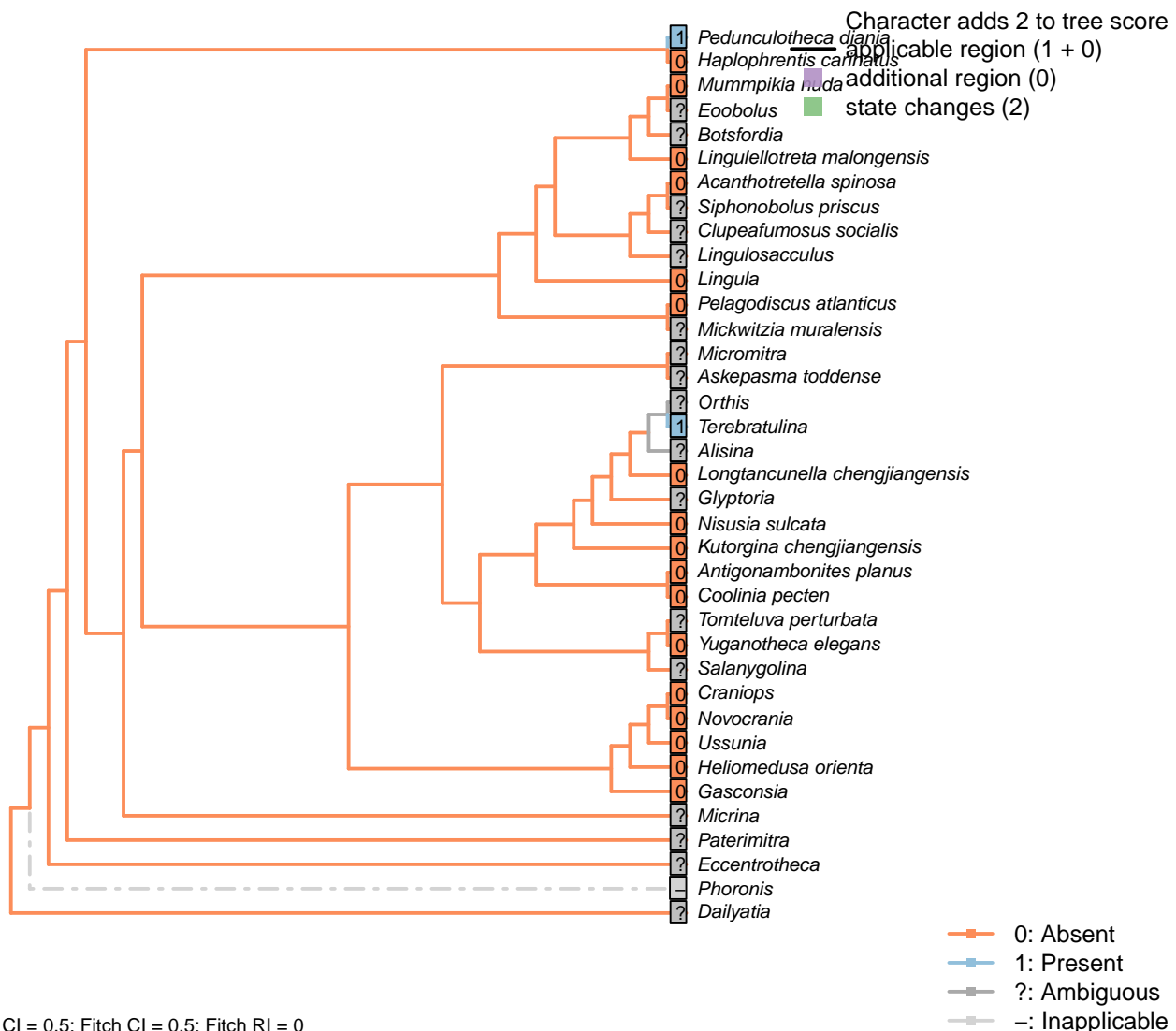
1: Present

Neomorphic character.

A bulb is an expanded region of the distal pedicle, often embedded into the sediment to improve anchorage.

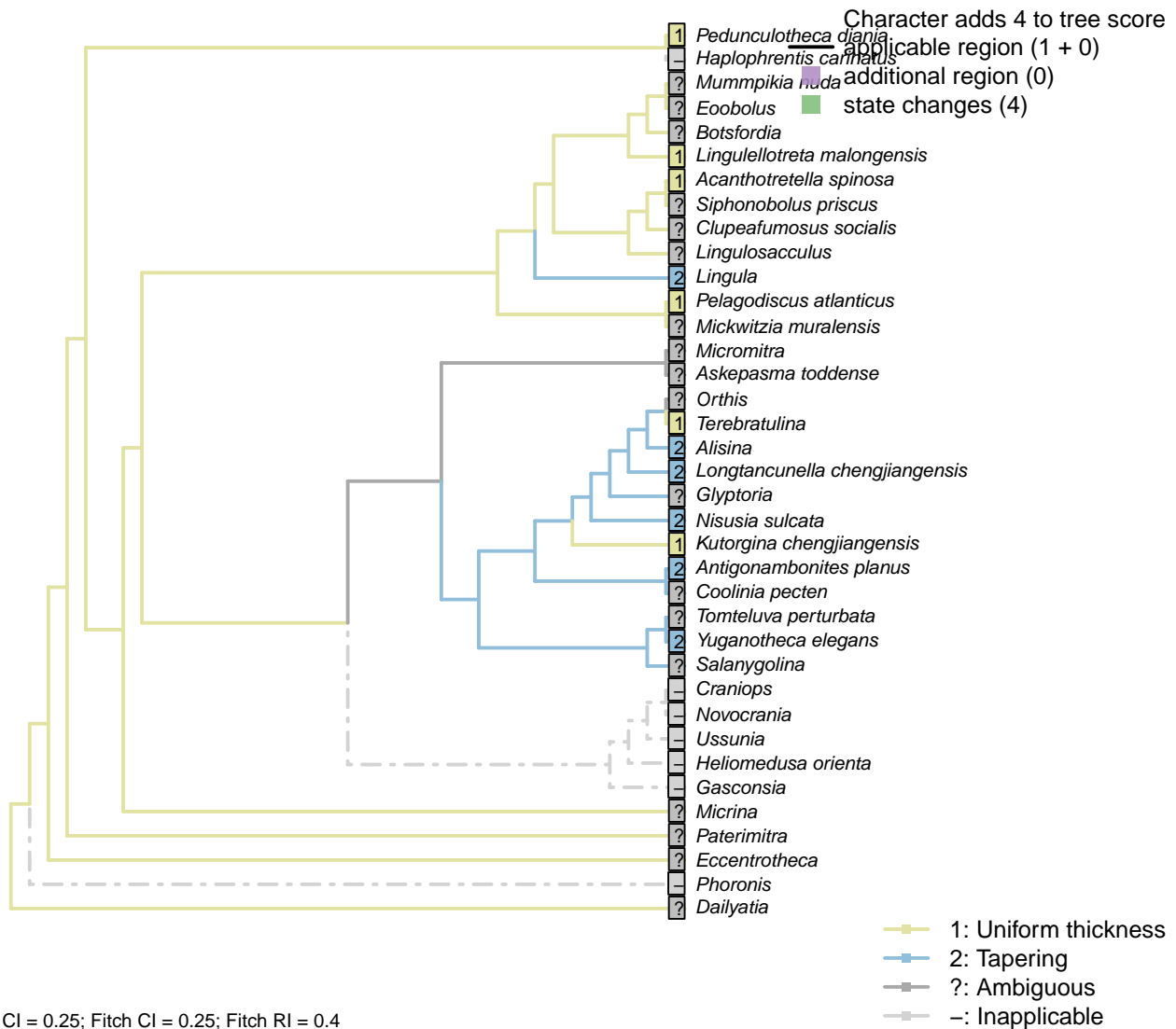
*Acanthotretella spinosa*: Holmer and Caron (2006) interpret the presence of a bulb as tentative; we score it as ambiguous.

## [87] Distal rootlets



Observed in *Pedunculotheca* and *Bethia* (Sutton et al., 2005).

## [88] Tapering



### Character 88: Pedicle: Tapering

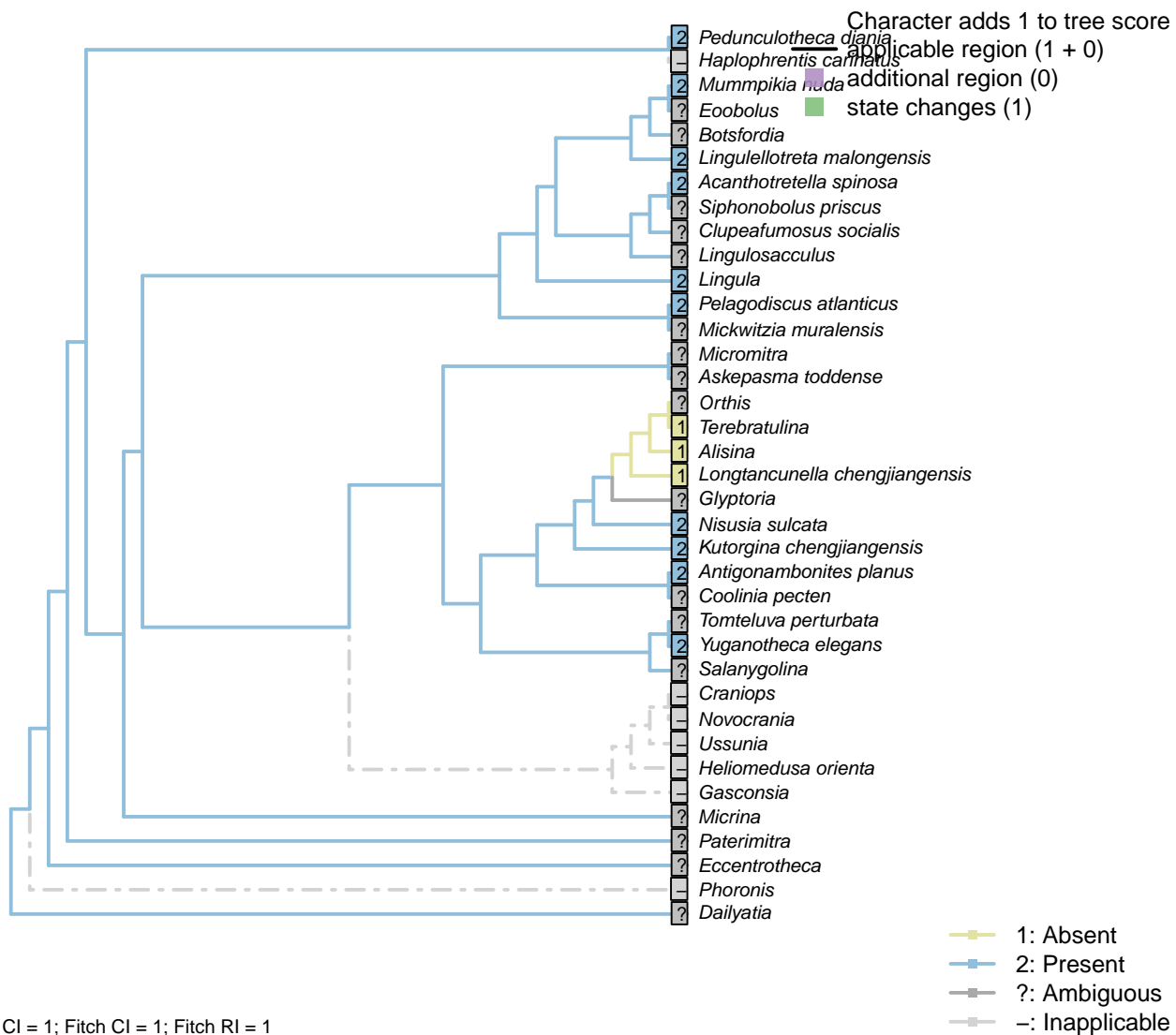
- 1: Uniform thickness
  - 2: Tapering
- Transformational character.

Holmer *et al.* (2018b) remark that the tapering aspect of the *Nisusia* pedicle recalls that of certain Chengjiang taxa (*Alisina*, *Longtancunella*) whilst distinguishing it from many other taxa (*Eichwaldia*, *Bethia*) in which the pedicle is a constant thickness.

*Antigonambonites planus*: Tapered pedicle sheath with holdfast.

*Pedunculotheca diana*: The pedicle thickness does not obviously change between the apex of the shell and the holdfast.

## [89] Coelomic region

**Character 89: Pedicle: Coelomic region**

1: Absent

2: Present

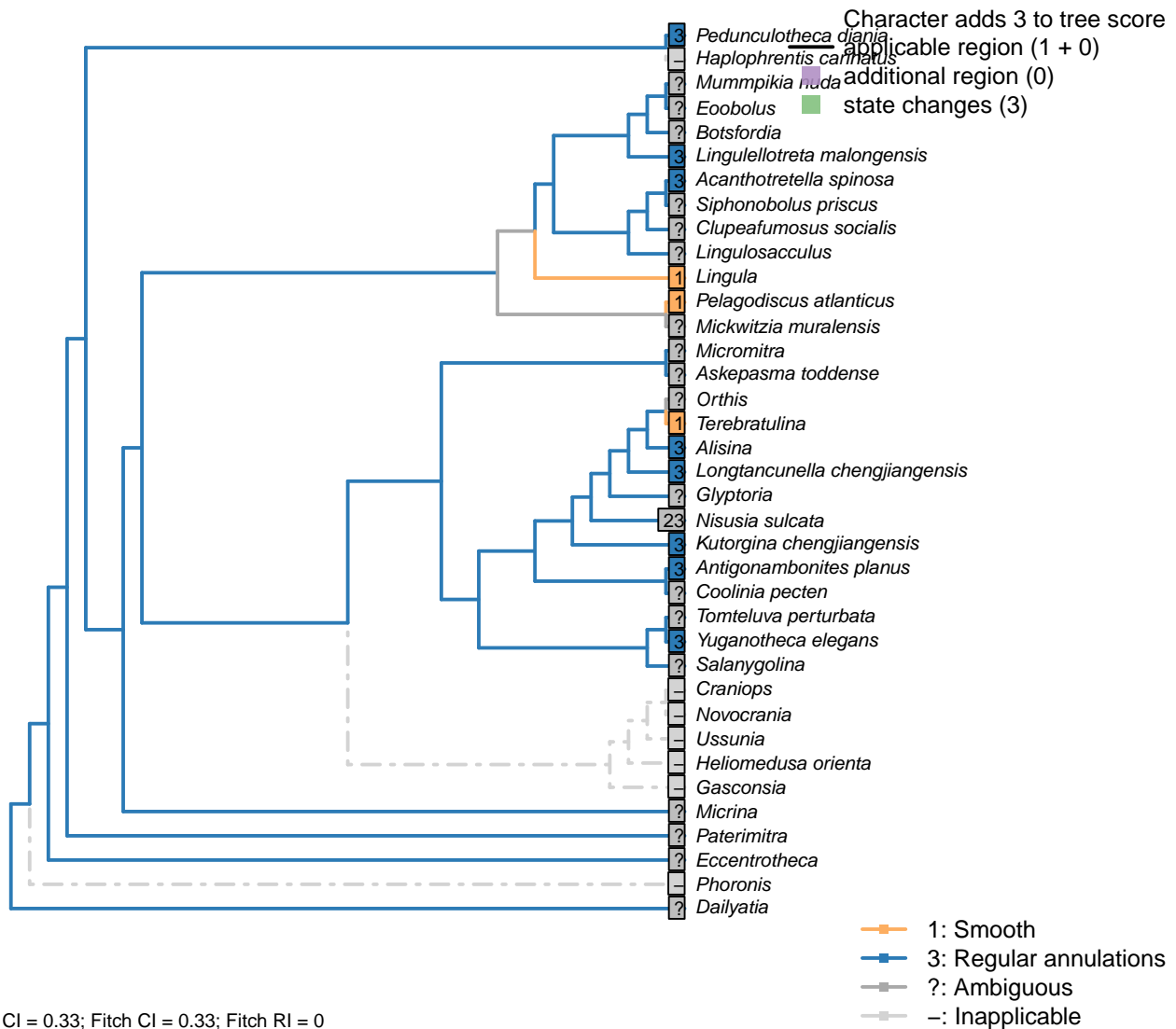
Transformational character.

Certain brachiopods, such as *Acanthotretella*, exhibit a coelomic cavity within the pedicle or pedicle sheath.

Treated as transformational as it is not clear that either state is necessarily ancestral.

*Nisusia sulcata*: A coelomic canal is inferred based on the ease with which the pedicle is deformed (Holmer et al., 2018a), but its presence is not known for certain so is coded ambiguous.

## [90] Surface ornament



### Character 90: Pedicle: Surface ornament

- 1: Smooth
  - 2: Irregular wrinkles
  - 3: Regular annulations
- Transformational character.

Annulations are regular rings that surround the pedicle, and are distinguished from wrinkles, which are irregular in magnitude and spacing, and may branch or fail to entirely encircle the pedicle.

*Acanthotretella spinosa*: “The pedicle surface is ornamented with pronounced annulated rings, disposed at intervals of about 0.2 mm”.

*Alisina*: “It appears that the pedicle lacks a coelomic space and is distinctly annulated, with densely stacked tabular bodies” – Zhang et al. (2011b).

*Antigonambonites planus*: “The emerging pedicle has a consistent shape in all the available specimens and

is strongly annulated and distally tapering” – Holmer et al. (2018a).

*Kutorgina chengjiangensis*: “Pronounced concentric annular discs disposed at intervals of  $0.6 < 96 > 1.0$  mm”.

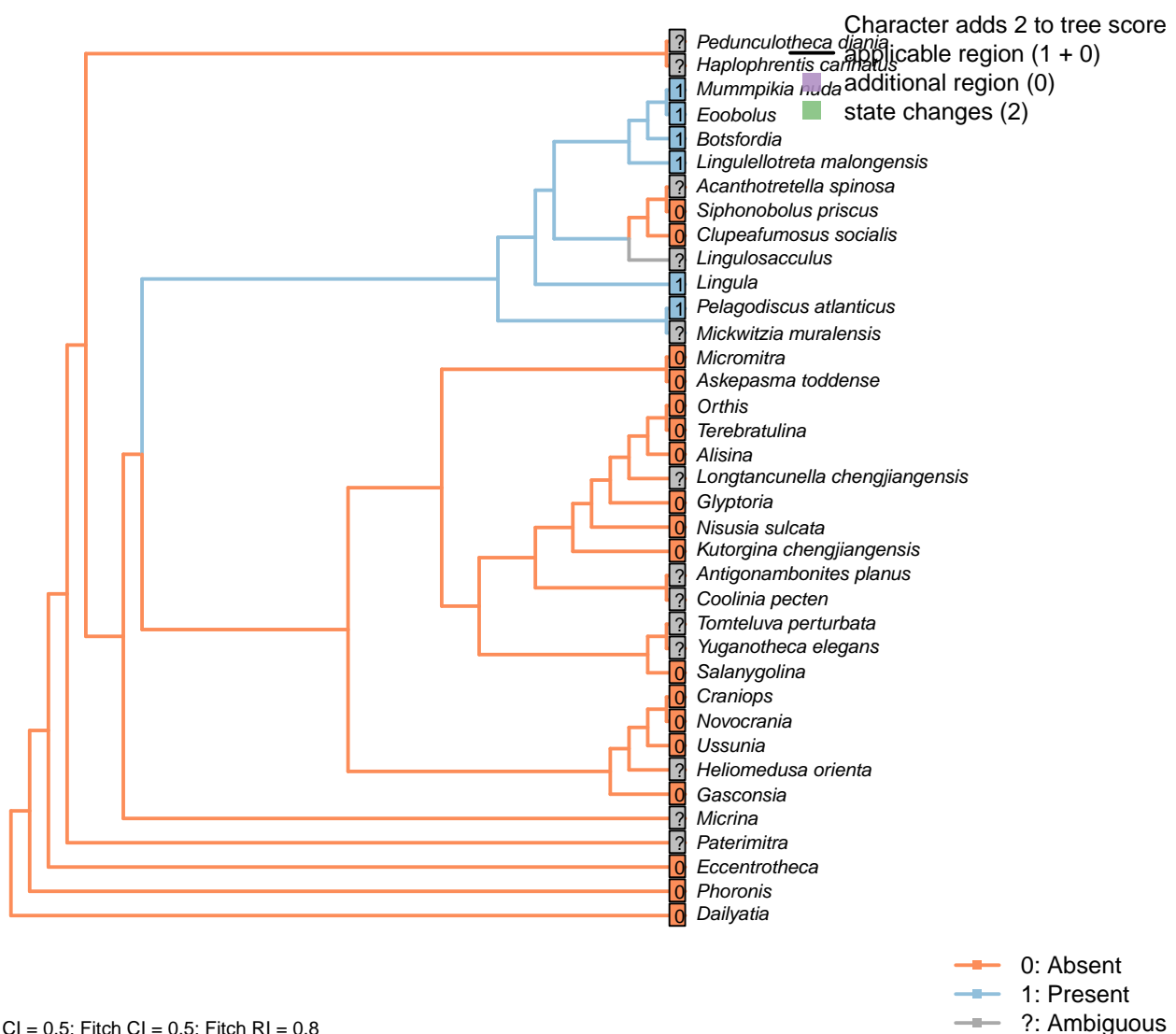
*Lingulellotreta malongensis*: Regularly annotated (see fig. 14.9 in Hou et al., 2017).

*Longtancunella chengjiangensis*: “The preserved pedicle has condensed annulations” – Zhang et al. (2011a).

*Nisusia sulcata*: The “strong annulations” vary significantly in transverse thickness (Holmer et al., 2018a), so it is not clear whether these represent true annulations or wrinkles.

*Yuganotheca elegans*: Annulations present in median collar.

## [91] Nerve impression



### Character 91: Pedicle: Nerve impression

0: Absent

1: Present

Neomorphic character.

In certain taxa the impression of the pedicle nerve is evident in the shell. See character 28 in Williams *et al.* (1998) appendix 1. Care must be taken not to code an impression as absent when the preservational quality is insufficient to safely infer a genuine absence. Treated as neomorphic as the presence of an innervation is considered a derived state.

*Alisina*: Not described by Williams *et al.* (2000).

*Askepasma toddense*, *Glyptoria*, *Kutorgina chengjiangensis*, *Micromitra*, *Salanygolina*: Following Williams *et al.* (1998), appendix 2.

*Botsfordia*: Documented by Skovsted *et al.* (2017).

*Clupeafumosus socialis*: Coded as absent in Acrotretidae (Williams *et al.*, 2000, table 6).

*Lingula*: Present in many lingulids (Williams *et al.*, 2000), and coded as present in Lingulidae (Williams *et al.*, 2000, table 6).

*Lingulellotreta malongensis*: Coded as present in Lingulellotretidae (Williams *et al.*, 2000, table 6).

*Mummpikia nuda*: Balthasar (2008, p. 274) identifies a canal as a probable impression of a pedicle nerve.

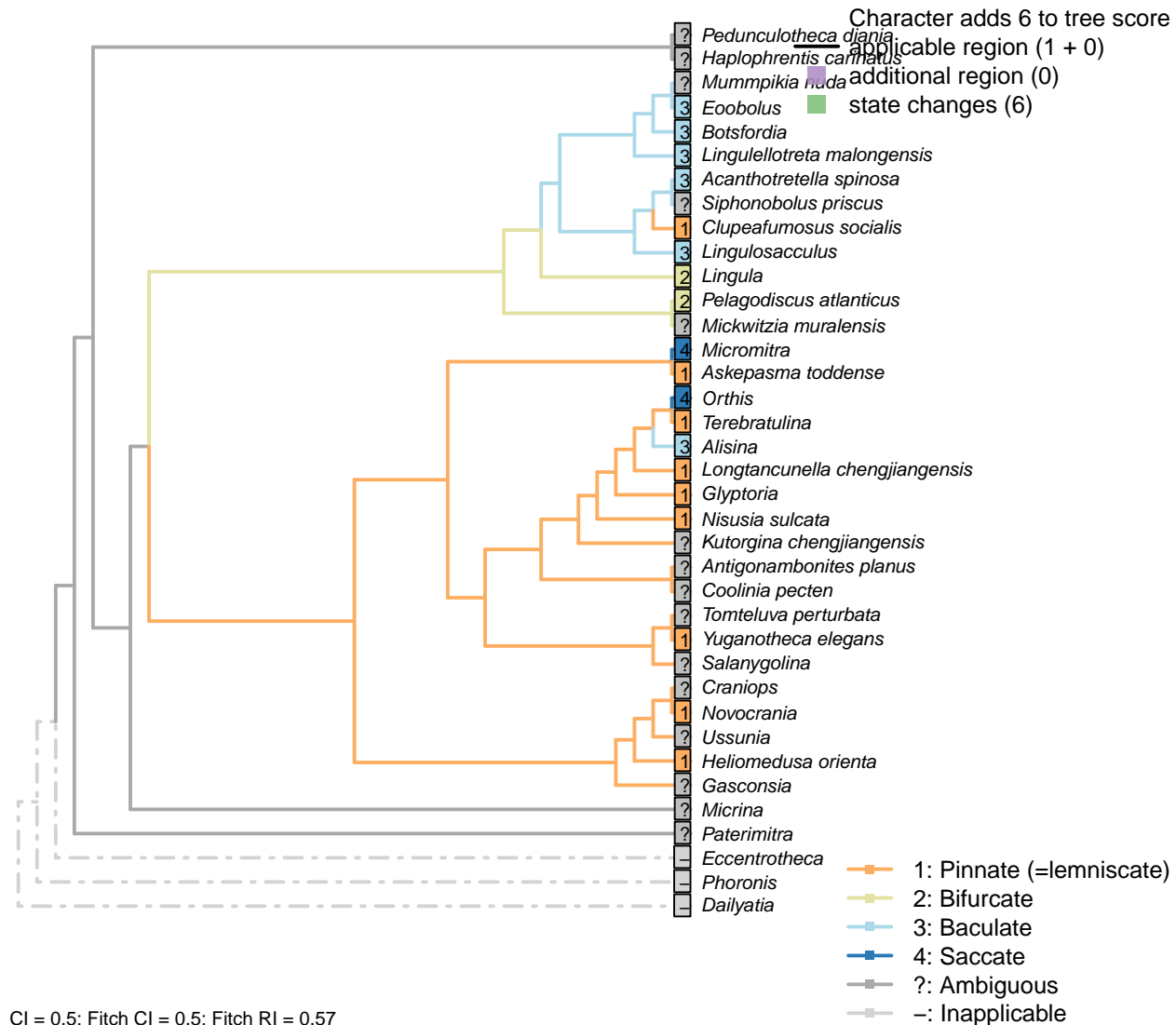
*Nisusia sulcata*, *Orthis*: Not reported in Williams *et al.* (2000).

*Pelagodiscus atlanticus*: Coded as present in Discinidae (Williams *et al.*, 2000, table 6).

*Siphonobolus priscus*: Coded as absent in Siphonotretidae (Williams *et al.*, 2000, table 6).

### 3.13 Mantle canals

#### [92] Morphology



#### Character 92: Mantle canals: Morphology

- 1: Pinnate (=lemniscate)
  - 2: Bifurcate
  - 3: Baculate
  - 4: Saccate
- Transformational character.

The morphology of dorsal and ventral canals is identical in all included taxa, so is assumed not to be independent – hence the use of a single character (contra Williams et al., 2000).

For a description of terms see Williams *et al.* (1997, 2000).

Pinnate = “rapidly branch into a number of subequal, radially disposed canals”

Bifurcate = “*vascula lateralia* in both valves divide immediately after leaving the body cavity”

Baculate = “extend forward without any major dichotomy or bifurcation” (Williams et al., 1997, p. 418)  
 Saccate = “pouchlike sinuses lying wholly posterior to the arcuate *vascula media*” (ibid., p412).

*Acanthotretella spinosa*: Following Table 6, for Siphonotretidae, in Williams et al. (2000).

*Alisina, Nisusia sulcata*: Following Table 15 in Williams et al. (2000).

*Antigonambonites planus*: Not reported in Treatise (Williams et al., 2000).

*Askepasma toddense*: Described as pinnate (at least in ventral valve) by Williams et al. (1998, p. 250).

*Botsfordia, Eoobolus*: Following Williams et al. (1998), appendix 2, and Williams et al. (2000), table 8.

*Clupeafumosus socialis*: Following Table 8 (for Acrotreta) in Williams et al. (2000), and the general pinnate condition for acrotretooids stated in Williams et al. (1997), p. 420.

*Coolinia pecten*: Not reported in Williams et al. (2000).

*Craniops*: Not reported from fossil material.

*Gasconsia*: Williams et al. (2000, table 15) appear to use Palaeotrimerella (as drawn in Williams et al., 1997) as a model for *Gasconsia*, which pre-supposes a close relationship. We are not aware of any report of mantle canals from *Gasconsia* itself.

*Glyptoria*: Following appendix 2 (char. 21) in Williams et al. (1998).

*Heliomedusa orienta*: Described as pinnate by Jin & Wang (1992).

*Kutorgina chengjiangensis, Novocrania*: Following table 15 in Williams et al. (2000) (for *Neocrania*).

*Lingula, Lingulellotreta malongensis*: Following table 6 in Williams et al. (2000).

*Lingulosacculus*: Baculate *vascula media* – Balthasar & Butterfield (2009).

*Longtancunella chengjiangensis*: Reported by Zhang et al. (2007c, 2011T) though the interpretation is tentative.

*Micromitra*: Described as saccate by Williams et al. (1998).

*Mummpikia nuda*: “Poorly resolved” – Balthasar (2008).

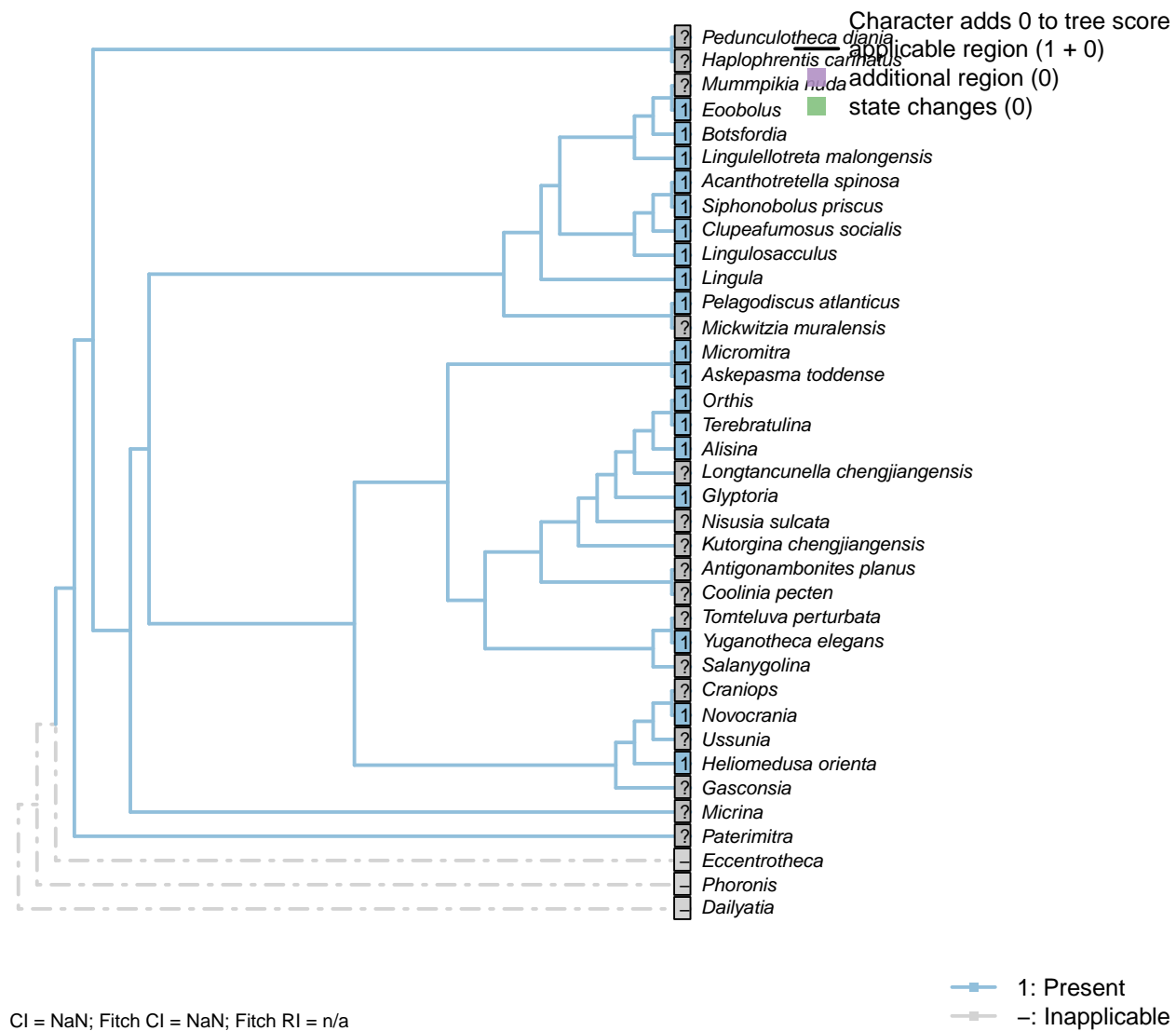
*Orthis*: Sacculate (sometimes digitate in dorsal valve) (Williams et al., 2000, p716).

*Pelagodiscus atlanticus*: Following table 6, for Discinidae, in Williams et al. (2000).

*Salanygolina*: Coded uncertain in appendix 2 in Williams et al. (1998).

*Terebratulina*: “In modern terebratulides, the *vascula media* are subordinate to the lemniscate or pinnate *vascula genitalia*” – Williams et al. (1997).

*Tomteluva perturbata*: Preservation not adequate to evaluate (Streng et al., 2016).

[93] *vascula lateralia***Character 93: Mantle canals: *vascula lateralia***

0: Absent

1: Present

Neomorphic character.

We treat the *vascula lateralia* as equivalent to the *vascula genitalia* of articulated brachiopods, allowing phylogenetic analysis to test their proposed homology.

Williams *et al.* (1997) write: “The mantle canal system of most of the organophosphate-shelled species consists of a single pair of main trunks in the ventral mantle (*vascula lateralia*) and two pairs in the dorsal mantle, one pair (*vascula lateralia*) occupying a similar position to the single pair in the ventral mantle and a second pair projecting from the body cavity near the midline of the valve. This latter pair may be termed the *vascula media*, but whether they are strictly homologous with the *vascula media* of articulated brachiopods is a matter of opinion. It is also impossible to assert that the *vascula lateralia* are the homologues of the *vascula myaria* or *genitalia* of articulated species, although they are likely to be so as they arise in a comparable position.”

"In inarticulated brachiopods, two main mantle canals (*vascula lateralia*) emerge from the main body cavity through muscular valves and bifurcate distally to produce an increasingly dense array of blindly ending branches near the periphery of the mantle (fig. 71.1–71.2)."

*Acanthotretella spinosa*: Following table 8 (which records presence in Siphonotreta) in Williams *et al.* (2000).

*Alisina, Kutorgina chengjiangensis, Nisusia sulcata*: Following table 15 in Williams *et al.* (2000).

*Askepasma toddense, Micromitra*: "Laurie (1987) has shown that arcuate *vascula media* were present in the mantles of both valves as were pouchlike *vascula genitalia*, especially in the ventral valve" – Williams *et al.* (1997).

*Botsfordia*: Following Popov (1992).

*Clupeafumosus socialis*: Presence indicated in Table 8 (for Acrotreta) in Williams *et al.* (2000).

*Gasconsia*: Williams *et al.* (2000, table 15) appear to use Palaeotrimerella (as drawn in Williams *et al.*, 1997) as a model for *Gasconsia*, which pre-supposes a close relationship. We are not aware of any report of mantle canals from *Gasconsia* itself.

*Heliomedusa orienta*: Present: Williams *et al.* (2000); Jin & Wang (1992).

*Lingulellotreta malongensis*: Present (Williams *et al.*, 2000).

*Longtancunella chengjiangensis*: Presence is possible but requires interpretation that is not unambiguous:

"In the dorsal valve, there can be seen two baculate grooves that arise from the anterior body wall at an antero-lateral position. These two grooves (Figs 4H, 5D) could be taken to represent the *vascula lateralia*" – Zhang *et al.* (2007c).

*Novocrania*: Following table 15 in Williams *et al.* (2000) (for *Neocrania*), who write that "Holocene craniides have only a single pair of main trunks in both valves, corresponding to the *vascula lateralia*". Williams *et al.* (2007) reiterate this position (p. 2875), at least for the ventral valve.

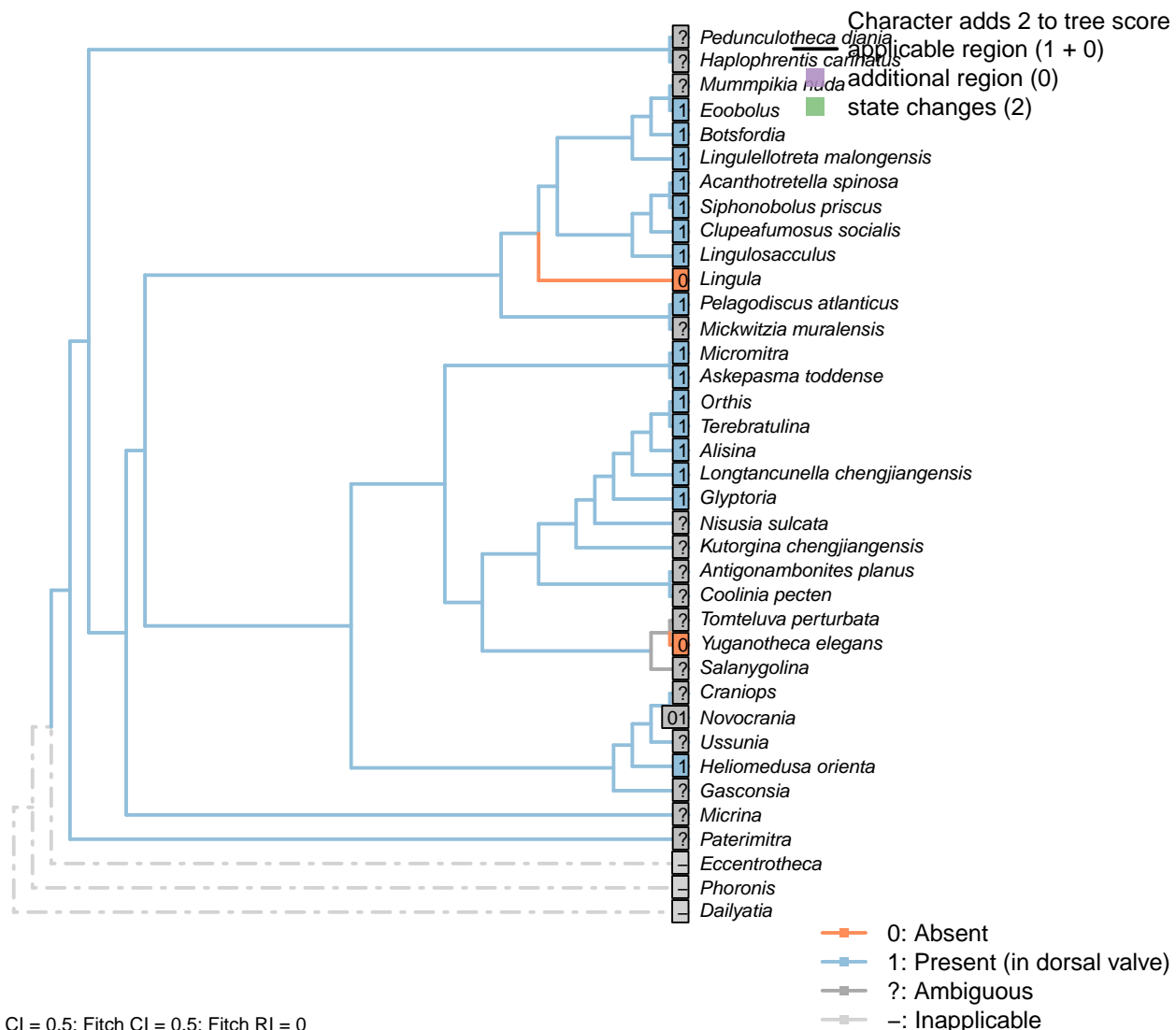
*Orthis, Terebratulina*: = *vascula genitalia*.

*Pelagodiscus atlanticus*: Following *Lochkothele* (Discinidae), Fig. 43.4a in Williams *et al.* (2000).

*Siphonobolus priscus*: Noted in *Siphonobolus* by Williams *et al.* (2000), with reference to Havlicek (1982).

*Tomteluva perturbata*: Preservation not adequate to evaluate (Streng *et al.*, 2016).

*Yuganotheca elegans*: Based on the figures and sketches in Zhang *et al.* (2014) (and supplementary material), the mantle canals are interpreted as lateral, with no clear *vascula media* present.

[94] *vascula media*Character 94: Mantle canals: *vascula media*

0: Absent

1: Present (in dorsal valve)

Neomorphic character.

Williams *et al.* (1997) note that in addition to the *vascula lateralia*, “*Discinisca* has two additional mantle canals emanating from the body cavity into the dorsal mantle (*vascula media*).”

These structures are only evident in the dorsal valve for the included taxa, so only a single character is

necessary.

*Acanthotretella spinosa*: Following table 6 (for Siphonotretidae) in Williams *et al.* (2000).

*Alisina, Kutorgina chengjiangensis, Nisusia sulcata*: Following table 15 in Williams *et al.* (2000).

*Askepasma toddense*: Following table 6 (for Paterinidae) in Williams *et al.* (2000).

*Botsfordia*: Following Popov (1992, fig. 2).

*Clupeafumosus socialis*: Following *Hadrotreta* schematic in Williams *et al.* (2000).

*Eoobolus*: Fig. 5 in Balthasar (2009).

*Gasconsia*: Williams *et al.* (2000, table 15) appear to use *Palaeotrimerella* (as drawn in Williams *et al.*, 1997) as a model for *Gasconsia*, which pre-supposes a close relationship. We are not aware of any report of mantle canals from *Gasconsia* itself.

*Glyptoria*: Present and divergent (Williams *et al.*, 2000).

*Heliomedusa orienta*: Present: Williams *et al.* (2000) p162, Jin & Wang (1992).

*Lingula, Lingulellotreta malongensis*: Following table 6 in Williams *et al.* (2000).

*Longtancunella chengjiangensis*: Reported by Zhang *et al.* (2007c) though the interpretation is tentative.

*Micromitra*: Reported by Williams *et al.* (1998).

*Novocrania*: Williams *et al.* (2000) write “Holocene craniides have only a single pair of main trunks in both valves, corresponding to the *vascula lateralia*” – an observation reflected in their table 15 (for *Neocrania*). But in contrast, Williams *et al.* (2007), p. 2875, identify the dorsal valve’s canals as a *vascula media* in living craniids (though both are *lateralia* in Ordovician craniides). This character is therefore coded as ambiguous.

*Orthis*: From idealised morphology in Williams *et al.* (2000).

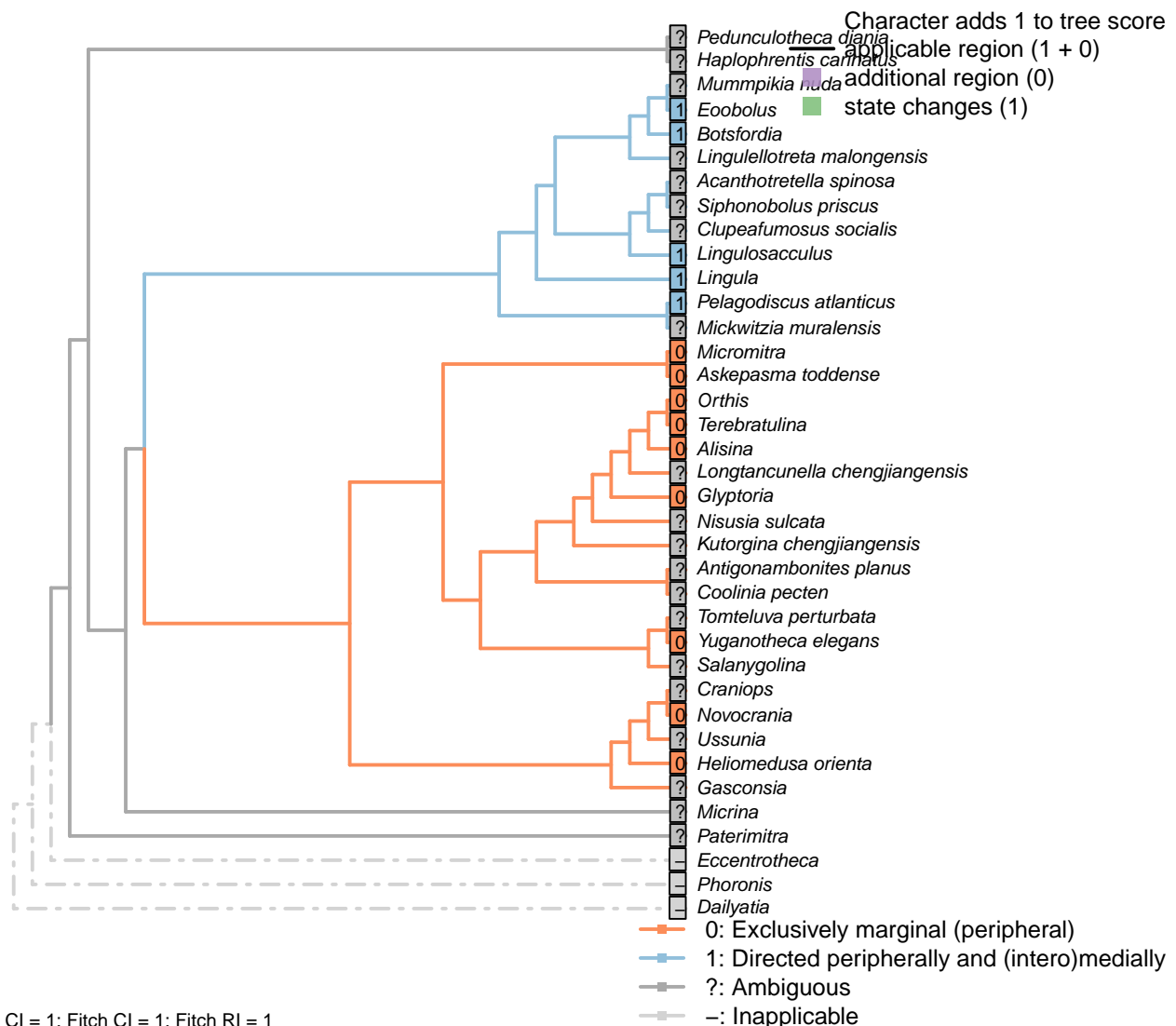
*Pelagodiscus atlanticus*: Following table 6 (for Discinidae) in Williams *et al.* (2000).

*Siphonobolus priscus*: Noted in *Siphonobolus* by Williams *et al.* (2000), with reference to Havlicek (1982).

*Terebratulina*: “In modern terebratulides, the *vascula media* are subordinate to the lemniscate or pinnate *vascula genitalia*” – Williams *et al.* (1997) p417.

*Tomteluva perturbata*: Preservation not adequate to evaluate (Streng *et al.*, 2016).

*Yuganotheca elegans*: Based on the figures and sketches in Zhang *et al.* (2014) (and supplementary material), the mantle canals are interpreted as lateral, with no clear *vascula media* present.

[95] *vascula terminalia***Character 95: Mantle canals: *vascula terminalia***

- 0: Exclusively marginal (peripheral)
- 1: Directed peripherally and (intero)medially
- Neomorphic character.

Presumed to be connected with setal follicles in life (Williams et al., 1998). See Williams *et al.* (2000) for

discussion.

*Acanthotretella spinosa*: Preservation not clear enough to score with certainty (Holmer and Caron, 2006).

*Alisina*: Interomedial *vascula terminalia* not reported by Williams *et al.* (2000).

*Askepasma toddense*, *Micromitra*: Peripheral only (Williams *et al.*, 1998, 2000).

*Botsfordia*, *Eoobolus*: Following Williams *et al.* (1998), appendix 2.

*Glyptoria*: Following appendix 2 in Williams *et al.* (1998).

*Heliomedusa orienta*: Inferred from Jin & Wang (1992).

*Kutorgina chengjiangensis*, *Salanygolina*: Coded uncertain in appendix 2 in Williams *et al.* (1998).

*Lingula*: Peripheral and medial for all Lingulata (Williams *et al.*, 2000).

*Lingulellotreta malongensis*: Not described in Williams *et al.* (2000).

*Lingulosacculus*: Strong indication of medially directed *vascula terminalia* from *vascula lateralia*; see fig. 1.A1 in Balthasar and Butterfield (2009).

*Novocrania*: Peripheral only (Williams *et al.*, 2000, p.158).

*Orthis*: See schematics in Williams *et al.* (2000).

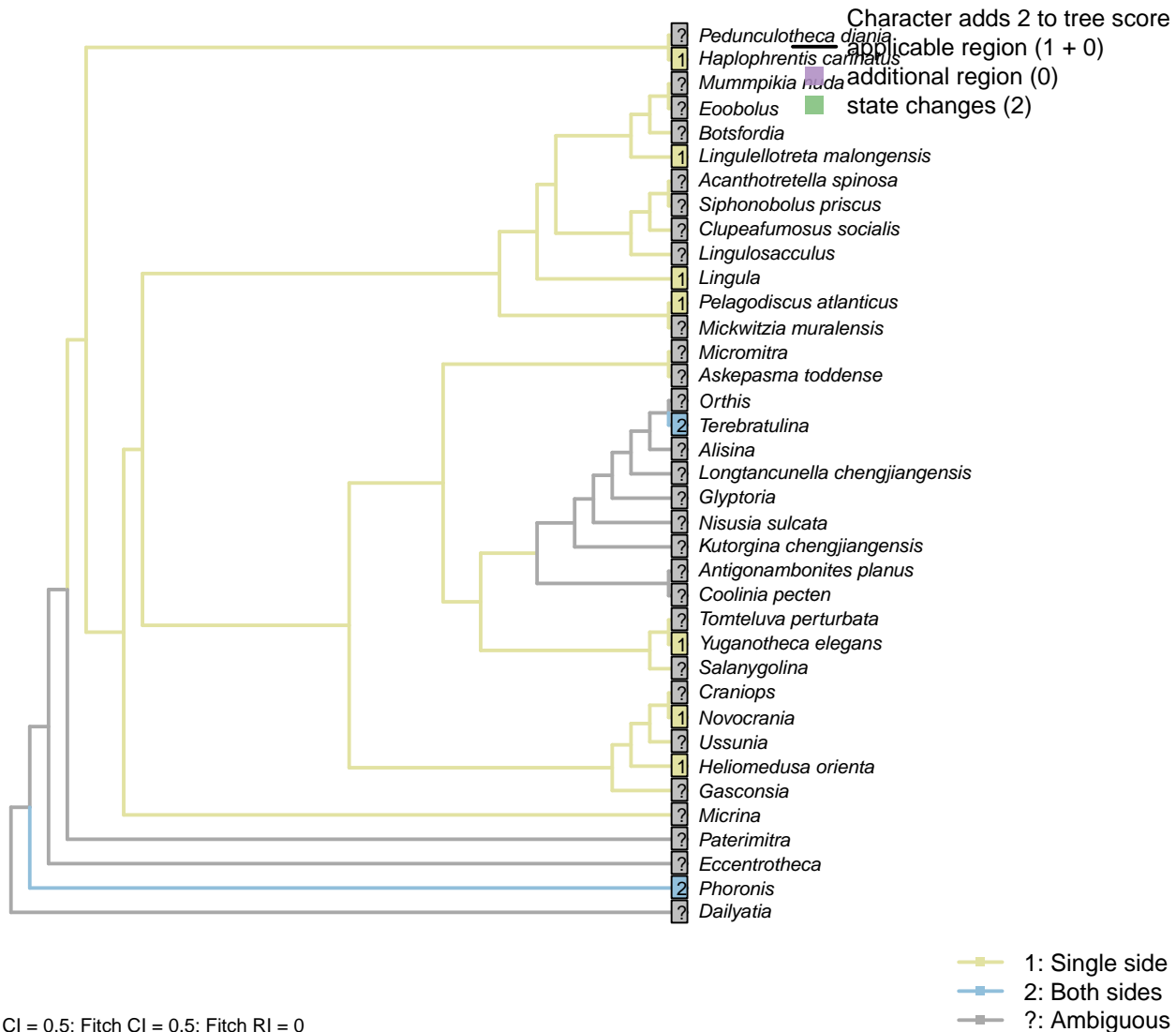
*Pelagodiscus atlanticus*: Following *Lochkothele* (Discinidae), fig. 43.4a in Williams *et al.* (2000).

*Siphonobolus priscus*: Not reported in Williams *et al.* (2000).

*Terebratulina*: Following idealised plectolophous terebratulid of Emig (1992).

## 3.14 Lophophore

### [96] Tentacle disposition



#### Character 96: Lophophore: Tentacle disposition

1: Single side

2: Both sides

Transformational character.

Tentacles may occur along one or both sides of the axis of the lophophore arm (Carlson, 1995).

*Acanthotretella spinosa*: Preservation insufficient to evaluate (Holmer and Caron, 2006).

*Alisina*: Preservation inadequate.

*Heliomedusa orienta*: "Each lophophoral arm bears a row of long, slender flexible tentacles" – Zhang et al. (2009).

*Kutorgina chengjiangensis*: Tentacles "cannot be confidently demonstrated in the available specimens." –

Zhang et al. (2007b).

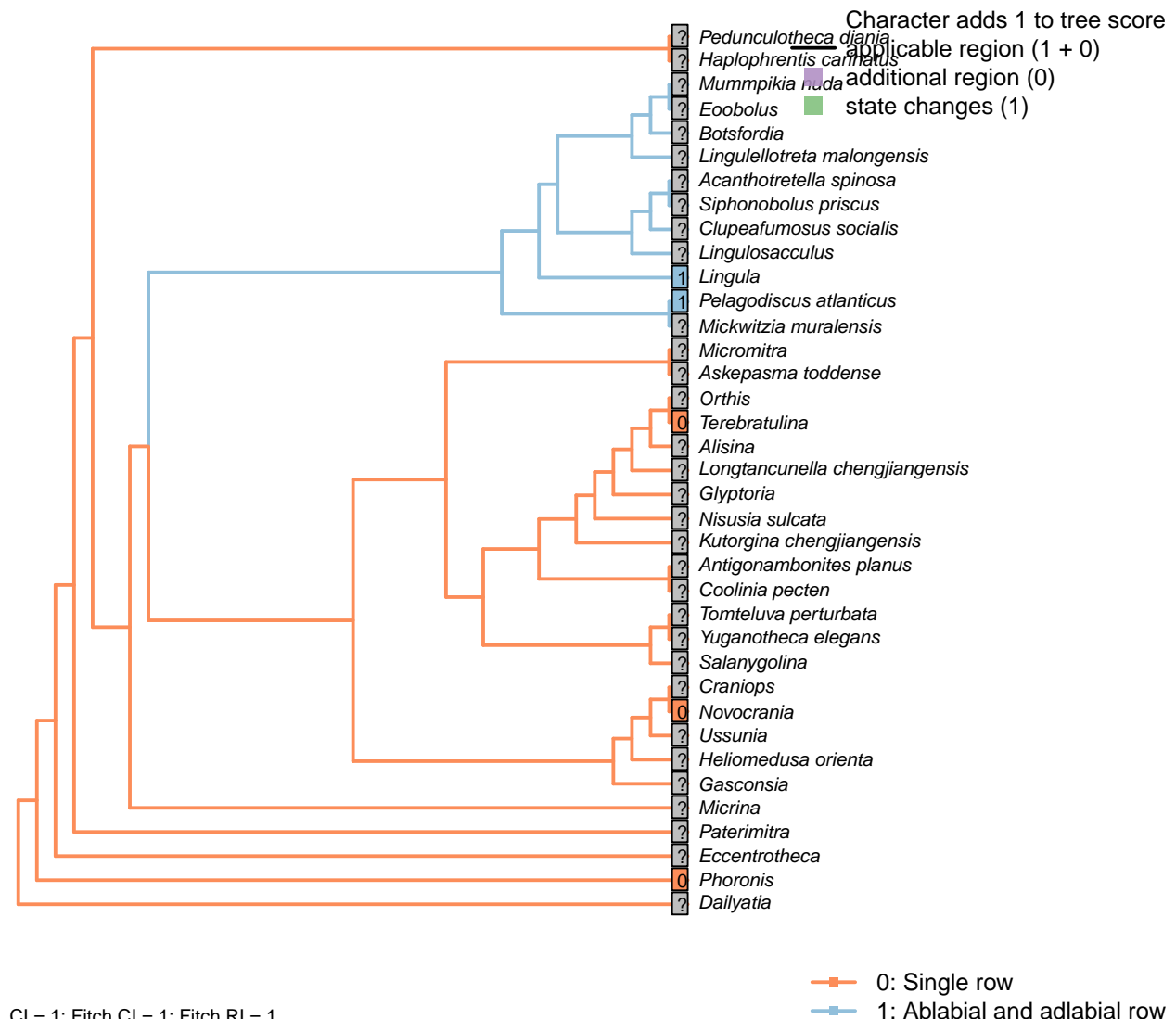
*Lingula*, *Novocrania*, *Pelagodiscus atlanticus*, *Phoronis*, *Terebratulina*: Following coding for higher group in Carlson (1995), appendix 1, character 36.

*Lingulellotreta malongensis*: “The tentacles are clearly visible, and closely arranged in a single palisade” – Zhang et al. (2004).

*Lingulosacculus*: Preservation insufficient to evaluate.

*Longtancunella chengjiangensis*: Inadequately preserved to evaluate.

### [97] Tentacle rows per side in trocholophe stage



#### Character 97: Lophophore: Tentacle rows per side in trocholophe stage

0: Single row

1: Ablabial and adlabial row

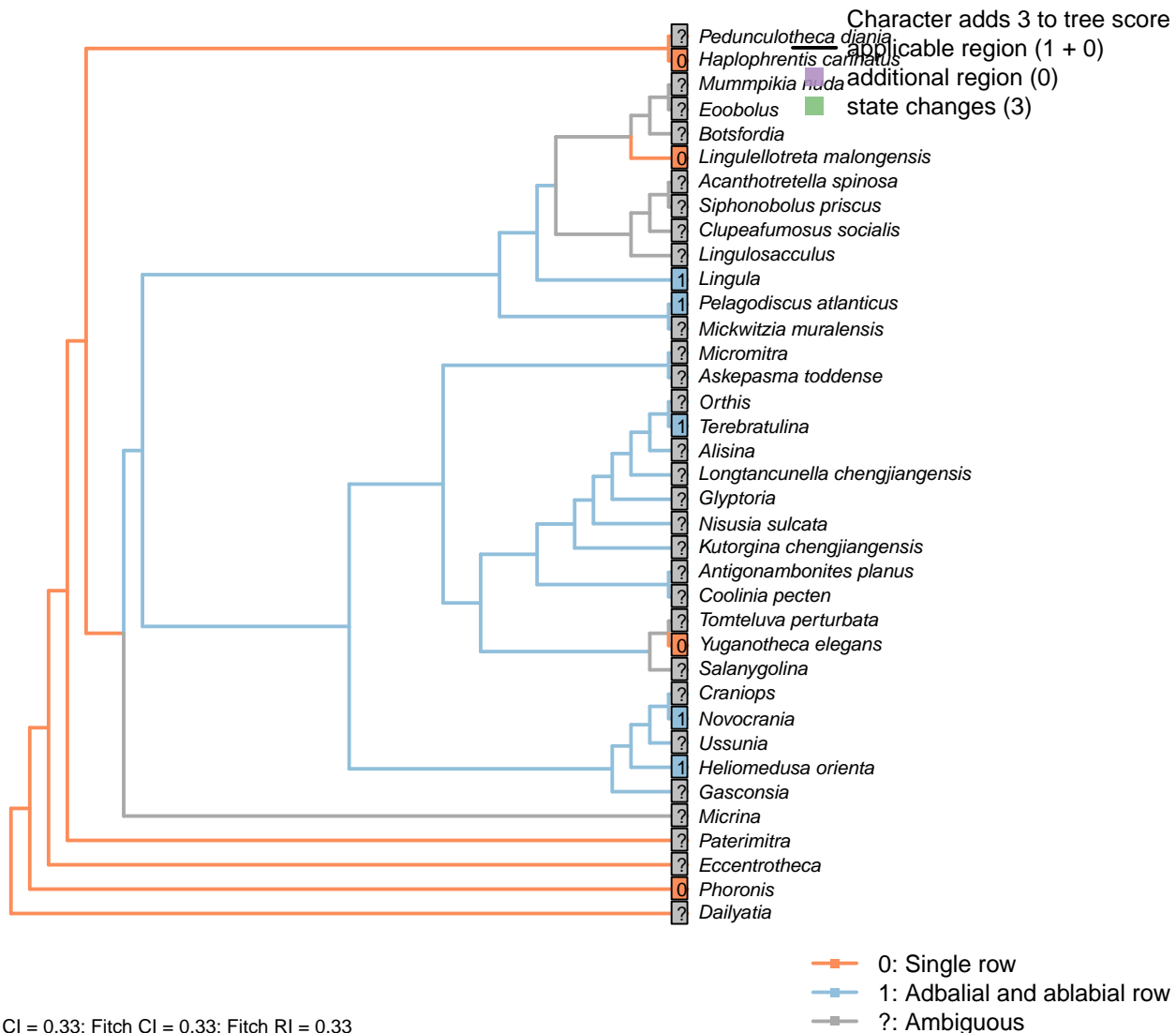
Neomorphic character.

After Carlson (1995), character 37. Lophophore tentacles are commonly arranged into an ablabial and adlabial row, with ablabial tentacles sometimes added later in development.

*Lingula, Pelagodiscus atlanticus, Phoronis, Terebratulina*: Following coding for higher taxon in Carlson (1995), appendix 1, character 37.

*Novocrania*: Following coding for higher taxon in Carlson (1995), appendix 1, character 37. Also states in Williams et al. (2000), p. 158.

### [98] Tentacle rows per side in post-trocholophe stage



#### Character 98: Lophophore: Tentacle rows per side in post-trocholophe stage

0: Single row

1: Adblarial and abblarial row

Neomorphic character.

After Carlson (1995), character 37. Lophophore tentacles are commonly arranged into an ablabial and

adlabial row, with ablabial tentacles sometimes added later in development.

*Acanthotretella spinosa*: Preservation insufficient to evaluate (Holmer and Caron, 2006).

*Heliomedusa orienta*: “The lophophoral arms bear laterofrontal tentacles with a double row of cilia along their lateral edge, as in extant lingulid brachiopods” – Zhang et al. (2009).

*Kutorgina chengjiangensis*: Tentacles “cannot be confidently demonstrated in the available specimens.” – Zhang et al. (2007b).

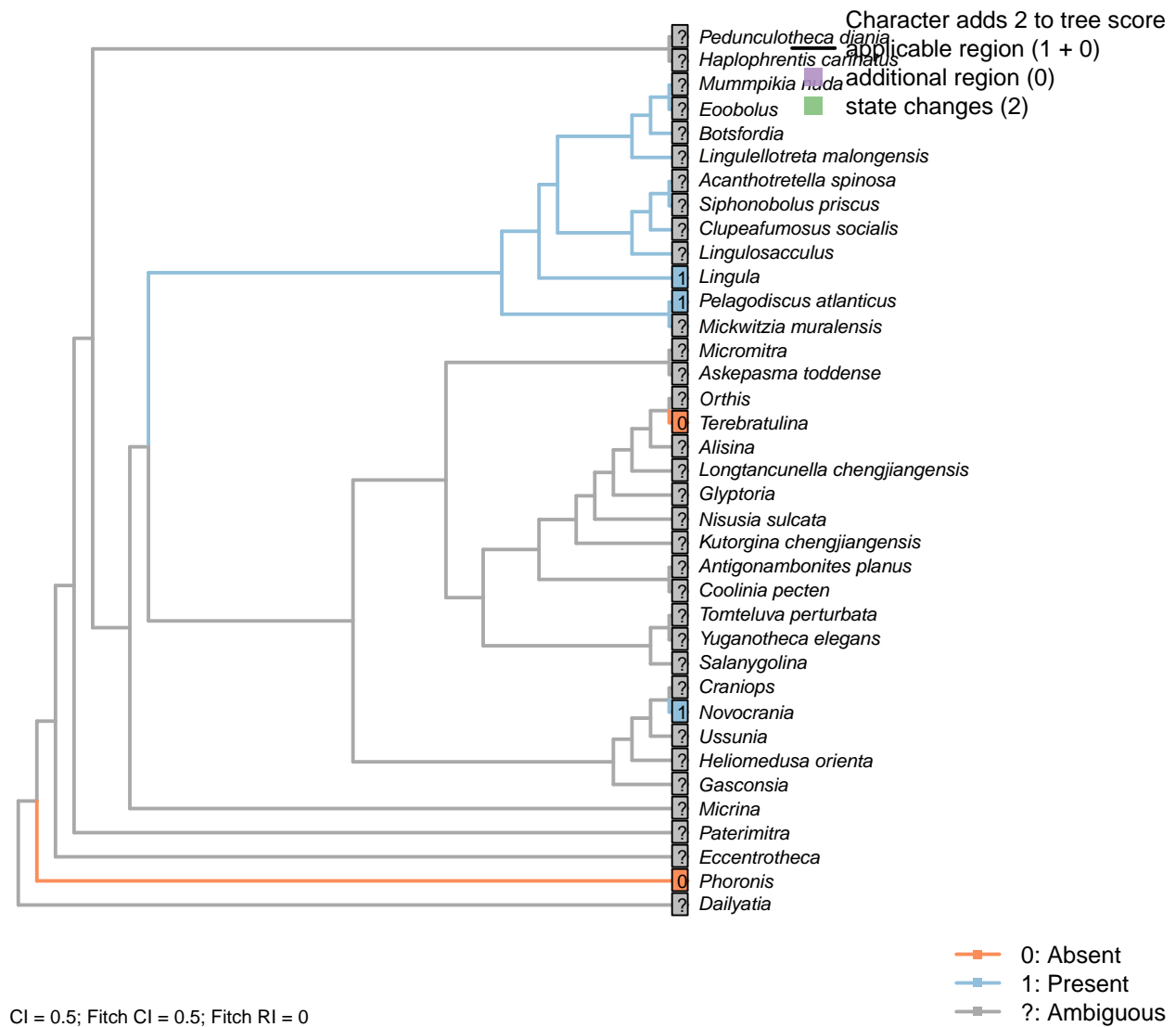
*Lingula*, *Novocrania*, *Pelagodiscus atlanticus*, *Phoronis*, *Terebratulina*: Following coding for higher taxon in Carlson (1995), appendix 1, character 37.

*Lingulellotretra malongensis*: Single palisade (Zhang et al., 2004).

*Lingulosacculus*: Preservation insufficient to evaluate.

*Yuganotheca elegans*: “helical lophophore fringed with a single row of thick, widely spaced, parallel-sided and hollow tentacles” – Zhang et al. (2014).

## [99] Median tentacle in early development



**Character 99: Lophophore: Median tentacle in early development**

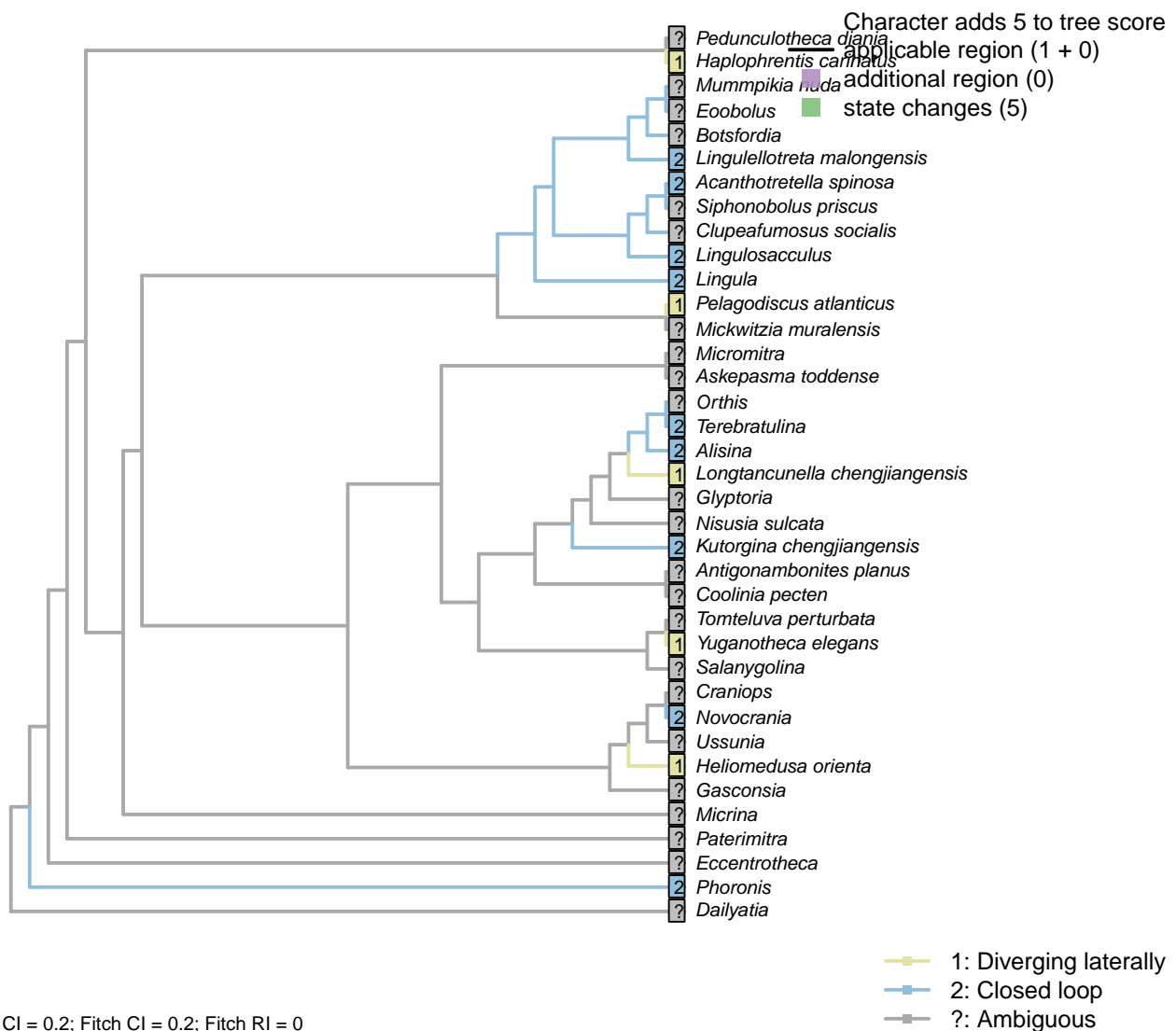
0: Absent

1: Present

Neomorphic character.

Following character 28 in Carlson (1995). Certain taxa exhibit a median tentacle early in development that is lost at some point in ontogeny.

*Acanthotretella spinosa, Alisina, Antigonambonites planus, Askepasma toddense, Clupeafumosus socialis, Coolinia pecten, Dailyatia, Eccentrotheca, Gasconsia, Glyptoria, Haplophrentis carinatus, Heliomedusa orienta, Kutorgina chengjiangensis, Lingulellotreta malongensis, Lingulosacculus, Longtancunella chengjiangensis, Micrina, Micromitra, Mummpikia nuda, Nisusia sulcata, Orthis, Paterimitra, Pedunculotheca diana, Salanygolina, Tomteluva perturbata, Yuganotheca elegans:* Lophophore ontogeny presently unknown.

**[100] Forms closed loop**

- 1: Diverging laterally  
 2: Closed loop  
 Transformational character.

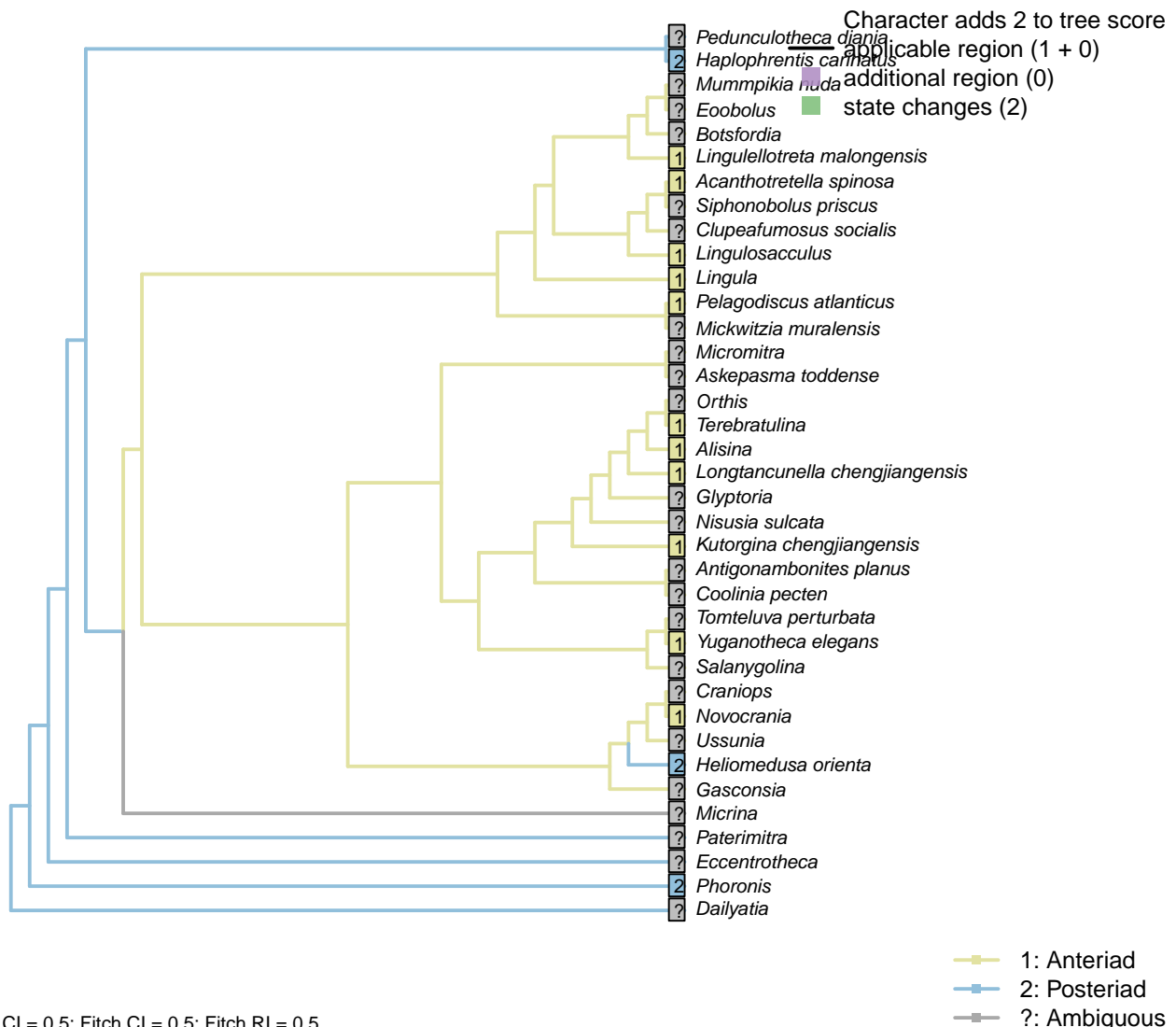
Whereas the lophophore of crown-group brachiopods typically forms a closed loop, those of *Haplophrentis* and *Heliomedusa* diverge laterally (Moysiuk et al., 2017).

*Lingulosacculus*: Two diverging arms of the lophophore are preserved (Balthasar and Butterfield, 2009).

*Longtancunella chengjiangensis*: Two distinct, diverging arms reconstructed by Zhang et al. (2007c).

*Nisusia sulcata*: No specimens of *Nisusia* preserve the lophophore.

## [101] Coiling direction



### Character 101: Lophophore: Coiling direction

- 1: Anteriad  
 2: Posteriad  
 Transformational character.

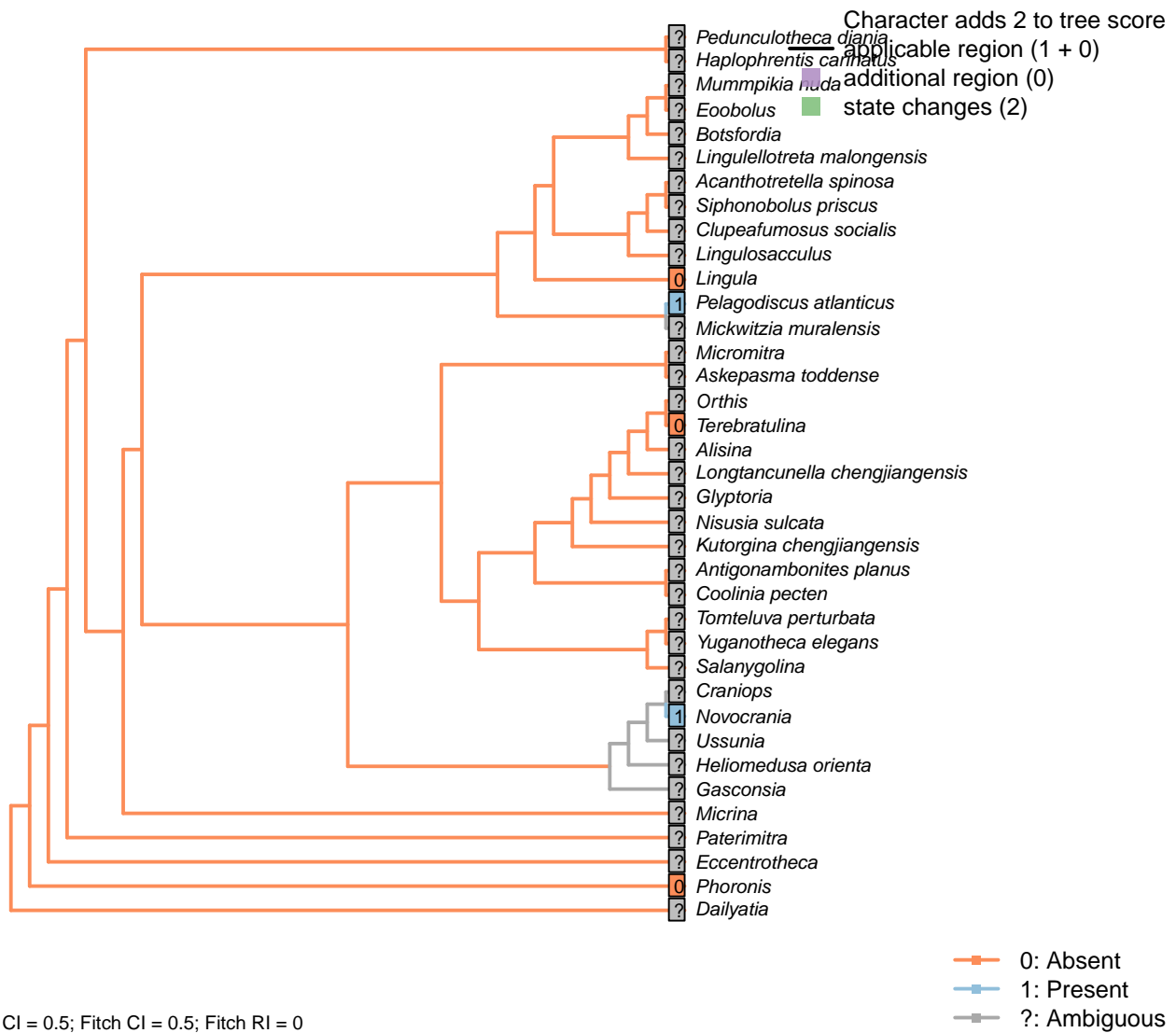
The lophophore arms of *Heliomedusa* and *Haplophrentis* arch posteriad, rather than anteriad as in lingulids. See Zhang et al. (2009); Moysiuk et al. (2017).

*Acanthotretella spinosa*, *Lingulellotreta malongensis*: Arms proceed anteriad before recurving.

*Pelagodiscus atlanticus*: “converging anteriorly and coiling anterior to the body cavity” – Zhang et al. (2009).

*Phoronis*: Coiling in direction of anus (i.e. posteriad).

## [102] Adjustor muscle



### Character 102: Lophophore: Adjustor muscle

0: Absent

1: Present

Neomorphic character.

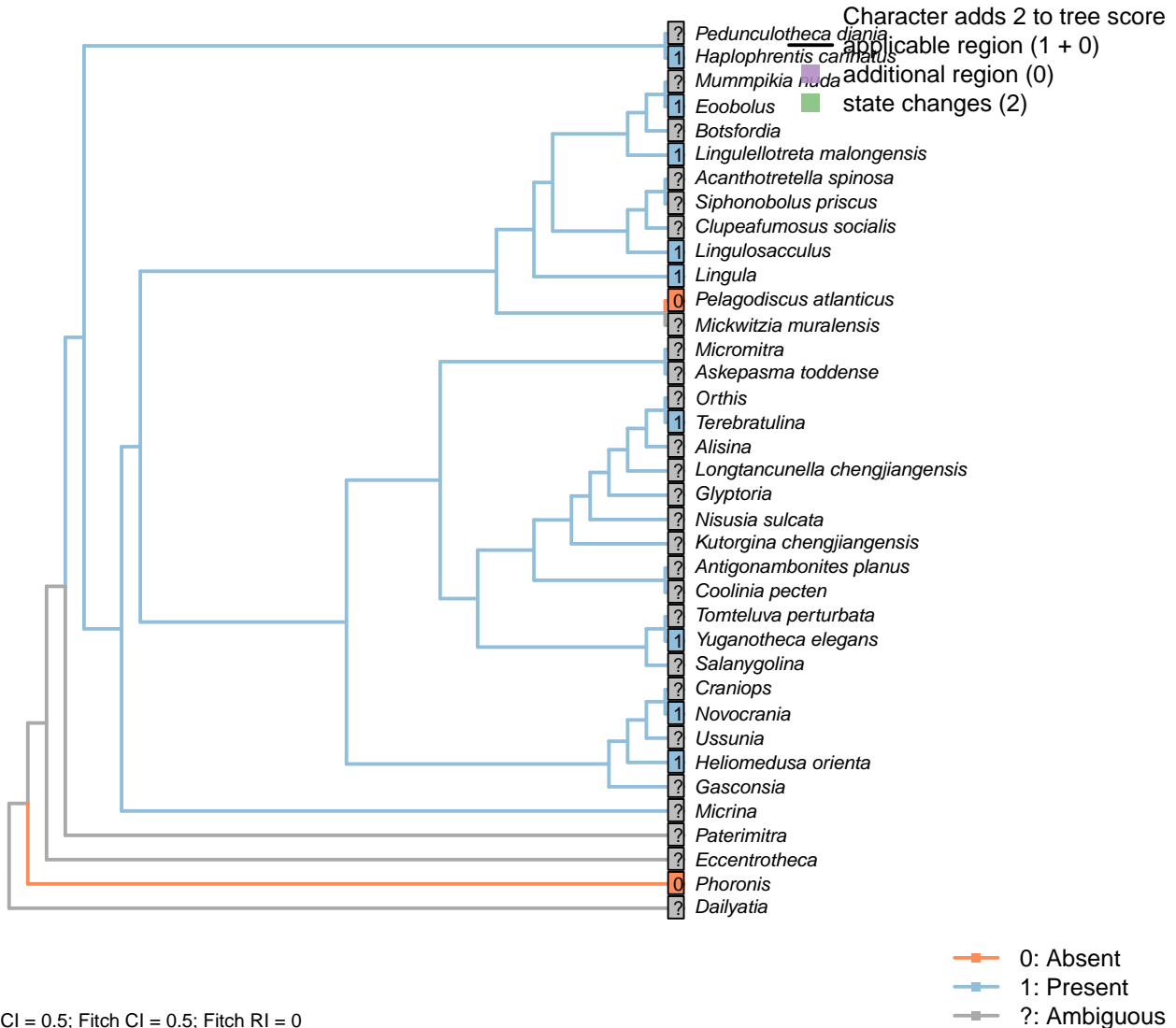
Following character 55 in Carlson (1995). Not possible to code in most fossil taxa.

*Acanthotretella spinosa*, *Alisina*, *Antigonambonites planus*, *Askepasma toddense*, *Clupeafumosus socialis*, *Coolinia pecten*, *Dailyatia*, *Eccentrotheca*, *Gasconsia*, *Glyptoria*, *Haplophrentis carinatus*, *Heliomedusa ori-*

*enta, Kutorgina chengjiangensis, Lingulellotreta malongensis, Lingulosacculus, Longtancunella chengjiangensis, Micrina, Micromitra, Mummpikia nuda, Nisusia sulcata, Orthis, Paterimitra, Pedunculotheca diana, Salanygolina, Tomteluva perturbata, Yuganotheca elegans:* Preservation not adequate to evaluate presence or absence of this muscle.

*Lingula, Novocrania, Pelagodiscus atlanticus, Phoronis, Terebratulina:* Following coding for higher taxon in Carlson (1995), appendix 1, character 55.

### 3.15 Prominent pharynx [103]



#### Character 103: Prominent pharynx

0: Absent

1: Present

Neomorphic character.

Hyoliths exhibit a prominent protrusible muscular pharynx at the base of the lophophore (Moysiuk et al., 2017). This is considered as potentially equivalent to the anterior projection of the visceral cavity in *He-*

*liomedusa*, and, by extension, in *Lingulosacculus* and *Lingulotreta*.

*Eoobolus*: Prominent extension of dorsal visceral platform (Balthasar, 2009).

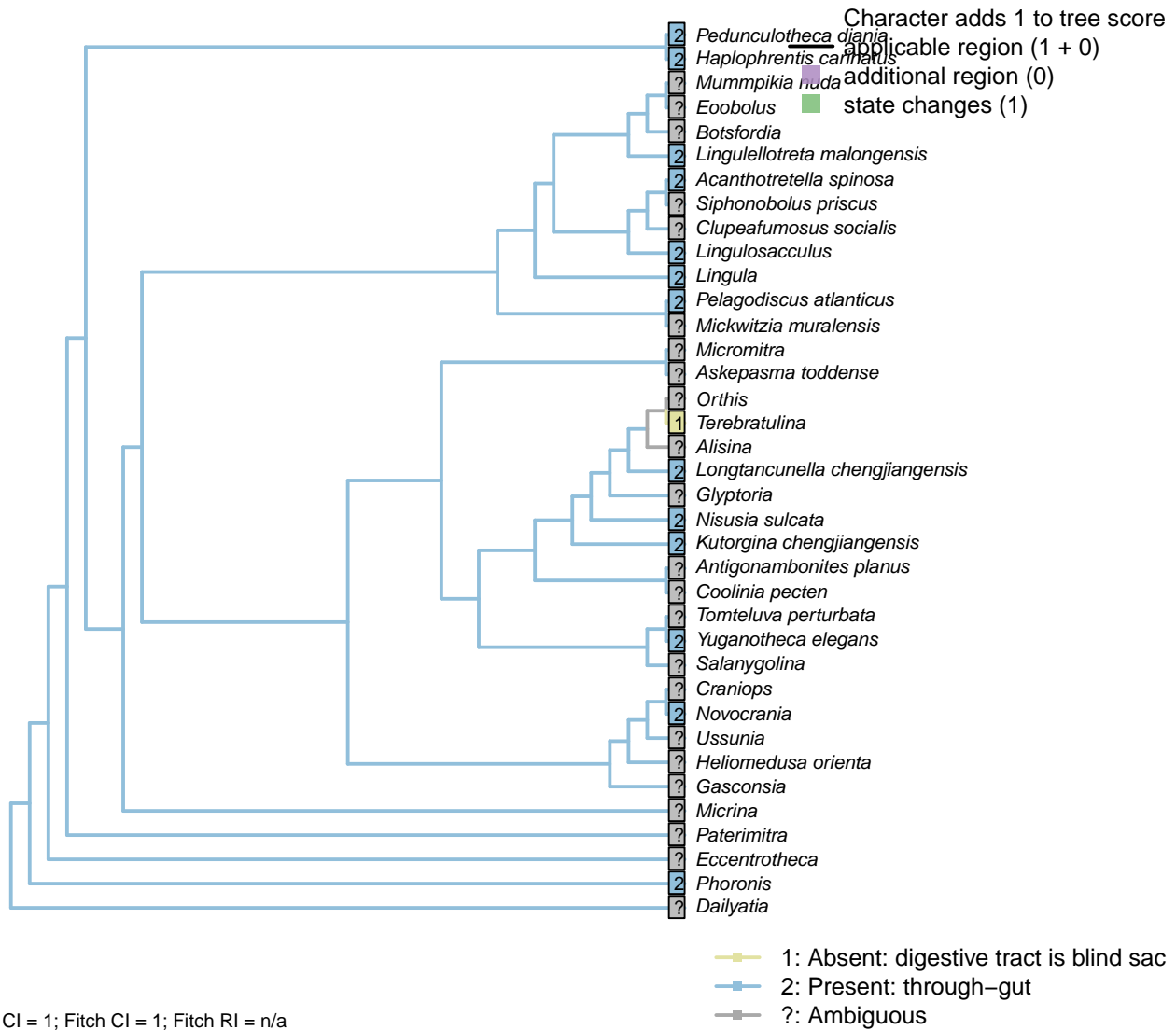
*Heliomedusa orienta*: Corresponding to the “neck” of the vase-shaped visceral cavity reported by Zhang et al. (2009).

*Lingulellotreta malongensis*: An anterior projection of the visceral area is noted by Williams *et al.* (2000) and considered equivalent to that observed in *Lingulosacculus* (Balthasar and Butterfield, 2009).

*Lingulosacculus*: The prominent anterior extension of the visceral area noted by Balthasar & Butterfield (2009) is considered as potentially homologous with that of *Heliomedusa* (Zhang et al., 2009) and, by extension, *Haplophrentis* (Moysiuk *et al.*, 2017).

*Yuganotheca elegans*: Possibly present, following interpretation of mouth (see fig. 2c, d in Zhang et al., 2014).

### 3.16 Anus [104]



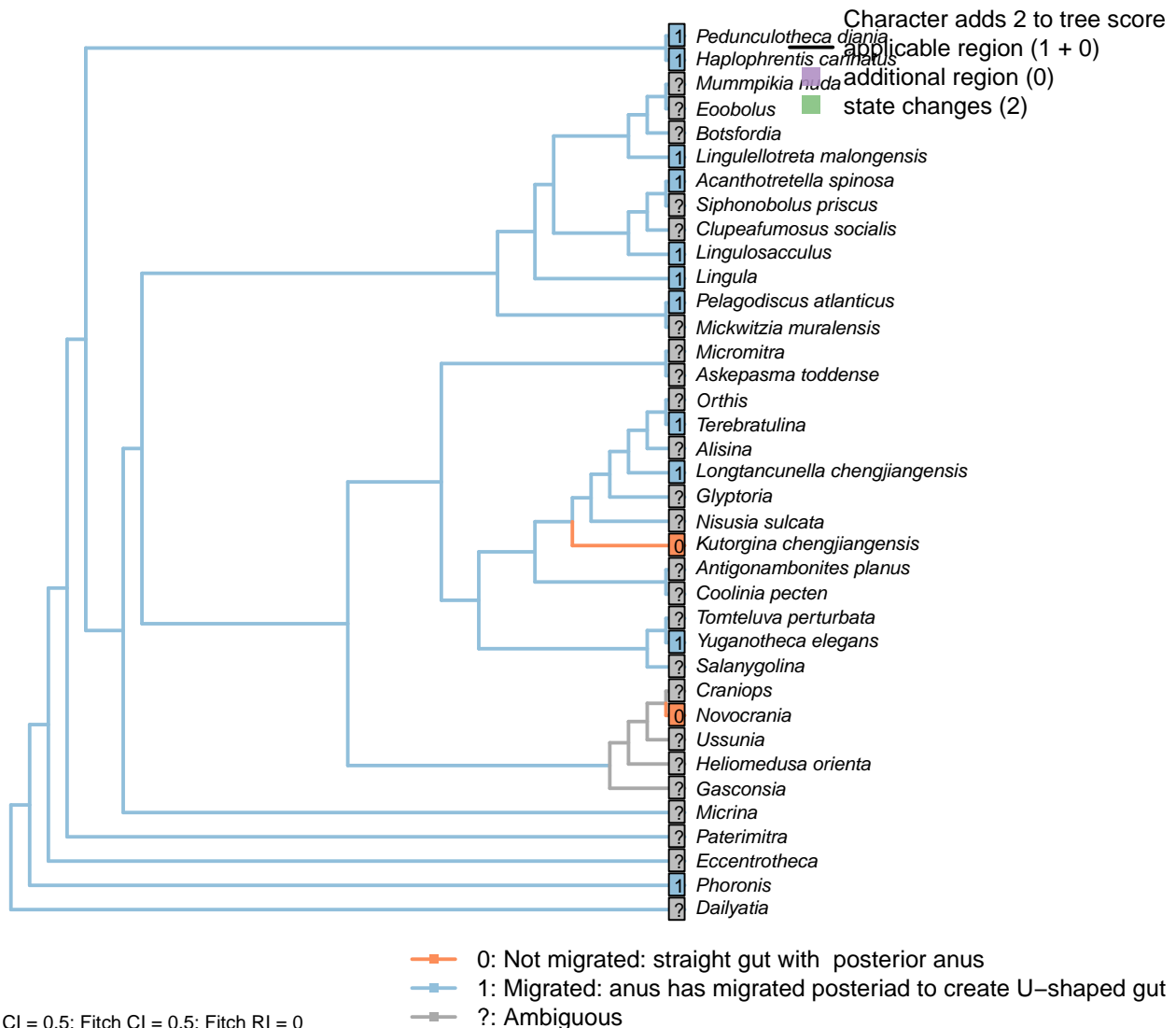
- 1: Absent: digestive tract is blind sac  
 2: Present: through-gut  
 Transformational character.

The digestive tract may either constitute a blind sac, or a through gut with anus.

*Glyptoria*: Scored according to familial level feature.

*Kutorgina chengjiangensis*: Although “the possibility of a blind ending may not be completely eliminated [...] the weight of evidence [...] leads us to reject the possibility of a blind-ending intestine” – Zhang et al. (2007b), p. 1399.

## [105] Migration



### Character 105: Anus: Migration

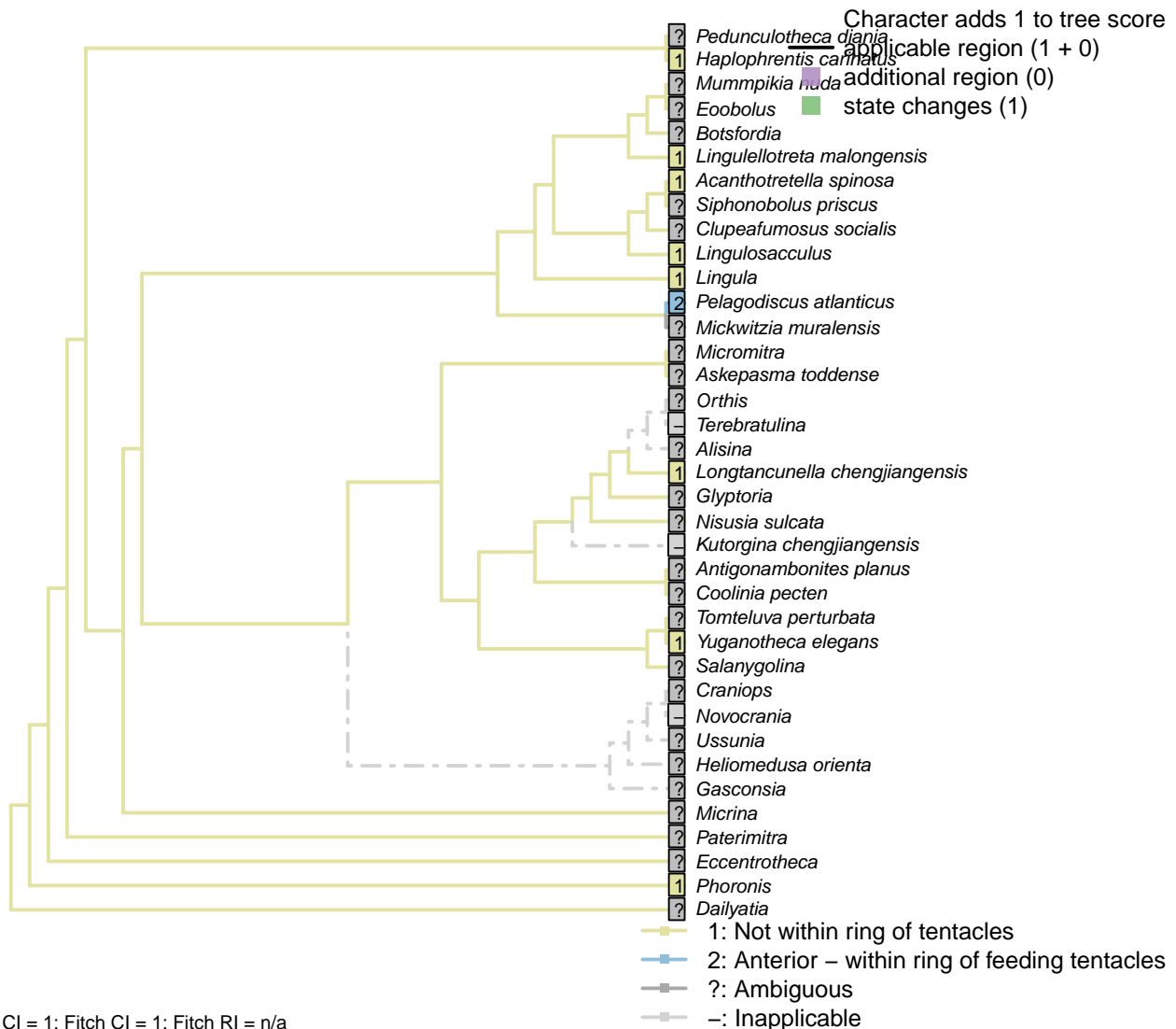
- 0: Not migrated: straight gut with posterior anus  
 1: Migrated: anus has migrated posteriad to create U-shaped gut  
 Neomorphic character.

"The relative position of the mouth and anus in the larvae of brachiopods and phoronids is similar: posterior anus and anterior mouth" – Williams et al. (2007), p. 2884.

*Kutorgina chengjiangensis*: "Five specimens have an exceptionally preserved digestive tract, dorsally curved, with a putative dorso-terminal anus located near the proximal end of a pedicle" – Zhang et al. (2007b).

*Terebratulina*: "In rhynchonelliforms, the gut curves somewhat into a C-shape and the (blind) anus becomes posteroventral in position." – Williams et al. (2007), p. 2884.

## [106] Within ring of tentacles



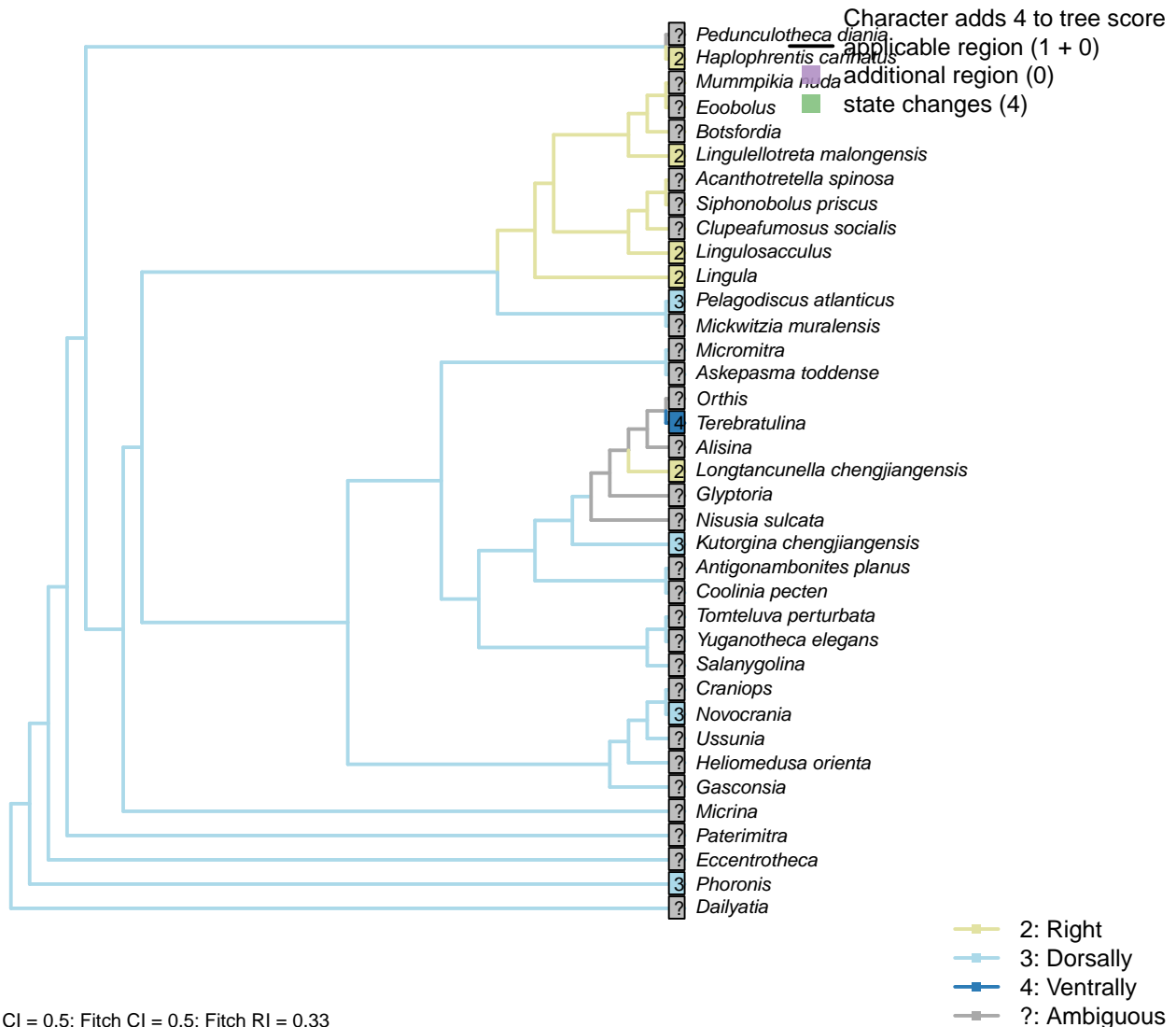
### Character 106: Anus: Migration: Within ring of tentacles

- 1: Not within ring of tentacles
- 2: Anterior - within ring of feeding tentacles
- Transformational character.

A migrated anus may be located laterally or within the lophophore ring (as in entoprocts).

*Kutorgina chengjiangensis*: “Presumed to terminate in a functional anus located near the proximal end of the pedicle.” – Zhang et al. (2007b).

## [107] Position



### Character 107: Anus: Migration: Position

- 1: Left
  - 2: Right
  - 3: Dorsally
  - 4: Ventrally
- Transformational character.

If the anus is not within the ring of tentacles, in which direction is it oriented?.

*Haplophrentis carinatus*: Opening to the right – see figures 1, 3, and extended data 5 in Moysiuk et al. (2017).

The text states in error that the anus is to the left of the midline.

*Kutorgina chengjiangensis*: “Five specimens have an exceptionally preserved digestive tract, dorsally curved, with a putative dorso-terminal anus located near the proximal end of a pedicle” – Zhang et al. (2007b).

*Lingula*: “In the lingulids, the [intestine] follows an oblique course anteriorly to open at the anus on the right body wall.” – Williams et al. (1997), p. 89.

*Lingulellotreta malongensis*: “finally terminating in an anal opening on the right anterior body wall” (Zhang et al., 2007a, p.66).

*Lingulosacculus*: “This same arrangement occurs in *L. nuda*, with the looped dark line tracking the same course as the exceptionally preserved guts of Chengjiang lingulellotretids, including the median position of its posterior loop and the sharp right turn as it exits the posterior extension of the ventral valve” (Balthasar and Butterfield, 2009, p.310).

*Longtancunella chengjiangensis*: “The intestine extends posteriorly, and then turns right to continue as a tortuous strand, finally terminating at the latero-median position of the anterior body wall” – Zhang et al. (2007c).

*Terebratulina*: “In rhynchonelliforms, the gut curves somewhat into a C-shape and the (blind) anus becomes posteroventral in position.” – Williams et al. (2007), p. 2884.

*Yuganotheca elegans*: The identification of the “very poorly impressed possible anus at the lateral side of the anterior body wall” is not yet confident, so this character is coded as not presently available.

# Chapter 4

## Fitch parsimony

Parsimony search was conducted in TNT v1.5 (Goloboff and Catalano, 2016) using ratchet and tree drifting heuristics (Goloboff, 1999; Nixon, 1999), repeating the search until the optimal score had been hit by 1500 independent searches:

```
xmult:rat10 drift10 hits 1500 level 4 chklevel 5;
```

Searches were conducted under equal weights and results saved to file:

```
piwe-; xmult; /* Conduct search with equal weighting */  
tsav *TNT/ew.tre;sav;tsav/; /* Save results to file */  
keep 0; hold 10000; /* Clear trees from memory */
```

Further searches were conducted under extended implied weighting (Goloboff, 1997, 2014), under the concavity constants 2, 3, 4.5, 7, 10.5, 16 and 24:

```
xpiwe=; /* Enable extended implied weighting */  
piwe=2; xmult; /* Conduct analysis at k = 2 */  
tsav *TNT/xpiwe2.tre; sav; tsav/; /* Save results to file */  
keep 0; hold 10000; /* Clear trees from memory */  
piwe=3; xmult; /* Conduct analysis at k = 3 */  
tsav *TNT/xpiwe3.tre; sav ;tsav/; /* Save results to file */
```

We acknowledge the Willi Hennig Society for their sponsorship of the TNT software.

### 4.1 Results

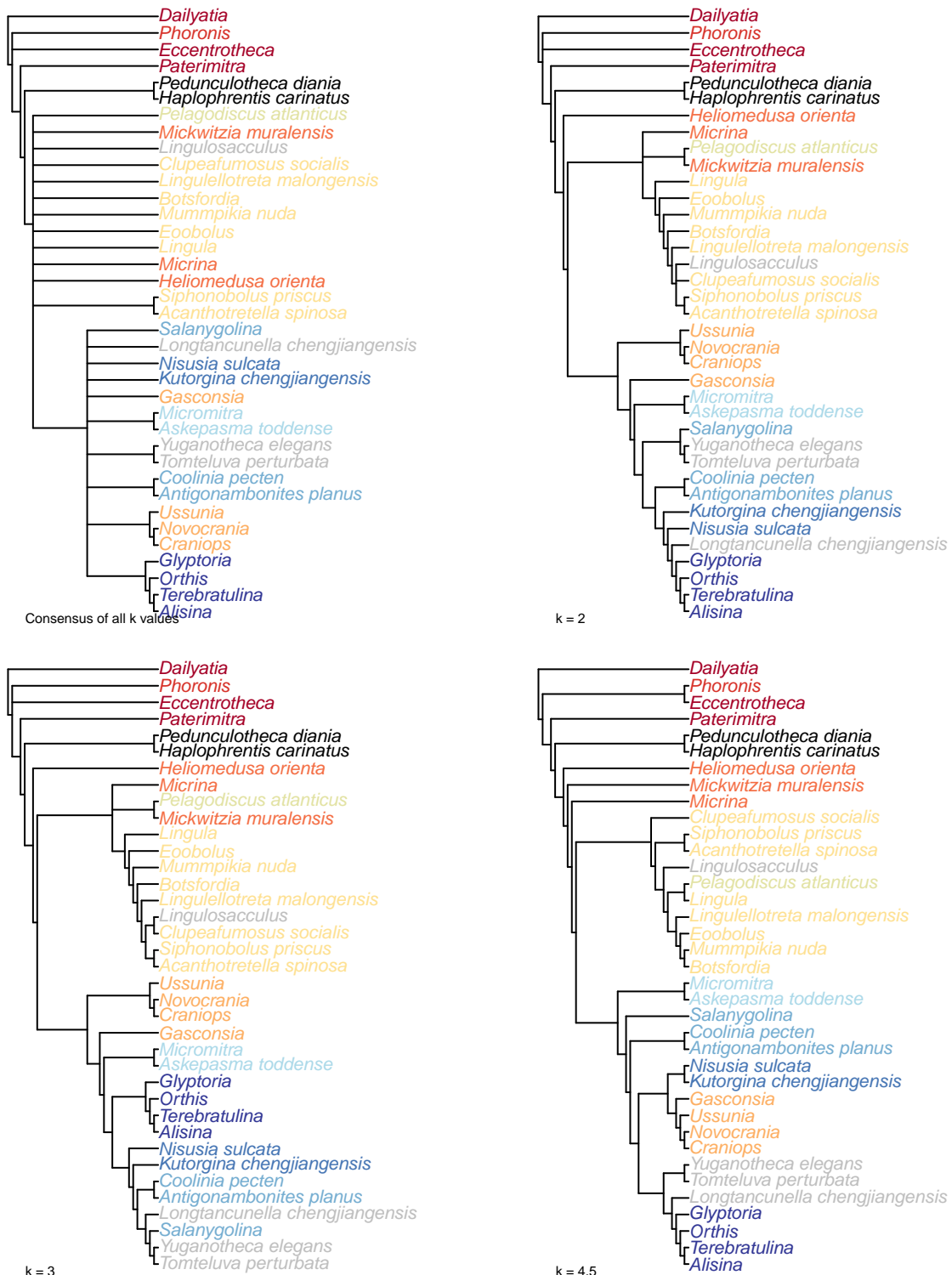


Figure 4.1: Strict consensus of all trees recovered by TNT using Fitch parsimony with implied weighting at all values of  $k$ , and at the individual values  $k = 2, 3$  and  $4.5$ . The consensus of all implied weights runs is not very well resolved, largely due to a few wildcard taxa, particularly at  $k = 4.5$ , which obscures a consistent set of relationships between the remaining taxa.

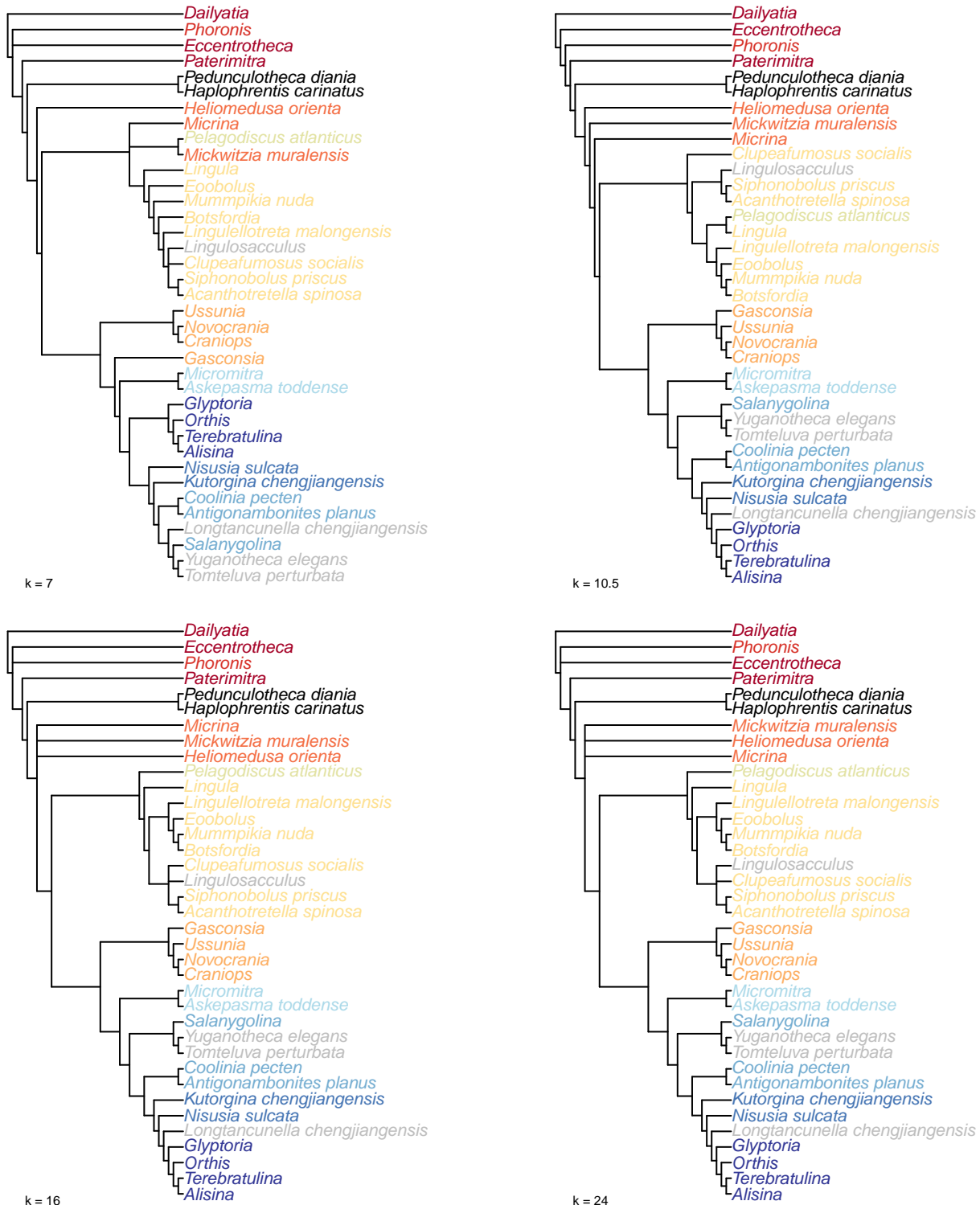


Figure 4.2: Strict consensus of all trees recovered by TNT using Fitch parsimony with implied weighting, at  $k = 7, 10.5, 16$ , and  $24$ .

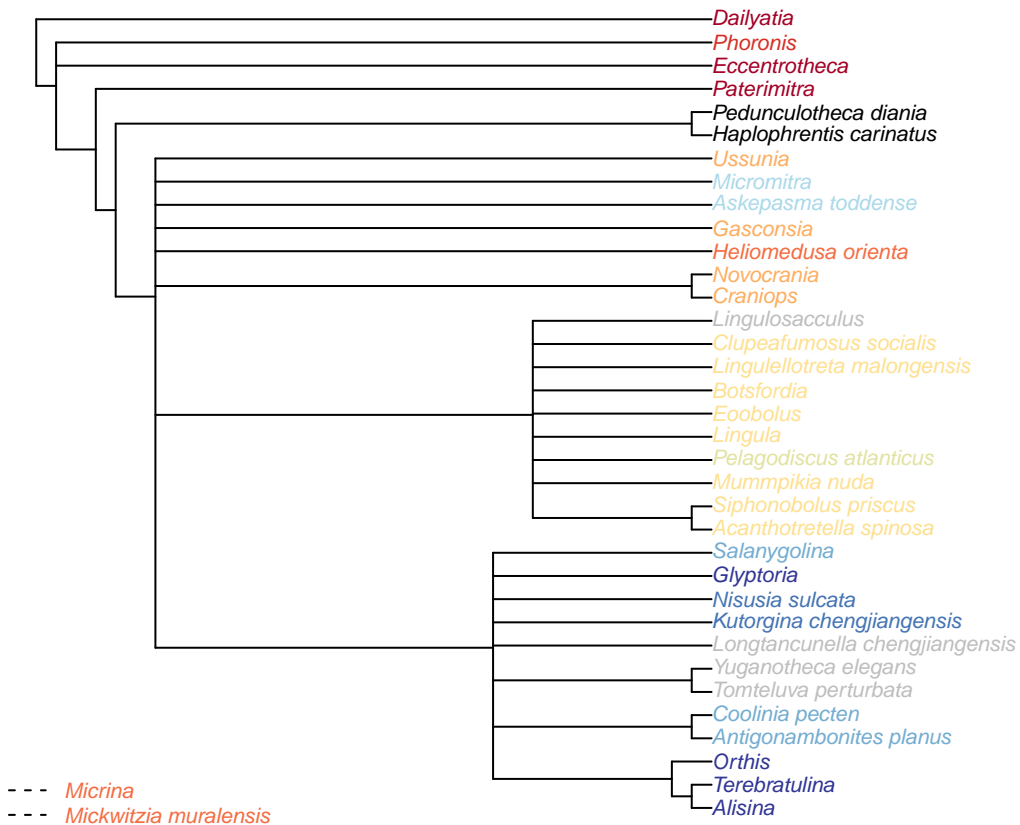


Figure 4.3: Consensus of all trees obtained using equally weighted Fitch parsimony in TNT. *Mickwitzia* and *Micrina* may equally parsimoniously be reconstructed in the basal region of the linguliform or rhynchonelliform lineages; as such, the inclusion of these taxa in the consensus tree reduces resolution. These taxa were still included in the analysis used to generate this tree, but were removed from each MPT before the consensus was calculated in order that the relationships that are present in each tree might be more easily observed.

# Chapter 5

## Bayesian analysis

Bayesian search was conducted in MrBayes v3.2.6 (Ronquist et al., 2012) using the Mk model (Lewis, 2001) with gamma-distributed rate variation across characters:

```
lset coding=variable rates=gamma;
```

Branch length was drawn from a dirichlet prior distribution, which is less informative than an exponential model (Rannala et al., 2012), but requires a prior mean tree length within about two orders of magnitude of the true value (Zhang et al., 2012). To satisfy this latter criterion, we specified the prior mean tree length to be equal to the length of the most parsimonious tree under equal weights, using a Dirichlet prior with  $\alpha_T = 1$ ,  $\beta_T = 1/(equal\ weights\ tree\ length/number\ of\ characters)$ ,  $\alpha = c = 1$ :

```
prset brlenspr = unconstrained: gammadir(1, 0.34, 1, 1);
```

Neomorphic and transformational characters (*sensu* Sereno, 2007) were allocated to two separate partitions whose proportion of invariant characters and gamma shape parameters were allowed to vary independently:

```
charset Neomorphic = 1 2 3 5 7 8 9 10 12 14 17 18 19 22 23 24 25 28 29 30 31 32 35 37 39 46 47  
49 50 51 52 53 54 57 61 62 63 64 66 67 69 70 71 72 73 77 78 79 81 83 86 87 91 93 94 95 97 98 99  
102 103 105;
```

```
charset Transformational = 4 6 11 13 15 16 20 21 26 27 33 34 36 38 40 41 42 43 44 45 48 55 56  
58 59 60 65 68 74 75 76 80 82 84 85 88 89 90 92 96 100 101 104 106 107;
```

```
partition chartype = 2: Neomorphic, Transformational;
```

```
set partition = chartype;
```

```
unlink shape=(all) pinvar=(all);
```

Neomorphic characters were not assumed to have a symmetrical transition rate – that is, the probability of the absent → present transition was allowed to differ from that of the present → absent transition, being drawn from a uniform prior:

```
prset applyto=(1) symdirihyperpr=fixed(1.0);
```

The rate of variation in neomorphic characters was also allowed to vary from that of transformational characters:

```
prset applyto=(1) ratepr=variable;
```

*Dailyatia* was selected as an outgroup:

```
outgroup Dailyatia;
```

Four MrBayes runs were executed, each sampling eight chains for 5 000 000 generations, with samples taken every 500 generations. The first 10% of samples were discarded as burn-in.

```
mcmc ngen=5000000 samplefreq=500 nruns=4 nchains=8 burninfrac=0.1;
```

A posterior tree topology was derived from the combined posterior sample of all runs. Convergence was indicated by PSRF = 1.00 and an estimated sample size of > 200 for each parameter.

## 5.1 Parameter estimates

Parameter	Mean	Variance	minESS	avgESS	PSRF
TL{all}	7.380	0.54000	3160	5380	0.99996
m{1}	0.609	0.00984	733	2790	1.00000

## 5.2 Results

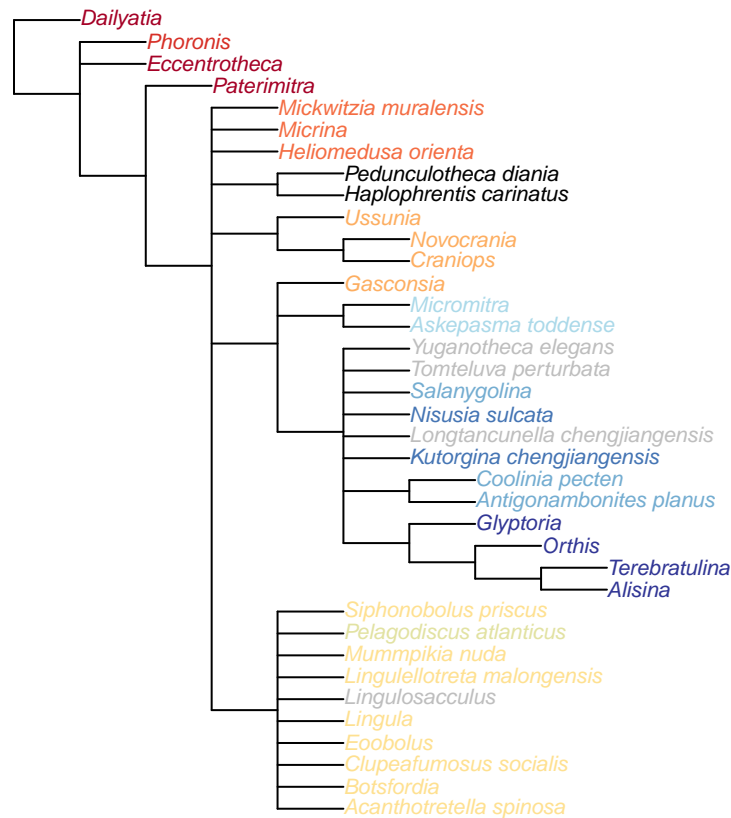


Figure 5.1: Results of Bayesian analysis, posterior probability &gt; 50%, all taxa

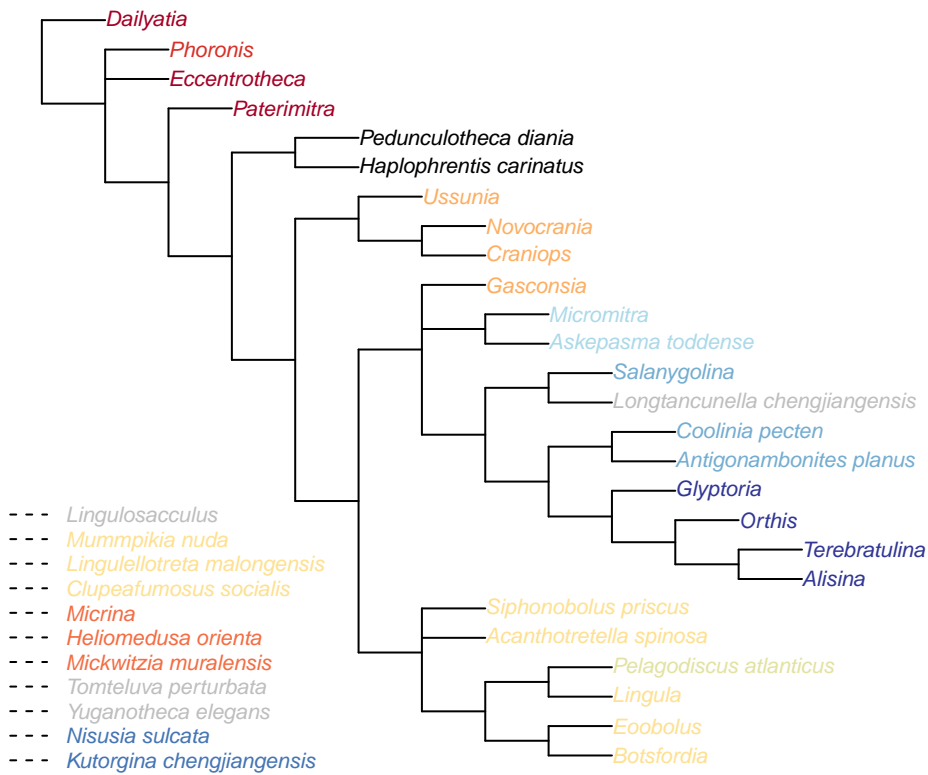


Figure 5.2: Results of Bayesian analysis, posterior probability &gt; 50%, wildcard taxa pruned

# Chapter 6

## Taxonomic implications

This section briefly places key features of our results in the context of previous phylogenetic hypotheses.

**Brachiopod crown and stem group** Crown- and stem-group terminology has great value in clarifying the early evolution of major lineages (Budd and Jensen, 2000; Carlson and Cohen, 2009). The crown group of a lineage is defined as the last common ancestor of all living members of a group, and all its descendants; the stem group as all taxa more closely related to the crown group than to any other extant taxon. In our analyses, the brachiopod crown group corresponds to the last common ancestor of *Terebratulina* and *Lingula*; the brachiopod stem group comprises anything between this node and the branching point of *Phoronis*.

**Craniiforms** Trimerellids are reconstructed as paraphyletic with respect to Craniiforms. This is consistent with the affinity commonly drawn between these groups (e.g. Williams et al., 2000), and helps to account for the stratigraphically late (Ordovician) appearance of Craniids in the fossil record. (Aragonite is underrepresented in early Palaeozoic strata due to taphonomic bias.)

The relationship of Craniiforms with respect to Linguliforms and Rhynchonelliforms remains unclear. Shell characters point to a relationship with the Rhynchonelliforms, which is countered by similarities between the spermatozoa of phoronids and terebratulids, which indicate a craniiform + linguliform clade.

It's worth noting that Bayesian and Fitch analyses place *Gasconsia* as the basalmost member of the Rhynchonellid lineage, upholding suggestions (Holmer et al., 2014) of a chileid rather than trimerellid affinity. This placement presumably represents an artefact resulting from the incorrect handling of inapplicable data. But if true, *Gasconsia* would be a close analogue for the common ancestor of Rhynchonelliforms + Craniiforms (+Linguliforms?).

**Rhynchonelliforms** The position of kutorginids within the rhynchonelliform stem lineage has been tricky to resolve (Holmer et al., 2018b); we resolve them as paraphyletic with respect to Rhynconellata (which encompasses the obolellate *Alisina*), which is broadly in accord to previous proposals (Holmer et al., 2018a). Chileids form the adelphiotaxon to this clade. *Longtancunella* (Zhang et al., 2011a) nests crownwards of the protorthid *Glyptoria*, but stemward of the obolellid *Alisina*.

*Salanygolina* has been interpreted as a stem-group rhynchonelliform based on its combination of paterinid and chileate features (Holmer et al., 2009). Our results position *Salanygolina* between paterinids and chileids, which directly corroborates this proposed phylogenetic position.

Basal rhynchonellids are characterized by a circular umbonal perforation in the ventral valve, associated with a colleplax. Partly on this basis, the aberrant taxa *Yuganotheca* and *Tomteluva* plot close to *Salanygolina*, the three often forming a clade – though the reliability of this grouping is perhaps liable to change as additional data comes to light. Nevertheless, an interpretation of *Yuganotheca* as a stem-group brachiopod (Zhang et al., 2014) is difficult to reconcile with the increasingly well-constrained

nature of the early brachiopod body plan.

**Linguliforms** The reconstruction of Linguloformea comprising Linguloidea as sister to Discinoidea is as expected, though it is notable that Acrotretids and Siphonotretids plot more closely to Linguloidea than Discinoidea does.

Lingulellotretids also sit within this lingulid grouping; a position in the phoronid stem lineage (advocated by Balthasar and Butterfield, 2009) is not upheld.

More novel is the reconstruction of the calcitic obbolellid *Mummpikia* in the linguliform total group: a rhynchonelliform affinity has been assumed based on its calcitic mineralogy. This said, Balthasar (2008) has highlighted the similarities between obbolellids and linguliform brachiopods, including sub- $m$  vertical canals and the detailed configuration of the posterior shell margin. Our analysis upholds the case for a linguliform affinity for *Mummpikia*; a calcitic shell seemingly arose through an independent change within this taxon. As such, *Mummpikia* has no direct bearing on the origin of ‘Calciata’, save that shell mineralogy is perhaps less static than commonly assumed.

More generally, our results identify Class Obbolellata as polyphyletic: *Alisina* (Trematobolidae) plots within Rhynchonellata; *Tomteluva* is harder to place, but tends to group with *Salanygolina* stemwards of the chileids.

**Paterinids** Paterinids have traditionally been placed within the Linguliforms on the basis of their phosphatic shell (Williams et al., 2007), which our analysis identifies as ancestral within the brachiopod crown group; our analysis places them within the Rhynchonelliforms instead. Characters supporting this position include the strophic hinge line, planar cardinal area, the absence of a pedicle nerve impression, and the morphology of the mantle canals.

More generally, although some lingulids can be found which share more generic characters (e.g. shell growth direction) with paterinids, the particular combination of characters exhibited in paterinids does not occur anywhere in the linguliform lineage, but is more similar to that of basal rhynchonelliforms, particularly *Salanygolina*.

**Tommotiids** Tommotiids represent a basal grade, paraphyletic to phoronids and crown-group brachiopods, in line with previous interpretations.

*Micrina* and *Mickwitzia* are the most crownwards of the tommotiids, but beyond this, their position is somewhat difficult to pin down; certain analytical configurations reconstruct them as stem-brachiopods; others place them closer to the discinids, the lingulids or the craniiforms. *Helomedusa* is commonly associated closely with *Mickwitzia*, reflecting the similarities emphasized by Holmer and Popov in Williams et al. (2007), but plots instead within the Craniiforms under certain analytical conditions, in line with earlier interpretations (Williams et al., 2000).

**Hyoliths** Hyoliths are interpreted as stem-group Brachiopods, which refines the broader phylogenetic position proposed by Moysiuk et al. (2017). This is to say, they sit closer to brachiopods than the phoronids do, but no analysis places them within the Brachiopod crown group.

Hyoliths thus represent derived tommotiids, and are the closest relatives to the Brachiopod crown group.

# Supplementary Figures

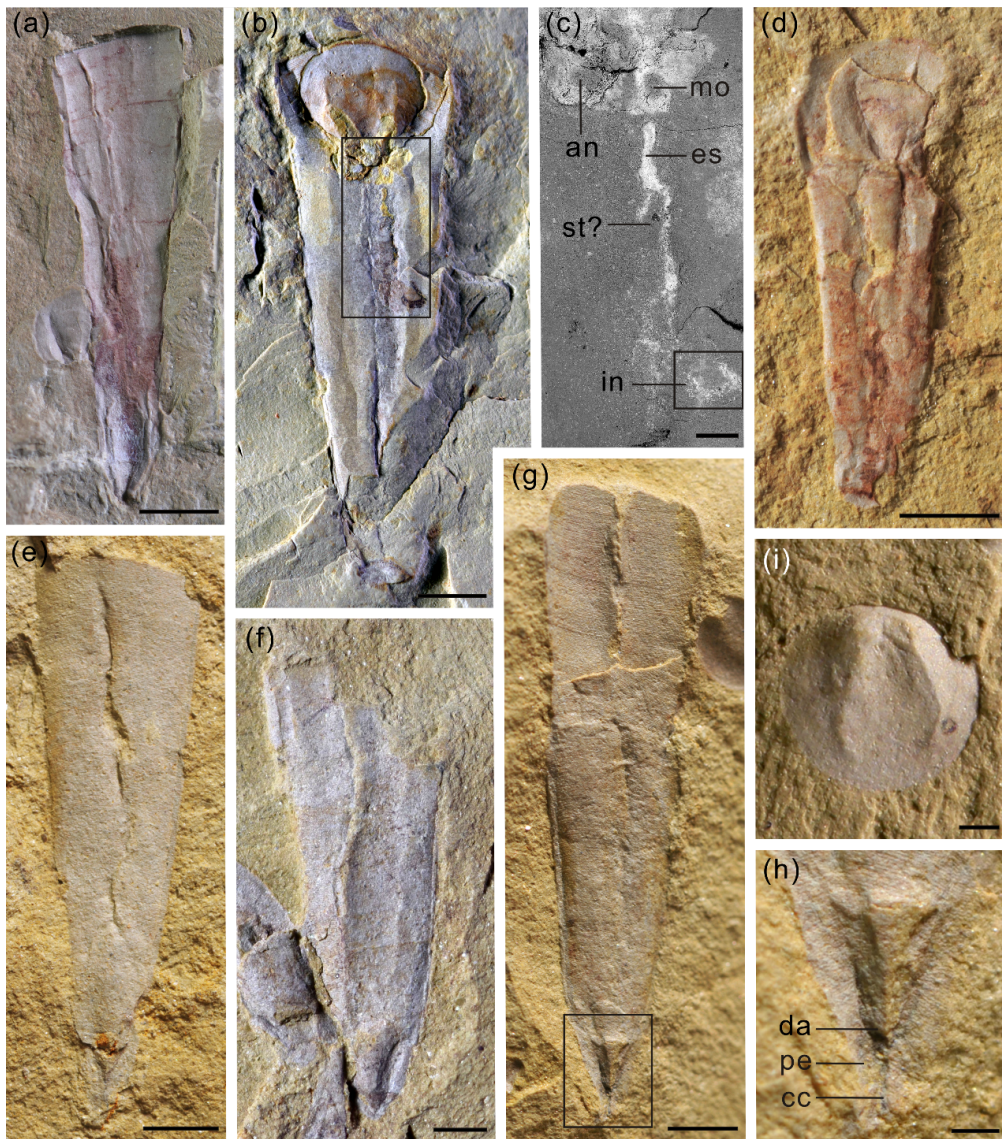


**Fig. S1.** *Pedunculotheca diania* Sun, Zhao et Zhu gen. et sp. nov. from the Chengjiang Biota, Yunnan Province, China. (a) NIGPAS 166601, external mould of dorsum with dorsal apex and pedicle foramen. (b) NIGPAS 166597, preserving conical shell, operculum and internal soft tissue, showing a compressed elliptic cross-section; backscatter electron micrograph of boxed region shown in (c). (d) NIGPAS 166599b, counterpart, juvenile conical shell with operculum showing two longitudinal ventral grooves and

circular larval shell. (e) NIGPAS 166602, conical shell with incomplete attachment structure. (f) NIGPAS 166598, broken shell with two ventral furrows and incomplete attachment structure. (g) NIGPAS 166596, incomplete shell with one medial ventral furrow and short attachment structure with coelomic cavity; detail of boxed region shown in (h). (i) NIGPAS 166603, exterior of operculum. Scale bars: 2mm (for a, b and e-g); 500 µm (for c, h and i).

Abbreviations: an = anus, cc = coelomic cavity, da = dorsal apex, es = esophagus, in = intestine, mo = mouth, pe = pedicle, st = stomach.

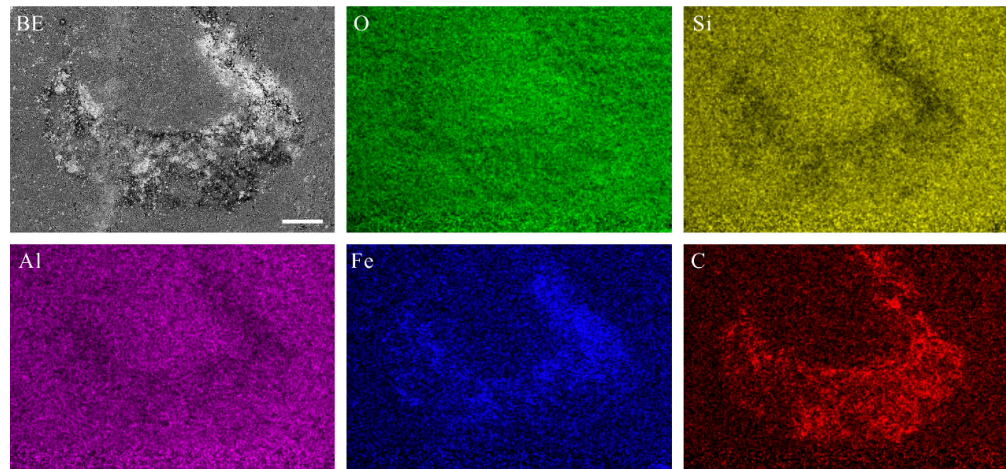


**Fig. S2. Elemental distribution in the gut of *Pedunculotheca diania* Sun, Zhao et Zhu gen. et sp. nov.** NIGPAS 166597. Region corresponds to boxed region in Fig. S1c. Scale bar = 100 µm.

Abbreviations: BE = backscatter electron image, O = Oxygen, Si = Silicon, Al = Aluminium, Fe = Iron, C = Carbon.

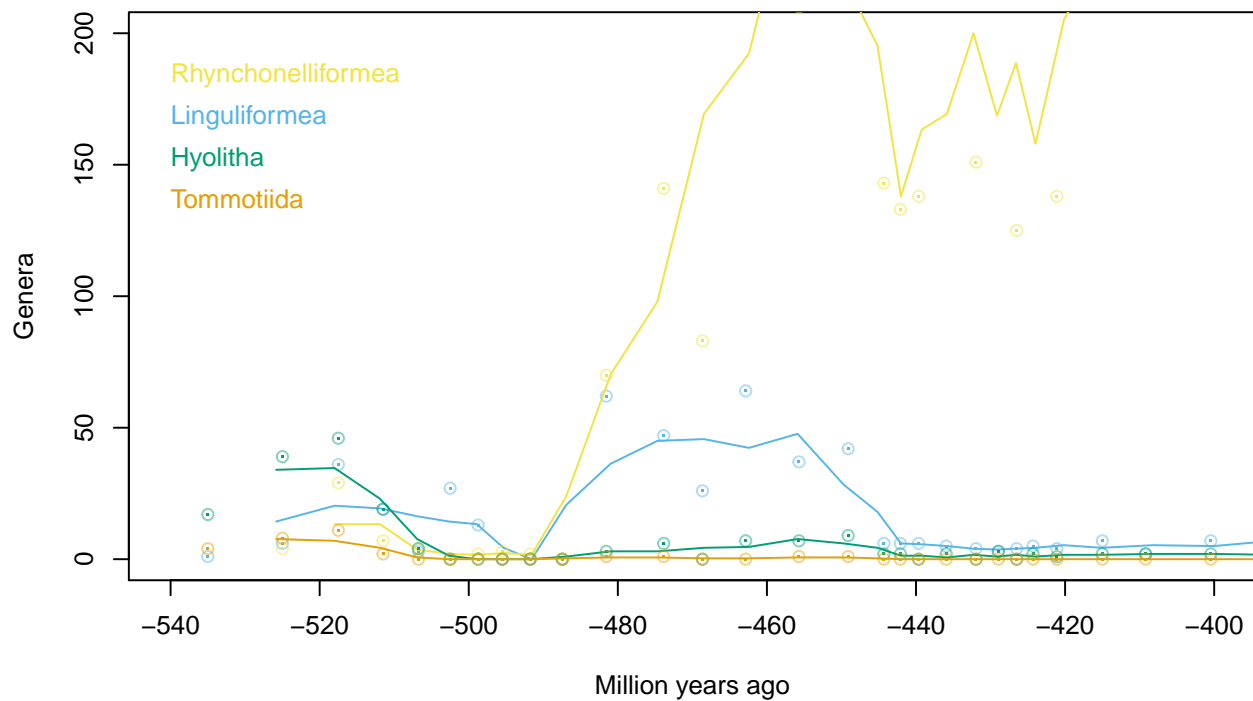


**Fig. S3. Global diversity of brachiopods through the Paleozoic.** Points represent number of genera reported in each time bin; lines represent rolling mean diversity over three consecutive time bins. Data from Paleobiology database.

# Supplementary Table

NIGPAS Specimen numbers	Fossil locality	Coordinates
166593, 166617	Shankou Village, Anning	24°49'53" N, 102°24'47.9" E
166594, 166595	Yaoying Village, Wuding	25°36'01.2" N, 102°20'04.6" E
166596–166616	Ma'anshan Village, Chengjiang	24°40'37.2" N, 102°58'40.2" E

**Table S1. Provenance of fossil material.** Individuals from the Yaoying section are usually bigger, with a thicker body wall, and have a smaller ratio of apertural width to shell length than specimens from other areas. In the absence of other differentiating features, we consider these deviations to represent ecophenotypical variation within a single species, perhaps reflecting the increased energetics and predation pressure that accompany the shallower water depth reported at the Yaoying section (Zhao et al., 2012).

# Bibliography

- Afzelius, B. A. and Ferraguti, M. (1978). Fine structure of brachiopod spermatozoa. *Journal of Ultrastructure Research*, 63(3):308–315, doi:10.1016/s0022-5320(78)80054-9.
- Archie, J. W. (1989). Homoplasy excess ratios: new indices for measuring levels of homoplasy in phylogenetic systematics and a critique of the Consistency Index. *Systematic Zoology*, 38(3):253, doi:10.2307/2992286.
- Balthasar, U. (2004). Shell structure, ontogeny, and affinities of the Lower Cambrian bivalved problematic fossil *Mickwitzia muralensis* Walcott, 1913. *Lethaia*, 37(4):381–400, doi:10.1080/00241160410002090.
- Balthasar, U. (2007). An early Cambrian organophosphatic brachiopod with calcitic granules. *Palaeontology*, 50(6):1319–1325, doi:10.1111/j.1475-4983.2007.00729.x.
- Balthasar, U. (2008). *Mummpikia* gen. nov. and the origin of calcitic-shelled brachiopods. *Palaeontology*, 51(2):263–279, doi:10.1111/j.1475-4983.2008.00754.x.
- Balthasar, U. (2009). The brachiopod *Eobolus* from the early Cambrian Mural Formation (Canadian Rocky Mountains). *Paläontologische Zeitschrift*, 83(3):407–417, doi:10.1007/s12542-009-0026-4.
- Balthasar, U. and Butterfield, N. J. (2009). Early Cambrian soft-shelled brachiopods as possible stem-group phoronids. *Acta Palaeontologica Polonica*, 54(2):307–314, doi:10.4202/app.2008.0042.
- Balthasar, U., Cusack, M., Faryma, L., Chung, P., Holmer, L. E., Jin, J., Percival, I. G., and Popov, L. E. (2011). Relic aragonite from Ordovician–Silurian brachiopods: Implications for the evolution of calcification. *Geology*, 39(10):967–970, doi:10.1130/g32269.1.
- Bassett, M. G. and Popov, L. E. (2017). Earliest ontogeny of the Silurian orthotetide brachiopod *Coolinia* and its significance for interpreting strophomenate phylogeny. *Lethaia*, 50(4):504–510, doi:10.1111/let.12204.
- Bassett, M. G., Popov, L. E., and Egerquist, E. (2008). Early ontogeny of some Ordovician–Silurian strophomenate brachiopods: Significance for interpreting evolutionary relationships within early Rhynchonelliformea. *Fossils and Strata*, 54:13–20.
- Bassett, M. G., Popov, L. E., and Holmer, L. E. (2001). Functional morphology of articulatory structures and implications for patterns of musculature in Cambrian rhynchonelliform brachiopods. In Brunton, H., Cocks, R. M., and Long, S. L., editors, *Brachiopods, Past and Present*, pages 163–176. Taylor & Francis.
- Benedetto, J. L. (2009). *Chaniella*, a new lower Tremadocian (Ordovician) brachiopod from northwestern Argentina and its phylogenetic relationships within basal rhynchonelliforms. *Paläontologische Zeitschrift*, 83(3):393–405, doi:10.1007/s12542-009-0023-7.
- Brazeau, M. D., Guillerme, T., and Smith, M. R. (2018). An algorithm for morphological phylogenetic analysis with inapplicable data. *Systematic Biology*, doi:10.1101/209775.
- Brazeau, M. D., Smith, M. R., and Guillerme, T. (2017). MorphyLib: a library for phylogenetic analysis of categorical trait data with inapplicability. doi:10.5281/zenodo.815371.

- Budd, G. E. and Jensen, S. (2000). A critical reappraisal of the fossil record of the bilaterian phyla. *Biological Reviews*, 75(2):253–295.
- Butler, A. D., Streng, M., Garwood, R., Lowe, T., and Holmer, L. E. (2012). Constructing Cambrian body-plans: critical evaluation of tommotiid and stem-brachiopod character homologies [Exceptional preservation of *Micrina* setae and 3D MicroCT reconstruction confirm the tommotiid stem-group brachiopod link]. In *Palaeontological Association Annual Meeting*, volume 56, page 61. The Palaeontological Association.
- Butler, A. D., Streng, M., Holmer, L. E., and Babcock, L. E. (2015). Exceptionally preserved *Mickwitzia* from the Indian Springs Lagerstätte (Cambrian Stage 3), Nevada. *Journal of Paleontology*, 89(6):933–955, doi:10.1017/jpa.2016.8.
- Carlson, S. J. (1995). Phylogenetic relationships among extant brachiopods. *Cladistics*, 11:131–197, doi:10.1111/j.1096-0031.1995.tb00084.x.
- Carlson, S. J. and Cohen, B. L. (2009). Separating the crown from the stem: defining Brachiopoda and Pan-Brachiopoda delineates stem-brachiopods. *Geological Society of America Annual Meeting Abstract Program*, 41:562.
- Chen, J.-Y., Huang, D.-Y., and Chuang, S.-H. (2007). Reinterpretation of the Lower Cambrian brachiopod *Heliomedusa orienta* Sun and Hou, 1987a as a discinid. *Journal of Paleontology*, 81(1):38–47, doi:10.1666/0022-3360(2007)81[38:rotlcb]2.0.co;2.
- Cooper, G. A. (1976). Lower Cambrian brachiopods from the Rift Valley (Israel and Jordan). *Journal of Paleontology*, 50(2):269–289.
- Cusack, M., Williams, A., and Buckman, J. O. (1999). Chemico-structural evolution of linguloid brachiopod shells. *Palaeontology*, 42(5):799–840, doi:10.1111/1475-4983.00098.
- Dewing, K. (2001). Hinge modifications and musculature of strophomenoid brachiopods: examples across the Ordovician–Silurian boundary, Anticosti Island, Quebec. *Canadian Journal of Earth Sciences*, 38:125–141, doi:10.1139/e00-027.
- Dzik, J. (1980). Ontogeny of *Bactrotheca* and related hyoliths. *Geologiska Föreningen i Stockholm Förhandlingar*, 102(3):223–233, doi:10.1080/11035898009455162.
- Emig, C. C. (1992). Functional disposition of the lophophore in living Brachiopoda. *Lethaia*, 25(3):291–302, doi:10.1111/j.1502-3931.1992.tb01398.x.
- Franzen, A. and Ahlfors, K. (1980). Ultrastructure of spermatids and spermatozoa in *Phoronis*, Phylum Phoronida. *Journal of Submicroscopic Cytology*, 12(4):585–597.
- Freeman, G. and Lundelius, J. W. (1999). Changes in the timing of mantle formation and larval life history traits in linguliform and craniiform brachiopods. *Lethaia*, 32:197–217, doi:10.1111/j.1502-3931.1999.tb00539.x.
- Fukumoto, M. (2003). The acrosome reaction of the spermatozoa of the inarticulate brachiopod *Lingula anatina*. In Brunton, H., Cocks, R. M., and Long, S. L., editors, *Brachiopods, Past and Present*, pages 40–45. Taylor & Francis.
- Goloboff, P. A. (1997). Self-weighted optimization: tree searches and character state reconstructions under implied transformation costs. *Cladistics*, 13(3):225–245, doi:10.1111/j.1096-0031.1997.tb00317.x.
- Goloboff, P. A. (1999). Analyzing large data sets in reasonable times: solutions for composite optima. *Cladistics*, 15(4):415–428, doi:10.1006/clad.1999.0122.
- Goloboff, P. A. (2014). Extended implied weighting. *Cladistics*, 30(3):260–272, doi:10.1111/cla.12047.
- Goloboff, P. A. and Catalano, S. A. (2016). TNT version 1.5, including a full implementation of phylogenetic morphometrics. *Cladistics*, 32(3):221–238, doi:10.1111/cla.12160.

- Gorjansky, V. Y. and Popov, L. E. (1986). On the origin and systematic position of the calcareous-shelled inarticulate brachiopods. *Lethaia*, 19:223–240, doi:10.1111/j.1502-3931.1986.tb00737.x.
- Hanken, N.-M. and Harper, D. A. T. (1985). The taxonomy, shell structure, and palaeoecology of the trimerellid brachiopod *Gasconsia* Northrop. *Palaeontology*, 28(2):243–254.
- Harper, D. A. T., Popov, L. E., and Holmer, L. E. (2017). Brachiopods: origin and early history. *Palaeontology*, 60:609–631, doi:10.1111/pala.12307.
- Havlicek, M. (1982). Lingulacea, Paterinacea, and Siphonotretacea (Brachiopoda) in the Lower Ordovician sequence of Bohemia. *Sbornik geologickych ved, Paleontologie*, 25:9–82, pl. 1–16.
- Herrmann, K. (1997). Phoronida. In Harrison, F. W. and Woollacott, R. M., editors, *Microscopic Anatomy of Invertebrates, 13: Lophophorates, Entoprocta, and Cycliophora*, pages 207–236. Wiley-Blackwell.
- Hodgson, A. N. and Reunov, A. A. (1994). Ultrastructure of the spermatozoon and spermatogenesis of the brachiopods *Discinisca tenuis* (Inarticulata) and *Kraussina rubra* (Articulata). *Invertebrate Reproduction & Development*, 25(1):23–31, doi:10.1080/07924259.1994.9672365.
- Holmer, L. E. (1989). Middle Ordovician phosphatic inarticulate brachiopods from Västergötland and Dalarna, Sweden. *Fossils and Strata*, 26:1–172.
- Holmer, L. E. and Caron, J.-B. (2006). A spinose stem group brachiopod with pedicle from the Middle Cambrian Burgess Shale. *Acta Zoologica*, 87:273–290, doi:10.1111/j.1463-6395.2006.00241.x.
- Holmer, L. E., Pettersson Stolk, P. S., Skovsted, C. B., Balthasar, U., and Popov, L. E. (2009). The enigmatic early Cambrian *Salanygolina* – A stem group of rhynchonelliform chileate brachiopods? *Palaeontology*, 52(1):1–10, doi:10.1111/j.1475-4983.2008.00831.x.
- Holmer, L. E., Popov, L. E., and Bassett, M. G. (2014). Ordovician–Silurian Chileida—first post-Cambrian records of an enigmatic group of Brachiopoda. *Journal of Paleontology*, 88(3):488–496, doi:10.1666/13-104.
- Holmer, L. E., Popov, L. E., Koneva, S. P., and Rong, J.-Y. (1997). Early Cambrian Lingulellotreta (Lingulata, Brachiopoda) from south Kazakhstan (Malyi Karatau Range) and South China (eastern Yunnan). *Journal of Paleontology*, 71(4):577–584, doi:10.1017/s0022336000040063.
- Holmer, L. E., Popov, L. E., Pour, M. G., Claybourn, T., Zhang, Z.-L., Brock, G. A., and Zhang, Z.-F. (2018a). Evolutionary significance of a middle Cambrian (Series 3) *in situ* occurrence of the pedunculate rhynchonelliform brachiopod *Nisusia sulcata*. *Lethaia*, doi:10.1111/let.12254.
- Holmer, L. E., Skovsted, C. B., Brock, G. A., Valentine, J. L., and Paterson, J. R. (2008). The Early Cambrian tommotiid *Micrina*, a sessile bivalved stem group brachiopod. *Biology Letters*, 4:724–728, doi:10.1098/rsbl.2008.0277.
- Holmer, L. E., Skovsted, C. B., Larsson, C. M., Brock, G. A., and Zhang, Z.-F. (2011). First record of a bivalved larval shell in Early Cambrian tommotiids and its phylogenetic significance. *Palaeontology*, 54(2):235–239, doi:10.1111/j.1475-4983.2010.01030.x.
- Holmer, L. E., Zhang, Z.-F., Topper, T. P., Popov, L. E., and Claybourn, T. M. (2018b). The attachment strategies of Cambrian kutoarginate brachiopods: the curious case of two pedicle openings and their phylogenetic significance. *Journal of Paleontology*, 92(1):33–39, doi:10.1017/jpa.2017.76.
- Hou, X.-G., Siveter, D. J., Siveter, D. J., Aldridge, R. J., Cong, P.-Y., Gabbott, S. E., and Purnell, M. A. (2017). Brachiopoda. In *The Cambrian Fossils of Chengjiang, China: The Flowering of Early Animal Life*. Blackwell.
- Hu, S.-X., Zhang, Z.-F., Holmer, L. E., and Skovsted, C. B. (2010). Soft-part preservation in a linguliform brachiopod from the lower Cambrian Wulongqing Formation (Guanshan Fauna) of Yunnan, South China. *Acta Palaeontologica Polonica*, 55(3):495–505, doi:10.4202/app.2009.1106.

- Jamieson, B. G. M. (1991). *Fish Evolution and Systematics: Evidence from Spermatozoa: With a Survey of Lophophorate, Echinoderm and Protochordate Sperm and an Account of Gamete Cryopreservation*. Cambridge University Press.
- Jin, Y.-G. and Wang, H.-Y. (1992). Revision of the Lower Cambrian brachiopod *Heliomedusa* Sun & Hou, 1987. *Lethaia*, 24:35–49, doi:10.1111/j.1502-3931.1992.tb01790.x.
- Kouchinsky, A. V. (2000). Skeletal microstructures of hyoliths from the Early Cambrian of Siberia. *Alcheringa: An Australasian Journal of Palaeontology*, 24(2):65–81, doi:10.1080/03115510008619525.
- Larsson, C. M., Skovsted, C. B., Brock, G. A., Balthasar, U., Topper, T. P., and Holmer, L. E. (2014). *Paterrimitra pyramidalis* from South Australia: scleritome, shell structure and evolution of a lower Cambrian stem group brachiopod. *Palaeontology*, 57(2):417–446, doi:10.1111/pala.12072.
- Laurie, J. (1987). The musculature and vascular systems of two species of Cambrian Paterinide (Brachiopoda). *Bureau of Mineral Resources Journal of Australian Geology and Geophysics*, 10:261–265.
- Lewis, P. O. (2001). A likelihood approach to estimating phylogeny from discrete morphological character data. *Systematic Biology*, 50(6):913–925, doi:10.1080/106351501753462876.
- Maddison, W. P. (1993). Missing data versus missing characters in phylogenetic analysis. *Systematic Biology*, 42(4):576–581, doi:10.1093/sysbio/42.4.576.
- Moore, J. L. and Porter, S. M. (2018). Plywood-like shell microstructures in hyoliths from the middle Cambrian (Drumian) Gowers Formation, Georgina Basin, Australia. *Palaeontology*, 61, doi:10.1111/pala.12352.
- Moysiuk, J., Smith, M. R., and Caron, J.-B. (2017). Hyoliths are Palaeozoic lophophorates. *Nature*, 541(7637):394–397, doi:10.1038/nature20804.
- Nixon, K. C. (1999). The Parsimony Ratchet, a new method for rapid parsimony analysis. *Cladistics*, 15(4):407–414, doi:10.1111/j.1096-0031.1999.tb00277.x.
- Owen, G. and Williams, A. (1969). The caecum of articulate Brachiopoda. *Proceedings of the Royal Society B: Biological Sciences*, 172:187–201, doi:10.1098/rspb.1969.0019.
- Popov, L. E. (1992). The Cambrian radiation of brachiopods. In Lipps, J. H. and Signor, P. W., editors, *Origin and Early Evolution of Metazoa*, pages 399–423. Pergamon.
- Popov, L. E., Bassett, M. G., Holmer, L. E., and Ghobadi Pour, G. M. (2009). Early ontogeny and soft tissue preservation in siphonotretide brachiopods: new data from the Cambrian-Ordovician of Iran. *Gondwana Research*, 16(1):151–161, doi:10.1016/j.gr.2009.01.009.
- Popov, L. E., Bassett, M. G., Holmer, L. E., Skovsted, C. B., and Zuykov, M. A. (2010). Earliest ontogeny of Early Palaeozoic Craniiformea: Implications for brachiopod phylogeny. *Lethaia*, 43(3):323–333, doi:10.1111/j.1502-3931.2009.00197.x.
- Rannala, B., Zhu, T.-Q., and Yang, Z.-H. (2012). Tail paradox, partial identifiability, and influential priors in Bayesian branch length inference. *Molecular Biology and Evolution*, 29(1):325–335, doi:10.1093/molbev/msr210.
- Reunov, A. A. and Klepal, W. (2004). Ultrastructural study of spermatogenesis in *Phoronopsis harmeri* (Lophophorata, Phoronida). *Helgoland Marine Research*, 58(1):1–10, doi:10.1007/s10152-003-0153-3.
- Robinson, J. (2014). The muscles, body wall and valve-opening mechanism of extant craniid (inarticulated) brachiopods. *Journal of Natural History*, 48:1231–1252, doi:10.1080/00222933.2013.840941.
- Ronquist, F., Teslenko, M., van der Mark, P., Ayres, D. L., Darling, A., Hohna, S., Larget, B., Liu, L., Suchard, M. A., and Huelsenbeck, J. P. (2012). MrBayes 3.2: efficient Bayesian phylogenetic inference and model choice across a large model space. *Systematic Biology*, 61(3):539–42, doi:10.1093/sysbio/sys029.

- Rowell, A. J. and Caruso, N. E. (1985). The evolutionary significance of *Nisusia sulcata*, an early articulate brachiopod. *Journal of Paleontology*, 59(5):1227–1242.
- Ruppert, E. E., Fox, R. S., and Barnes, R. D. (2004). *Invertebrate zoology: a functional evolutionary approach*, volume 53. Thompson Learning.
- Sereno, P. C. (2007). Logical basis for morphological characters in phylogenetics. *Cladistics*, 23(6):565–587, doi:10.1111/j.1096-0031.2007.00161.x.
- Skovsted, C. B., Betts, M. J., Topper, T. P., and Brock, G. A. (2015). The early Cambrian tommotiid genus *Dailyatia* from South Australia. *Memoirs of the Association of Australasian Palaeontologists*, 48(1):1–117.
- Skovsted, C. B., Brock, G. A., Topper, T. P., Paterson, J. R., and Holmer, L. E. (2011). Scleritome construction, biofacies, biostratigraphy and systematics of the tommotiid *Eccentrotheeca helenia* sp. nov. from the early Cambrian of South Australia. *Palaeontology*, 54:253–286, doi:10.1111/j.1475-4983.2010.01031.x.
- Skovsted, C. B. and Holmer, L. E. (2003). Early Cambrian (Botomian) stem group brachiopod *Mickwitzia* from Northeast Greenland. *Acta Palaeontologica Polonica*, 48(1):1–20.
- Skovsted, C. B. and Holmer, L. E. (2005). Early Cambrian brachiopods from north-east Greenland. *Palaeontology*, 48(2):325–345, doi:10.1111/j.1475-4983.2005.00450.x.
- Skovsted, C. B., Holmer, L. E., Larsson, C. M., Höglström, A. E. S., Brock, G. A., Topper, T. P., Balthasar, U., Stolk, S. P., and Paterson, J. R. (2009). The scleritome of *Paterimitra*: an Early Cambrian stem group brachiopod from South Australia. *Proceedings of the Royal Society B: Biological Sciences*, 276:1651–1656, doi:10.1098/rspb.2008.1655.
- Skovsted, C. B., Knight, I., Balthasar, U., and Boyce, W. D. (2017). Depth related brachiopod faunas from the lower Cambrian Forteau Formation of southern Labrador and western Newfoundland, Canada. *Palaeontologia Electronica*, 20.3.54A:1–52, doi:10.26879/775.
- Skovsted, C. B. and Peel, J. S. (2010). Early Cambrian brachiopods and other shelly fossils from the basal Kinzers Formation of Pennsylvania. *Journal of Paleontology*, 84(4):754–762, doi:10.1666/09-123.1.
- Smith, M. R. (2017). Quantifying and visualising divergence between pairs of phylogenetic trees: implications for phylogenetic reconstruction. *bioRxiv*, doi:10.1101/227942.
- Smith, M. R. (2018). TreeSearch: phylogenetic tree search using custom optimality criteria.
- Streng, M., Butler, A. D., Peel, J. S., Garwood, R. J., and Caron, J.-B. (2016). A new family of Cambrian rhynchonelliformean brachiopods (Order Naukatida) with an aberrant coral-like morphology. *Palaeontology*, 59(2):269–293, doi:10.1111/pala.12226.
- Sun, H.-J., Smith, M. R., Zeng, H., Zhao, F.-C., Li, G.-X., and Zhu, M.-Y. (2018). Hyoliths with pedicles constrain the origin of the brachiopod body plan. page submitted.
- Sutton, M. D., Briggs, D. E. G., Siveter, D. J., and Siveter, D. J. (2005). Silurian brachiopods with soft-tissue preservation. *Nature*, 436(7053):1013–1015, doi:10.1038/nature03846.
- Topper, T. P., Harper, D. A. T., and Ahlberg, P. (2013a). Reappraisal of the brachiopod *Acrotreta socialis* von Seebach, 1865: clarifying 150 years of confusion. *GFF*, 135(2):191–203, doi:10.1080/11035897.2013.811440.
- Topper, T. P., Holmer, L. E., Skovsted, C. B., Brock, G. A., Balthasar, U., Larsson, C. M., Petterson Stolk, P. S., and Harper, D. A. T. (2013b). The oldest brachiopods from the lower Cambrian of South Australia. *Acta Palaeontologica Polonica*, 58(1):93–109, doi:10.4202/app.2011.0146.
- Ushatinskaya, G. T. (2016). Protegulum and brephic shell of the earliest organophosphatic brachiopods. *Paleontological Journal*, 50(2):141–152, doi:10.1134/s0031030116020088.

- Ushatinskaya, G. T. and Korovnikov, I. V. (2016). Revision of the superfamily Acrotheloidea (Brachiopoda, class Linguliformea, order Lingulida) from the Lower and Middle Cambrian of the Siberian Platform. *Paleontological Journal*, 50(5):450–462, doi:10.1134/s0031030116050130.
- Vogt, L. (2017). The logical basis for coding ontologically dependent characters. *Cladistics*, doi:10.1111/cla.12209.
- Watkins, R. (2002). New record of the trimerellid brachiopod *Gasconsia*, a rare Silurian Lazarus taxon. *Journal of Paleontology*, 76(1):185–186, doi:10.1666/0022-3360(2002)076<0185:nottb>2.0.co;2.
- Wiens, J. J. (1998). Does adding characters with missing data increase or decrease phylogenetic accuracy? *Systematic Biology*, 47(4):625–640, doi:10.1080/106351598260635.
- Wiens, J. J. (2003). Missing data, incomplete taxa, and phylogenetic accuracy. *Systematic Biology*, 52(4):528–538, doi:10.1080/10635150390218330.
- Williams, A. and Brunton, C. H. C. (1993). Role of shell structure in the classification of the orthotetidine brachiopods. *Palaeontology*, 36:931–966.
- Williams, A., Carlson, S. J., Brunton, C. H. C., Holmer, L. E., and Popov, L. E. (1996). A supra-ordinal classification of the Brachiopoda. *Philosophical Transactions of the Royal Society B: Biological Sciences*, 351(1344):1171–1193, doi:10.1098/rstb.1996.0101.
- Williams, A., Carlson, S. J., Brunton, C. H. C., Holmer, L. E., Popov, L. E., Mergl, M., Laurie, J. R., Bassett, M. G., Cocks, L. R. M., Rong, J.-Y., Lazarev, S. S., Grant, R. E., Racheboeuf, P. R., Jin, Y.-G., Wardlaw, B. R., Harper, D. A. T., and Wright, A. D. (2000). Linguliformea, Craniiformea, and Rhynchonelliformea (part). In *Treatise on Invertebrate Paleontology, Part H, Brachiopoda (Revised)*, volume 2 & 3, pages 1–919. Geological Society of America & Paleontological Institute.
- Williams, A., Cusack, M., and Mackay, S. (1994). Collagenous chitino-phosphatic shell of the brachiopod *Lingula*. *Philosophical Transactions of the Royal Society B: Biological Sciences*, 346:223–266, doi:10.1098/rstb.1994.0143.
- Williams, A., Holmer, L. E., and Cusack, M. (2004). Chemico-structure of the organophosphatic shells of siphonotretide brachiopods. *Palaeontology*, 47(5):1313–1337, doi:10.1111/j.0031-0239.2004.00404.x.
- Williams, A., James, M. A., Emig, C. C., Mackay, S., Rhodes, M. C., Cohen, B. L., Gawthrop, A. B., Peck, L. S., Curry, G. B., Ansell, A. D., Cusack, M., Walton, D., Brunton, C. H. C., Mackinnon, D. I., and Richardson, J. R. (1997). Introduction. In *Treatise on Invertebrate Paleontology, Part H, Brachiopoda (Revised)*, volume 1, pages 1–539. Geological Society of America & Paleontological Institute.
- Williams, A., Mackay, S., and Cusack, M. (1992). Structure of the organo-phosphatic shell of the brachiopod *Discina*. *Philosophical Transactions of the Royal Society B: Biological Sciences*, 337:83–104, doi:10.1098/rstb.1992.0086.
- Williams, A., Popov, L. E., Holmer, L. E., and Cusack, M. (1998). The diversity and phylogeny of the paterinate brachiopods. *Palaeontology*, 41:221–262.
- Williams, A., Racheboeuf, P. R., Savage, N. M., Lee, D. E., Popov, L. E., Carlson, S. J., Logan, A., Luter, C., Cusack, M., Curry, G. B., Wright, A. D., Harper, D. A. T., Cohen, B. L., Cocks, L. R. M., MacKinnon, D. I., Smirnova, T. N., Baker, P. G., Carter, J. L., Gourvennec, R., Mancenido, M. O., Brunton, C. H. C., Dong-Li, D.-S., Boucot, A. J., Bassett, M. G., Alvarez, F., Holmer, L. E., Mergl, M., Emig, C. C., Rubel, M., and Jia-Yu, J.-R. (2007). Supplement. In *Treatise on Invertebrate Paleontology, Part H, Brachiopoda (Revised)*, volume 6, pages 2321–3226. Geological Society of America & Paleontological Institute.
- Williams, A., Sandy, M. R., Carlson, S. J., Lee, D. E., Johnson, J. G., Smirnova, T. N., Jin, Y.-G., Hou, H.-F., Carter, J. L., Gourvennec, R., Racheboeuf, P. R., Brunton, C. H. C., Dagys, A. S., Curry, G. B., Baker, P. G., Sun, D.-L., and MacKinnon, D. I. (2006). Rhynchonelliformea (part). In *Treatise on Invertebrate Paleontology, Part H, Brachiopoda (Revised)*, volume 5, pages 1689–2320. Geological Society of America & Paleontological Institute.

- Zhang, C., Rannala, B., and Yang, Z.-H. (2012). Robustness of compound Dirichlet priors for Bayesian inference of branch lengths. *Systematic Biology*, 61(5):779–84, doi:10.1093/sysbio/sys030.
- Zhang, Z.-F., Han, J., Zhang, X.-L., Liu, J.-N., Guo, J.-F., and Shu, D.-G. (2007a). Note on the gut preserved in the Lower Cambrian *Lingulellotreta* (Lingulata, Brachiopoda) from southern China. *Acta Zoologica*, 88(1):65–70, doi:10.1111/j.1463-6395.2007.00252.x.
- Zhang, Z.-F., Holmer, L. E., Ou, Q., Han, J., and Shu, D.-G. (2011a). The exceptionally preserved Early Cambrian stem rhynchonelliform brachiopod *Longtancunella* and its implications. *Lethaia*, 44(4):490–495, doi:10.1111/j.1502-3931.2011.00261.x.
- Zhang, Z.-F., Holmer, L. E., Popov, L. E., and Shu, D.-G. (2011b). An obolellate brachiopod with soft-part preservation from the Early Cambrian Chengjiang fauna of China. *Journal of Paleontology*, 85(3):460–463, doi:10.1666/10-121.1.
- Zhang, Z.-F., Li, G.-X., Emig, C. C., Han, J., Holmer, L. E., and Shu, D.-G. (2009). Architecture and function of the lophophore in the problematic brachiopod *Heliomedusa orienta* (Early Cambrian, South China). *Geobios*, 42(5):649–661, doi:10.1016/j.geobios.2009.04.001.
- Zhang, Z.-F., Li, G.-X., Holmer, L. E., Brock, G. A., Balthasar, U., Skovsted, C. B., Fu, D.-J., Zhang, X.-L., Wang, H.-Z., Butler, A. D., Zhang, Z.-L., Cao, C.-Q., Han, J., Liu, J.-N., and Shu, D.-G. (2014). An early Cambrian agglutinated tubular lophophorate with brachiopod characters. *Scientific Reports*, 4:4682, doi:10.1038/srep04682.
- Zhang, Z.-F., Shu, D.-G., Emig, C. C., Zhang, X.-L., Han, J., Liu, J.-N., Li, Y., and Guo, J.-F. (2007b). Rhynchonelliformean brachiopods with soft-tissue preservation from the early Cambrian Chengjiang Lagerstätte of South China. *Palaeontology*, 50:1391–1402, doi:10.1111/j.1475-4983.2007.00725.x.
- Zhang, Z.-F., Shu, D.-G., Han, J., and Liu, J.-N. (2004). New data on the lophophore anatomy of Early Cambrian linguloids from the Chengjiang Lagerstätte, Southwest China. *Carnets de géologie (Notebooks on geology)*, 4:1–7, doi:10.4267/2042/310.
- Zhang, Z.-F., Shu, D.-G., Han, J., and Liu, J.-N. (2007c). A gregarious lingulid brachiopod *Longtancunella chengjiangensis* from the Lower Cambrian, South China. *Lethaia*, 40(1):11–18, doi:10.1111/j.1502-3931.2006.00002.x.
- Zhang, Z.-L., Skovsted, C. B., and Zhang, Z.-F. (2018). A hyolithid without helens preserving the oldest hyolith muscle scars; palaeobiology of *Paramicrocornus* from the Shujingtuo Formation (Cambrian Series 2) of South China. *Palaeogeography, Palaeoclimatology, Palaeoecology*, 489:1–14, doi:10.1016/j.palaeo.2017.07.021.
- Zhang, Z.-L., Zhang, Z.-F., and Wang, H.-Z. (2016). Epithelial cell moulds preserved in the earliest acrotretid brachiopods from the Cambrian (Series 2) of the Three Gorges area, China. *GFF*, 138(4):455–466, doi:10.1080/11035897.2016.1143528.
- Zhao, F.-C., Hu, S.-X., Caron, J.-B., Zhu, M.-Y., Yin, Z.-J., and Lu, M. (2012). Spatial variation in the diversity and composition of the Lower Cambrian (Series 2, Stage 3) Chengjiang Biota, Southwest China. *Palaeogeography, Palaeoclimatology, Palaeoecology*, 346–347:54–65, doi:10.1016/j.palaeo.2012.05.021.
- Zhao, F.-C., Smith, M. R., Yin, Z.-J., Zeng, H., Li, G.-X., and Zhu, M.-Y. (2017). *Orthrozanclus elongata* n. sp. and the significance of sclerite-covered taxa for early trochozoan evolution. *Scientific Reports*, 7(1):16232, doi:10.1038/s41598-017-16304-6.